



TECHNISCHE UNIVERSITÄT MÜNCHEN

FAKULTÄT FÜR CHEMIE

FACHBEREICH ORGANISCHE CHEMIE

**New Ligand Structures for Homogeneous Transition-  
Metal Catalysis:  
Synthesis and Applications of New Dimethylphosphine  
Donors and Benzoannulated Dialkylbiaryl Phosphines**

Katja Reinhardt

Vollständiger Abdruck der von der Fakultät für Chemie der Technischen Universität München zur Erlangung des akademischen Grades einer

Doktorin der Naturwissenschaften (Dr. rer. nat.)

genehmigten Dissertation.

Vorsitzende/-r: apl. Prof. Dr. Wolfgang Eisenreich

Prüfende/-r der Dissertation:

1. Prof. Dr. Lukas Hintermann
2. Prof. Dr. Shigeyoshi Inoue

Die Dissertation wurde am 08.10.2021 bei der Technischen Universität München eingereicht und durch die Fakultät für Chemie am 11.11.2021 angenommen.



*Feel the rain on your skin  
No one else can feel it for you  
Only you can let it in  
No one else [...] can speak the words on your lips  
Drench yourself in words unspoken  
Live your life with arms wide open  
Today is where your book begins  
The rest is still unwritten*

*Natasha Bedingfield – “Unwritten”*





This thesis was carried out from March 2018 to September 2021 under the supervision of Prof. Dr. Lukas Hintermann at the Technical University of Munich.



## Acknowledgments

First of all, I would like to thank Prof. Dr. Lukas Hintermann for giving me the opportunity to conduct my PhD Thesis as part of his group. I truly appreciate always being able to turn to you for advice, be it of theoretically scientific nature or about practical laboratory work. At the same time, you allowed me to conduct my research independently with the freedom to develop my own ideas, which gave me the ability to grow into a more and more independently thinking researcher.

Furthermore, I want to thank Verena Widhopf and Christine Kretschmer for the support with all kinds of bureaucratic paper works.

Of course, the years I spent in the lab during my PhD would not have been the same without my colleagues: Dr. Philippe Klein, Dr. Sebastian Helmbrecht, Dr. Sebastian Koller, Christian Weindl, Dr. Junlin Zhang, Dr. Zhai Lianjie, Theresa Appleson, Corvin Lossin, Anna Gradenegger, Lukas Rast, Donato Pasculli and Nicolas Hilgert. I fondly remember our various AK Rumbles, and I hope we can repeat those in the future when we are all fully vaccinated.

Thank you, Philippe, for many fruitful scientific discussions, but also for being a friend and coffee drinking partner throughout the last years. A special thanks also goes to you for measuring and solving my crystal structures.

Helmi, I'd like to thank you for being the one to help me settle in the laboratory when I first came here as a Master's student, but especially for sharing the same kind of – sometimes dumb – humour with me.

Thank you also to Christian Weindl, who first entered the lab as one of my research students, and now advanced to a promising PhD candidate at our laboratory. Thank you for always helping out with general maintenance tasks in the laboratory. Especially the last 6 months of my lab work would have been way more frustrating for me if it weren't for your help.

Moreover, I would like to thank my helpers, the talented Bachelor's and Master's students that I supervised during my Thesis: Christian Weindl, Ekaterina Khrameshina, Raphael Bühler and Yueer Zhu. I am sure everyone of you has a promising future as a chemist ahead of you.

A very special thanks goes to my beloved friends in Munich, Laufen and the rest of the world, who I can always turn to for support, or simply for enjoying life together: Julia Loftus, Luise Mirdita, Rüya Inan, Verena Uher and Leela Klein. Whether we live far away or in the same city, no matter how regularly we meet up, I know I can always count on everyone of you and I will always appreciate and value our friendships.

My dear Seiji, I want to thank you for keeping up with me throughout the years, for always being there for me, supporting me and accepting me just the way I am. Even though we did not meet for more than a year due to the pandemic, I know you will always be there for me and I will always be there for you. Mahal kita at miss na kita.

Last but not least, I want to thank my parents, Klaus-Dietrich and Brita Reinhardt, for raising me and supporting me in all of my plans and endeavors. You're truly the best parents I could imagine and I love you so much. I also want to thank my brother Steffen: You have always been there to help me whenever I needed you.

## Abstract

This work deals with the exploration of novel ligand structures and their applicability in transition-metal catalyzed cross-coupling reactions. In the first part of this thesis, the incorporation of the dimethyl phosphino donor motif into ligand structures starting from the air-stable platform chemical dimethyl phosphine *P*-oxide (**4**) was studied. C-P bond formation was realized either by a direct addition of **4** to *p*-quinones *via* Brønsted acid catalyzed 1,2-*Michael* addition, or by alkylation of **4** *via* lithiation to a nucleophilic phosphinylium anion and its subsequent reaction with haloalkanes. This approach avoids handling of air-sensitive materials until the last deoxygenation step of the synthesis. This was exemplified by deoxygenation of **20** to afford new bis(dimethyl)phosphine alkane **23**, which was conveniently isolated as air-stable palladium(II) complex **27**. A further exploration of the dimethyl phosphino ligand motif and specifically the complexation chemistry of **4** as secondary phosphine oxide preligand was realized by the synthesis of the labile anionic dimethylphosphinous acid / phosphinito complex **30**.

The deoxochlorination of **4** with  $\text{PCl}_3$  gave  $\text{Men}_2\text{PCl}$  (**3**) as an established precursor for dimethylphosphine ligands *via* reaction with metalated (bi)aryl precursors, affording (aryl)dimethyl monophosphine ligands **L1-L5**, among them menthyl analogues of *Buchwald* ligands SPhos and JohnPhos. Ligands **L1-L5** and **4** as well as complexes **7** and **8** were evaluated in various transition-metal catalyzed test reactions. While **4** and its palladium complexes showed limited activity in catalysis, ligands **L1-L4** showed activity in Suzuki-Miyaura, Mizoroki-Heck and Kumada-Corriu couplings. The ligand (2-chlorophenyl)dimethyl phosphine **L3** in particular showed asymmetric Suzuki-Miyaura couplings forming sterically hindered in up to e.r. 93:7.

As a further novel ligand motif, a benzoannulated version of *Buchwald* ligand BrettPhos was synthesized, namely KatPhos (dicyclohexyl(1,4-dimethoxy-3-(2,4,6-triisopropylphenyl)naphthalen-2-yl)phosphine; **L6**). With CyAnPhos (dicyclohexyl(3-(3,5-di-*tert*-butyl-4-methoxyphenyl)-1,4-dimethoxynaphthalen-2-yl)phosphine; **L7**) and AnPhos ((3-(3,5-di-*tert*-butyl-4-methoxyphenyl)-1,4-dimethoxynaphthalen-2-yl)diphenylphosphine; **L8**), two more benzoannulated ligands were synthesized which exhibit a *meta,meta* substitution at the aryl' moiety (as opposed to the usual *ortho*-substitution with *Buchwald*'s biaryl dialkyl monophosphine ligands) as novel structural motif. The key phosphination step of each ligand synthesis was optimized using  $^{31}\text{P}$ -qNMR as a proof of concept to explore the potential of  $^{31}\text{P}$ -qNMR as quantification method in the synthesis of phosphine ligands.

The benzoannulated ligands were screened in palladium-catalyzed cross-coupling reactions and KatPhos was directly compared to its *Buchwald* analogue in BrettPhos-typical couplings. As KatPhos (**L6**) proved to be superior in the *Buchwald-Hartwig* coupling of 4-chloro anisole and aniline, its substrate scope in the coupling of primary amines and aryl chlorides was explored. Here, the coupling of simple primary aryl amines and activated or unactivated aryl chlorides was accomplished in excellent yields, but limitations were seen in the coupling of more sterically hindered or heterocyclic substrates.

# Zusammenfassung

Diese Arbeit thematisiert die Erforschung neuer Ligandstrukturen und ihrer Anwendbarkeit in Übergangsmetallkatalysierten Kreuzkupplungsreaktionen. Im ersten Teil dieser Dissertation wurde der Einbau des Dimethylphosphino-Donormotives in Ligandenstrukturen ausgehend von Dimethylphosphinoxid (**4**) als luftstabiler Ausgangskemikalie untersucht. Die C-P Bindungsbildung wurde zum Einen durch direkte Addition von **4** an *p*-Chinone *via* Brønsted-säurekatalysierte 1,2-*Michael* Addition oder durch Alkylierung von **4** *via* Lithiierung zu einem nukleophilen Phosphanylanion und darauffolgende Reaktion mit Halogenalkanen erreicht. Diese Herangehensweise vermeidet den Umgang mit luftempfindlichen Materialien bis zum letzten Schritt der Synthese, der Deoxygenierung. Dies wurde beispielhaft durch die Deoxygenierung von **20** zu Bis(dimethylphosphino)alkan **23** demonstriert, welches als luftstabiler Palladium(II)-Komplex **27** isoliert wurde. Weiters wurde das Dimethylphosphan-Ligandmotiv und besonders die Komplexierungschemie des sekundären Phosphinoxid-Präliganden **4** durch die Synthese des labilen, anionischen Dimethylphosphinige Säure/ -phosphinitokomplexes **30** untersucht. Die Deoxychlorierung von **4** mit  $\text{PCl}_3$  lieferte  $\text{Men}_2\text{PCl}$  (**3**) als etablierten Vorläufer für Dimethylphosphan-Liganden *via* Reaktion mit metallierten (Bi)aryl-Vorläufern. Dies lieferte (Aryl)dimethylphosphan-Liganden L1-L5, unter ihnen auch Menthyl-Analoga der *Buchwald*-Liganden SPhos und JohnPhos. Liganden **L1-L5** und **4** sowie die Palladiumkomplexe **7** und **8** wurden in diversen Übergangsmetallkatalysen evaluiert.

Während **4** und seine Palladiumkomplexe begrenzte Aktivität in der Katalyse zeigten, zeigten Liganden L1-L4 Aktivität in *Suzuki-Miyaura*, *Mizoroki-Heck* und *Kumada-Corriu* Kupplungen. Insbesondere der Ligand (2-Chlorophenyl)dimethylphosphan **L3** zeigte Aktivität in asymmetrischen *Suzuki-Miyaura* Kupplungen, welche zu sterisch gehinderten Biarylen in e.r.-Werten von bis zu 93:7 führten.

Als ein weiteres Ligandmotiv wurde KatPhos (Dicyclohexyl(1,4-dimethoxy-3-(2,4,6-triisopropylphenyl)naphthalen-2-yl)phosphan; **L6**), eine benzoaniellierte Version des *Buchwald*-Liganden BrettPhos, synthetisiert. Mit CyAnPhos (Dicyclohexyl(3-(3,5-di-*tert*-butyl-4-methoxyphenyl)-1,4-dimethoxynaphthalen-2-yl)phosphan; **L7**) und AnPhos (((3-(3,5-Di-*tert*-butyl-4-methoxyphenyl)-1,4-dimethoxynaphthalen-2-yl)diphenylphosphan; **L8**) wurden zwei weitere benzoaniellierte Liganden synthetisiert, die eine *meta,meta*-Substitution an der Aryl'-Einheit (anstelle der üblichen *ortho*-Substitution an *Buchwald*'s Biaryldialkyl Monophosphinliganden) als neuartige Strukturmodifikation aufweisen. Der Schlüsselschritt der Phosphinierung jeder Ligandsynthese wurde mithilfe von  $^{31}\text{P}$ -qNMR-Analyse als

Machbarkeitsstudie, um das Potential von  $^{31}\text{P}$ -qNMR als Quantifizierungsmethode in der Synthese von Phosphanliganden zu untersuchen, optimiert.

Die benzoanellierten Liganden wurden in Palladium-katalysierten Kreuzkupplungsreaktionen getestet. Zudem wurde KatPhos direkt mit seinem *Buchwald*-Analogon in BrettPhos-typischen Kupplungsreaktionen getestet. Da KatPhos (**L6**) in der Buchwald-Hartwig Kupplung von 4-Chloranisol und Anilin überlegen war, wurde seine Anwendbarkeit auf weitere Substrate in Kupplungen von primären Amininen und Arylchloriden untersucht. Hierbei wurde die Kupplung von einfachen primären Arylaminen und aktivierten oder nicht-aktivierten Arylchloriden in sehr guten Ausbeuten erreicht. Limitationen gab es bei der Kupplung von sterisch gehinderten und heterozyklischen Substraten.



# Table of Contents

<b>1</b>	<b>GENERAL INTRODUCTION AND THEORY</b>	<b>15</b>
1.1	Dialkylbiaryl Phosphine Ligands: Properties and Applications in Catalysis	16
1.2	Variations of the Dialkylbiaryl Phosphine Motif	21
1.3	Secondary Phosphine Oxides: Properties and Application in Catalysis	26
1.4	Introducing Chirality to Phosphorus Ligands	29
<b>2</b>	<b>DIMETHYLPHOSPHINE P-OXIDE AS AIR-STABLE PLATFORM CHEMICAL FOR THE SYNTHESIS OF LIGANDS AND TRANSITION METAL COMPLEXES AND THEIR APPLICATION IN CATALYSIS</b>	<b>33</b>
2.1	Dimethylphosphine P-Oxide as Air-Stable Platform Chemical for Men <sub>2</sub> P Donor Ligands	34
2.2	Aim of this Work	37
2.3	Direct Functionalization of Dimethylphosphine P-Oxide Towards Novel Ligand Structures	38
2.3.1	1,4-Addition of Men <sub>2</sub> P(O)H to p-Quinones	38
2.3.2	Direct Arylation and Alkylation of Men <sub>2</sub> P(O)H	44
2.4	Synthesis of Transition-Metal Complexes Incorporating the Dimethylphosphino Structural Motif	49
2.4.1	Synthesis of Transition-Metal Complexes Starting from Bis(dimethylphosphino)propane	49
2.4.2	Synthesis of [ $\{(\text{Men}_2\text{P}-\text{O}-\text{H}-\text{O}-\text{PMen}_2\text{-k}_2\text{P,P}')\text{Pd}\}_2(\text{m-Cl})_2$ ]	52
2.5	Synthesis and Complexation Chemistry of Ligands Containing the Dimethylphosphino Structural Motif <i>via</i> Arylation of Men <sub>2</sub> PCl	58
2.6	Exploration of New Dimethylphosphino Derivatives as Steering Ligands in Catalysis	64
2.6.1	Brønsted Acid Catalyzed Enantioselective Friedel Crafts Alkylation of Indoles with 2-Alkene-1,4-diones	64
2.6.2	Pd-Catalyzed Transformations of Alkynes with Dimethylphosphine Oxide	66
2.6.3	Dimethylphosphine P-Oxide as Ligand in Palladium-Catalyzed Cross-Couplings	69
2.7	(Aryl)dimethylphosphine Ligands and their Application in Catalysis	74
2.7.1	Catalytic Test Reactions Using (Aryl)dimethylphosphine Ligands	74
2.7.2	(Aryl)dimethylphosphines in Catalytic Coupling Reactions: Investigation on Substrate Scopes	85
2.8	<i>In situ</i> Ligand Modification of L2 and L3	97
2.8.1	Investigations on In Situ Ligand Modification of L3	97
2.8.2	Investigation of In Situ Modification of L2	100
2.9	Conclusion and Outlook	105
2.9.1	The Dimethylphosphino Structural Motif and its Application in Catalysis	105
<b>3</b>	<b>SYNTHESIS OF BENZOANNULATED LIGANDS OF THE BUCHWALD TYPE AND THEIR APPLICATION IN CATALYSIS</b>	<b>107</b>
3.1	New Variations of the Dialkylbiaryl Phosphine Ligand type: KatPhos, AnPhos and CyAnPhos	108
3.1.1	Previously Established Ligand Syntheses	109
3.1.2	Aim of this Work	111

<b>3.2</b>	<b>Syntheses of ligands KatPhos, CyAnPhos and AnPhos</b>	<b>112</b>
3.2.1	Synthesis of the Ligand Precursors	112
3.2.2	Optimization of the KatPhos Synthesis	114
3.2.3	Optimization of the CyAnPhos Synthesis	123
3.2.4	Optimization of the AnPhos Synthesis	126
3.2.5	General Remarks on the Applicability of <sup>31</sup> P-qNMRs	126
<b>3.3</b>	<b>Catalytic Test Reactions Employing Benzoannulated Ligands of the Buchwald Type</b>	<b>128</b>
3.3.1	KatPhos and CyAnPhos in Suzuki-Miyaura Coupling Reactions	128
3.3.2	KatPhos and CyAnPhos in the Mizoroki-Heck Reaction	132
3.3.3	Further Tests in Cross-Coupling Reactions	134
<b>3.4</b>	<b>Evaluation of KatPhos and CyAnPhos in BrettPhos-Typical Couplings</b>	<b>141</b>
3.4.1	Arylation of Primary Amines	141
3.4.2	Denitrative Suzuki-Miyaura Coupling of Nitroarenes	142
3.4.3	Evaluations of the Substrate Scope in the Arylation of Primary and Secondary Amines using KatPhos as Ligand	143
<b>3.5</b>	<b>Conclusion and Outlook</b>	<b>145</b>
<b>4</b>	<b>EXPERIMENTAL PART</b>	<b>147</b>
<b>4.1</b>	<b>Materials and Methods</b>	<b>148</b>
4.1.1	Chemicals and Reagents	148
4.1.2	Working Techniques	148
4.1.3	Analytical Techniques	149
<b>4.2</b>	<b>Synthetic Procedures</b>	<b>153</b>
4.2.1	General Procedures	153
4.2.2	Synthesis Procedures	161
4.2.3	Analytical Data of Cross-Coupling Products	183
<b>5</b>	<b>APPENDIX</b>	<b>189</b>
<b>5.1</b>	<b>Glossary</b>	<b>190</b>
<b>5.2</b>	<b>Crystallographic Data</b>	<b>192</b>
5.2.1	Sample and crystal Data for (1,3-Bis(dimethylphosphaneyl)propane-κ <sup>2</sup> P,P')palladium(II) Chloride (27)	192
5.2.2	Sample and crystal data for [ {(Men <sub>2</sub> P–O–H–O–PMen <sub>2</sub> - κ <sup>2</sup> P,P')Pd} <sub>2</sub> (μ-Cl) <sub>2</sub> ] (30)	193
5.2.3	Sample and crystal data for KatPhos (L6)	194
<b>5.3</b>	<b>Chiral HPLC Chromatograms</b>	<b>195</b>
5.3.1	Chromatograms for 2-Methoxy-binaphthyl	195
7.2.2	Chromatograms for 2-Methyl-binaphthyl	197
7.2.3	Chromatogram for 2,3-Dimethoxy-binaphthyl	198
<b>7.3</b>	<b>Exemplary <sup>1</sup>H-qNMR Analysis</b>	<b>199</b>
<b>7.4</b>	<b>References</b>	<b>200</b>

# **1 General Introduction and Theory**

## 1.1 Dialkylbiaryl Phosphine Ligands: Properties and Applications in Catalysis

Dialkylbiaryl phosphine ligands were first reported by Buchwald and co-workers in 1998<sup>1</sup> and have since found application in a variety of transition-metal catalyzed cross-coupling reactions, such as Buchwald-Hartwig aminations, Suzuki-Miyaura couplings and others. Their distinct structural features fulfill different functions which are of importance for general stability of the phosphines and in the different steps of the catalytic cycle (figure 1).<sup>2</sup>

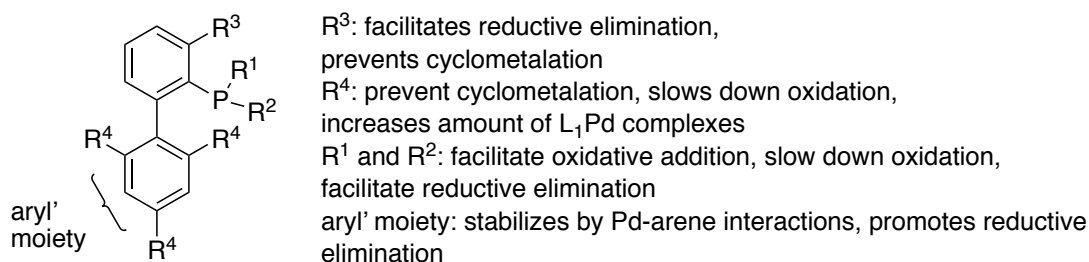
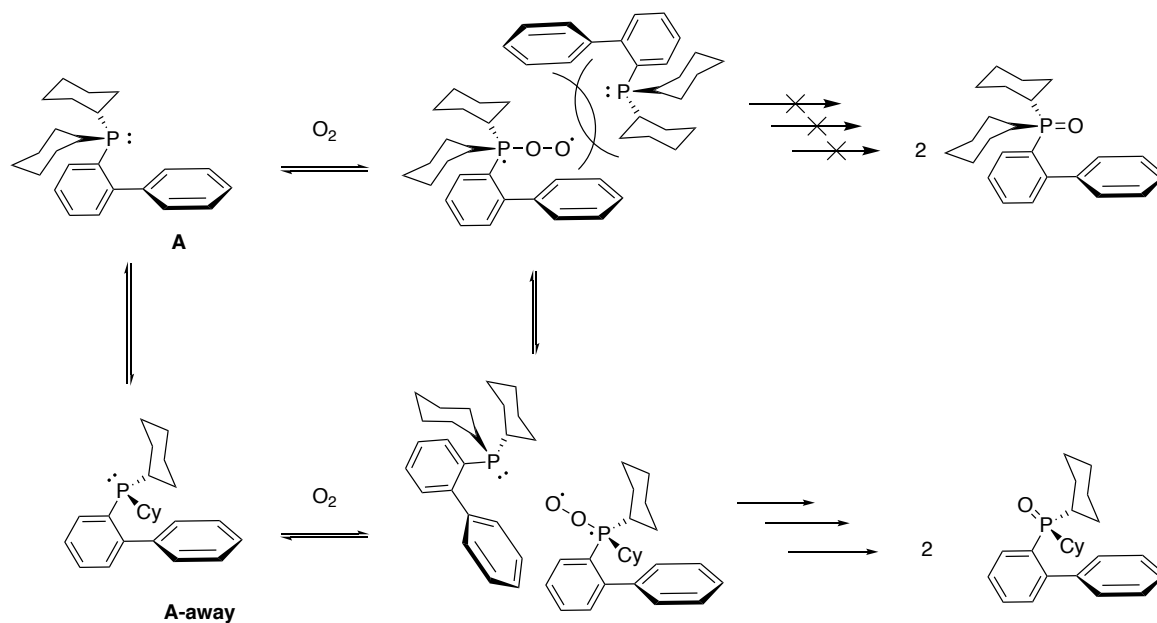


**Figure 1.** Structural features of dialkylbiaryl phosphines and their functions as described by Buchwald and co-workers.<sup>2</sup>

### Low Susceptibility of Dialkylbiaryl Phosphine Ligands Towards Oxidation

One pronounced characteristic of *Buchwald's* dialkylbiaryl phosphine ligands is their low susceptibility towards oxidation, which is enabled by the bulky alkyl substituents attached to phosphorous as well as the *ortho* substituents of the aryl' moiety. *Barder et al.* postulated that this might be due to the mechanism of phosphine oxidation, as depicted in scheme 1.<sup>3</sup>



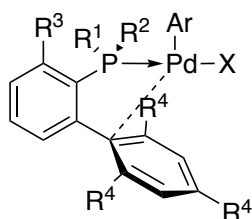
**Scheme 1.** Oxidation mechanism explaining the low susceptibility of dialkylbiaryl phosphines towards oxidation, as postulated by *Barder et al.*<sup>3</sup>

A dialkylbiaryl phosphine can potentially exist in two conformations, with the phosphorus lone-pair facing either in the direction of the aryl' moiety (**A**, scheme 1) or away (**A-away**). If oxygen reacts with phosphine in conformation **A**, subsequent reaction of a second phosphine (forming two molecules of phosphine oxide as a final reaction product) is hampered due to the sterical bulk of the phosphine. Thus, rotation of the phosphorus center has to happen before a second phosphine can react with oxygen. According to Barder *et al.*, this rotation is aggravated with increasing sterical bulk of the alkyl groups connected to phosphorous (*iso*-propyl < cyclohexyl < *tert*-butyl), and ratios of **A** : **A-away** conformation are favored towards the **A** conformation.<sup>3</sup>

### Functions of the Structural Features of Dialkylbiaryl Phosphines in the Catalytic Cycle

The different structural features of dialkylbiaryl phosphines also contribute favorably to the different steps of the catalytic cycle.

As far as the oxidative addition step in a typical cross-coupling reaction is concerned, the sterical demand of the *Buchwald* ligands stabilize the monoligated LPd(0) species, which is more reactive towards oxidative addition. Furthermore, the biaryl moiety contributes to the stability of the dialkylbiaryl phosphine palladium complexes by arene interactions of the aryl' moiety and the palladium center (scheme 2).<sup>4, 5</sup>

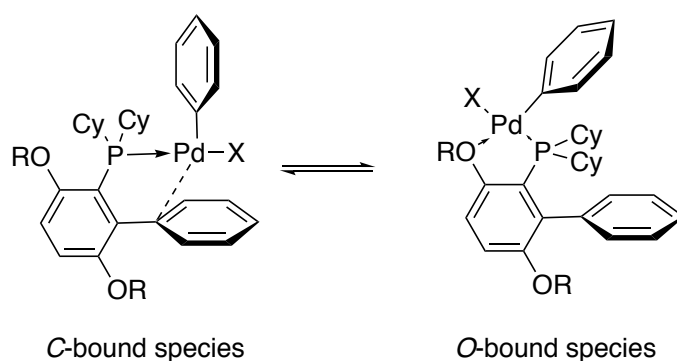


**Scheme 2.** Schematic depiction of the Pd-arene interactions of a dialkylbiaryl phosphine Pd(II) oxidative addition complex.

The electron-donating properties of the alkyl moieties attached to phosphorus contribute to a faster oxidative addition as well.<sup>6,2</sup>

Reductive elimination generates the final product of a cross-coupling reaction. This step of the catalytic cycle is influenced by both electronic and steric factors. For most dialkylbiaryl phosphine ligands, sterical factors facilitate reductive elimination. The bulkiness of the alkyl substituents cause steric congestion around the metal center, which makes the palladium complex more reactive towards reductive elimination resulting in the regeneration of the sterically less hindered LPd(0) complex.<sup>7,2</sup> Furthermore, three-coordinate complexes are generally more prone to reductive elimination than four-coordinate complexes. As the palladium-aryl' interactions are merely weak, the preferred T-shaped conformation for

reductive elimination is more easily adapted for dialkylbiaryl phosphines.<sup>8,2</sup> Reductive elimination can furthermore be facilitated by the substituent in *ortho*-position to phosphorus of the upper aryl moiety ( $R^3$  in figure 1). For the ligand BrettPhos, which exhibits a methoxy substituent in *ortho*-position of phosphorus, it was shown that the corresponding Pd(II) complexes exist either in an *O*-bound or *C*-bound state, as shown in scheme 3 ( $R = \text{Me}$ ). The *O*-bound state is less reactive in reductive elimination, and it was postulated that a bulkier alkoxide substituent ( $R = \text{}^i\text{Pr}$ ) facilitated reductive elimination by shifting the equilibrium to the *C*-bound state.<sup>8,9, 10,</sup>



**Scheme 3.** *C*-bound vs. (less reactive) *O*-bound state of a BrettPhos ( $R = \text{Me}$ ) ligated oxidative addition complex.

Another important factor for catalyst activity in a catalytic reaction is potential catalyst deactivation by cyclometallation. It was found that, during Pd-catalyzed C-N bond formation, for ligands with *ortho*-substitution at aryl', the formation of palladacycles is avoided, thus upholding high intrinsic activity of the ligands.<sup>11</sup>

Figure 2 depicts a selection of commonly used dialkylbiaryl phosphines reported by Buchwald and co-workers along with some of their typical applications. It is worth noting that the range of applications exceed those mentioned here, as this class of ligands is commonly used also for other groups' research endeavors.

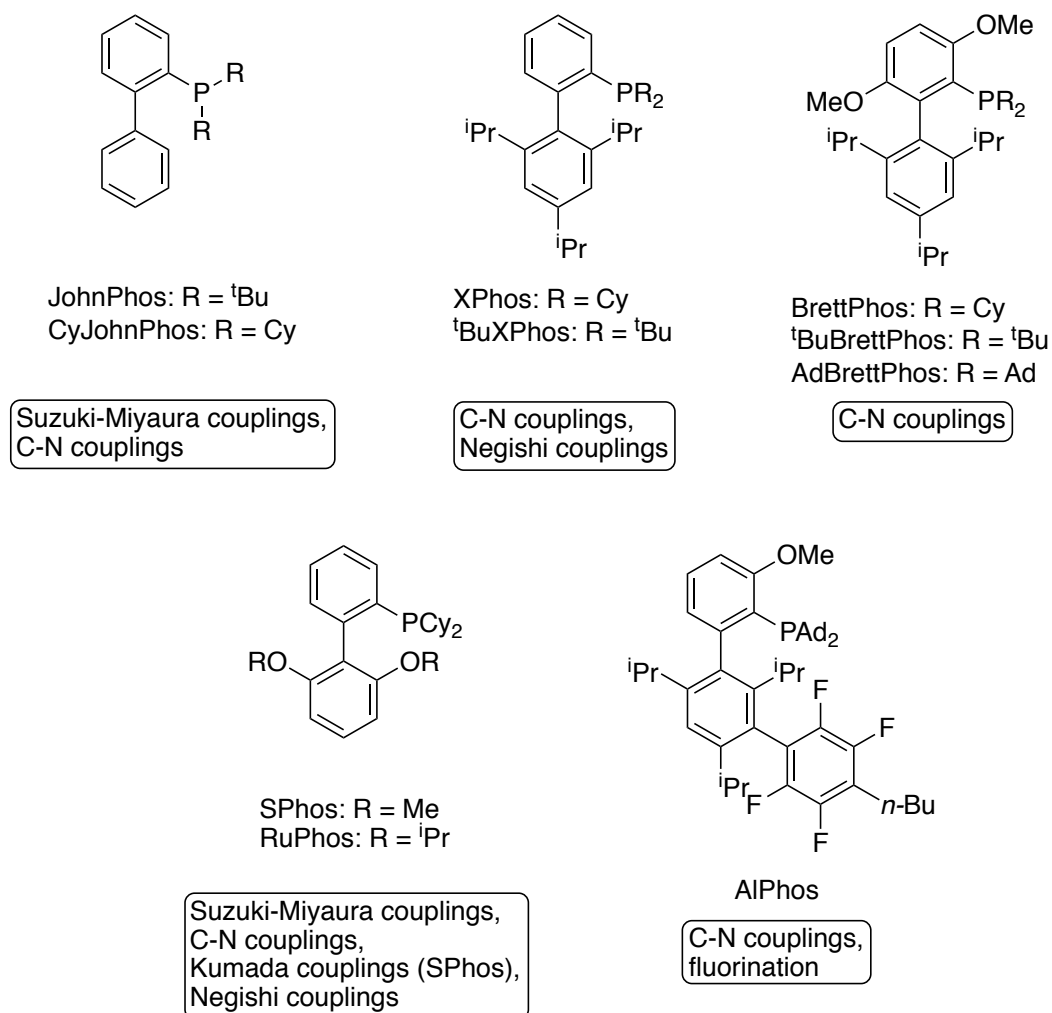
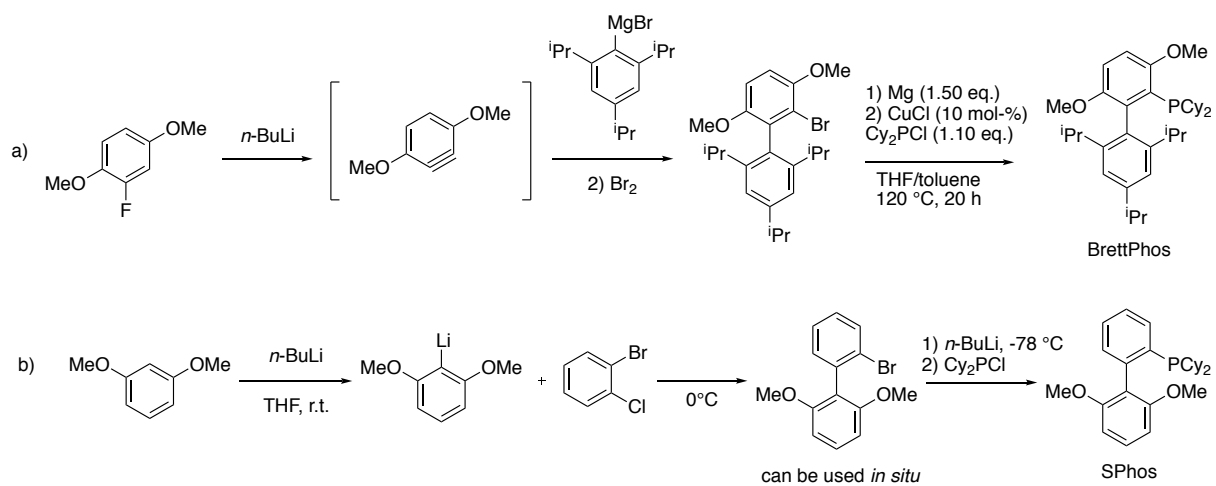


**Figure 2.** A selection of Buchwald's dialkylbiaryl phosphine ligands and some of their typical applications.<sup>5,12,13,14,15, 16,17,18,19,2</sup>

### Synthesis of Dialkylbiaryl Phosphine Ligands

For most of the structurally more complex dialkylbiaryl phosphines, Buchwald and co-workers use aryne chemistry for the construction of the biaryl moiety (scheme 4). The ensuing phosphination is either performed after isolating the respective biaryl halides (as seen in scheme 4a)<sup>20</sup> or *in situ* (scheme 4b).<sup>21</sup> In some cases, such as the synthesis of BrettPhos or AlPhos, the use of catalytic to stoichiometric amounts of copper(I) salt is necessary in the phosphination step.<sup>15</sup>



**Scheme 4.** Approaches for a) the synthesis of BrettPhos, and b) the synthesis of SPhos using aryne chemistry.<sup>21</sup>

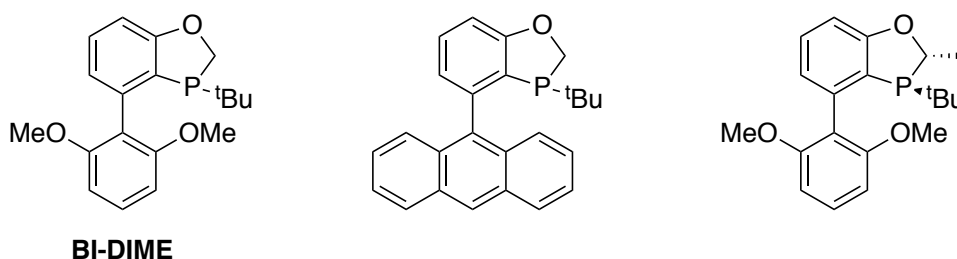


## 1.2 Variations of the Dialkylbiaryl Phosphine Motif

Since Buchwald and co-workers developed their dialkylbiaryl phosphine ligands, other groups have taken up on these catalytically useful structural features and further diversified ligand structures. Among these variations, some examples are presented in the following.

### Variations of the Dialkyl Motif: The 2,3-Dihydrobenzo[*d*][1,3]oxaphosphole Framework by Boehringer-Ingelheim

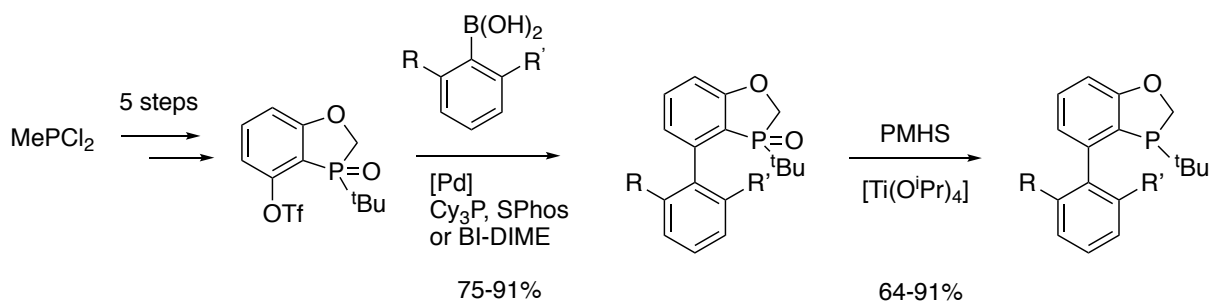
While Buchwald and co-workers had mainly focused on dicyclohexyl, *-tert*-butyl and *-adamantyl* monophosphines, which can rotate rather freely around the phosphorus center, Boehringer-Ingelheim developed a class of dihydrobenzooxaphosphole-based biaryl monophosphine ligands (scheme 5), whose distinctive feature exhibits a rotational and conformational rigidity around the phosphorus center, forcing the phosphorus lone pair into a fixed orientation for coordination to a metal center.<sup>22</sup>



*Scheme 5.* Dihydrobenzooxaphosphole-based dialkylbiaryl ligand variation by Boehringer-Ingelheim.<sup>23, 24, 25</sup>

This ligand class was successfully applied in palladium-catalyzed Suzuki-Miyaura couplings of aryl boronic acids and esters with aryl bromides and chlorides, aminations of aryl bromides and chlorides, the borylation of di-*ortho* substituted aryl bromides and aryl chlorides and also asymmetric Suzuki-Miyaura and Negishi cross-coupling reactions.<sup>25,24</sup>

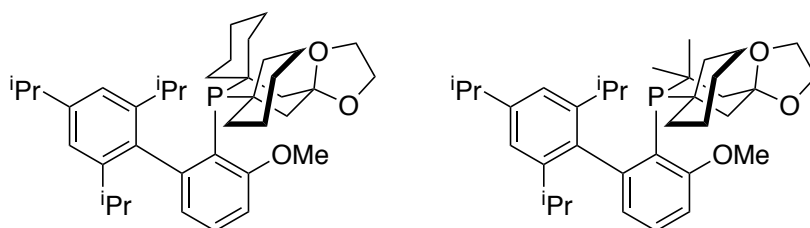
The synthesis of these ligands is achieved starting from methyldichlorophosphine (scheme 6). First, the dihydrobenzooxaphosphole scaffold is constructed,<sup>26</sup> which is then coupled with the respective phenylboronic acid to afford ligand oxide. The oxide is reduced using PMHS/Ti(O<sup>*i*</sup>Pr)<sub>4</sub> to afford the free ligand as a last step of the synthesis.<sup>22</sup>



**Scheme 6.** Multi-step synthesis of dihydrobenzooxaphosphole-based dialkylbiaryl phosphine ligand variation by Boehringer-Ingelheim.<sup>22, 23</sup>

### Variations of the Dialkyl Motif: Biaryl Phosphorinane Ligands

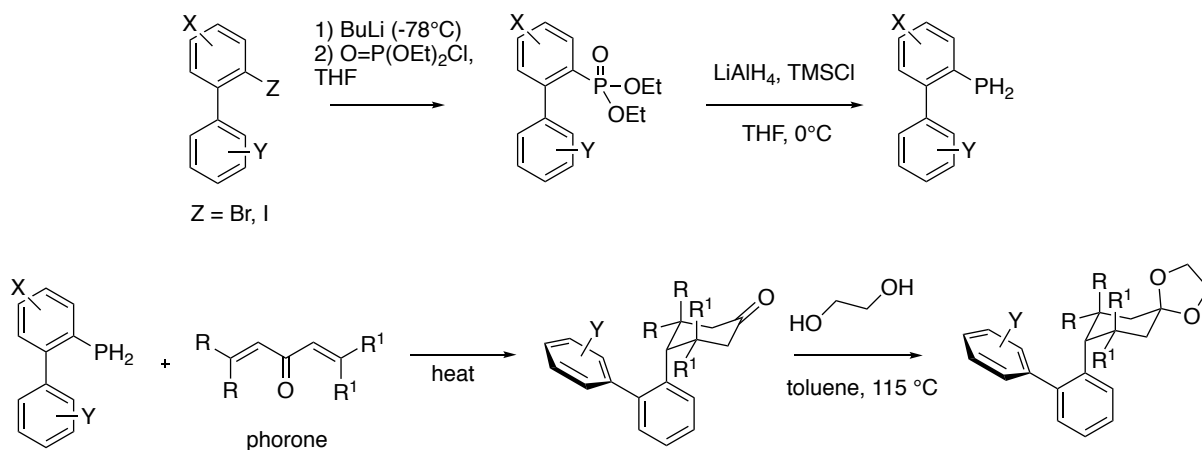
A phosphacycle was also included in a further variation of the dialkyl motif: Laffoon *et al.* reported the synthesis of a series of biaryl phosphorinane ligands, as shown in scheme 7.



**Scheme 7.** Biaryl phosphorinane ligands as reported by Laffoon *et al.*<sup>27</sup>

The ligands proved to be beneficial for palladium-catalyzed sulfonamidation, C-O coupling and C-N coupling reactions. Structural analysis of the ligands and comparison to their *Buchwald* counter-parts revealed less electron-donating properties and a bigger sterical bulk of the phosphorinane ligands, which facilitates reductive elimination in the catalytic cycle.<sup>27</sup>

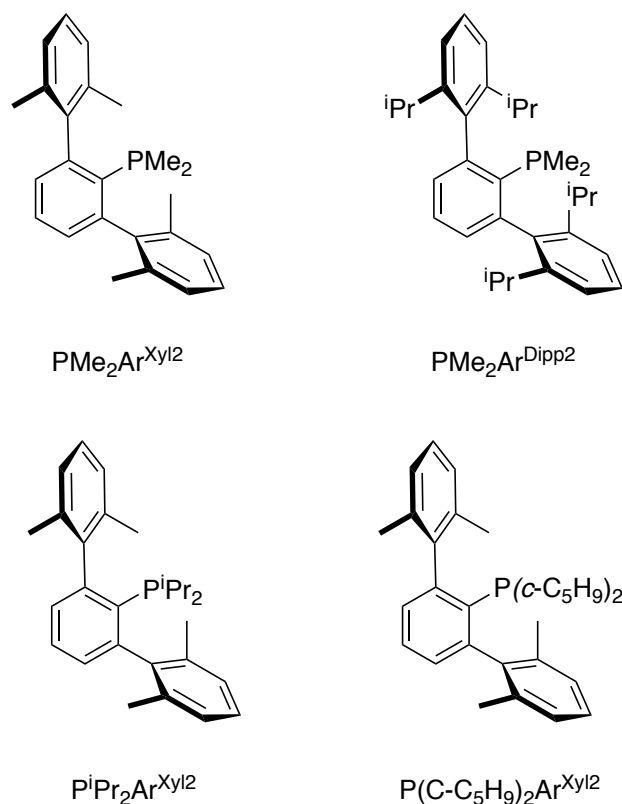
The phosphorinane scaffold is synthesized by reaction of a primary biaryl phosphine with phorone and subsequent formation of the ketal (scheme 8).



**Scheme 8.** General synthesis of biaryl phosphorinane ligands reported by Laffoon *et al.*<sup>27</sup>

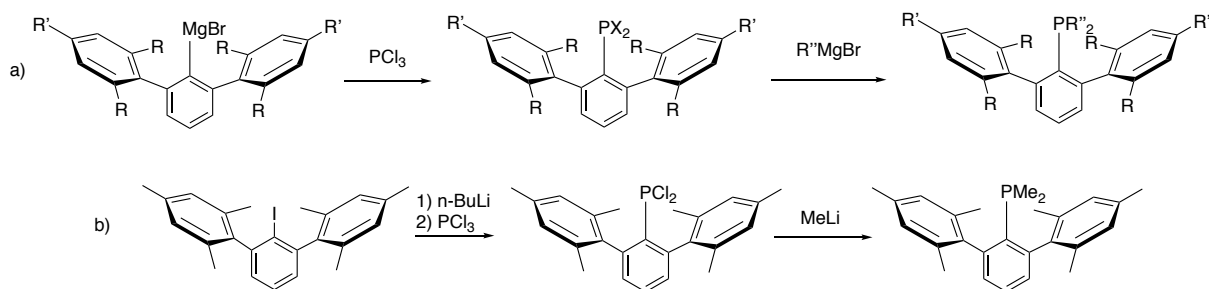
### Variations of the Biaryl Backbone: Dialkylterphenyl Phosphine Ligands

As a variation of the biaryl backbone, the groups of *Nicasio* and *Carmona* and the group of *Protasiewicz* synthesized and characterized several bulky dialkylterphenyl phosphine ligands and their palladium precatalysts and demonstrated their applications in Suzuki-Miyaura couplings and C-N couplings (scheme 9).<sup>28,29,30</sup>



**Scheme 9.** Selected terphenyl ligands synthesized by *Nicasio* and *Carmona* and co-workers.

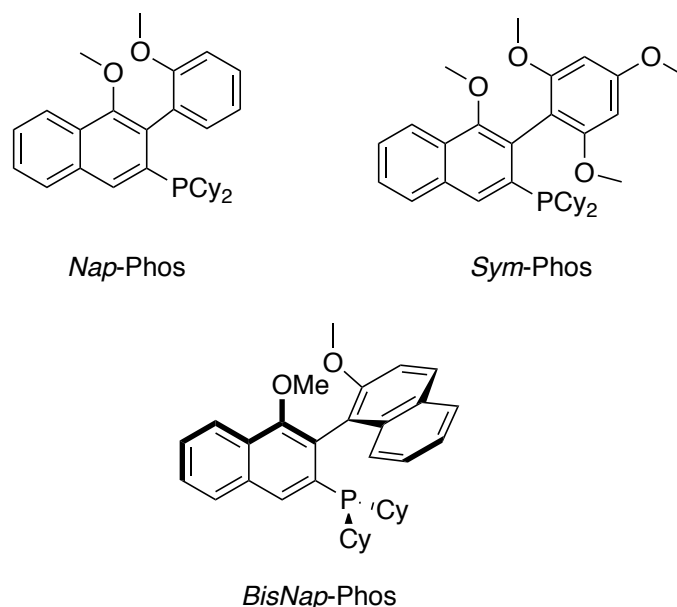
Surprisingly, high yields were reached in a C-N coupling reaction with this class of ligands even when using the palladium precatalyst based on  $\text{PMe}_2\text{Ar}^{\text{Dipp}2}$ , which exhibits two methyl groups connected to phosphorous, which are not as sterically hindered and electron-donating as the alkyl moieties typically seen with phosphine ligands. The authors suggest that the sterical encumberment by the terphenyl moiety contributes to the good performance of this ligand.<sup>30</sup> The terphenyl phosphine scaffold is constructed by reaction of either terphenyl-*Grignard* or lithium reagent with  $\text{PCl}_3$ . Subsequent reaction with either alkyl lithium or alkyl *Grignard* reagent provides the phosphine ligand (scheme 10).<sup>28,31,32</sup>



**Scheme 10.** Synthetic access to terphenyl dialkyl ligands via a) aryl Grignard<sup>31</sup> and b) aryl lithium species.<sup>32</sup>

### Variations of the Biaryl Backbone: Phenyl-Naphthyl Dialkyl Phosphine Ligands

In 2006, Demchuk *et al.* reported the synthesis and application of *Nap-Phos*, a phenyl-naphthyl dialkyl phosphine ligand, which constitutes a formal annulation of the phosphorus-containing aryl moiety of the usual biphenyl motif.<sup>33</sup> Later, this structural motif was diversified with the synthesis of further ligands (scheme 11), with additional methoxy-substituents on the phenyl-moiety to prevent cyclometallation and to reach more electron-density at the metal center of the corresponding Pd(II)-ligand complex.<sup>33 34</sup>

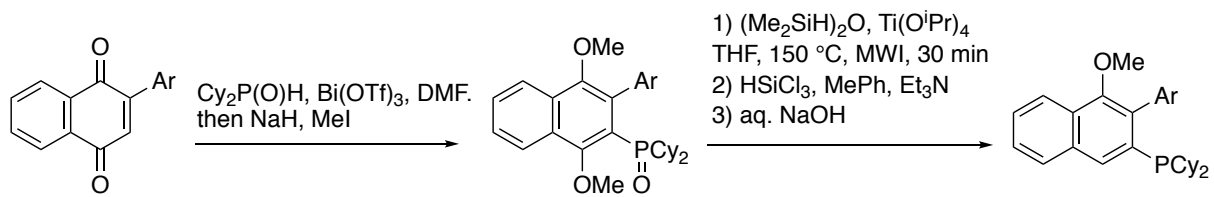


**Scheme 11.** Phenyl-naphthyl dialkyl phosphines as reported by Demchuk *et al.*<sup>33,34</sup>

This class of ligands proved to be useful for palladium-catalyzed Suzuki-Miyaura couplings (in organic solvent as well as in water), Mizoroki-Heck reactions and hydrodehalogenation reactions. As for *Sym-Phos*, Pd(II)-arene interactions of the phenyl moiety were also observed in X-ray crystallographic studies.<sup>35</sup>

The synthesis of these ligands is achieved *via* phospho-*Michael*-addition to the naphthoquinone derivative, subsequent twofold methylation and a final deoxygenation step of the tertiary phosphine oxide (scheme 12). This route suffers from cleavage of the methoxy group in *ortho*-

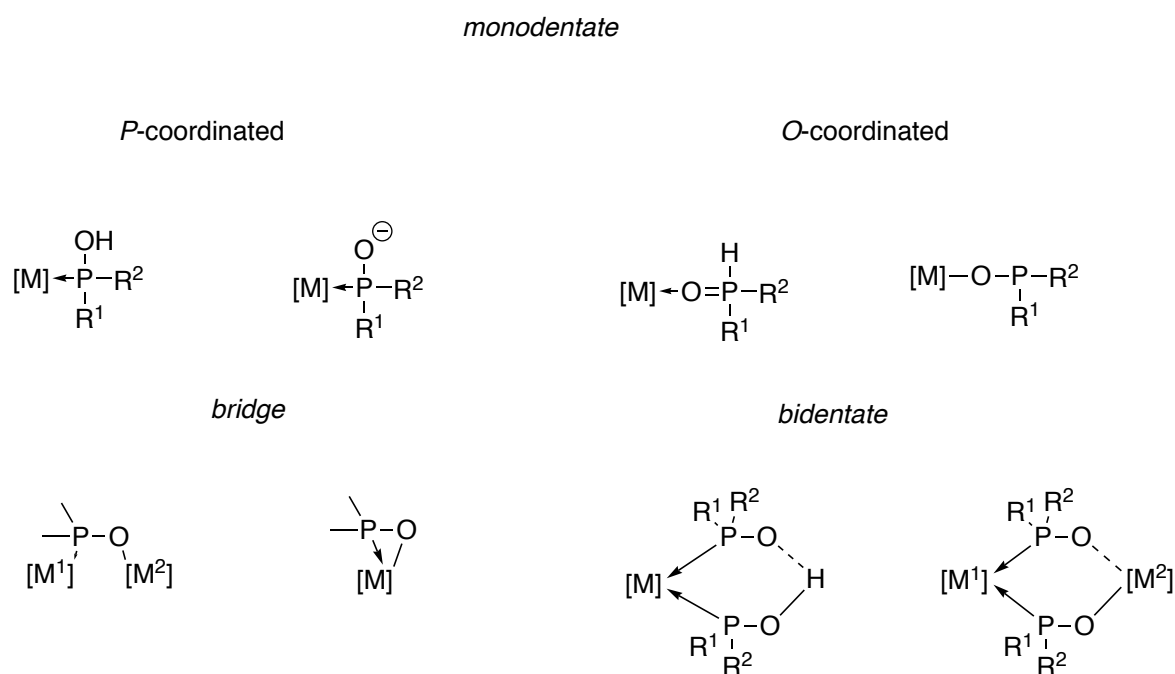
position to phosphorus upon deoxygenation, thus somewhat limiting the potential for structural diversification of the ligands.<sup>34</sup>



**Scheme 12.** Exemplary synthesis route of phenyl-naphthyl dialkyl phosphine ligands.<sup>34</sup>

### 1.3 Secondary Phosphine Oxides: Properties and Application in Catalysis

Another class of ligands of relevance to this work are secondary phosphine oxides (SPOs). The traditional, trivalent phosphine ligands are often difficult to handle, as they are prone to oxidation and may require protection, for example as  $\text{BH}_3$  adduct, which requires an additional deprotection step before use in catalysis.<sup>36</sup> SPOs, due to their pentavalent phosphorus, circumvent this problem and are usually bench-stable. They exist in tautomerism with their corresponding trivalent phosphinous acid, thus they retain *P*-donating abilities and can act as ligand in catalysis. The SPO/phosphinous acid equilibrium is usually shifted to the side of the phosphine oxide in the free ligand, however coordination to transition metals favors the side of the phosphinous acid.<sup>37</sup> Secondary phosphine oxides can bind to metal centers either in bidentate or monodentate fashion. Furthermore, the P-O moiety can, in principle, undergo two different coordination modes, as it exhibits a soft binding site (phosphorus) and hard binding site (oxygen). The former preferably coordinates late transition metals, whereas the latter preferably coordinates early transition metals (scheme 13).<sup>36</sup>

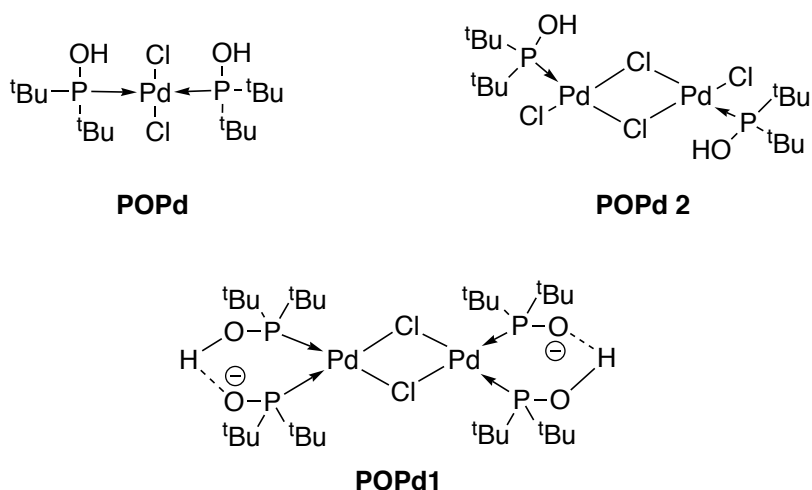


**Scheme 13.** Different coordination modes of SPOs to metal centers.<sup>36</sup>

Buono *et al.* showed in 2011 that the electron-donating properties of phosphinous acids do not reach those of their corresponding trisubstituted phosphines, but upon deprotonation, leading to phosphinito ligands, they become strongly electron-donating.<sup>38</sup> Bidentate

phosphinito/phosphinous acid ligands are of varying electron-donicity depending on their substituents. Dialkylphosphine oxide based phosphinito/phosphinous acid ligands, for example, surpass *N*-heterocyclic carbenes in this matter.

The first use of a secondary phosphine oxide in catalysis was reported already in 1986 by van Leeuwen and co-workers in a platinum-catalyzed hydroformylation reaction.<sup>39,40</sup> But only in the early 2000s did SPO chemistry and their application in catalysis become of wider interest, when Li *et al.* prepared some air- and moisture-stable SPOs and demonstrated the applicability of the [Pd<sub>2</sub>(dba)<sub>3</sub>]/RR'P(O)H systems and air-stable dialkyl phosphine oxide palladium complexes (POPd) in Mizoroki-Heck, Suzuki-Miyaura, Kumada, C-N and C-S couplings of aryl chlorides (scheme 14).<sup>39,41,42</sup>

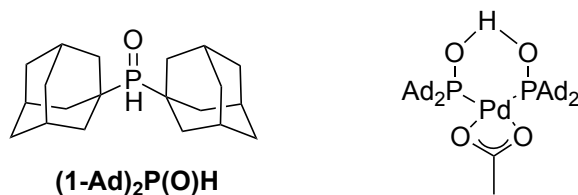


**Scheme 14.** Secondary phosphinous acid complexes by Li *et al.*<sup>41,42</sup>

Later, Wolf and co-workers examined the use of POPd, POPd1 and POPd2 in cross-coupling reactions of chloroquinolines. Generally, POPd was found to be a superior precatalyst compared to POPd1 and POPd2, and the authors postulated that the anionic nature of the palladium/phosphinous acid complexes (upon deprotonation by base) might result in low solubility of the catalysts and is therefore detrimental to the outcome of the catalytic reaction. Tuning of the reaction conditions towards a better homogeneity of the reaction (such as use of organic amine base Cy<sub>2</sub>NMe or use of DMF as polar solvent) improved the yields.<sup>43</sup>

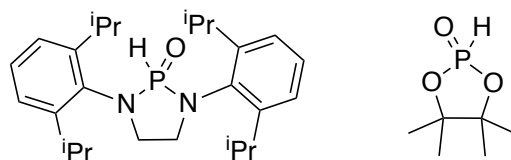
A noteworthy addition to the SPO scope was made by Ackermann and co-workers, who developed sterically hindered di(1-adamantyl)phosphine oxide (scheme 15). This ligand and its corresponding palladium complex was successfully used in Pd-catalyzed intramolecular  $\alpha$ -arylations with chloroarenes and C-H bond activations, and Kumada-Corriu cross-couplings

with 2-pyridyl *Grignard* reagents, among others.<sup>44,45,46</sup> For the latter, it was assumed that *in situ* formation of a heterobimetallic complex is responsible for the high activity of the catalyst<sup>46</sup>.



**Scheme 15.** Di(1-adamantyl)phosphine oxide as (*pre-*)ligand for a Pd(II) complex as reported by Ackermann and co-workers<sup>44,45</sup>

Another notable class of secondary phosphine oxides are heteroatom-substituted secondary phosphine oxides (HASPOs). This type of ligands was employed by Ackermann and co-workers (scheme 16).<sup>47</sup> One of their main asset is their easy accessibility: While conventional SPOs usually require a synthesis starting from air- and moisture-sensitive organometallic reagents, HASPOs can conveniently be synthesized from the corresponding diamines or diols and cheap PCl<sub>3</sub>. Ackermann's HASPOs and their palladium complexes demonstrated activity in palladium-catalyzed *Suzuki-Miyaura* couplings of aryl chlorides and nickel-catalyzed *Kumada* couplings of aryl chlorides, fluorides, (hetero)aryl tosylates and alkenyl tosylates, among others.<sup>48,49</sup>



**Scheme 16.** Examples of HASPOs employed by Ackermann and co-workers.<sup>49</sup>



## 1.4 Introducing Chirality to Phosphorus Ligands

The synthesis of enantiomerically pure compounds has posed a problem to industrial chemists in the production of e.g. pharmaceuticals for decades and fueled research in catalytic asymmetric synthesis. Besides organo- and biocatalysts, the use of chiral phosphorus ligands for asymmetric transition-metal catalysis has played a vital role in the synthesis of chiral compounds.<sup>50,51</sup> The first chiral phosphorus ligands were developed for asymmetric hydrogenation reactions, when Knowles and Horner developed chiral analogues of the Wilkinson's catalyst  $[\text{RhCl}(\text{PPh}_3)_3]$ .<sup>52,53,54,55</sup> Later, the development of bisphosphine ligand DIOP by Kagan and co-workers<sup>56,57,58</sup> led to some groundbreaking realizations: Had it before been widely assumed that the stereocenter of a ligand has to be as close to the metal center as possible to achieve good enantiomeric enrichment, it was now recognized that *P*-chiral phosphorus ligands are not a necessity, but chirality can also be introduced through the ligand's backbone. Moreover, the potential of chelating bisphosphines and  $C_2$ -symmetry were found to be beneficial for ligand design for asymmetric catalysis.<sup>53</sup> Up to now, numerous chiral phosphorus ligands have been developed and applied in asymmetric catalytic transformations. These can roughly be classified into chelating bisphosphines and monophosphines, and these again can be classified into those ligands exhibiting *P*-stereogenic chirality and those with a chiral backbone, be it a unit with a chiral center connected to phosphorous or a backbone exhibiting axial or planar chirality.<sup>59, 60</sup> This classification is depicted in figure 3, along with some examples reported in the literature for each classification. Notably, combinations of each ligand classes have found application as well, such as the prominently used JosiPhos,<sup>61</sup> a bisphosphine ligand combining both a planar chiral element and a central chiral unit. Because of their relatively easier synthesis, the exploration of ligands with a chiral backbone has been prevalent so far.<sup>62</sup>

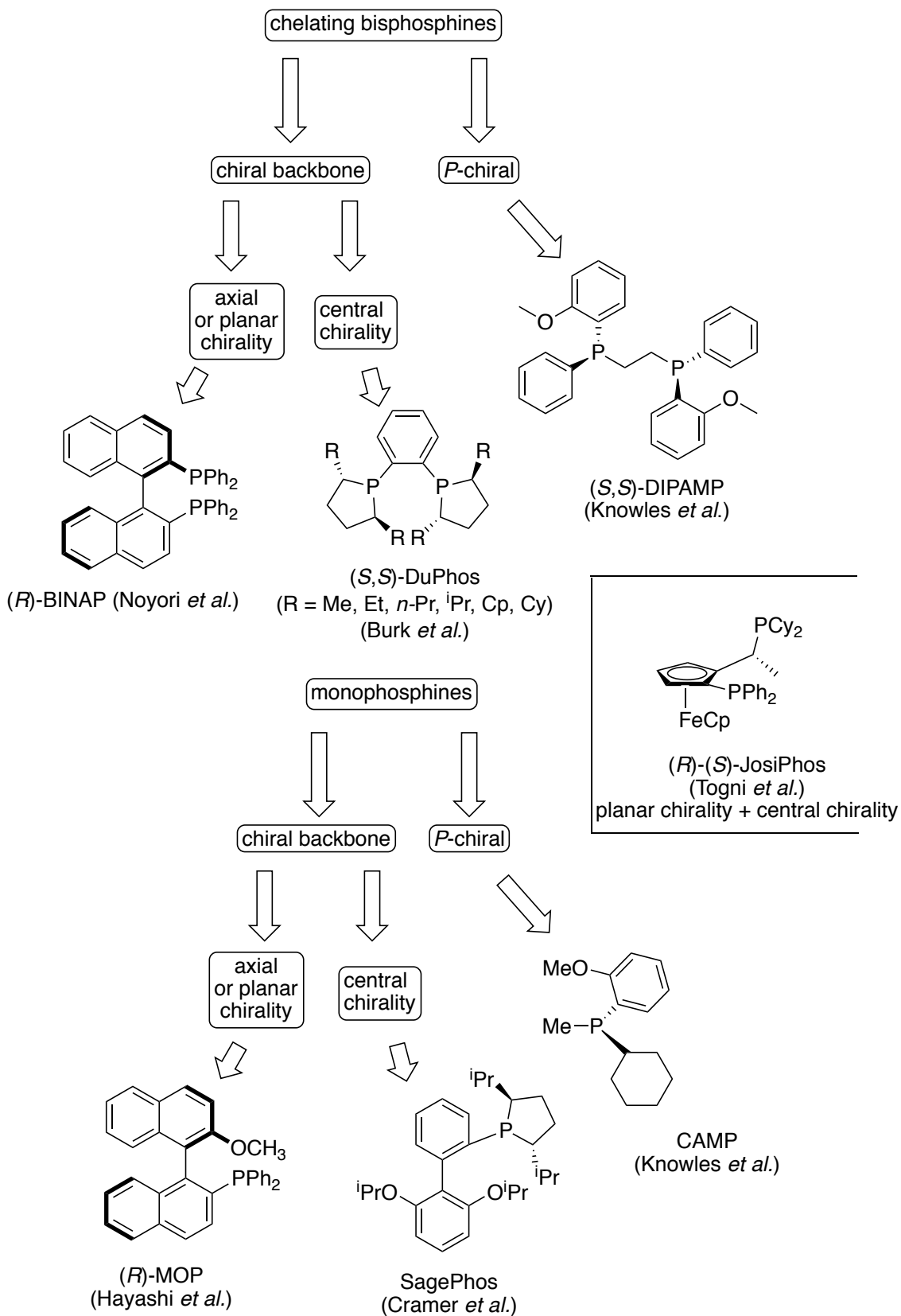


**Figure 3.** Rough classification of chiral phosphorus ligands.<sup>61,63, 64, 65, 66, 67, 68</sup>

The here cited examples show that the aforementioned popular dialkylbiaryl phosphine ligand motif has also been used for the design of chiral ligands (e.g. SagePhos). Needless to say, chiral SPOs have also found application in asymmetric catalytic reactions.<sup>36</sup>

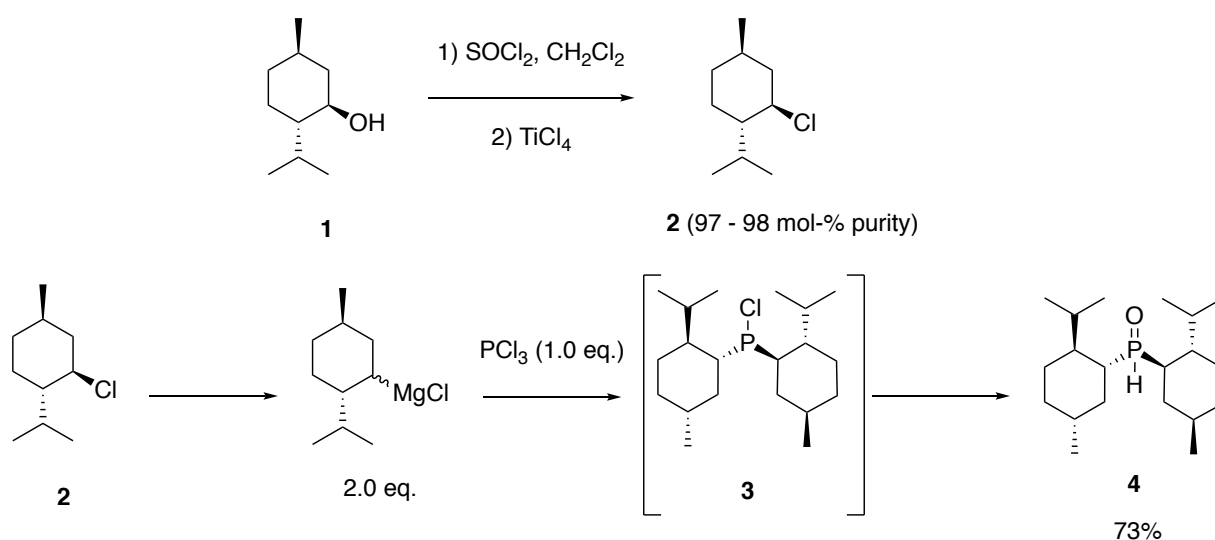


## **2 Dimethylphosphine *P*-Oxide as Air-Stable Platform Chemical for the Synthesis of Ligands and Transition Metal Complexes and their Application in Catalysis**

## 2.1 Dimethylphosphine *P*-Oxide as Air-Stable Platform Chemical for Men<sub>2</sub>P Donor Ligands

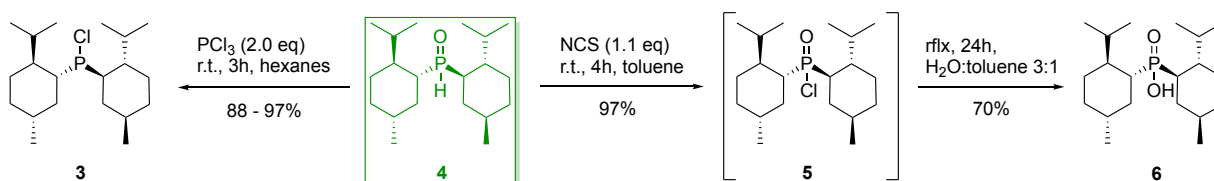
The enantiomeric (–)- and (+)-menthols and derivatives thereof are commonly used chiral auxiliaries in asymmetric organic synthesis,<sup>69</sup> including the synthesis of chiral phosphorus ligands. Besides, the menthyl- or dimethylphosphino structural motif can be found as chiral donor group in a variety of ligands which have been applied in various asymmetric catalytic transformations, including rhodium(I) catalyzed asymmetric hydrogenation<sup>70,71</sup> or asymmetric Ni-catalyzed alka-1,3-diene codimerization, especially in the early days of asymmetric catalysis.<sup>72,59</sup>

In our group, dimethylphosphine *P*-oxide **4** has become available<sup>73</sup> (meanwhile, its preparation was also reported by Black *et al.*<sup>74</sup>). The synthesis sequence for this enantiopure SPO is presented in scheme 17. Starting from (–)-menthol **1**, an improved synthesis of menthyl chloride **2** was developed. While commonly used synthesis pathways are accompanied with the generation of cationic rearrangement products in 18-25 mol-%, our group has developed a convenient synthesis and purification protocol leading to menthyl chloride of 97-98 mol-% purity.<sup>75</sup> With menthyl chloride at hand, a method for the synthesis of dimethylphosphine oxide **4** *via* menthyl Grignard reagent was developed. The use of menthyl magnesium chloride generated from the regioisomerically pure **2** enabled an easily scalable and highly diastereoselective synthesis of dimethylphosphine oxide, in which the final product was obtained pure and crystalline by simple trituration from hexanes.<sup>73,76,77</sup>



**Scheme 17.** Previously achieved multi-step synthesis of **4**.

Further research efforts in our group focused on simple transformations of the air-stable platform chemical dimethylphosphine *P*-oxide to the corresponding chlorophosphine **3**, phosphinic chloride **5**, phosphinic acid **6** or other derivatives (scheme 18).<sup>76,77,78</sup>



**Scheme 18.** Previously achieved syntheses starting from  $\text{Men}_2\text{P}(\text{O})\text{H}$  **4**.

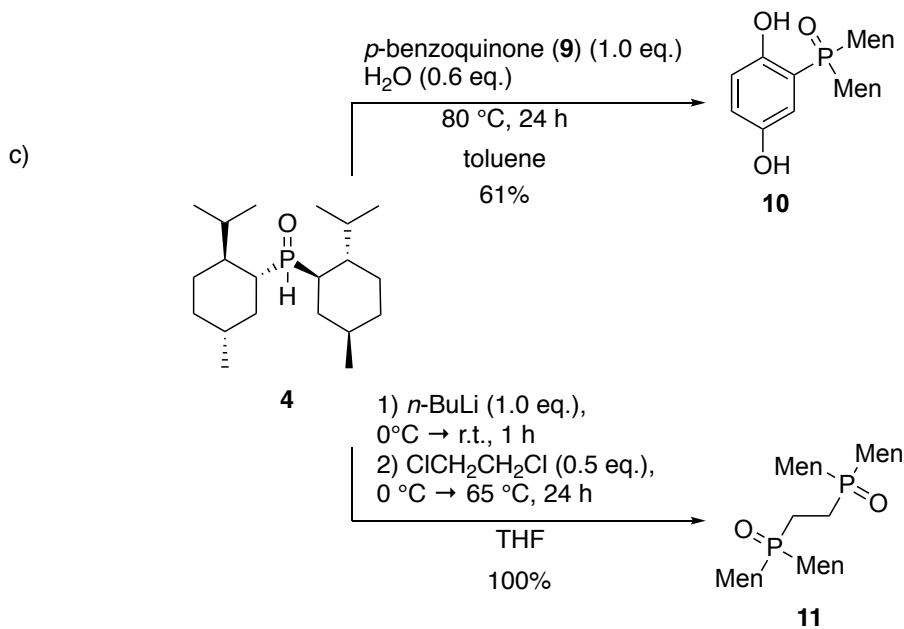
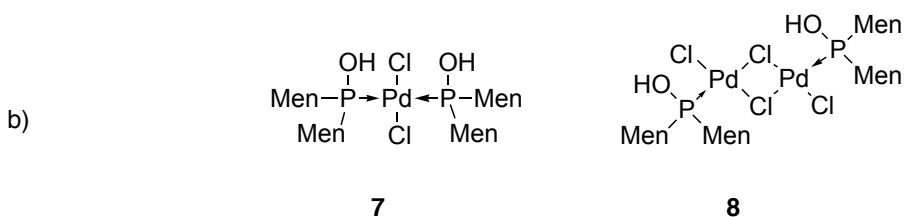
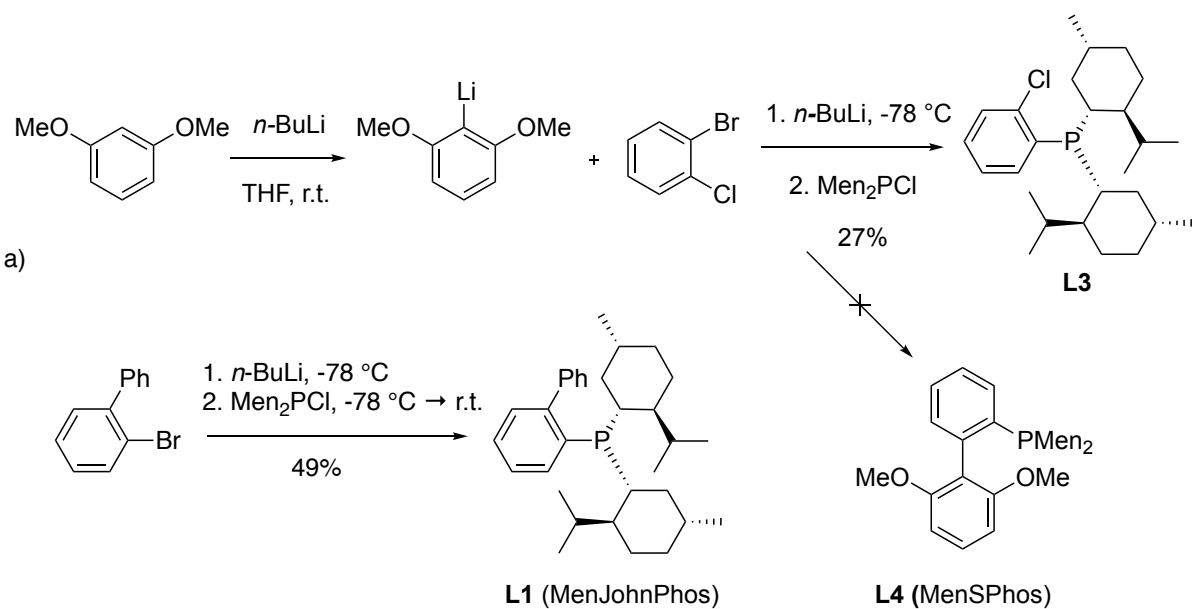
According to earlier literature reports, the synthesis of dimethylchlorophosphine succeeded by direct isolation of the compound from the reaction mixture of menthyl magnesium chloride with  $\text{PCl}_3$ , however this route provides low yields and requires tedious purification procedures under air- and moisture exclusion.<sup>79,80</sup> Our new synthesis from dimethylphosphine oxide as air-stable platform chemical provided easy access to dimethylchlorophosphine **3** in excellent yields.<sup>78</sup>

The aim was now to incorporate the bulky and chiral dimethylphosphino donor motif into ligands suitable for catalysis. To do so, different strategies were attempted in preliminary works by Corvin Lossin during earlier works in our group: Firstly, starting from dimethylchlorophosphine **3**, the synthesis of a *Buchwald* type dimethylbiaryl phosphine ligand **L1** (MenJohnPhos) was achieved (scheme 19a). Efforts to obtain **L4** afforded (2-chlorophenyl)dimethylphosphine **L3** instead.<sup>77</sup>

A second strategy for the incorporation of the dimethylphosphino donor motif into ligand structures is the direct use of  $\text{Men}_2\text{P}(\text{O})\text{H}$  **4** as secondary phosphine oxide in catalysis. As such, the synthesis of complexes **7** and **8**, which are menthyl analogs of Li's POPd and POPd2, respectively, was achieved in our laboratory (scheme 19b).

The third strategy for the incorporation of the dimethylphosphino structural motif into ligand structures is the direct transformation of air-stable  $\text{Men}_2\text{P}(\text{O})\text{H}$  by alkylation or arylation with an envisioned deoxygenation step as a final step. As such, a first proof of principle was shown by Corvin Lossin in the water-promoted phospho-*Michael*-addition to *p*-benzoquinone, providing 2,5-dihydroxyphenyl-1-dimethylphosphine oxide **10** (scheme 19c). An alkylation was demonstrated by reacting lithiated **4** with 1,2-dichloroethane, affording ethane-1,2-diylbis(dimethylphosphineoxide) **11**.

First catalytic test reactions in Suzuki-Miyaura and Buchwald-Hartwig couplings suggested applicability of the synthesized phosphine ligands **L1** and **L3**, as well as (pre-)ligand dimethylphosphine oxide **4** in catalysis.<sup>77</sup>

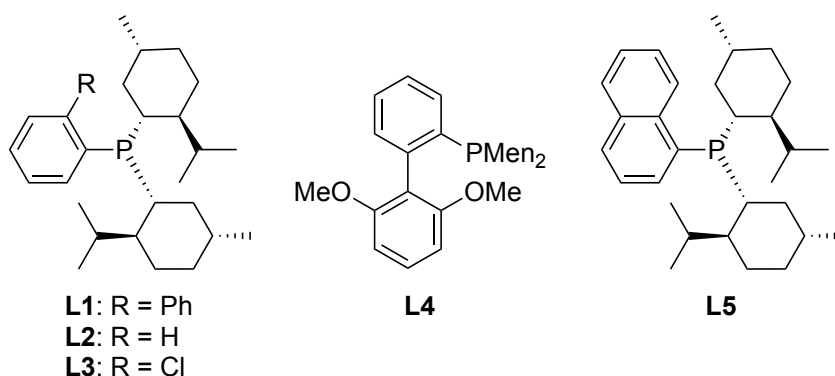


**Scheme 19.** Previously synthesized ligands and Pd(II) complexes exhibiting the  $\text{Men}_2\text{P}$  structural motif.



## 2.2 Aim of this Work

One aim of this work was to further demonstrate the potential of dimethylphosphine oxide as an air-stable platform chemical for the synthesis of PMen<sub>2</sub>-containing ligand motifs. As such, the previously established scope of transformations of Men<sub>2</sub>P(O)H by alkylations and arylations should be improved and expanded. In the quest for accessing new chiral ligand structures, improvement and scale-up of the already existing syntheses of (aryl)dimethylphosphine ligands **L1** and **L3** was mapped out, as well as syntheses of further dimethylphosphine ligands. In particular, the synthesis of a menthyl analogue of *Buchwald* ligand SPhos, which had failed before, was envisaged (scheme 20).



*Scheme 20.* (Aryl)dimethylphosphine ligands studied in this work.

**L3** had shown promising results in first tests in catalytic transformations,<sup>77</sup> and the (2-chlorophenyl)phosphine structural motif has proven applicability in *Suzuki-Miyaura* couplings in the literature.<sup>81</sup> Thus, further studies of **L3** in catalytic transformations were envisaged in this work. As a comparison, its dehalogenated variant **L2** (Men<sub>2</sub>PPh) should be synthesized as well. The general (aryl)dimethylphosphine ligand motif offers great potential for structural diversification of the aryl moiety, which could lead to interesting new activities in catalysis. As such, the synthesis of **L5** (NapPMen<sub>2</sub>) was envisaged. This ligand exhibits a benzoannulation in *ortho*-position to phosphorus, a structural motif that has so far not been extensively studied in catalysis,<sup>82</sup> but could lead to interesting activities due to its bigger sterical bulk compared to dimethyl(phenyl)phosphine.

With ligands **L1** – **L5** and dimethylphosphine oxide **4** at hand, their examination in a variety of transition-metal catalyzed cross-coupling reactions was envisaged. In this manner, the influence of menthyl as bulky, electron-donating alkyl group in phosphine ligands on catalytic transformations should be examined, as well as its potential to induce asymmetric transformations.

## 2.3 Direct Functionalization of Dimethylphosphine *P*-Oxide Towards Novel Ligand Structures

### 2.3.1 *1,4-Addition of Men<sub>2</sub>P(O)H to *p*-Quinones*

#### 1,4-Addition of Men<sub>2</sub>P(O)H to *p*-Benzoquinone

The water-promoted 1,4-addition of dimethylphosphine *P*-oxide to *p*-benzoquinone had previously been conducted in our group<sup>77</sup> following a modified protocol by Li-Bao and co-workers<sup>83</sup> in moderate yield. However, as the isolated compound still contained some impurities of *p*-benzoquinone after a rather tedious purification protocol, further attempts to optimize the synthesis were undertaken. As such, the previously employed conditions were first varied with respect to reaction time, concentration, solvent and stoichiometry, and the crude mixtures analyzed by <sup>31</sup>P-NMR spectroscopy after work-up. Figure 4 shows an exemplary <sup>31</sup>P-NMR spectrum of entry 1 (table 1).

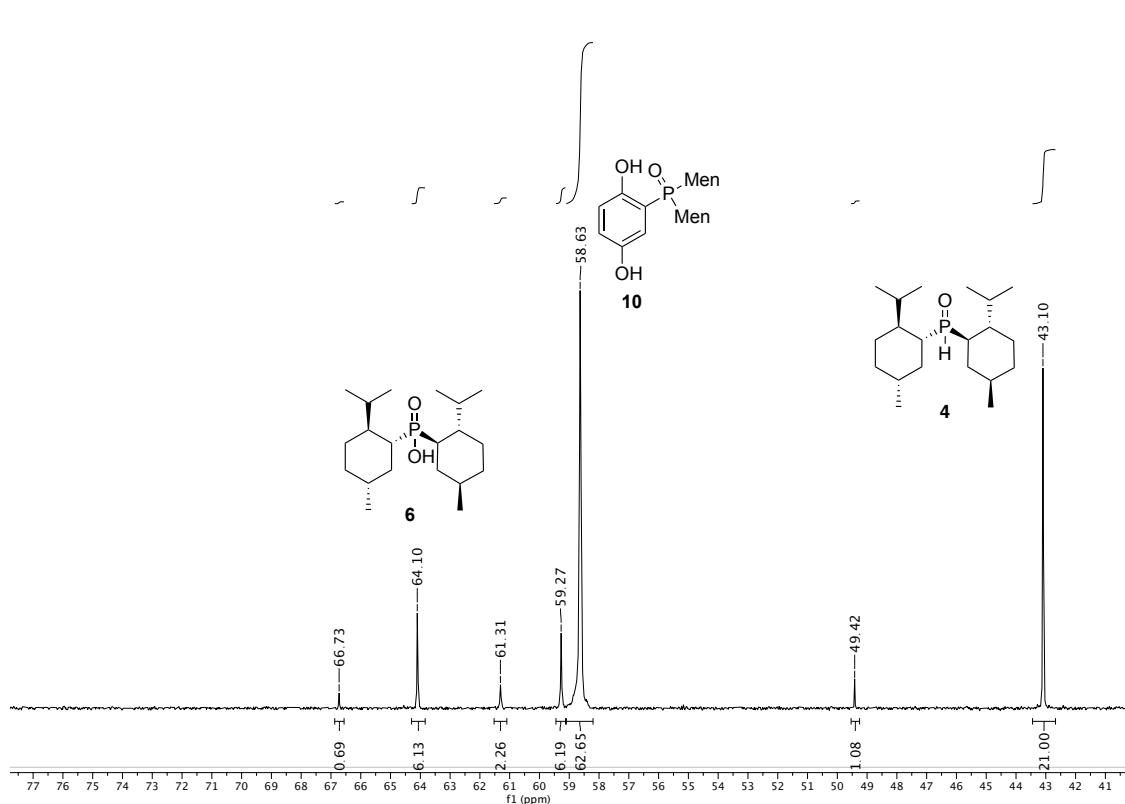
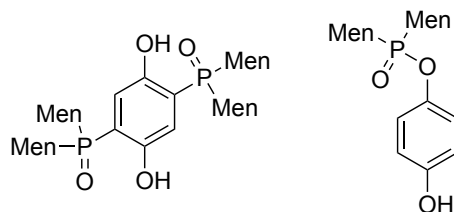


**Figure 4.** Excerpt of an exemplary <sup>31</sup>P-NMR spectrum of entry 1 (table 1) for the optimization of the 1,4-addition of Men<sub>2</sub>POH to *p*-benzoquinone.

Besides the signals stemming from target material **10** ( $\delta_P$  58.63) and starting material **4** ( $\delta_P$  43.10), the spectrum shows signals of several side products. Presumably, the signal arising at  $\delta_P$  64.10 stems from dimethylphosphinic acid **6** (Men<sub>2</sub>POOH, ref.:  $\delta_P$  63.6<sup>76</sup>), which could

have been formed by 1,6-addition of Men<sub>2</sub>POH to *p*-benzoquinone, followed by hydrolysis of the resulting 4-hydroxyphenyl dimethylphosphinate. Besides the aforementioned 1,6-addition product, a twofold 1,4-addition could also be responsible for one of the emerging side products, as was previously discussed by Li-Bao and co-workers (scheme 21). A definite identification of the by-products was, however, not carried out.



**Scheme 21.** Other possible by-products and their postulated mechanistic generation.<sup>83</sup>

The optimization for the water-promoted 1,4-addition of Men<sub>2</sub>POH to *p*-benzoquinone is shown in table 1. An analysis by <sup>1</sup>H-qNMR was considered, but rejected due to the lack of a proton signal which would be suitable for an accurate analysis. <sup>31</sup>P-qNMR analysis was attempted, but gave inaccurate results (see section 3.2 of this work). Therefore, an analysis of relative <sup>31</sup>P-NMR integrals was envisioned for comparing the results.

**Table 1.** Variation of reaction conditions for the water-promoted 1,4-addition of Men<sub>2</sub>POH to *p*-benzoquinone.

entry	solvent	12 /x eq.	time /h	conc. [4] /M	NMR yield <sup>a</sup> /mol-%	conversion <sup>a</sup> /mol-%
1	toluene	1.0	22	0.5	62	79
2	toluene	1.5	15	0.5	66	94
3	toluene	1.0	48	0.5	60	88
4	toluene	1.0	22	1	66	89
5	1,4-dioxane	1.0	24	0.5	48	85

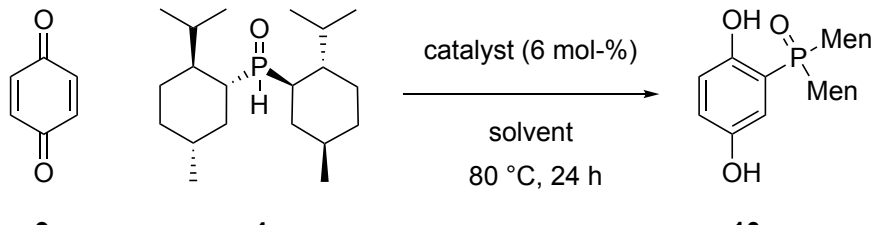
a) Analytical yields and conversions (mol-%) based on <sup>31</sup>P-NMR area integration.

The formerly established conditions (entry 1) provide a moderate yield and incomplete conversion. Raising the equivalents of *p*-benzoquinone gave a comparable yield (entry 2), but

a higher conversion, which indicates lower selectivity of the reaction. The same applies to doubling the reaction time or increasing the nominal concentration of the reactants (entries 3 and 4). Changing the solvent to 1,4-dioxane led to a considerable decrease in yield and selectivity (entry 5).

Another procedure to perform 1,4-additions of secondary phosphine oxides to *p*-benzoquinone involves the use of Bi(OTf)<sub>3</sub> as Lewis acid catalyst.<sup>33,35</sup> The results of this approach as applied to the target reaction are summarized in table 2. In addition, the use of *p*TsOH·H<sub>2</sub>O as Brønsted acid catalyst was explored.

**Table 2.** Variation of reaction conditions for the Lewis- or Brønsted acid catalyzed 1,4-addition of Men<sub>2</sub>POH to *p*-benzoquinone. Isolated yields in brackets.



entry	solvent	catalyst	NMR yield <sup>a</sup> /mol-%	conversion <sup>a</sup> /mol-%
1	toluene	Bi(OTf) <sub>3</sub>	73	82
2	toluene	<i>p</i> TsOH·H <sub>2</sub> O	85	92
3	toluene	/	68	85
4	DMF	Bi(OTf) <sub>3</sub>	81	96
5	DMF	<i>p</i> TsOH·H <sub>2</sub> O	87 (62) <sup>b</sup>	100
6	DMF	/	41	85

a) Analytical yields and conversions (mol-%) based on <sup>31</sup>P-NMR area integration.

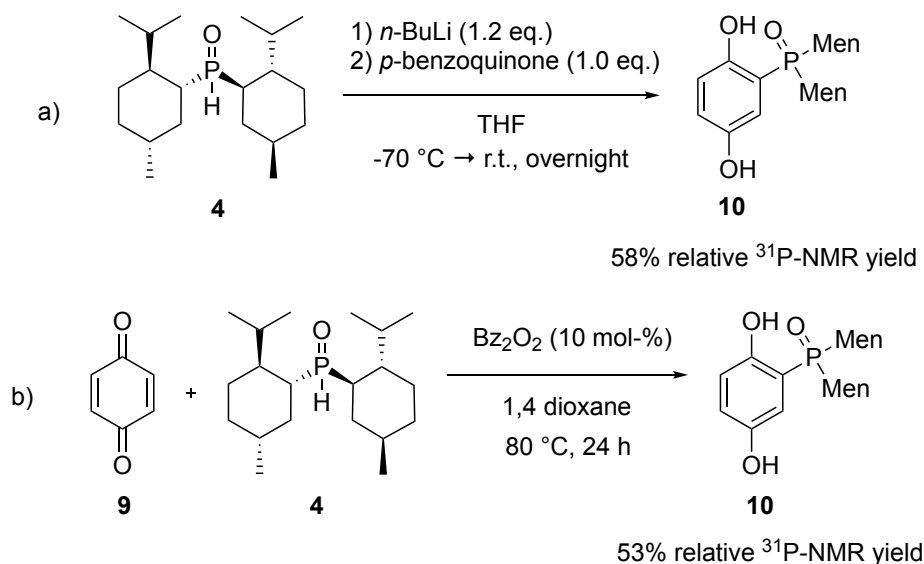
b) Isolated yield in brackets.

It appears that the relative <sup>31</sup>P-NMR yield is generally higher when *p*TsOH·H<sub>2</sub>O is used (entries 2 and 5), followed by Bi(OTf)<sub>3</sub> (entries 1 and 4). In the case of toluene as a solvent, when no additive is used (entry 3), the yield is slightly lower than for Bi(OTf)<sub>3</sub> (entry 1), but interestingly comparable to the yield achieved by water promotion (compare table 1 entry 1). This result debates the assumption that the reaction is, in fact, promoted by water, or that an additional amount of water is necessary to promote the reaction. It is possible that residual amounts of water in the solvent or reagents are already sufficient for promoting the reaction, and that adding more water does not further contribute to improving the yield. When using DMF as a solvent,

Bi(OTf)<sub>3</sub> as catalyst showed slightly better results (entry 4), however not as good as *p*TsOH·H<sub>2</sub>O (entry 5) in the same solvent. When no additive was used, the yield of **10** was considerably lower (entry 6). This is attributed to the generation of more side products and thus to a lower selectivity rather than a lower conversion. Although toluene and DMF show comparable yields when working with a catalytic amount of *p*TsOH·H<sub>2</sub>O, the conditions of entry 5 showed a more narrow product distribution, which implied that purification would be easier. Thus, the conditions of this entry was chosen for conducting the reaction on a preparative scale, affording 62% of pure compound **10** on the 2.5 mmol scale (entry 5). Compared to the formerly applied reaction conditions, this is not a substantial improvement in yield, but the procedure was simple and purification by recrystallization very effective.

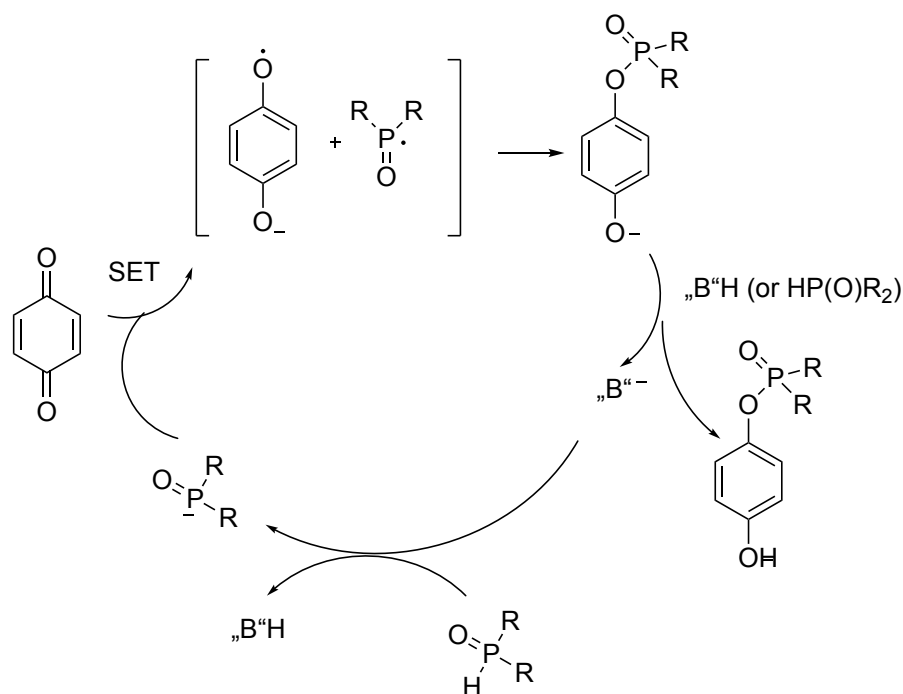
### Alternative Reaction Modes

As an alternative access to **10**, *n*-butyl lithium was used for deprotonation of Men<sub>2</sub>P(O)H to mediate 1,4-addition to *p*-benzoquinone (scheme 22a). Analysis of the crude product showed a slightly lower <sup>31</sup>P NMR yield compared to the former reaction modes.



**Scheme 22.** Alternative reaction modes for the addition of Men<sub>2</sub>POH to *p*-benzoquinone.

The relative integrals of the signals at  $\delta_P$  64.1 and  $\delta_P$  61.3 were much higher, implying that the 1,6-addition pathway is more prevalent for this reaction mode. Li-Bao and co-workers postulated that the 1,6-adduct is generated by deprotonation of the P(O)-H compound followed by SET to the *p*-quinone and radical recombination with C-O bond formation (see scheme 23).



**Scheme 23.** Mechanism for the base-promoted formation of 1,6 adduct as proposed by Li-Bao and co-workers. (“B” = base)<sup>83</sup>

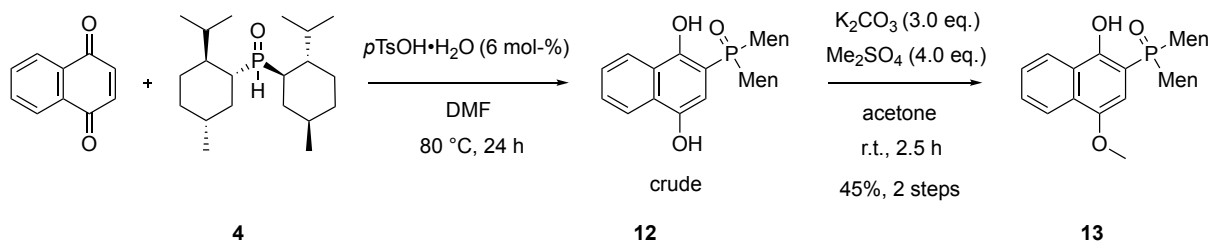
This postulate correlates well with these findings, presuming that the signals at  $\delta_P$  64.1 and  $\delta_P$  61.3 can be assigned to  $\text{Men}_2\text{P}(\text{O})\text{OH}$  and the 1,6 addition product, respectively. For a definite assignment, an isolation and characterization of the by-products have to be carried out. This, however, would not have contributed to solve the synthetic problem at hand.

As an alternative reaction mode, a radical addition of dimethylphosphine oxide to *p*-benzoquinone was also attempted, using dibenzoyl peroxide as radical starter (scheme 22b). A similar reaction mode has been reported by Wang *et al.* in 2016 in the addition of *P*-stereogenic secondary phosphine oxide to activated alkenes (however using AIBN as radical starter).<sup>84</sup> This method, with a <sup>31</sup>P-NMR yield of 53%, did not show significant advantages compared to the former experiments.

### 1,4-Addition of $\text{Men}_2\text{P}(\text{O})\text{H}$ to Naphthoquinone

The same conditions established for the 1,4-benzoquinone adduct were applied to the 1,4-addition of **4** to 1,4-naphthoquinone. After work-up, the crude material turned out to be a sticky, poorly soluble solid. Recrystallization from hot ethyl acetate/hexanes required a large amount of solvent and furnished a slushy-like, voluminous mass which underwent considerable shrinkage after removing the residual solvent *in vacuo*, affording 33% of **12**. As this yield is rather low and other ways of isolating the target material were deemed difficult due to its low solubility, an *in situ* methylation of both OH groups was envisioned. In a first attempt, when

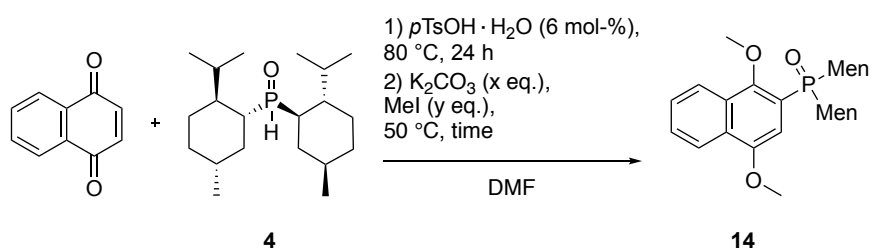
using an excess of base and  $\text{Me}_2\text{SO}_4$  as methylating reagent, only the monomethylated species **13** was obtained in 45% yield (scheme 24).



**Scheme 24.** 1,4-Addition of naphthoquinone and  $\text{Men}_2\text{POH}$  and subsequent monomethylation.

Another approach envisaged a one-pot 1,4-addition and subsequent two-fold methylation in DMF. As  $\text{Me}_2\text{SO}_4$  typically reacts with this solvent,<sup>85</sup> MeI was instead used as methylation reagent, which is also advantageous because of its lower toxicity.<sup>86,87</sup> While monitoring the reaction by TLC, more  $\text{K}_2\text{CO}_3$  and MeI were added during the course of the reaction (table 3 entry 1). It became evident that the limiting factor for complete methylation was the amount of base added. A substantial excess of base is needed to deprotonate the second OH-group, supposedly because its proton engages in hydrogen bonding to the neighbouring  $\text{P}(\text{O})\text{Men}_2$  oxygen. With these findings at hand, the one-pot 1,4-addition and methylation sequence was repeated using a larger excess of base (entry 2). These conditions produced compound **14** in 79% yield, however still containing about 1 mol-% of  $\text{Men}_2\text{P}(\text{O})\text{H}$  and some other unidentified impurities. Washing with cold methanol afforded 67% of pure compound **14**.

**Table 3.** One-pot 1,4-addition of  $\text{Men}_2\text{POH}$  to naphthoquinone and subsequent methylation.



entry	x	y	time	yield /%
1 <sup>a,b</sup>	3.0	4.0	>2 d	81
2	8.8	5.0	17 h	79 <sup>c</sup> (67) <sup>d</sup>

a) Second addition of 1.0 eq. of  $\text{K}_2\text{CO}_3$  and 2.0 eq. of MeI after 20h.

b) Crude material subjected to further methylation (4.0 eq. of  $\text{K}_2\text{CO}_3$  and 2.0 eq. of MeI, 24 h).

c) Containing around 1 mol-%  $\text{Men}_2\text{POOH}$  and other unidentified impurities.

d) Yield in brackets after wash with cold MeOH.

$^1\text{H-NMR}$  analysis of **13** shows a considerable down-field shift of the hydroxy group ( $\delta_H$  12.31), indicating  $\text{Men}_2\text{PO}\cdots\text{HO}$  hydrogen bonding. This is also confirmed by the  $^{31}\text{P-NMR}$  shifts of the unmethylated, mono- and dimethylated species: While the chemical shifts of **12** and **13** are comparable ( $\delta_P$  57.5 and 59.5, respectively), the signal for **14** is considerably shifted towards a higher frequency ( $\delta_P$  46.6).

### 2.3.2 *Direct Arylation and Alkylation of $\text{Men}_2\text{P(O)H}$*

#### Attempted Copper-Catalyzed Arylation of $\text{Men}_2\text{P(O)H}$

Following a literature procedure for the copper(I)-catalyzed arylation of dicyclohexylphosphine oxide with aryl iodide<sup>88</sup>, an arylation of dimethylphosphine oxide was attempted accordingly. This coupling had already been attempted in previous works with triphenyl phosphine or (*S*)-1-phenylethylamine as ligand.<sup>77</sup> In the following approaches, the reaction conditions were further varied with respect to base, solvent and ligand and compared with the previous results, as shown in table 4, and the crude mixtures analyzed by  $^1\text{H-}$  and  $^{31}\text{P-NMR}$  spectroscopy.

**Table 4.** Attempted arylation of dimethyl phosphine oxide.

entry	base	ligand	solvent	ratio 15/4/6 <sup>b</sup>
1	$\text{K}_2\text{CO}_3$	$\text{PPh}_3$	DMF	6/77/17
2	$\text{K}_3\text{PO}_4$	$\text{PPh}_3$	toluene	6/93/1
3	$\text{K}_2\text{CO}_3$	$\text{Me}_2\text{DACH}$	toluene	0/4/96
4 <sup>a</sup>	$\text{K}_2\text{CO}_3$	1-phenethylamine	toluene	9/88/3
5 <sup>a</sup>	$\text{K}_2\text{CO}_3$	$\text{PPh}_3$	toluene	1/99/0

a) These experiments were part of a previous work in this group, but are presented here for a full overview.<sup>77</sup>

b) as estimated by  $^{31}\text{P-NMR}$  area integration

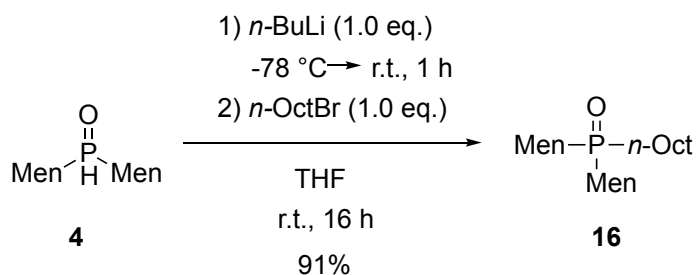
Besides the signal of the starting material, almost all mixtures show a new signal with a down-field shift of  $\sim 1$  ppm compared to the  $\text{Men}_2\text{POH}$  signal. Previously, this signal ( $\sim \delta_P$  42) had been dismissed as unidentified by-product, but more recent experiments with phosphine ligand



Men<sub>2</sub>PPh (see section 2.8) helped with assigning this signal to phosphine oxide **15**. Compared to a previous experiment with PPh<sub>3</sub> as a ligand (entry 5), changing the solvent to DMF (entry 1) or using K<sub>3</sub>PO<sub>4</sub> as a base (entry 2) slightly increased the generation of target material, but still its amount remained unsatisfyingly low. Interestingly, the <sup>31</sup>P-NMR spectra show another signal near δ<sub>P</sub> 60, which can be assigned to dimethylphosphinic acid **6** (ref: δ<sub>P</sub> 63.6<sup>76</sup>). The amount of **6** increases with DMF as solvent, and it is generated almost exclusively when using Me<sub>2</sub>DACH as ligand (entry 3). The conversion of Men<sub>2</sub>P(O)H to Men<sub>2</sub>P(O)OH represents a formal oxidation. Copper-mediated oxidations and oxidative P-O couplings of P(O)-H compounds in alkaline media are described in the literature,<sup>89</sup> however, they require the presence of an oxidant. Since all reactions were conducted under the exclusion of air, a pathway *via* oxidative coupling seems unlikely. An example for an oxidant-free, dehydrogenative copper-catalyzed P-C bond formation was reported involving a copper-hydride species under evolution of hydrogen.<sup>90</sup> A similar mechanism might have taken place here forming a P-O bond, although such a mechanism has only been reported using an iron catalyst in the literature.<sup>91</sup>

### **P-Alkylation of Men<sub>2</sub>P(O)H**

As a further transformation of dimethylphosphine oxide, *P*-alkylation with haloalkanes and base was studied. As such, the deprotonation of dimethylphosphine oxide by *n*-butyl lithium and subsequent alkylation by *n*-octyl bromide was first studied (scheme 25). An excess of 2.0 equivalents of *n*-octyl bromide was first used. The reaction was quenched with D<sub>2</sub>O prior to work-up, and the crude mixture analyzed by <sup>31</sup>P-NMR. <sup>31</sup>P-NMR analysis showed full conversion of Men<sub>2</sub>P(O)H. However, besides the signal of the desired product, further signals of unidentified by-products are visible. In an attempt to avoid the formation of by-products, the quantity of *n*-octyl bromide was reduced to an equimolar amount. <sup>31</sup>P-NMR analysis of the crude material showed, apart from a few negligible impurities, almost complete transformation to the alkylated target material, and a filtration over a short column afforded **16** in 91% yield (scheme 25).

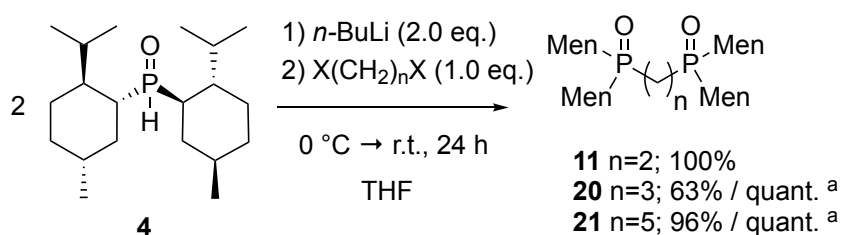


**Scheme 25.** Alkylation of dimethyl phosphine oxide using *n*-octyl bromide.

These conditions also proved advantageous with respect to purification, as it leaves no excess (halo)alkane as by-product.

### Reaction of 1,*n*-Dihaloalkanes with Dimethylphosphine *P*-Oxide

After previous work had successfully accomplished the alkylation reaction of lithiated dimethylphosphine oxide with 1,2-dichloroethane **17** to yield **11**,<sup>77</sup> the conditions were applied to other 1,*n*-dihaloalkanes in this work (scheme 26). Using 1,3-dichloropropane **18** and 1,5-dibromopentane **19**, respectively, compounds **20** and **21** were synthesized in moderate to high yields. As for **20**, Men<sub>2</sub>P(O)OH was isolated as by-product, but on a larger scale, the alkylation was achieved in quantitative yield.



**Scheme 26.** Alkylation of **4** with 1,*n*-dihaloalkanes (scale: 0.5 mmol).  $X = \text{Cl}$  for **11**, **20**,  $\text{Br}$  for **21**. The synthesis of **11** was established in previous works. <sup>a</sup>) Scale: 2.0 mmol.

Generally, the crude materials were considered pure enough to be used in follow-up reactions. Purification efforts only succeeded by crystallization in the case of **11** at  $-20^\circ\text{C}$ . Compounds **20** and **21** were soluble in all solvents tested (hexane, Et<sub>2</sub>O, methanol, acetone) even at low temperature, which is why crystallization was not feasible. In these cases, purification was achieved by a short filtration over silica.

### Deoxygenation of Alkane-1,*n*-diyl-bis(dimethylphosphine)oxides

As a route to alkane-1,*n*-diyl-bis(dimethylphosphine)oxides, the deoxygenation of **11** and **20** was envisioned. Following a modified procedure by Baldwin and co-workers<sup>92</sup> for the deoxygenation of ethane-1,2-diyl-bis(dialkylphosphine)oxides R<sub>2</sub>P(O)CH<sub>2</sub>CH<sub>2</sub>(O)PR<sub>2</sub> (where R = Ph, Cy, <sup>i</sup>Pr), deoxygenation using an excess of HSiCl<sub>3</sub> (10 equivalents) at elevated temperature was envisioned. Fritzsche *et al.*<sup>93</sup> have elaborated that an excess of at least 2 equivalents of trichlorosilane is required for this reaction, because HCl is generated from the reduction of the phosphine oxide, which then reacts with a further equivalent of HSiCl<sub>3</sub> to generate H<sub>2</sub>. As table 5 shows, using ethane-1,2-diyl-bis(dimethylphosphine)oxide **11** as substrate gave no reaction (entry 1). Supposedly, the four menthyl groups constitute too much sterical hindrance, and the ethylene bridge is too short to keep the hindered dimethylphosphino

moieties in sufficient distance from each other. The propane derivative **20** showed a better result, with an approximately 1:1 molar ratio of starting material and desoxygenated material (entry 2). This material was subjected to another deoxygenation reaction. This time, to avoid emerging H<sub>2</sub> and reduce the amount of HSiCl<sub>3</sub>, triethylamine was added to trap HCl formed during the reaction.<sup>93</sup> <sup>1</sup>H-NMR analysis of the crude material showed almost full reduction to bisphosphine (entry 3). In entry 5, the conditions were applied to crude compound **20**. After stirring for 13 hours at 60°C, <sup>31</sup>P-NMR analysis of the reaction mixture showed almost complete conversion to the bisphosphine **23**. The target material was isolated in 26% yield. Problematic work-up due to the sluggish nature of the formed siloxanes, which hampered phase separation, may have contributed to the substantial loss of yield. Under the same conditions, the deoxygenation of ethane-1,2-diyl-bis(dimethylphosphine)oxide as substrate was attempted once more, but showed no conversion (entry 4).

**Table 5.** Attempted desoxygenation of bis(dimethylphosphineoxide)alkanes

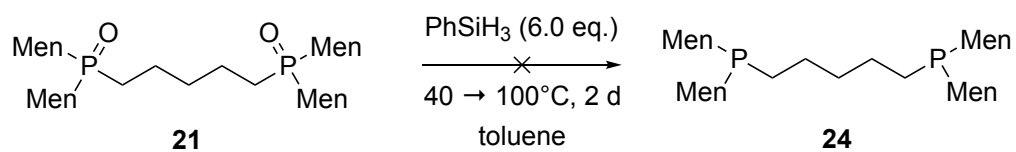
entry	substrate (n = x)	conditions	result
1	n = 2	HSiCl <sub>3</sub> (10.0 eq.), toluene, 110 °C, 4 h	no conversion
2	n = 3	HSiCl <sub>3</sub> (10.0 eq.), toluene, 110 °C, 4 h	50 mol-% <b>20</b> , 50 mol-% <b>23</b> <sup>a</sup>
3	n = 3 <sup>b)</sup>	HSiCl <sub>3</sub> (5.00 eq.), NEt <sub>3</sub> (5.00 eq.), toluene, 50 °C, 9 h	nearly complete conversion to the phosphine
4	n = 2	HSiCl <sub>3</sub> (5.00 eq.), NEt <sub>3</sub> (5.00 eq.), toluene, 50 °C, 9 h	no conversion
5	n = 3	HSiCl <sub>3</sub> (6.00 eq.), Net <sub>3</sub> (6.00 eq.), 60 °C, 12 h	26% isolated yield

a) as estimated by <sup>31</sup>P-NMR integrals

b) crude mixture of entry 2

As another reagent for deoxygenation, phenyl silane was tested (scheme 27) with pentane-1,5-diyl-bis(dimethylphosphine)oxide as a substrate. As opposed to trichlorosilane, phenyl silane has a high boiling point, which enables heating the reaction to a higher temperature, and it was assumed that this might be beneficial for this reaction. The reaction was monitored by <sup>31</sup>P-NMR

spectroscopy. However, after 19 hours, no reaction was observed. Adding  $\text{CF}_3\text{SO}_3\text{H}$  as catalyst, as described in the literature,<sup>94</sup> did not have any effect.



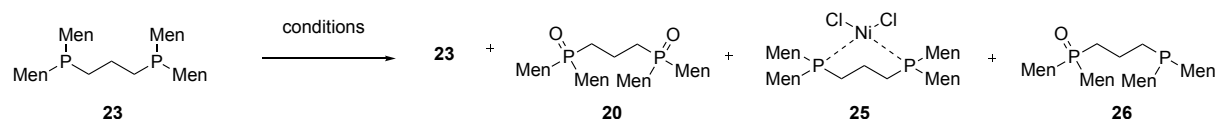
**Scheme 27.** Attempted deoxygenation of **21**. The reaction was monitored by  $^{31}\text{P}$ -NMR sampling. After 22 hours,  $\text{CF}_3\text{SO}_3\text{H}$  (10 mol-%) was added to the reaction mixture.

## 2.4 Synthesis of Transition-Metal Complexes Incorporating the Dimethylphosphino Structural Motif

### 2.4.1 Synthesis of Transition-Metal Complexes Starting from Bis(dimethylphosphino)propane

Section 2.3.2 of this work deals with the synthesis of bis(dimethylphosphino)alkanes. In order to avoid handling the phosphines under air-exclusion, one objective was to convert them to their corresponding transition metal complexes without prior isolation. The synthesis of nickel complex **25** was first envisioned starting from bisphosphine **23**. Table 6 shows the conditions applied in this synthesis. The conditions from entries 1 and 2 were both adapted from a known literature procedure with dppe, dcpe or dcpp as substrates.<sup>95,96,97</sup>

**Table 6.** Conditions for the attempted synthesis of **25**.



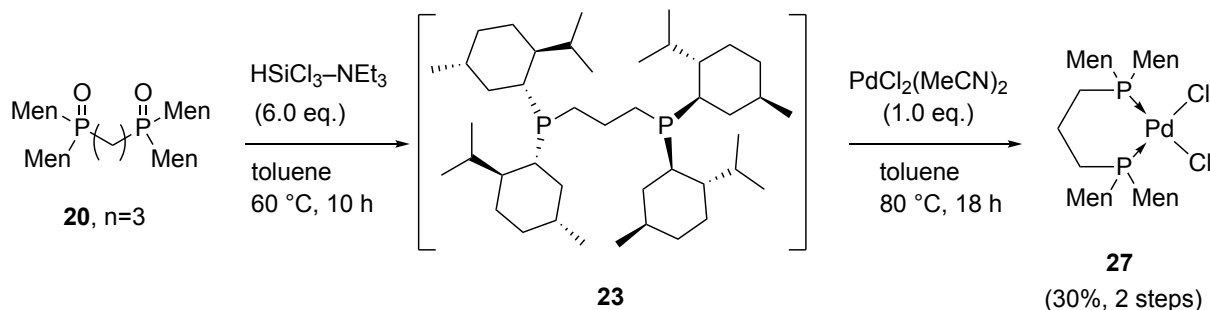
entry	conditions	starting material	products
1	(dme)NiCl <sub>2</sub> (1.00 eq.), THF, r.t. overnight	crude	(dme)NiCl <sub>2</sub> recovered
2	NiCl <sub>2</sub> ·6H <sub>2</sub> O (1.00 eq.), EtOH, 80 °C, overnight	crude	18% of <b>23</b> re-isolated
3	(dme)NiCl <sub>2</sub> (1.00 eq.), CH <sub>2</sub> Cl <sub>2</sub> , r.t.	purified <sup>b</sup>	<b>20</b> (12 mol-%), <b>25</b> (12 mol-%), <b>26</b> (23 mol-%), <b>23</b> (50 mol-%) <sup>a</sup>
4	(dme)NiCl <sub>2</sub> (1.00 eq.), toluene, 80 °C	purified <sup>b</sup>	<b>20</b> (7 mol-%), <b>25</b> (9 mol-%), <b>26</b> (25 mol-%), <b>23</b> (57 mol-%) <sup>a</sup>

a) Molar ratios estimated by <sup>31</sup>P-NMR area integration. The structures of **25** and **26** were not confirmed.

b) The material was purified by Celite filtration and recrystallization.

While the conditions of entries 1 and 2 were not successful, entries 3 and 4 showed some formation of an unknown species, as judged by <sup>31</sup>P-NMR analysis. The signal appeared at  $\delta_P$  5.66, which indicates the formation of the desired compound **25** (compare the cyclohexyl derivative:  $\delta_P$  18.2<sup>95</sup>). It is to be noted that for entries 3 and 4, ligand **23**, purified by Celite filtration and recrystallization, was used. The crude material still contained siloxanes which are formed as by-product of the desoxygenation reaction, which could have hampered complex

formation in entries 1 and 2. However, since no selective reaction took place, the idea of isolating the phosphine as nickel complex was dismissed, and a further effort focused on the isolation as Pd species using  $\text{PdCl}_2(\text{MeCN})_2$  as a precursor. A small scale preliminary experiment showed complete conversion to complex **27**. Finally, the complex was directly isolated after reaction with crude phosphine in 30% isolated yield over 2 steps (scheme 28).



**Scheme 28.** Synthesis of bis(dimethylphosphine)propane palladium(II) dichloride.

Compound **27** was characterized by X-ray crystallography (figure 5).

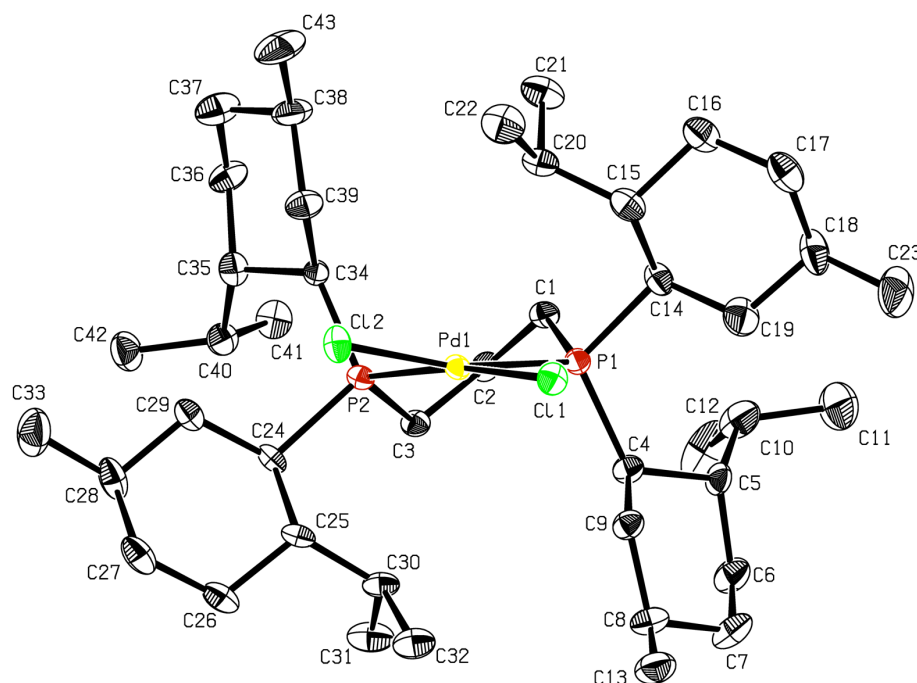


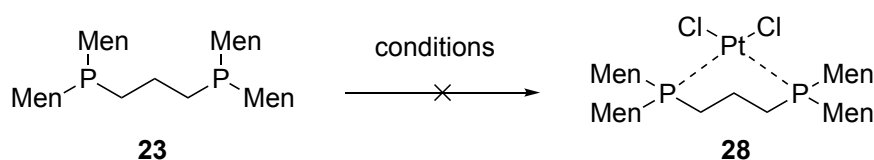
**Figure 5.** Solid-state molecular structure of **27**. Ellipsoids are shown at 50% probability. Hydrogens are omitted for clarity.

The bisphosphine chelate-complex **27** exhibits idealized square-planar geometry, although the  $\text{P1-Pd1-Cl2}$  and  $\text{P2-Pd1-Cl1}$  bond angles ( $168.99(6)^\circ$  and  $171.34(5)^\circ$ , respectively) show a slight abbreviation from the  $180^\circ$  expected for a perfectly square planar geometry. This slightly

distorted geometry might be a consequence of sterical crowding due to the bulky menthyl groups.

The synthesis of a corresponding platinum complex **28** was envisaged as well (table 7). For this purpose, small scale experiments were set up and monitored by  $^{31}\text{P}$ -NMR sampling of the reaction mixtures. The reaction in MeCN with  $\text{PtCl}_2$  as precursor gave a complex mixture (table 7, entry 1), with a multitude of unassignable signals in the range of  $\delta_P$  25 – 96 in the  $^{31}\text{P}$ -NMR spectrum. Assumedly, these signals are due to phosphine-bridged coordination polymers formed in the reaction. Another approach involved a room temperature reaction with acetone as solvent (entry 2), which gave rise to three major (broadened) signals between  $\delta_P$  50 – 52. This is in the range of oxidized starting material, but the broadened nature of the singlets rather supports the formation of a (partly oxidized) phosphine-bridged coordination polymer.

**Table 7.** Attempted synthesis of a platinum complex **28**.



entry <sup>a</sup>	conditions	results <sup>b</sup>
1	$\text{PtCl}_2$ (1.00 eq.), MeCN, 70 °C, 8 h	complex mixture
2	$\text{PtCl}_2$ (1.00 eq.), acetone, r.t. 22 h <sup>98</sup>	major (broadened) signals between $\delta_P \sim 50 - 52$
3	$\text{PtCl}_2(\text{MeCN})_2$ (1.00 eq.), toluene, 110 °C, 3 d	major (broadened) signal at $\delta_P$ 1.15

a) Scale: 33.3  $\mu\text{mol}$ .

b) As judged by  $^{31}\text{P}$ -NMR analysis of the reaction/crude mixture

As the synthesis of Pd complex **27** had worked out cleanly with  $\text{PdCl}_2(\text{MeCN})_2$  as palladium(II) precursor, the analogous platinum complex  $\text{PtCl}_2(\text{MeCN})_2$  **29** was synthesized according to a literature procedure (scheme 29).<sup>99</sup> Heating **29** and ligand **23** in toluene at higher temperature resulted in a cleaner reaction (entry 3), giving rise to a major broadened signal at  $\delta_P$  1.15. However, purification attempts (Celite filtration, crystallization by layering of THF with hexanes) failed, and further attempts to synthesize **28** were not undertaken.

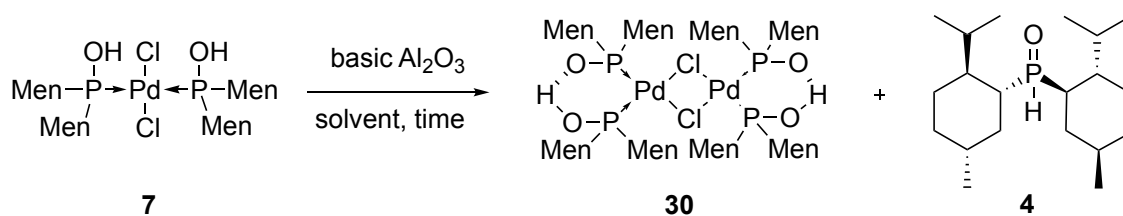


**Scheme 29.** Synthesis of  $\text{PtCl}_2(\text{MeCN})_2$ .

### 2.4.2 Synthesis of [ $\{(Men_2P-O-H-O-PMen_2-k_2P,P')Pd\}_2(m-Cl)_2$ ]

As part of studying the complexation chemistry of dimethylphosphine oxide, the synthesis of a pseudo-chelating dimeric dimethylphosphinito palladium complex **30** by base-promoted HCl abstraction of compound **7** had hitherto failed due to the presumed instability of the target material in a variety of media.<sup>76,77</sup> As an alternative reaction mode, a solid phase reaction with aluminum oxide as base was envisaged. This would ensure easy separation of the base·HCl adduct. To circumvent possible side reactions of the Pd-complexes with solvent during the reaction, chlorinated solvents were avoided. Elution of the reaction products from aluminum oxide was conducted by subsequent use of toluene and then Et<sub>2</sub>O as relatively inert solvents. Table 8 shows an overview of the preliminary optimization experiments in the quest to obtain compound **30**.

**Table 8.** Preliminary optimization experiments for the solid-phase synthesis of compound **30**.



entry	solvent <sup>a</sup>	time	column dimensions	result <sup>b</sup>	comment
1	Et <sub>2</sub> O	2 days	h = 5.5 cm, d = 3.5 cm	complex	
2	toluene	5 hours	h = 5.5 cm, d = 3.5 cm.	no material eluted	heatgun activation of Al <sub>2</sub> O <sub>3</sub>
3	Et <sub>2</sub> O	immediate elution	h = 0.5 cm, d = 0.6 cm.	<b>7</b> (57 mol-%), <b>30</b> (40 mol-%), <b>4</b> (2 mol-%)	
4	toluene	immediate elution	h = 0.5 cm, d = 0.6 cm.	<b>7</b> (8 mol-%), <b>30</b> (92 mol-%)	

a) Solvents used for the solution of **7** and for elution. For elution with toluene, a second fraction was gathered using Et<sub>2</sub>O as eluant.

b) Only the first (main) elution fractions were compared. Molar ratios are estimated by <sup>31</sup>P-NMR area integration.



A first test reaction involved loading a short, dry aluminum oxide column with a solution of starting material in the designated solvent and letting the column stand overnight before elution with Et<sub>2</sub>O (entry 1). The crude material was analyzed by <sup>31</sup>P-NMR spectroscopy, an exemplary spectrum of which is shown in figure 6.

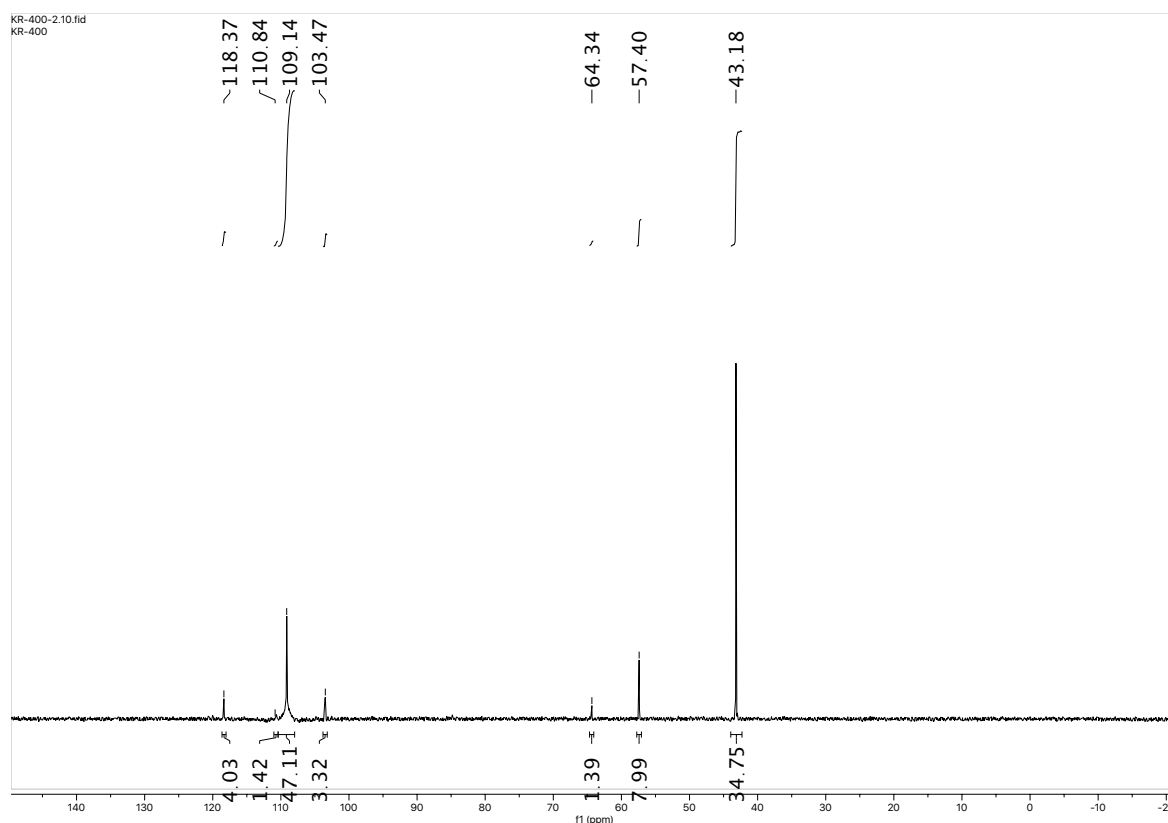


**Figure 6.** <sup>31</sup>P-NMR analysis of crude entry 1 (table 8)

It is evident that almost complete consumption of starting material (**7**;  $\delta_P$  118.37) took place. Besides the formation of a substantial amount of target material (**30**;  $\delta_P$  107.89), dimethylphosphine oxide (**4**;  $\delta_P$  44.25) was formed as the main by-product. This might be due to dissociation of the target complex as a consequence of its instability. An adverse factor to the stability of the target material might be the rather old batch of aluminum oxide used, which might have drawn moisture upon storage. This possibility was investigated by activating the aluminum oxide using a heat gun prior to the experiment (entry 2). However, with this set-up, surprisingly no material was eluted at all. This led to the conclusion that some residual moisture is needed for a successful reaction and elution of the complex. Moreover, it was assumed that the long retention time on the aluminum oxide column might be detrimental to the integrity of the target material. Therefore, in the next experiments (entries 3 and 4), a short pad (h = 0.5 cm) of aluminum oxide was used to ensure fast elution. The columns were then eluted with only Et<sub>2</sub>O (entry 3) or toluene followed by Et<sub>2</sub>O (entry 4) and the crude material was analyzed by

<sup>31</sup>P-NMR spectroscopy. Eluting directly with Et<sub>2</sub>O resulted in incomplete conversion and minor formation of Men<sub>2</sub>P(O)H as by-product. On the other hand, direct elution by toluene resulted in relatively pure target material with only little amount of starting material (around 8 mol-% as calculated by <sup>31</sup>P-NMR area integration). A second fraction, which was eluted by Et<sub>2</sub>O, showed full conversion of the starting material, however formation of Men<sub>2</sub>POH as by-product. These experiments lead to the conclusion that firstly, elution with toluene is more beneficial, as it leads to higher conversion of starting material and formation of less by-product. Using Et<sub>2</sub>O might either enhance degradation of the target material or elute Men<sub>2</sub>POH formed by side-reactions from the column. Secondly, extended contact times on the column should be avoided by immediate elution and use of a rather short column. As shown in entries 3 and 4, the reduction of column length is necessary due to the slow elution of the target material when using toluene as eluent, but is also necessary in order to prevent the degradation of target material.

**Table 9.** Scale-up of the optimized reaction conditions.

entry <sup>a</sup>	time <sup>b</sup>	column dimensions	yield <sup>c</sup>	purity <sup>c</sup>
1	immediate elution	h = 0.5 cm, d = 5 cm	55%	82 mol-%
2	5 min	h = 0.5 cm, d = 5 cm	52%	98 mol-%

a) scale: 120 μmol.

b) standing time on the column after loading with solution of **7**. c) as calculated by <sup>1</sup>H-NMR analysis.

c) Isolated yields.

For a scale-up of these preliminary experiments, a broader column diameter was chosen, but column length was kept the same. The first attempt at scaling up (table 9, entry 1) still resulted in incomplete conversion. The standing time of starting material and aluminum oxide was therefore prolonged by leaving the starting material on the column for 5 minutes before eluting with toluene (entry 2). These conditions were the most beneficial, affording **30** in 52% yield in 98 mol-% purity (as judged by <sup>1</sup>H-NMR analysis) without further purification. Crystallization attempts by CH<sub>2</sub>Cl<sub>2</sub>/hexanes diffusion experiments had failed earlier. As the formation of grey solids suggested instability of the compound in chlorinated solvents, NMR analysis was performed in benzene-*d*<sub>6</sub> as deuterated solvent, and crystals suitable for X-ray analysis were

obtained by evaporation from this solution. The structure obtained by X-ray crystallography is depicted in figure 7.

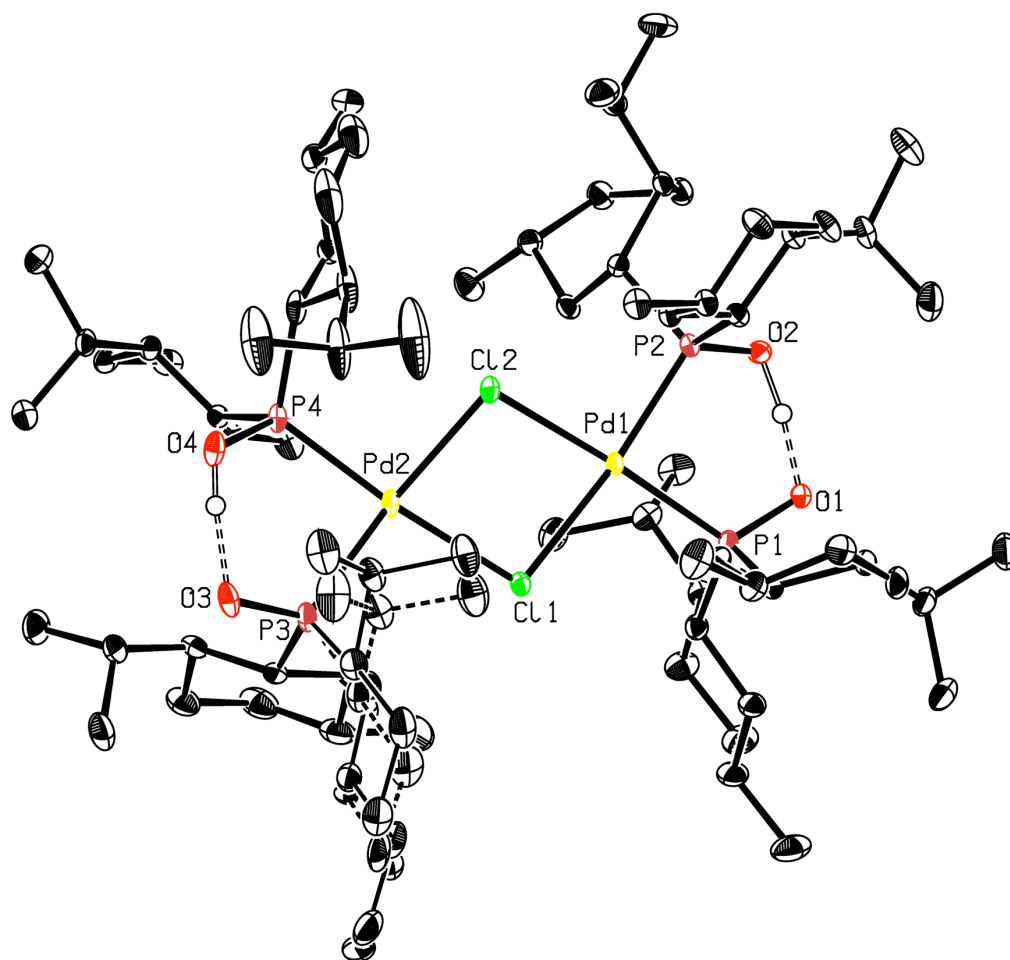


**Figure 7.** Solid-state molecular structure of **30**. Ellipsoids are shown at 50% probability. Hydrogens are omitted for clarity. The disorder of  $\text{Men}_2\text{POH}$  on the right is omitted for clarity.

As expected, the anionic character of the dimethyl phosphinito moieties is reflected by the P3-O3 (1.54 Å) and P1-O1 bond lengths (1.55 Å), respectively, which are in the range of a P-O single bond. OH $\cdots$ O hydrogen bonding is also confirmed. Strikingly, one of the P2-adjacent menthyl moieties has taken a disfavored boat conformation. Assumedly, the steric crowding of the compound forces the menthyl moiety into this usually unfavored conformation.<sup>100</sup> The aforementioned instability of the compound is also observed in the  $^1\text{H-NMR}$  spectrum. The OH $\cdots$ O proton signal gives rise to a singlet at  $\delta_{\text{H}}$  15.2, with a substantial downfield shift due to hydrogen bonding. However, integration of the aliphatic region results in values that are too high compared to the integral stemming from the two OH $\cdots$ O protons. Presumably, the *pseudo*-chelating complex is in equilibrium with other species with **30** existing as the major species in  $\text{C}_6\text{D}_6$  solution in about 80 mol-%, as judged by  $^1\text{H-NMR}$ . This assumption is further supported

by the rather broad  $^{31}\text{P}$ -NMR signal which **30** gives rise to, indicating a fluctuation of different species.

Comparing the spectra of eluted fractions of the different experiments, a singlet appearing at  $\delta_H$  4.3 stands out. This singlet only seems to appear in those fractions eluted with  $\text{Et}_2\text{O}$  and cannot be assigned to the starting material (in  $\text{C}_6\text{D}_6$ , the corresponding  $\text{POH}$  singlet appears at  $\delta_H$  5.96) or  $\text{Men}_2\text{POH}$ . Assumedly, it stems from a partial dissociation of the dimethyl phosphinite and the dimethyl phosphinous acid moiety, leaving a free OH group, which could give rise to said singlet. Figure 8 shows the  $^1\text{H}$ -NMR spectrum of the  $\text{Et}_2\text{O}$ -eluted fraction of entry 2, table 9. Comparing the  $\text{OH}\cdots\text{O}$  ( $\delta_H$  15.2) integral to the aliphatic region this time indicates an abundance of **30** of ~60 mol-%.

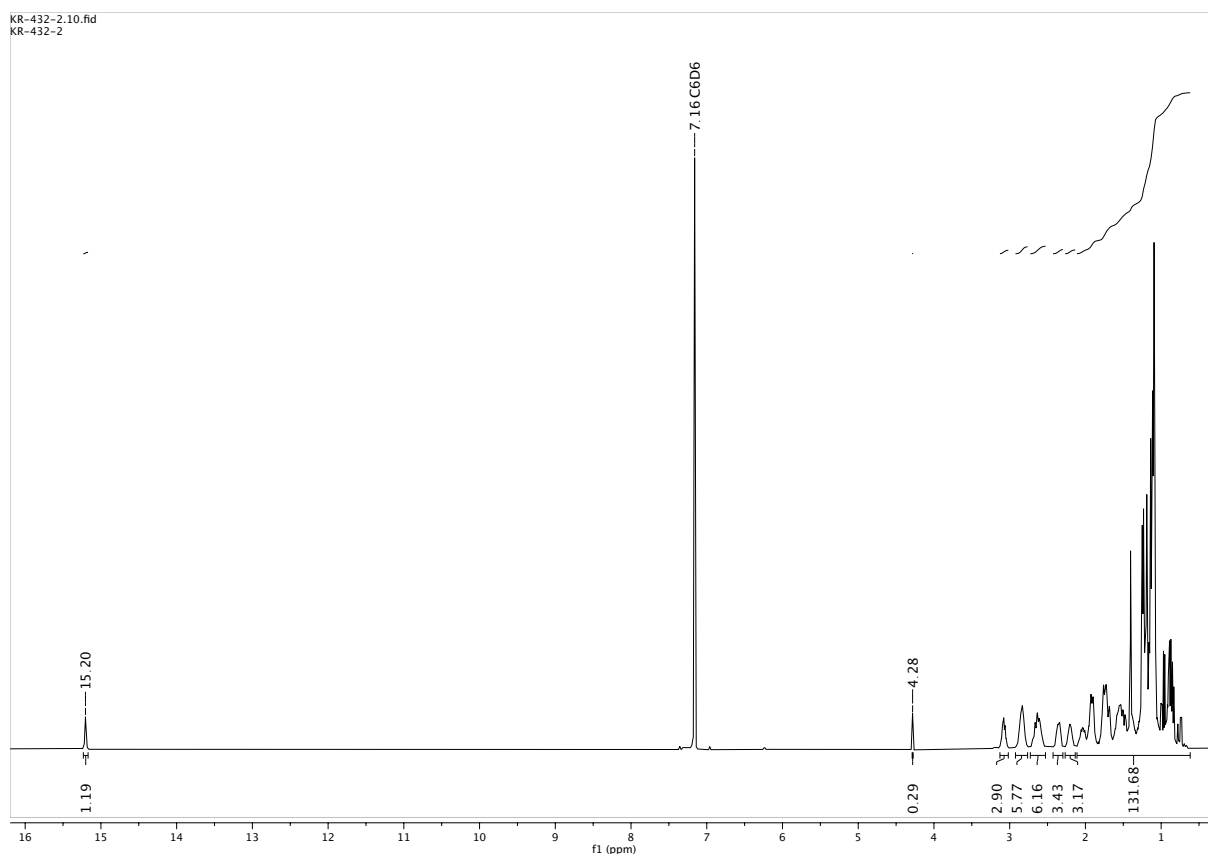
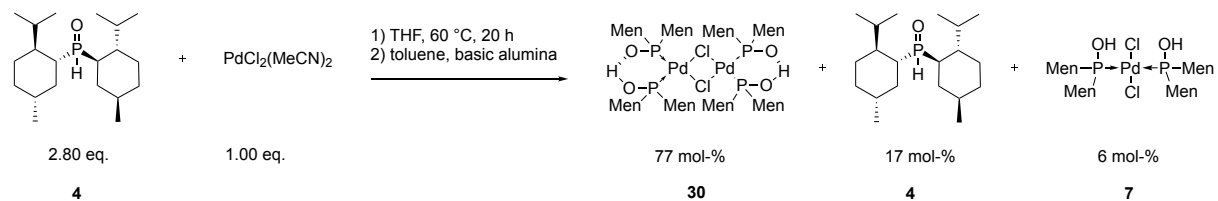


**Figure 8.** Excerpt of the  $^1\text{H}$ -NMR spectrum of the  $\text{Et}_2\text{O}$ -eluted fraction of entry 2, table 9.

When comparing the amount of dimethyl phosphine oxide present in the mixture with the integral of the singlet, a correlation can be found. Generally speaking, the more **4** is present in the mixture, the higher the integral of the singlet at  $\delta_H$  4.28 seems to be, thus indicating that presence of  $\text{Men}_2\text{POH}$  in the mixture destabilizes species **30** to form a new (supposedly dissociated) species. However, since some exemptions from this correlation were observed, other unknown factors might contribute as well. A further elucidation of these factors was not possible within the scope of this thesis.

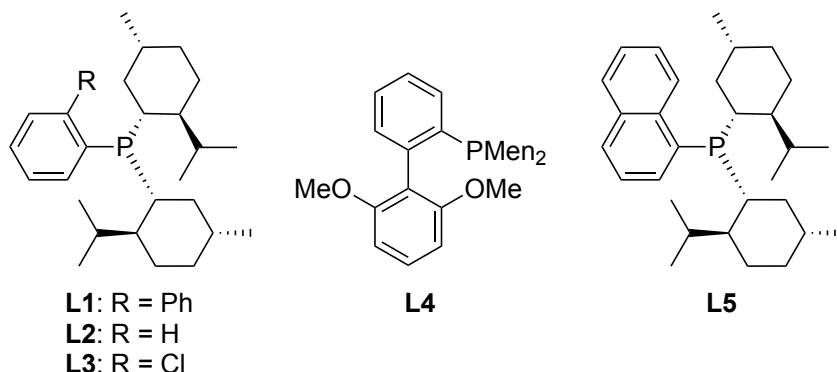
The synthesis of **30** was also attempted directly from a suitable Pd precursor and **4**, forming crude **7**, which was then directly filtered over a pad of basic alumina (scheme 30). This, however, led to insufficient purity, thus it was concluded that pure **7** is needed for a successful synthesis.



**Scheme 30.** Attempted synthesis of **30** directly from **4** and  $\text{PdCl}_2(\text{MeCN})_2$ . Molar ratios are estimated by  $^{31}\text{P}$ -NMR of the crude material.

## 2.5 Synthesis and Complexation Chemistry of Ligands Containing the Dimethylphosphino Structural Motif *via* Arylation of $\text{Men}_2\text{PCl}$

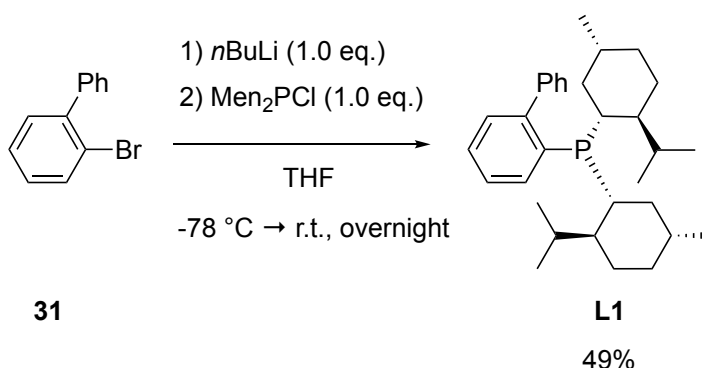
For the evaluation of the dimethylphosphino structural motif in steering ligands for catalysis, the synthesis of a series of dimethyl(bi)aryl phosphines **L1-L5** was envisaged (scheme 31).



*Scheme 31. The dimethyl(bi)aryl phosphines synthesized in this work.*

### Synthesis of MenJohnPhos (**L1**)

The formerly established conditions for the synthesis of **L1** (MenJohnPhos)<sup>77</sup> were reproduced affording the same yield on a higher scale (scheme 32). The purification process was improved by recrystallizing once from hot MeOH/EtOAc, as opposed to two successive recrystallization processes in the earlier synthesis. Compared to the synthesis of CyJohnPhos by Buchwald and co-workers which uses a similar procedure, the yield of **L1** is lower.<sup>101</sup> This could be explained by the added sterical bulk of the menthyl moieties compared to the cyclohexyl moieties.



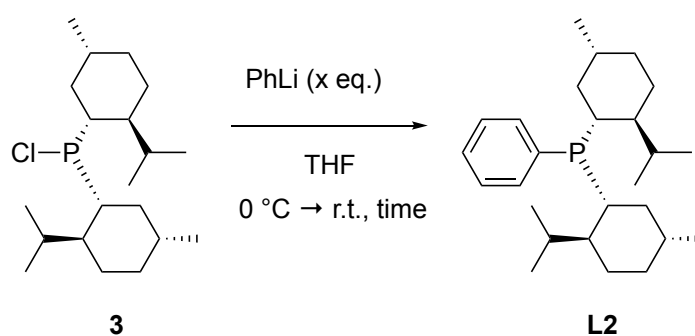
*Scheme 32. Synthesis of L1.*

### Synthesis of Dimethyl(phenyl)phosphine (**L2**)

The synthesis of **L2** ( $\text{Men}_2\text{PPh}$ ) on a small scale by reaction of  $\text{Men}_2\text{PCl}$  with phenyl lithium afforded the compound in low yield at first (table 10, entry 1). Scaling up the reaction revealed purification difficulties, as the compound did not crystallize. Presumably, this is due to a higher

amount of not easily volatile di-*n*-butyl ether stemming from the phenyl lithium solution. Purification by column chromatography was not successful due to fast oxidation of the phosphine in solution. These results prompted a further investigation of the reaction in order to obtain a purer product. Monitoring the reaction by <sup>1</sup>H-qNMR using an internal standard showed a yield of 94% already after one hour of reaction time.<sup>i</sup> Thus, low isolated yields are not a result of incomplete conversion, but rather of suboptimal purification conditions. A complete work-up under argon with subsequent removal of most di-*n*-butyl ether *via* high vacuum and recrystallization under argon led to a satisfying, optimized yield of 77% (entry 2).

**Table 10.** Synthesis of **L2**.



entry	x	time	scale	work-up and purification	yield /% <sup>a</sup>
1	1.0	overnight	1.0 mmol	under air	37
2	1.2	2.5 h	2.5 mmol	under argon	77

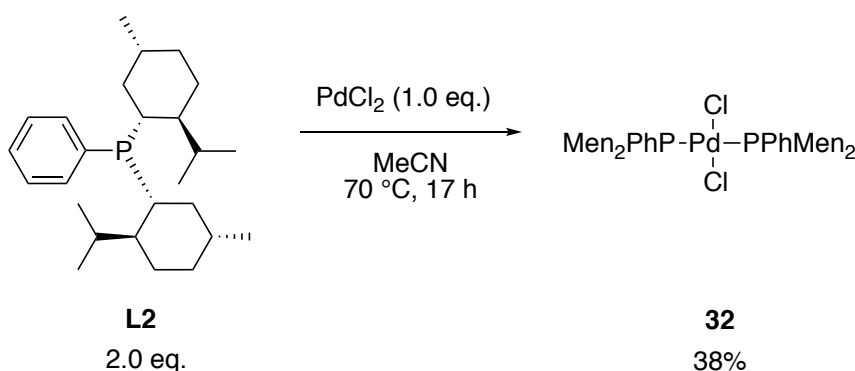
a) Yields are isolated yields.

Surprisingly, the ligand was relatively air-stable as a solid. Although it was preferably stored in a Schlenk tube under argon, it could be easily weighed in under air, and only a minor amount of oxidized ligand formed over a month of extensive use.

For studying the complexation chemistry of dimethyl(phenyl)phosphine (**L2**) and in an effort to synthesize a more bench-stable precursor complex for this ligand, the synthesis of bis(dimethylphenylphosphine) palladium (II) chloride **32** was envisioned. Heating dimethyl(phenyl)phosphine with palladium(II) chloride in acetonitrile at 70 °C overnight afforded a yellow crude material. <sup>31</sup>P-NMR analysis showed full conversion of the phosphine and emergence of a new signal at  $\delta_P$  24.06, which constitutes a significant downfield shift compared to the free phosphine ( $\delta_P$  -10.1). This finding supports the coordination of phosphorous to the palladium center. While handling the crude material in air, some

<sup>ii</sup> For a detailed procedure, see Experimental Part.

inhomogeneous yellow and red solids formed during rotary evaporation. It is assumed that the material disintegrates while heating under air, forming PdCl<sub>2</sub> as red solid. Thus, in a further experiment, purification was conducted under argon and without heating, affording pure compound **32** in 38% yield (scheme 33). Loss of yield is attributed to the small scale of the reaction and the purification by hexane wash, causing a part of the target material to remain in the filtrate.



**Scheme 33.** Synthesis of bis(dimethylphosphine palladium(II) dichloride).

The <sup>1</sup>H-NMR spectrum of **32** shows (compared to the free phosphine) two sets of rather broad signals instead of the multiplet stemming from the *meta*-aryl protons (figure 9). When comparing their integrals to the remaining proton signals, two species (with a ratio of around 0.8:1) can be assumed. These could be explained by slow rotation of the phenyl groups caused by steric congestion of the bulky menthyl moieties, thus causing anisochrony of the *meta*-aryl protons. These findings suggest potential applicability in asymmetric catalysis, if taken as indication that the coordination space around Pd is more tightly controlled through the presence of the bulky ligand **L2**.



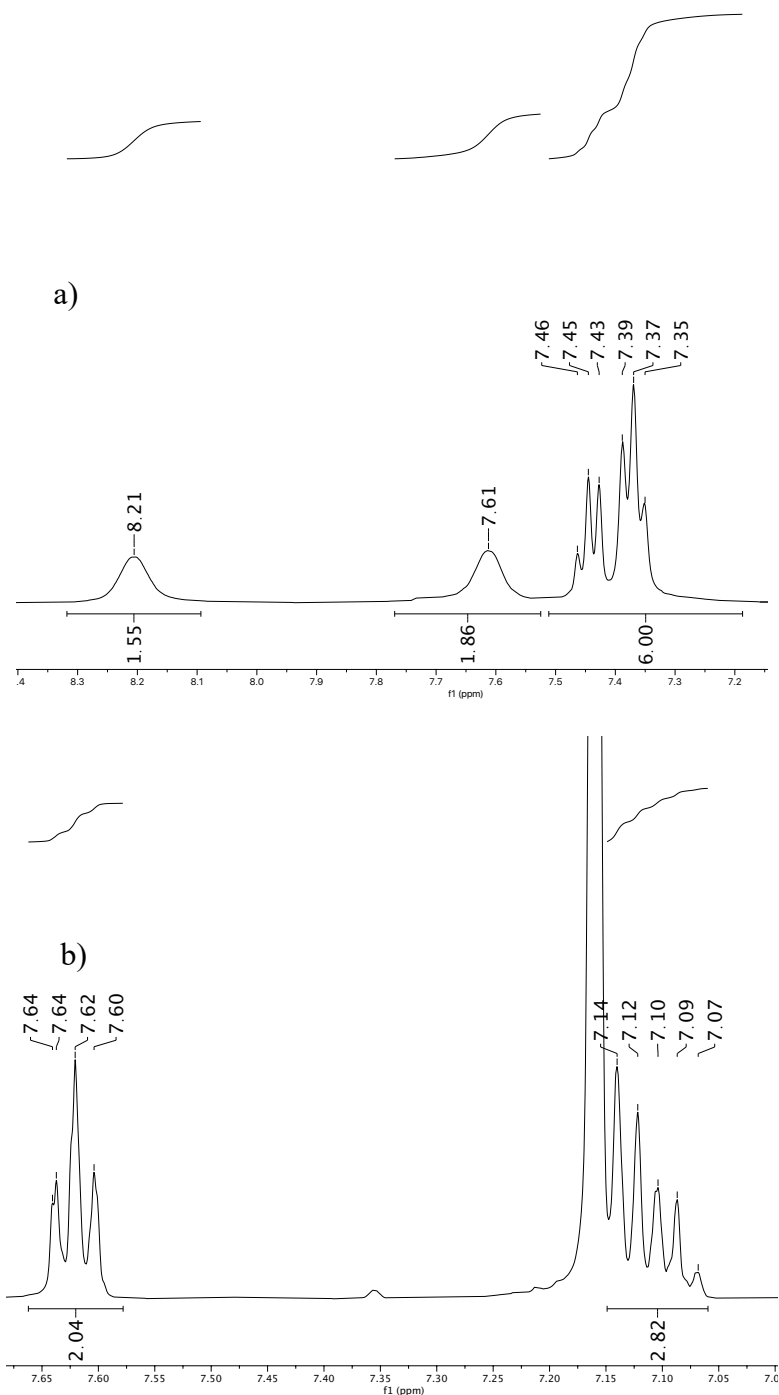


**Figure 9.** Excerpt of the aromatic region of the <sup>1</sup>H-NMR spectra of **32** in CD<sub>2</sub>Cl<sub>2</sub> (a) and free phosphine **L2** in C<sub>6</sub>D<sub>6</sub> (b).

Line broadening is also observed in the aromatic region of the <sup>13</sup>C-APT spectrum (figure 10). The *pseudo*-triplet at δ<sub>C</sub> 127.58 stems from the phosphorus-bound C-atoms. Three sets of broadened signals are observed for the C-H units in *ortho*- and *meta*- position (δ<sub>C</sub> 126.87, 132.81 and 138.56), which agrees with the assumption slow rotation of the phenyl groups. The sharp C-H signal at δ<sub>C</sub> 130.45, on the other hand, is likely to stem from *para*-C-H, whose

chemical environment does not change by rotation of the phenyl groups, and therefore does not give rise to a broadened signal.

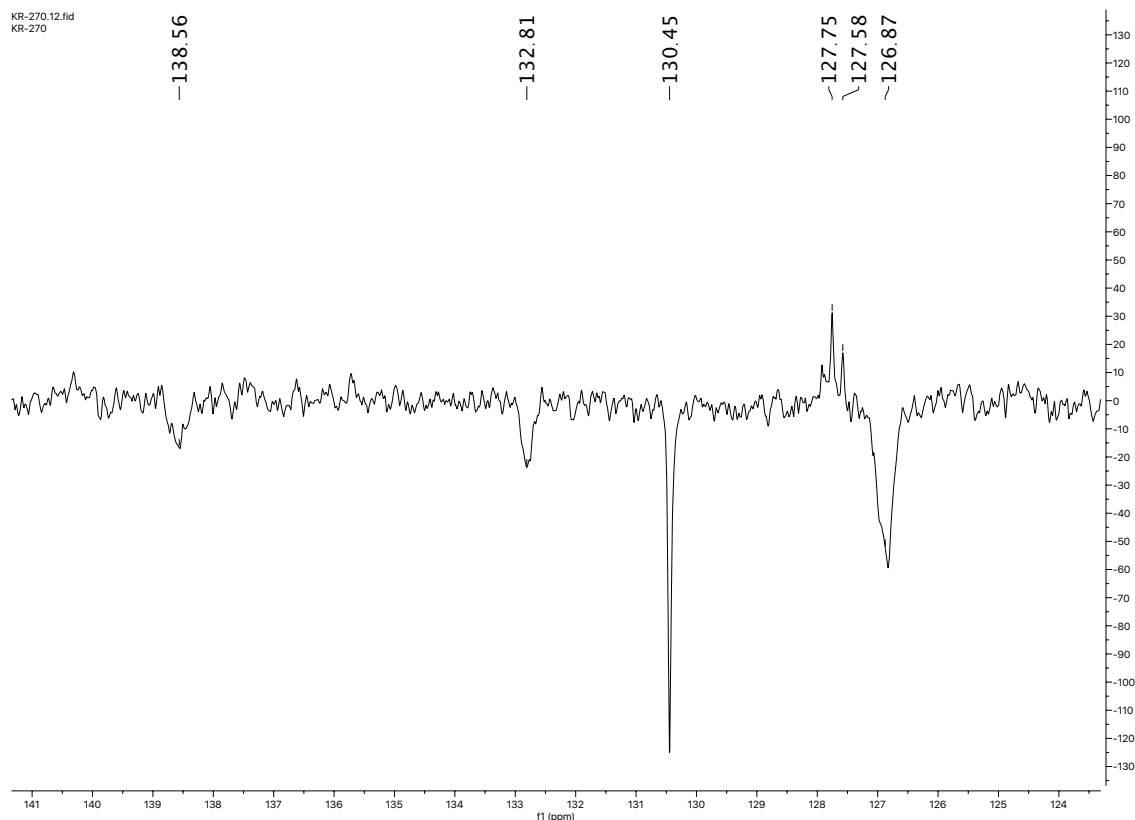
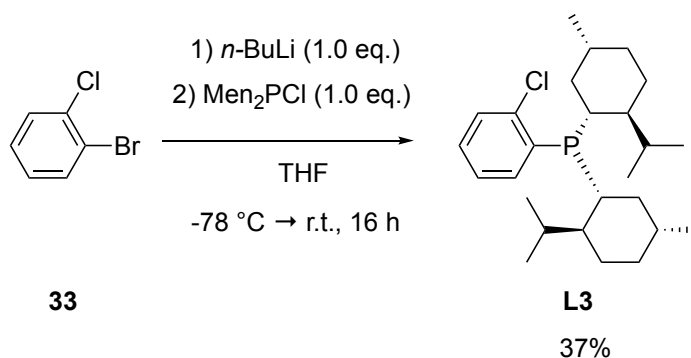


**Figure 10.** Excerpt of the aromatic region of the  $^{13}\text{C}$ -APT spectrum of **32** in  $\text{CD}_2\text{Cl}_2$ . Negative Integrals are C-H-, positive integrals are C atoms with no attached protons.

### Synthesis of (2-chlorophenyl)dimenthyl phosphine (**L3**)

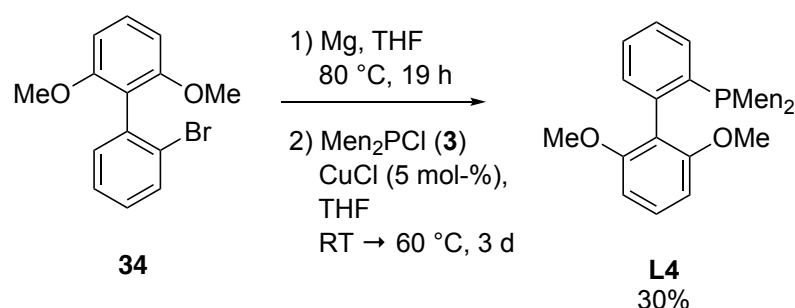
The synthesis of **L3** was realized directly from 1-bromo-2-chloro benzene *via* halogen-lithium exchange and subsequent phosphination, although the yield was low. Attempts to improve the conditions by adding stoichiometric amounts of  $\text{CuCl}$  or conducting the synthesis at higher temperatures ( $-40\text{ }^\circ\text{C}$  as opposed to  $-78\text{ }^\circ\text{C}$ ) did not bring about significant improvements.<sup>102</sup> The isolated yield was slightly improved when precipitation instead of crystallization was used as purification method (scheme 34).



**Scheme 34.** Synthesis of **L3**.

### Synthesis of MenSPhos (L4)

The synthesis of **L4** (MenSPhos) was accomplished in moderate yield (scheme 35). As opposed to the synthesis of *Buchwald's* SPhos, which is performed by *in situ* aryne addition and phosphination,<sup>21</sup> isolation of precursor **34** and phosphination of the corresponding aryl magnesiumbromide was preferred.

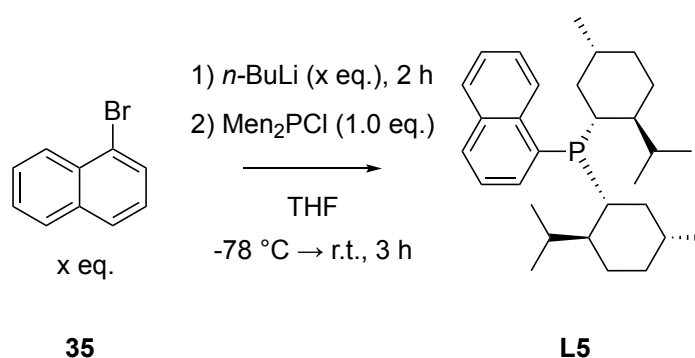


*Scheme 35. Synthesis of L4.*

### Synthesis of Dimethyl(1-naphthyl)phosphine (L5)

The synthesis of **L5** was achieved by lithiation of 1-bromonaphthalene and subsequent reaction with Men<sub>2</sub>PCl and was optimized in two steps (table 11). The yield was moderate when equimolar amounts of aryl lithium were used (entry 1), but improved slightly with an excess of ArLi (entry 2). A further optimization of the synthesis was not undertaken, since the potential of the ligand in catalysis was first to be explored.

*Table 11. Optimization of the synthesis of L5.*



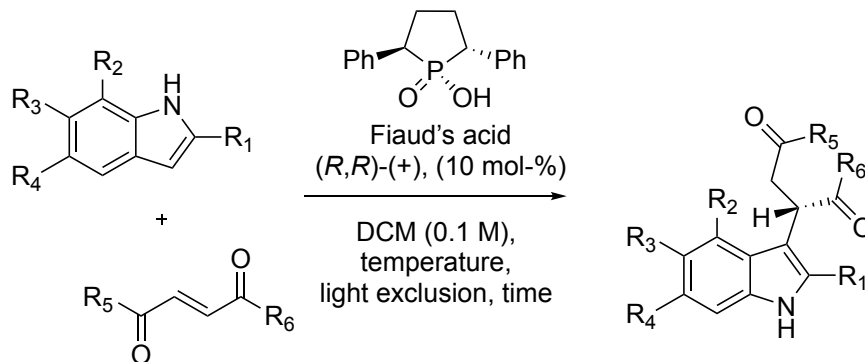
entry	<i>x</i> eq.	yield /% <sup>a</sup>
1	1.0	37
2	2.0	54

a) Isolated yields.

## 2.6 Exploration of New Dimethylphosphino Derivatives as Steering Ligands in Catalysis

### 2.6.1 *Brønsted Acid Catalyzed Enantioselective Friedel Crafts Alkylation of Indoles with 2-Alkene-1,4-diones*

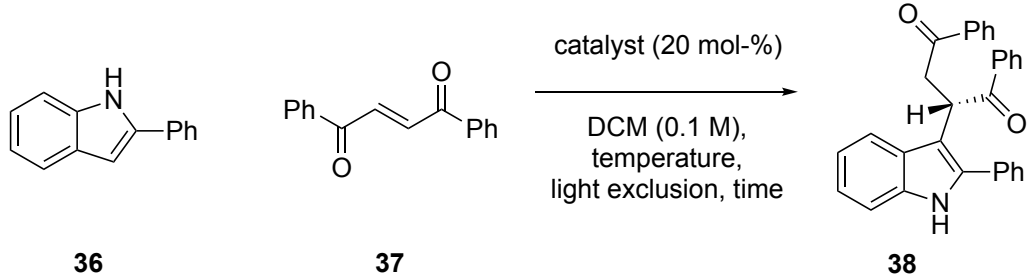
Jaisankar *et al.* have reported on the use of Fiaud's acid as a Brønstedt acid catalyst for enantioselective Friedel Crafts alkylation of indoles with alkene-1,4-diones (scheme 36).<sup>103</sup>



**Scheme 36.** Enantioselective Friedel Crafts alkylation of indoles with alkene-1,4-diones catalyzed by Fiaud's acid as reported by Jaisankar and co-workers.<sup>103</sup>

With dimethylphosphinic acid **6** available as chiral, enantiopure phosphinic acid, it was of interest to explore its performance in the same reaction. Using 1-phenyl indole and *trans*-1,2-dibenzoyl ethylene as substrates, the applicability of dimethylphosphinic acid **6** as a chiral Brønstedt acid catalyst was examined. For this purpose, two experiments using dimethylphosphinic acid (table 12, entry 1) and Fiaud's acid (entry 2) as a reference were set up and the progress of the reaction monitored by TLC.

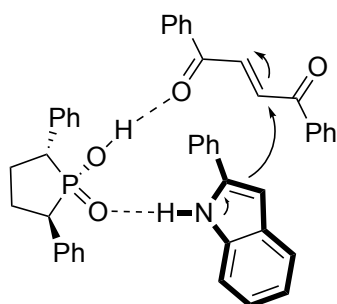
**Table 12.** Catalytic test reactions for the enantioselective Brønsted acid catalyzed Friedel Crafts alkylation of 1-phenylindole and *trans*-1,2-dibenzoyl ethylene



entry	catalyst	temperature	time	result <sup>a</sup>
1	Men <sub>2</sub> POOH ( <b>6</b> )	r.t. → 30°C	3 days	only traces of <b>38</b>
2	Fiaud's acid	30°C	17 hours	near complete formation of <b>38</b>

a) as judged by <sup>1</sup>H-NMR of the crude material

When conducting the reaction at room temperature, TLC analysis showed no reaction for entry 1. Considering warmer temperatures in Kolkata, where large parts of Jaisankar's work were conducted, compared to Munich,<sup>104,105</sup> the reaction temperature was slightly elevated to 30°C. However, even after 3 days, no reaction product was detected by TLC analysis. <sup>1</sup>H-NMR of the crude material after work-up showed only unchanged starting material. The control reaction with Fiaud's acid as a catalyst (entry 2) showed formation of target material after stirring overnight for 17 hours as judged by TLC analysis. <sup>1</sup>H-NMR analysis of the crude material also showed near complete conversion, which is comparable to the literature results. In conclusion, **6** is not a suitable catalyst for this reaction. Its inferior performance compared to Fiaud's acid might be explained by more sterical demand, which might hinder the two substrates from approaching the catalytically active phosphinic acid site. Furthermore, the five-membered ring of Fiaud's acid constitutes a relatively rigid environment of the catalytically active site, which might benefit the formation of the very confined catalytic transition state. The two menthyl moieties of dimethyl phosphinic acid, on the other hand, exhibit more rotational freedom, which might be an obstacle (scheme 37).

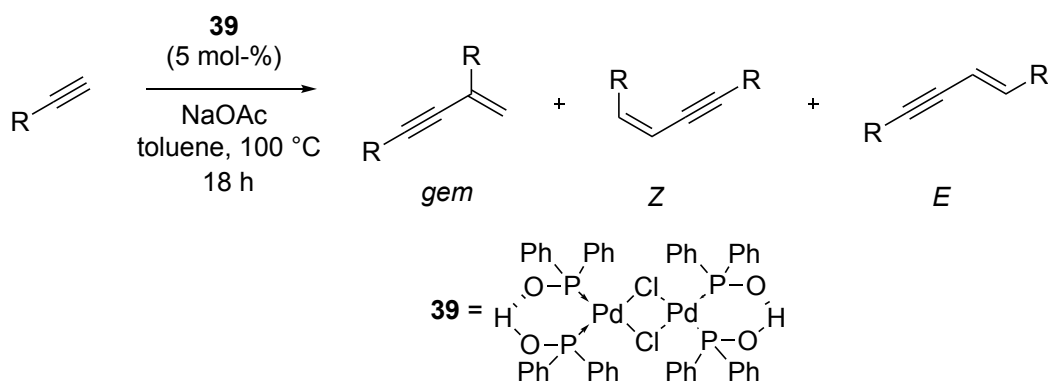


**Scheme 37.** Catalytic transition state of the Fiaud's acid catalyzed enantioselective Friedel Crafts alkylation of indoles and alkene-1,4-diones proposed by Jaisankar et al.<sup>103</sup>

### 2.6.2 Pd-Catalyzed Transformations of Alkynes with Dimethylphosphine Oxide

#### Palladium-Catalyzed Dimerization of Phenylethyne

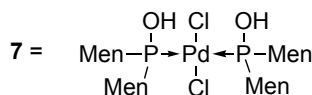
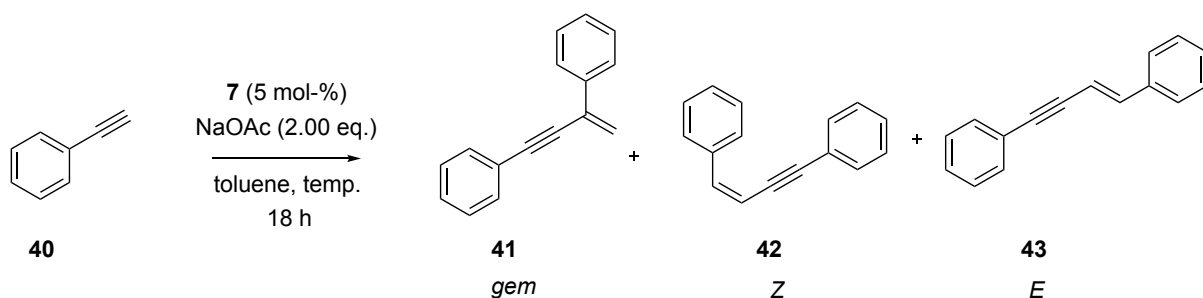
Morales-Serna and co-workers recently reported a phosphinito palladium(II) complex catalyzed synthesis of 1,3-enynes by dimerization of terminal alkynes.<sup>106</sup> In their work, complex **39**, which is derived from diphenylphosphine oxide, served as a catalyst (scheme 38).



**Scheme 38.** Synthesis of 1,3-enynes by dimerization of terminal alkynes as reported by Morales-Serna and co-workers.

In the present work, the utility of a dimethylphosphine oxide ligated complex was assessed. As the dimethylphosphinite/phosphinous acid palladium(II) complex **30** was not accessible yet by synthetic methods at that point, use of complex **7** and *in situ* generation of **30** by deprotonation using NaOAc as base was envisaged. Table 13 shows the employed reaction conditions using phenyl ethyne as model substrate and the outcomes analyzed by <sup>1</sup>H-qNMR spectroscopy of the crude material. This type of reaction can produce three different isomers, namely the geminal alkene *gem*, the *Z* and the *E* alkene.

**Table 13.** Palladium-catalyzed dimerization of phenyl ethyne



entry	temperature	<b>40</b> /%	<b>41</b> /% <sup>a</sup>	<b>42</b> /% <sup>a</sup>	<b>43</b> /% <sup>a</sup>	recovery /% <sup>a</sup>
1	100 °C	-	23	6	3	32
2	60 °C	16	10	trace	trace	26

a) Analytical yields and recoveries (mol-%) determined by quantitative <sup>1</sup>H-NMR analysis using an internal standard.

At a high reaction temperature of 100 °C (entry 1), the desired 1,3-enyne (**41**; *gem*) was the major reaction product, however with a low yield of 23%. Besides small amounts of *E* and *Z* isomers, no starting material was detected. Notably, the recovery of the experiment is too low, which could be explained by polymerization. As shown in figure 11, the <sup>1</sup>H-NMR spectrum shows clear signs of polymerization in the aromatic chemical shift range. Assuming that polymerized product initially stems from 1,3-enyne formed as an intermediate, it was concluded that lowering the reaction temperature might hamper polymerization and therefore produce higher yields of the *gem* isomer. Thus, in entry 2, the temperature was lowered to 60°C. However, these conditions led to a lower yield and incomplete conversion of the alkyne, while still showing signs of polymerization. Further efforts to improve the reaction conditions were not undertaken.

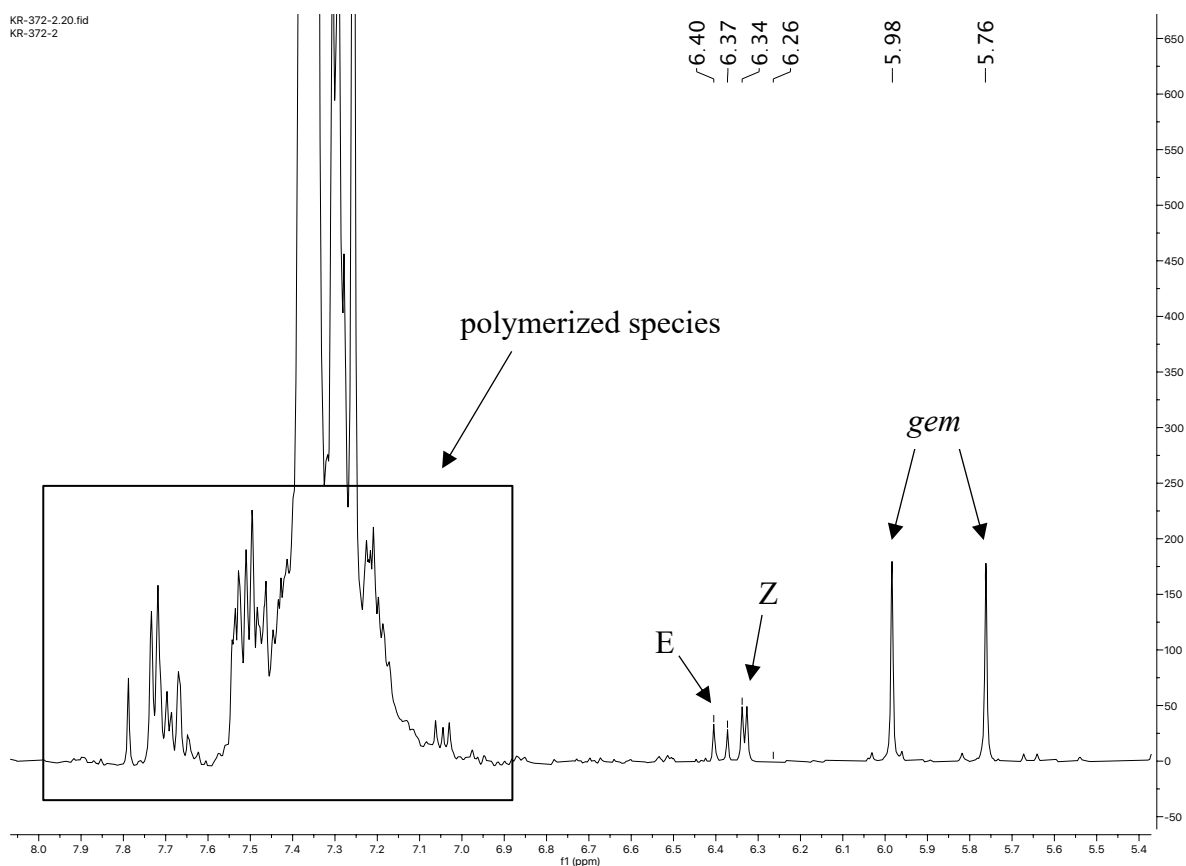
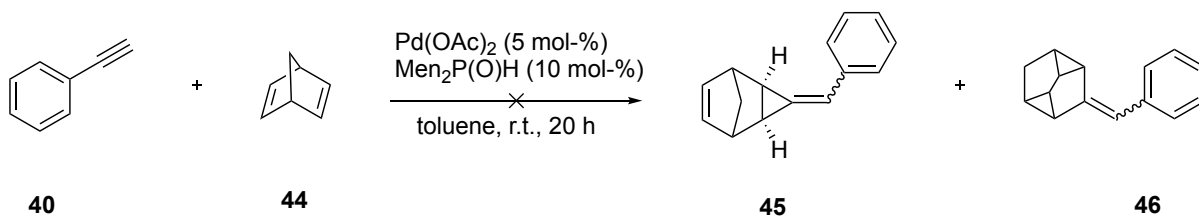


**Figure 11.** Excerpt of the  $^1\text{H}$ -NMR spectrum of entry 2, table 13 showing polymerized species in the aromatic chemical shift range.

### Pd-Catalyzed [2+1] Cycloaddition of Phenyl Ethyne to Norbornadiene

In 2005, Buono and co-workers reported a palladium catalyzed [2+1] cycloaddition of terminal alkynes to norbornene derivatives using dicyclohexylphosphine oxide as a ligand.<sup>107</sup> In the current work, the assessment of dimethylphosphine oxide as a ligand in a model reaction using phenyl ethyne and norbornadiene as substrates was envisaged (scheme 39).



**Scheme 39.** Failed [2+1] cycloaddition of phenyl acetylene to norbornadiene.

$^1\text{H}$ -qNMR analysis of the crude material showed, besides partially recovered norbornadiene and phenyl acetylene, no formation of target material. Again, the fate of unrecovered starting material can be explained by dimerization of **40** or polymerization of both starting materials. This is confirmed by proton signals in the aromatic region, as shown in figure 12.



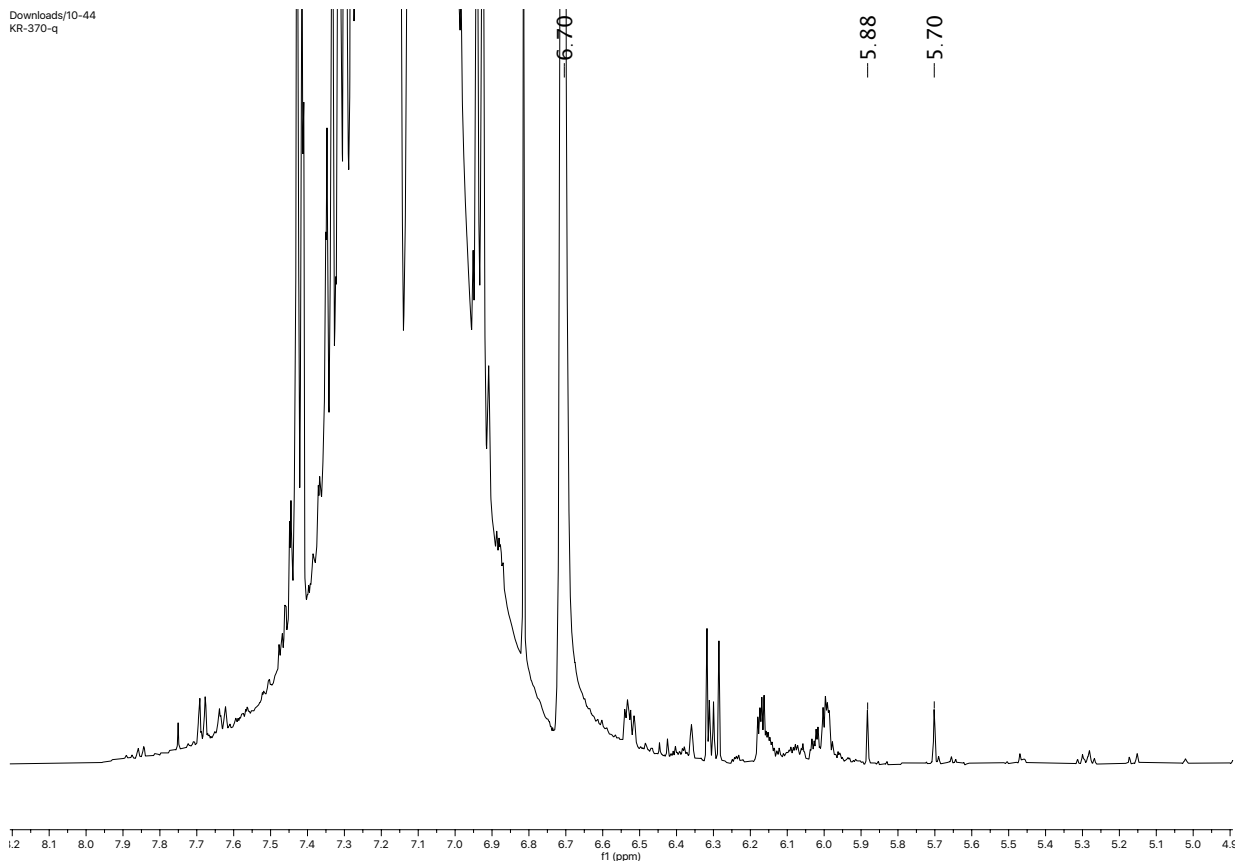


**Figure 12.** Excerpt of the  $^1\text{H}$ -NMR spectrum of the Pd-catalyzed [2+1] cycloaddition of phenyl ethyne to norbornadiene showing dimerization and polymerization of starting material.

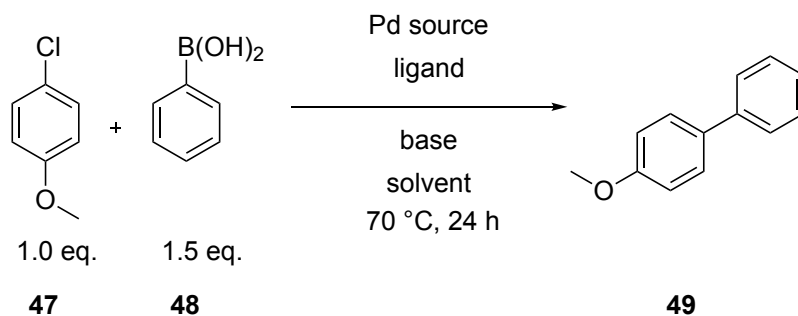
Attempts at optimizing the reaction conditions were not undertaken. Combined with the results of section the palladium-catalyzed dimerization of dimethylphosphine oxide, it became clear that catalytic transformations of terminal alkynes are prone to polymerization when using dimethylphosphine oxide as ligand.

### 2.6.3 Dimethylphosphine P-Oxide as Ligand in Palladium-Catalyzed Cross-Couplings

#### **Dimethylphosphine P-Oxide as Ligand in Palladium-Catalyzed Suzuki-Miyaura Couplings**

Dimethylphosphine oxide and dimethylphosphine oxide incorporating palladium complexes were evaluated as a ligand/catalyst systems in Suzuki-Miyaura couplings. The first model reaction envisaged the coupling of phenylboronic acid and 4-chloroanisole as an electron-rich aryl chloride. The two tested conditions are listed in table 14.

**Table 14.** Tested conditions for the Suzuki-Miyaura coupling of 4-chloroanisole and phenylboronic acid.



entry	Pd source	ligand	solvent	base	yield /% <sup>a</sup>
1 <sup>b</sup>	Pd(OAc) <sub>2</sub> (2 mol-%)	Men <sub>2</sub> POH (4 mol-%)	THF	K <sub>2</sub> CO <sub>3</sub> (3.0 eq.)	9
2 <sup>b</sup>	(Men <sub>2</sub> POH) <sub>2</sub> PdCl <sub>2</sub> (2 mol-%)	-	THF	K <sub>2</sub> CO <sub>3</sub> (3.0 eq.)	33
3 <sup>b</sup>	[(Men <sub>2</sub> POH)PdCl <sub>2</sub> ] <sub>2</sub> (1 mol-%)	-	THF	K <sub>2</sub> CO <sub>3</sub> (3.0 eq.)	25
4 <sup>c</sup>	Pd(OAc) <sub>2</sub> (1 mol-%)	Men <sub>2</sub> POH (2 mol-%)	toluene	K <sub>3</sub> PO <sub>4</sub> (2.0 eq.)	2
5 <sup>c</sup>	(Men <sub>2</sub> POH) <sub>2</sub> PdCl <sub>2</sub> (1 mol-%)	-	toluene	K <sub>3</sub> PO <sub>4</sub> (2.0 eq.)	7
6 <sup>c</sup>	[(Men <sub>2</sub> POH)PdCl <sub>2</sub> ] <sub>2</sub> (0.5 mol-%)	-	toluene	K <sub>3</sub> PO <sub>4</sub> (2.0 eq.)	10

a) Analytical yields (mol-%) determined by <sup>1</sup>H-qNMR analysis using an internal standard.

b) Condition A: Procedure according to general procedure GP-5-A.

c) Condition B: Procedure according to general procedure GP-5-B.

It should be noted that the two tested conditions are not the result of a systematic optimization of reaction conditions, but were selected independently from another based on reported conditions.<sup>1,108</sup> While none of the reactions give satisfying results, it is apparent that generally, condition A gives higher yields. This is probably not only attributable to the higher catalyst loading with this condition, because the yield should rise proportionally to the catalyst loading if both conditions afford the same TON. Therefore, either the solvent, base or amount of base or a combination of all of these could be responsible for the better yields with condition A. Possibly, anionic Men<sub>2</sub>POH-Pd complexes, which are formed upon deprotonation of the *in situ* generated Pd species, are better soluble in the more polar solvent THF, which may lead to a better catalytic activity. Since the overall performance of dimethylphosphine oxide and its

palladium complexes in the Suzuki-Miyaura coupling of 4-chloroanisole and phenylboronic acid were not satisfying, a more detailed optimization of the conditions was not conducted.

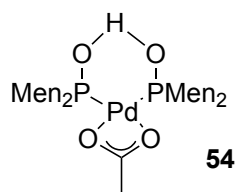
**Table 15.** Suzuki-Miyaura coupling of phenylboronic acid and 1-bromo-2-methoxynaphthalene

entry	Pd source	ligand	50 /% <sup>a</sup>	52 /% <sup>a</sup>	53 /% <sup>a</sup>	recovery /% <sup>a</sup>
1	Pd(OAc) <sub>2</sub> (2 mol-%)	Men <sub>2</sub> POH (4 mol-%)	12	70	18	100
2	(Men <sub>2</sub> POH) <sub>2</sub> PdCl <sub>2</sub> (2 mol-%)	-	30	43	25	98
3	[(Men <sub>2</sub> POH)PdCl <sub>2</sub> ] <sub>2</sub> (2 mol-%)	-	49	30	20	99

a) Analytical yields (mol-%) and recoveries (mol-%) determined by <sup>1</sup>H-qNMR analysis using an internal standard.

As another model substrate, electron-rich and sterically more hindered aryl bromide 1-bromo-2-methoxynaphthalene **50** was coupled with phenylboronic acid **51**. The results of this test reaction are presented in table 15. Overall, the coupling with aryl bromide as electrophile showed better results than that with aryl chloride. Furthermore, it is evident that a substantial amount of hydrodehalogenated product **53** is formed as a by-product with all of the used catalyst systems.

Especially the dimethylphosphine oxide/Pd(OAc)<sub>2</sub> system afforded a good yield of 70% (entry 1), which is in stark contrast to the very low yield (9%) using aryl chloride. These differences suggest that oxidative addition is the rate-limiting step for all of the tested catalyst systems. While [(Men<sub>2</sub>POH)PdCl<sub>2</sub>]<sub>2</sub> and (Men<sub>2</sub>POH)<sub>2</sub>PdCl<sub>2</sub> show a mediocre performance (entries 2 and 3), the dimethyl phosphine oxide/Pd(OAc)<sub>2</sub> system could be a promising candidate for further investigation. The good results might be attributed to formation of acetate bridged complex **54** (scheme 40) *in situ* or the absence of halide anions. Complex **54** had already been observed in earlier work within the research group, but not obtained in a high purity.<sup>77</sup> Further attempts to synthesize **54** and an investigation of its performance in catalysis could be an intriguing task for future endeavors.

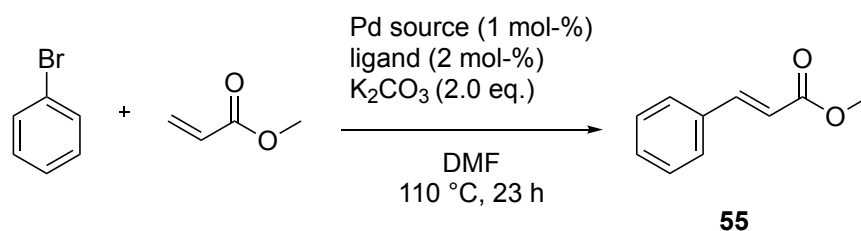


**Scheme 40.** Proposed *in situ* formation of complex **54**.

### Dimethylphosphine *P*-Oxide as Steering Ligand in Mizoroki-Heck Couplings

In a further catalytic test reaction, the Pd-catalyzed Mizoroki-Heck coupling of bromobenzene and methyl acrylate was attempted using dimethylphosphine oxide as ligand (table 16).<sup>1</sup>

**Table 16.** Mizoroki-Heck coupling of bromobenzene and methyl acrylate using dimethylphosphine oxide as ligand.



entry	Pd source	ligand	yield /% <sup>a</sup>
1	Pd(OAc) <sub>2</sub>	Men <sub>2</sub> POH	7
2	(Men <sub>2</sub> POH) <sub>2</sub> PdCl <sub>2</sub>	-	4
3	[(Men <sub>2</sub> POH)PdCl <sub>2</sub> ] <sub>2</sub> <sup>b</sup>	-	18
4	Pd(OAc) <sub>2</sub>	-	trace

a) Yield (mol-%) calculated by <sup>1</sup>H-qNMR analysis using toluene as internal standard.

b) 0.5 mol-% of the Pd source was used.

None of the catalyst systems show promising results under the tested condition, but dimeric complex [(Men<sub>2</sub>POH)PdCl<sub>2</sub>]<sub>2</sub> (entry 3) afforded a considerably higher yield than the other two catalyst systems (entries 1 and 2). As control reaction, the same coupling was implemented using only Pd(OAc)<sub>2</sub> as catalyst (entry 4). This set-up afforded only a trace amount of product, which leads to the conclusion that Men<sub>2</sub>POH does contribute to the catalytic cycle as a ligand for entries 1 – 3.

<sup>1</sup> Conditions in literature for this model reaction vary with respect to solvent, base, Pd precursor and temperature; at the time of writing (2021/09), a search in the Reaxys database resulted in 211 different conditions for this particular reaction.

## Dimethylphosphine *P*-Oxide as Steering Ligand in Kumada-Corriu Couplings

A further catalytic test reaction involved the Kumada-Corriu coupling of phenylmagnesium bromide and 1-bromo-2-methoxynaphthalene (table 17).

**Table 17.** Kumada-Corriu coupling of phenylmagnesium bromide and 1-bromo-2-methoxynaphthalene.

Reaction scheme showing the Kumada-Corriu coupling of 1-bromo-2-methoxynaphthalene (**50**) with phenylmagnesium bromide (PhMgBr) to form 1-phenyl-2-methoxynaphthalene (**52**) and 1-methoxynaphthalene (**53**). Conditions: Pd source (1 mol-%), ligand (2 mol-%), PhMgBr (1.5 eq.), THF, r.t., 18 h.

entry	Pd source	ligand	<b>50</b> /% <sup>a</sup>	<b>52</b> /% <sup>a</sup>	<b>53</b> /% <sup>a</sup>	recovery /% <sup>a</sup>
1	Pd(OAc) <sub>2</sub>	Men <sub>2</sub> POH	71	20	4	95
2	(Men <sub>2</sub> POH) <sub>2</sub> PdCl <sub>2</sub>	-	72	19	4	95
3	[(Men <sub>2</sub> POH)PdCl <sub>2</sub> ] <sub>2</sub> <sup>b</sup>	-	69	21	3	93
4	Pd(OAc) <sub>2</sub>	-	34	11	39	84

a) Analytical yields (mol-%) and recoveries (mol-%) calculated by <sup>1</sup>H-qNMR analysis using an internal standard.

b) 0.5 mol-% of Pd species was used.

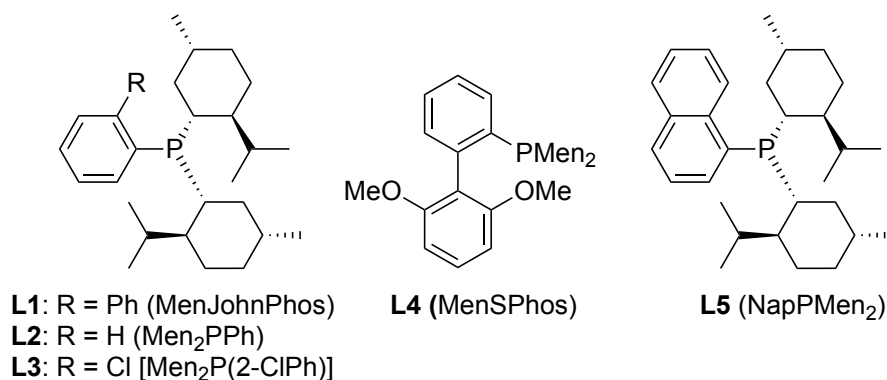
<sup>1</sup>H-qNMR analysis of the crude materials shows that the Men<sub>2</sub>P(O)H-based tested catalytic systems (entries 1 – 3) yield a comparable, low amount (~ 20%) of target material **52**, but still higher than that of the control reaction using only Pd(OAc)<sub>2</sub> without a ligand (entry 4). Moreover, only a small amount of hydrodehalogenated compound **53** was formed. When using only Pd(OAc)<sub>2</sub>, **53** was formed in a much higher yield. Thus, using Men<sub>2</sub>POH as ligand suppresses the formation of **53**, which might be formed outside of the catalytic cycle by transmetalation. A further optimization of the reaction conditions was not performed within the scope of this work.

## 2.7 (Aryl)dimenthylphosphine Ligands and their Application in Catalysis

### 2.7.1 Catalytic Test Reactions Using (Aryl)dimenthylphosphine Ligands

#### (Aryl)dimenthylphosphine Ligands in a Buchwald-Hartwig coupling

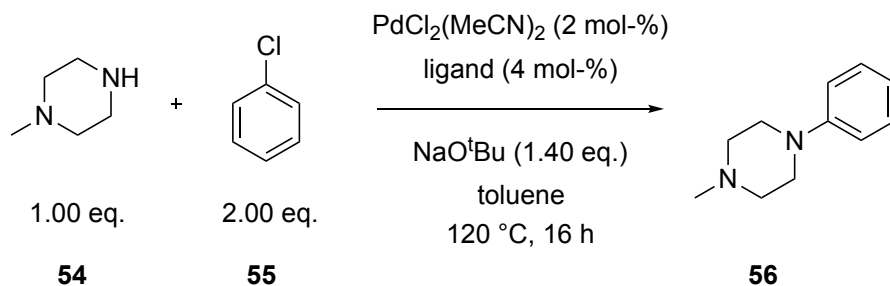
The (aryl)dimenthylphosphine ligands **L1-L5** (scheme 41) whose synthesis was described in section 2.5 of this work were tested in a variety of transition-metal catalyzed cross-coupling reactions.



**Scheme 41.** Ligands L1-L5 assessed in cross-coupling reactions in this work.

The palladium-catalyzed Buchwald-Hartwig amination of chlorobenzene with *N*-methyl piperazine was used as a model reaction based on reported literature<sup>109</sup> and the crude materials were analyzed by <sup>1</sup>H-qNMR. The results of the ligand assessment are presented in table 18. While *ortho*-biarylphosphine ligands **L1** and **L4** (entries 1 and 4) afforded rather low yields, arylphosphine ligands **L2** and **L3** (entries 2 and 3) performed excellently. This comes to a surprise, as dialkylbiarylphosphine ligands are known as privileged ligand class in catalysis due to Pd-aryl interactions of the *ortho*-aryl' moiety. For all ligands, the recovery based on **54** is not quantitative. As Reddy *et al.* proposed, decomposition of the amine starting material is likely to take place in these harsh, basic conditions.<sup>109</sup>

**Table 18.** Ligand assessment for the Buchwald-Hartwig coupling of chlorobenzene and *N*-methylpiperazine.



entry	ligand	yield /% <sup>a</sup>	conversion /% <sup>b</sup>
1	<b>L1</b> (MenJohnPhos)	19 <sup>c</sup>	53
2	<b>L2</b> (Men <sub>2</sub> PPh)	92 (90) <sup>d</sup>	92
3	<b>L3</b> (Men <sub>2</sub> P(2-ClPh))	88	88
4	<b>L4</b> (MenSPhos)	28 (25) <sup>d</sup>	68

a) Analytical yields (mol-%) calculated by <sup>1</sup>H-qNMR analysis using an internal standard.

b) Conversions (mol-%) of **54** determined by <sup>1</sup>H-qNMR analysis using an internal standard.

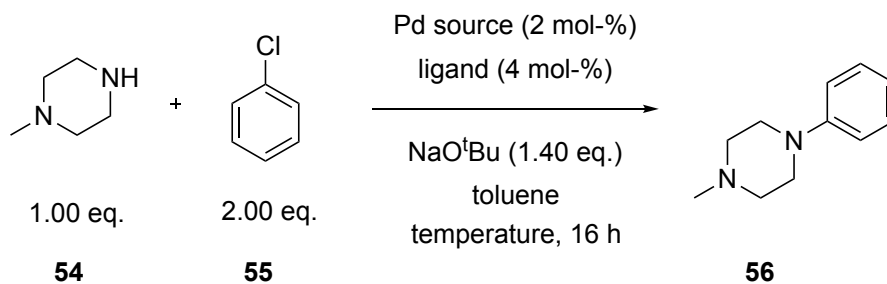
c) These results were produced by a co-worker and are listed for a complete overview.

d) Isolated yields in brackets.

### Investigations of the Use of Phenyl dimethylphosphine in the Buchwald-Hartwig Coupling

Based on the initial assessment, ligand **L2** appeared to be a promising candidate for application in Buchwald-Hartwig coupling. However, the high temperature and strong basicity in the first test reaction are unfavorable in terms of substrate tolerance and environmental impact. Therefore, the performance of **L2** (Men<sub>2</sub>PPh) was tested at lower temperatures (table 19).

**Table 19.** Buchwald-Hartwig coupling of *N*-methylpiperazine using **L2** as steering ligand at lower temperatures.



entry	Pd source	ligand	temperature	yield /% <sup>a</sup>	comment
1	PdCl <sub>2</sub> (MeCN) <sub>2</sub>	<b>L2</b>	r.t.	-	-
2	PdCl <sub>2</sub> (MeCN) <sub>2</sub>	<b>L2</b>	60 °C	-	-
3	Pd(OAc) <sub>2</sub>	<b>L2</b>	r.t.	3	-
4	PdCl <sub>2</sub> (PPhMen) <sub>2</sub>	-	r.t.	-	-
5	PdCl <sub>2</sub> (PPhMen) <sub>2</sub>	-	60 °C	2	-
6	PdCl <sub>2</sub> (MeCN) <sub>2</sub>	<b>L2</b>	60 °C	-	with Pd “preactivation” <sup>b</sup>

a) Analytical yields (mol-%) calculated by <sup>1</sup>H-qNMR analysis using an internal standard.

b) Pd preactivation: PdCl<sub>2</sub>(MeCN)<sub>2</sub> (2 mol-%), **L2** (4 mol-%), NaOtBu (16 mol-%) were heated in toluene (1 mL) to 120°C for 30 minutes in a Schlenk tube under argon.

Using PdCl<sub>2</sub>(MeCN)<sub>2</sub> as a palladium precursor did not afford any target material (entries 1 – 2). Assuming that PdCl<sub>2</sub>(MeCN)<sub>2</sub> might have low solubility in toluene at lower temperatures, the palladium precursor was switched to the more soluble Pd(OAc)<sub>2</sub> (entry 3), which gave only a low yield. Palladium complex PdCl<sub>2</sub>(PPhMen)<sub>2</sub> showed no reaction at room temperature (entry 4) and gave a very low yield at 60°C (entry 5). Following the assumption that the rate limiting step of the reaction might be the Pd(II)/Pd(0) reduction which is required for entering the catalytic cycle, a Pd preactivation process was envisaged (entry 6).

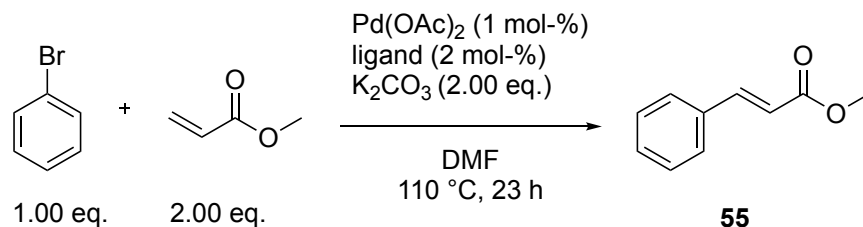
As reported by *Grushin* and *Alper*, the reduction of Pd(II) species to the catalytically active Pd(0) species is likely caused by residual amounts of OH<sup>-</sup> in the organic or inorganic base used in palladium(II)-catalyzed cross-coupling reactions.<sup>110</sup> It was therefore assumed that, in order to conduct the coupling at lower temperature, heating only palladium precursor and ligand with a small amount of base might be necessary to obtain the desired palladium(0) species prior to the cross-coupling reaction. This procedure, however, did not afford any desired target material. Further attempts of conducting the model reaction at lower temperature were not undertaken, but a water preactivation as reported by Buchwald and co-workers or the direct use of a Pd(0) species might be promising to attempt in future endeavours.<sup>111</sup>



## Ligands L1-L5 in the Mizoroki-Heck Coupling

Ligands **L1-L5** were tested in the palladium-catalyzed Mizoroki-Heck coupling of bromobenzene and methyl acrylate (table 20).

**Table 20.** Screening of (aryl)dimenthylphosphine ligands in the Mizoroki-Heck model reaction.



entry	ligand	yield /% <sup>a</sup>
1	<b>L1</b> (MenJohnPhos)	25
2	<b>L2</b> (Men <sub>2</sub> PPh)	94
3	<b>L3</b> (Men <sub>2</sub> P(2-ClPh))	16
4	<b>L4</b> (MenSPhos)	2
5	<b>L5</b> (Men <sub>2</sub> PNap)	0 <sup>b</sup>

a) Analytical yields (mol-%) calculated by <sup>1</sup>H-qNMR analysis using an internal standard.

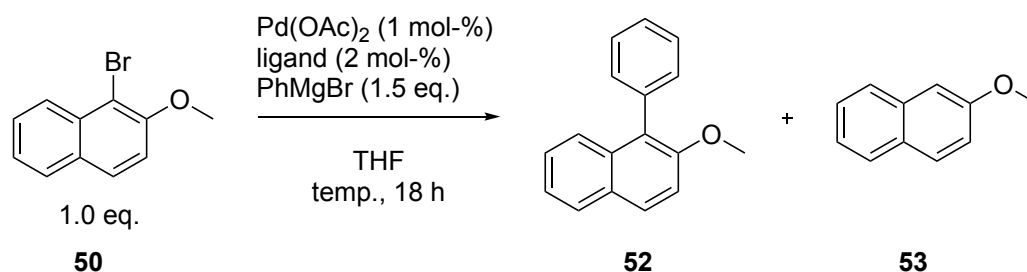
b) Formation of dimerized methyl acrylate was observed in trace amounts.

The best result was obtained with (aryl)dimenthylphosphine ligand **L2** (entry 2) with a near quantitative yield. The *ortho*-biaryl ligands **L1** and **L4**, on the other hand, gave low to almost no yield (entries 1 and 4). This agrees with the findings in literature, where dialkylbiaryl phosphine ligands have been reported seldomly as ligands in Heck coupling, but classic monophosphine ligands like PPh<sub>3</sub> and P(*o*-tolyl)<sub>3</sub> are more common.<sup>112</sup> Interestingly, **L3**, which is only distinguished from **L2** by a chlorine moiety in *ortho*-position to the dimethyl phosphino donor group, performed rather poorly. The use of (1-naphthyl)dimenthylphosphine **L5** did not result in any formation of *E*-styrene, but dimerization product was formed in trace amounts, presumably *via* an 1,4 addition elimination mechanism (entry 5).

## Ligands L1-L5 in Pd- and Ni-catalyzed Kumada-Corriu Coupling

As another model reaction, the palladium catalyzed Kumada-Corriu coupling of phenylmagnesium bromide and 1-bromo-2-methoxy naphthalene was tested using ligands **L1-L5** (table 21). For comparison, the ligand SPhos by Buchwald and co-workers<sup>5</sup> was also tested.

**Table 21.** Ligand evaluation in a Kumada-Corriu coupling



entry	ligand	temperature	<b>50</b> /% <sup>a</sup>	<b>52</b> /% <sup>a</sup>	<b>53</b> /% <sup>a</sup>	recovery /% <sup>a</sup>
1	<b>L2</b> ( $\text{Men}_2\text{PPh}$ )	70 °C	2	98	0	100
2	SPhos	70 °C	0	88	4	92
3	<b>L1</b> ( $\text{MenJohnPhos}$ )	r.t.	77	7	11	95
4	<b>L2</b> ( $\text{Men}_2\text{PPh}$ )	r.t.	13	79	3	95
5	<b>L3</b> ( $\text{Men}_2\text{P}(2\text{-ClPh})$ )	r.t.	62	26	7	95
6	<b>L4</b> ( $\text{MenSPhos}$ )	r.t.	75	3	9	87
7	<b>L5</b> ( $\text{Men}_2\text{PNap}$ )	r.t.	61	27	10	98
8	SPhos	r.t.	0	86	7	93

a) Analytical yields (mol-%) calculated by <sup>1</sup>H-qNMR analysis using an internal standard.

At first, the coupling was conducted with heating using **L2** or SPhos as steering ligands (entries 1, 2). **L2** gave excellent, near quantitative yield, which was considerably higher than benchmark ligand SPhos. These promising results implied that the reaction might also be feasible at room temperature. Indeed, the model reaction afforded good results even at room temperature with **L2** as ligand (entry 4). Compared to SPhos, however, its performance is slightly poorer (entry 8). The other tested ligands afforded only low yields. Surprisingly, **L4**, which is the menthyl analogue of SPhos, afforded almost no target material. MenJohnPhos (**L1**) also afforded a very low yield. All in all, the biaryl motif combined with the bulky menthyl moieties attached to phosphorus seem to be detrimental for the Kumada-Corriu coupling, whereas monoaryl combined with a dimethyl moiety is beneficial. An interesting addition for this ligand screening would be dicyclohexylphenyl phosphine to assess the combination of monoaryl and cyclohexyl moieties. Substituents on the phenyl moiety in *o*-position to phosphorus (Cl for **L3**,

entry 5, and a benzoannulation for **L5**, entry 7) other than phenyl are more beneficial, but still afford low yields.

### Further Investigations of **L2** as Steering Ligand in Kumada-Corriu Cross-Coupling

The promising activities obtained with **L2** in palladium catalyzed Kumada-Corriu coupling justified further investigations. Figure 13 compares the rate of the formation of **52** when using **L2** or SPhos as ligands. After 4.5 hours, the use of Men<sub>2</sub>PPh already afforded near 70% of product. On the other hand, SPhos provides a rather slow rate of product formation in the first few hours, with only 24% yield after 4.5 hours. These findings show that **L2** is competitive with the benchmark *Buchwald* ligand SPhos, and further examinations into its substrate scope might be promising.

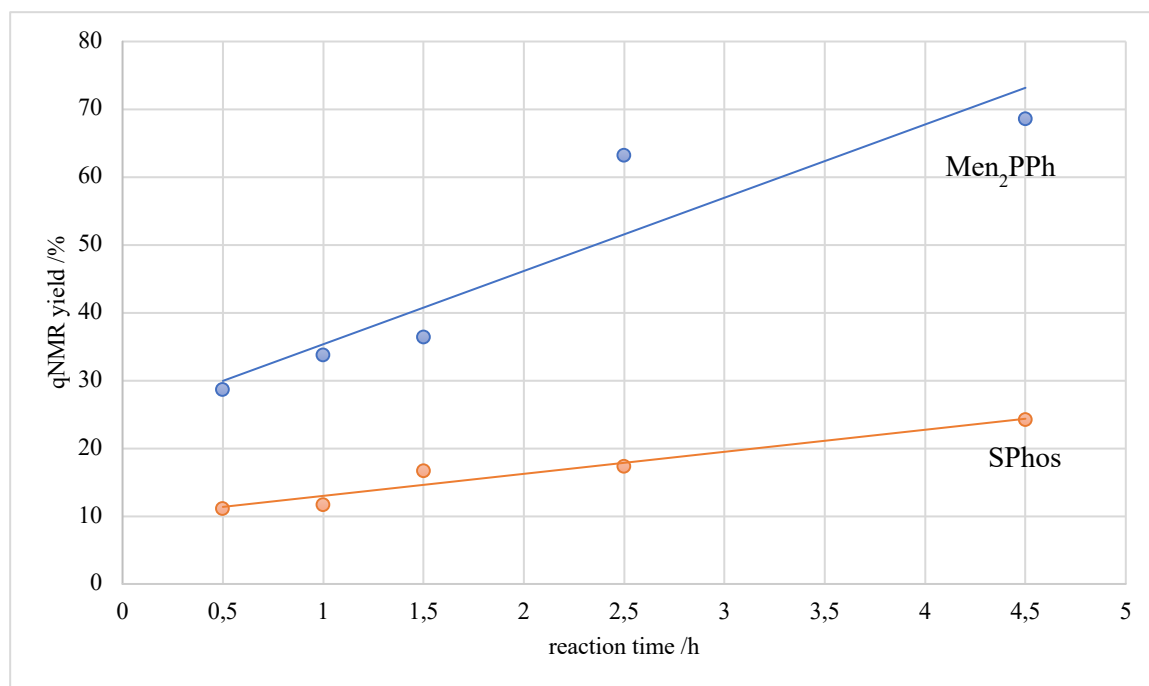
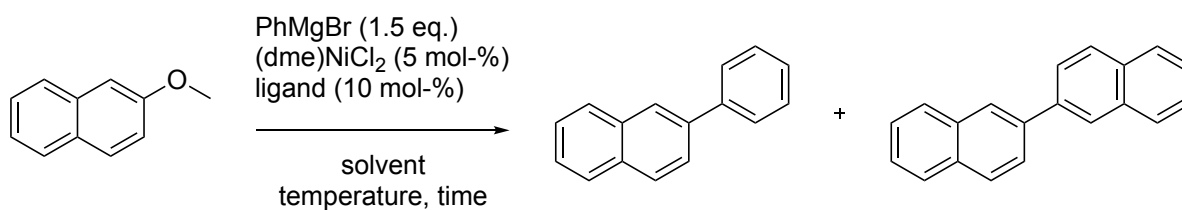


**Figure 13.** Reaction progress of **52** when using Men<sub>2</sub>PPh (**L2**) (blue) vs. SPhos (orange) as ligand.

As another Kumada-Corriu type transformation, the demethoxylative nickel-catalyzed coupling of phenylmagnesium bromide and 2-methoxynaphthalene was investigated, with the ultimate insight to enable sequential Pd- and Ni- catalyzed Kumada-Corriu coupling using only one ligand. The performance of **L2** compared to PCy<sub>3</sub>, which is a commonly used ligand in this transformation, as described by Dankwardt (table 22).<sup>113</sup>

**Table 22.** Ni-catalyzed demethoxylative coupling of 2-methoxynaphthalene and phenylmagnesium bromide.



entry	solvent	ligand	time /h	temperature	<b>58</b> /% <sup>a</sup>	<b>59</b> /% <sup>a, b</sup>
1	THF	<b>L2</b>	21	60 °C	59	17
2	toluene-THF	<b>L2</b>	14	r.t.	61	18
3	toluene-THF	PCy <sub>3</sub>	14	r.t.	83	10

a) Analytical yields (mol-%) calculated by <sup>1</sup>H-qNMR analysis using an internal standard.

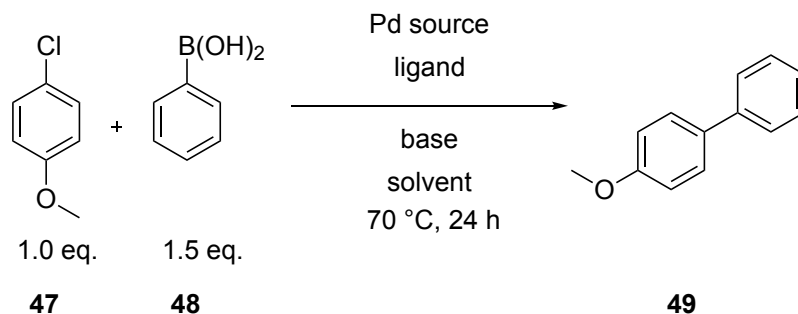
b) Yield of the dimer based on naphthyl monomer unit.

In a first attempt, the reaction was performed in THF with heating (entry 1), which resulted in a rather humble yield. As Dankwardt reported, nonpolar solvents are preferred for this transformation due to assumed poisoning of the catalysis by MgBr(OMe) formed during this reaction.<sup>113</sup> Therefore, a toluene-THF solvent mixture was tested and compared directly to the use of PCy<sub>3</sub> under the same condition (entries 2, 3). Since this model reaction was performed at room temperature in the literature using PCy<sub>3</sub>, the same conditions were chosen using **L2** for a direct comparison. This gave comparable results to the first condition, while standard ligand PCy<sub>3</sub> clearly outperforms **L2**. However, both conditions using **L2** show complete conversion, with formation of homocoupled 2,2'-binaphthyl as by-product.

## Evaluation of L1-L5 in Suzuki-Miyaura Coupling

The performance of **L1-L5** was evaluated in the palladium-catalyzed Suzuki-Miyaura coupling of 4-chloroanisole and phenylboronic acid under two different conditions, as presented in table 23.

**Table 23.** Evaluation of ligands **L1-L5** in the Suzuki-Miyaura coupling of 4-chloroanisole and phenyl boronic acid.



entry	Pd source	ligand	solvent	base	yield /% <sup>a</sup>
1 <sup>b</sup>	Pd(OAc) <sub>2</sub> (1 mol-%)	<b>L1</b> (MenJohnPhos) (2 mol-%)	toluene	K <sub>3</sub> PO <sub>4</sub> (2.0 eq.)	>99%
2 <sup>b</sup>	Pd(OAc) <sub>2</sub> (1 mol-%)	<b>L2</b> (Men <sub>2</sub> PPh) (2 mol-%)	toluene	K <sub>3</sub> PO <sub>4</sub> (2.0 eq.)	12
3 <sup>b</sup>	Pd(OAc) <sub>2</sub> (1 mol-%)	<b>L4</b> (MenSPhos) (1 mol-%)	toluene	K <sub>3</sub> PO <sub>4</sub> (2.0 eq.)	93
4 <sup>c</sup>	Pd(OAc) <sub>2</sub> (2 mol-%)	<b>L1</b> (MenJohnPhos) (4 mol-%)	THF	K <sub>2</sub> CO <sub>3</sub> (3.0 eq.)	66
5 <sup>c</sup>	Pd(OAc) <sub>2</sub> (2 mol-%)	<b>L2</b> (Men <sub>2</sub> PPh) (4 mol-%)	THF	K <sub>2</sub> CO <sub>3</sub> (3.0 eq.)	3
6 <sup>c</sup>	Pd(OAc) <sub>2</sub> (2 mol-%)	<b>L3</b> (Men <sub>2</sub> P(2-ClPh)) (4 mol-%)	THF	K <sub>2</sub> CO <sub>3</sub> (3.0 eq.)	69
7 <sup>c</sup>	Pd(OAc) <sub>2</sub> (2 mol-%)	<b>L4</b> (MenSPhos) (4 mol-%)	THF	K <sub>2</sub> CO <sub>3</sub> (3.0 eq.)	59
8 <sup>c</sup>	Pd(OAc) <sub>2</sub> (2 mol-%)	<b>L5</b> (Men <sub>2</sub> PNap) (4 mol-%)	THF	K <sub>2</sub> CO <sub>3</sub> (3.0 eq.)	1

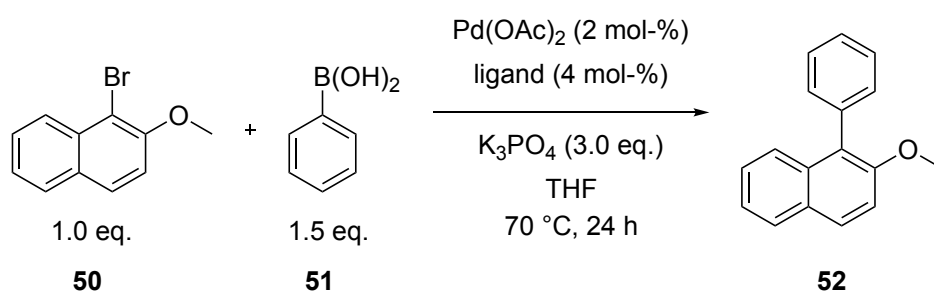
- a) Analytical yields (mol-%) calculated by <sup>1</sup>H-qNMR analysis using an internal standard.
- b) Condition A: Performed according to general procedure GP-5-A.
- c) Condition B: Performed according to general procedure GP-5-B.

Again, the two tested conditions are not results of systematic optimizations, but were tested independently from another based on conditions reported in literature.<sup>1,108</sup> The use of

MenJohnPhos (**L1**) gave an excellent yield using condition A (entry 1), but a considerably lower yield with condition B (entry 4). The same applies to MenSPhos (**L4**) (compare entries 3 and 7). Notably, condition A actually uses a lower catalyst loading. **L2** did not perform well in both conditions (entries 2 and 5). **L3** gave a decent yield for condition B (entry 6). **L5** performed very poorly.

Next, **L1-L5** were tested in the Pd-catalyzed *Suzuki-Miyaura* coupling of sterically hindered aryl bromide 1-bromo-2-methoxynaphthalene and phenyl boronic acid, as seen in table 24.

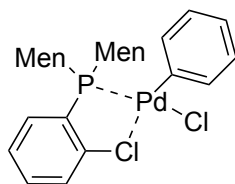
**Table 24.** Ligand screening for the Pd-catalyzed *Suzuki-Miyaura* coupling of 1-bromo-2-methoxy naphthalene and phenyl boronic acid.



entry	ligand	52 /% <sup>a</sup>
1	<b>L1</b> (MenJohnPhos)	69
2	<b>L2</b> (Men <sub>2</sub> PPh)	94
3	<b>L3</b> (Men <sub>2</sub> P(2-ClPh))	86
4	<b>L4</b> (MenSPhos)	97
5	<b>L5</b> (Men <sub>2</sub> PNap)	27

a) Analytical yields (mol-%) calculated by <sup>1</sup>H-qNMR analysis using an internal standard.

In this model reaction, dimethyl(phenyl)phosphine (**L2**) and MenSPhos (**L4**) performed best with near quantitative yields (entries 2 and 4). **L3** performed almost as good (entry 3), and the use of **L1** afforded moderate results (entry 1). **L5** gave poor results (entry 5). The excellent performance of **L2** comes as a surprise, as it afforded almost no target material for the coupling of chloroanisole (table 23). This implies that with this ligand, oxidative addition is slow with less activated substrates. In contrast, **L3** gives good results with both aryl bromide and chloride. Assumedly, the chlorine in *ortho*-position stabilizes Pd(0) and Pd(II) complexes formed in the catalytic cycle by donating electron-density of the chlorine lone pairs to palladium, and the same interaction could also be responsible for accelerating oxidative addition similar to the case of Buchwald ligands (scheme 42). Such a halogen-metal interaction involving 2-haloaryl phosphine ligands has been reported in the case of Ir and Rh.<sup>114,115</sup>



**Scheme 42.** Proposed Pd(II) complex of **L3** formed by oxidative addition with stabilizing *o*-Cl-Pd interactions.

### Evaluation of L1-L4 in as Steering Ligands in Asymmetric Suzuki-Miyaura Coupling

In order to assess the dimethylphosphino motif's ability to induce asymmetry in enantioselective reactions, the coupling of 1-naphthylboronic acid and 1-bromo-2-methoxynaphthalene was tested with ligands **L1-L4** and the product was analyzed by chiral HPLC. As **L5** had performed poorly in previous Suzuki-Miyaura couplings, assessment of its performance was omitted for this model reaction. The obtained yields and enantiomeric ratios are presented in table 25.

**Table 25.** Asymmetric Suzuki-Miyaura coupling of 1-naphthylboronic acid and 1-bromo-2-methoxynaphthalene.

entry	ligand	yield /% <sup>a</sup>	e.r. <sup>b</sup>
1	<b>L1</b> (MenJohnPhos)	33	57:43
2	<b>L2</b> (Men <sub>2</sub> PPh)	52	74:26
3	<b>L3</b> (Men <sub>2</sub> P(2-ClPh))	62	74:26
4	<b>L4</b> (MenSPhos)	56	69:31

a) Analytical yields (mol-%) calculated by <sup>1</sup>H-qNMR analysis using an internal standard.

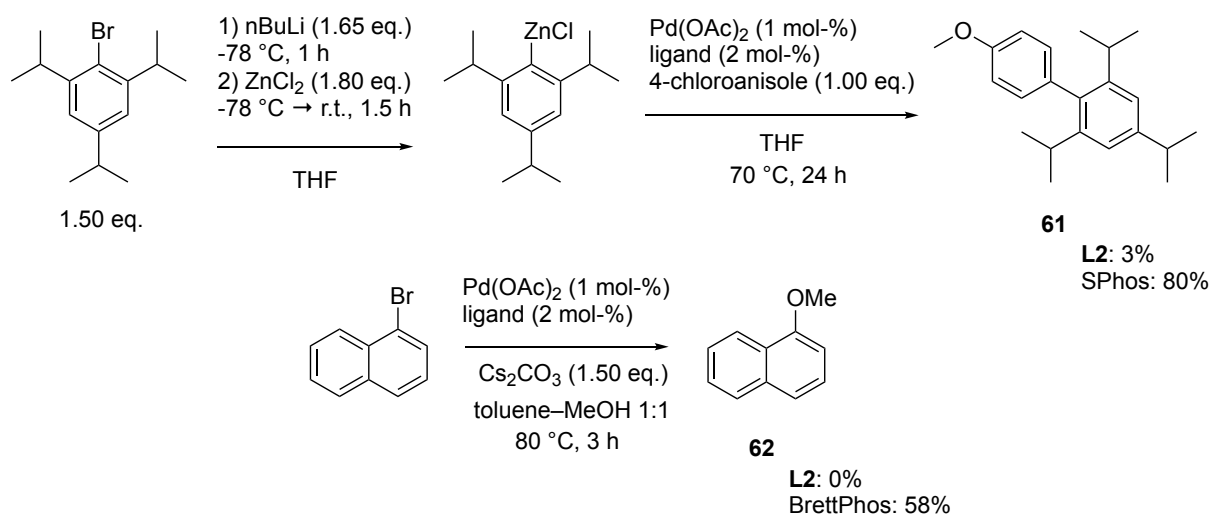
b) Enantiomeric ratios from chiral HPLC analysis of purified product.

MenJohnPhos (**L1**) showed the poorest activity with a low yield and only a low, but distinct enantiomeric enrichment (entry 1). MenSPhos (**L4**) performed better with a moderate yield and a moderate enantiomeric ratio (entry 4). The best ligands for the asymmetric coupling was (aryl)dimethyl phosphine ligands **L2** and **L3**, which, while still only delivering a moderate

yield, showed a better enantiomeric enrichment (entries 2 and 3). These results demonstrate the potential of the dimethylphosphino moiety to act as chiral ligands in asymmetric catalysis.

### Further Catalytic Test Reactions Using L2 as Ligand

Men<sub>2</sub>PPh (**L2**) was furthermore tested in the Pd-catalyzed Negishi coupling of 2,4,6-triisopropylphenylzinc chloride and 4-chloroanisole<sup>13</sup> and in the C-O coupling of 1-bromonaphthalene with methoxide<sup>116</sup> (scheme 43) and its performance was compared to that of *Buchwald* ligands. Both couplings were adapted from literature procedures. However, both tested couplings were unsuccessful, and no further examination was undertaken.



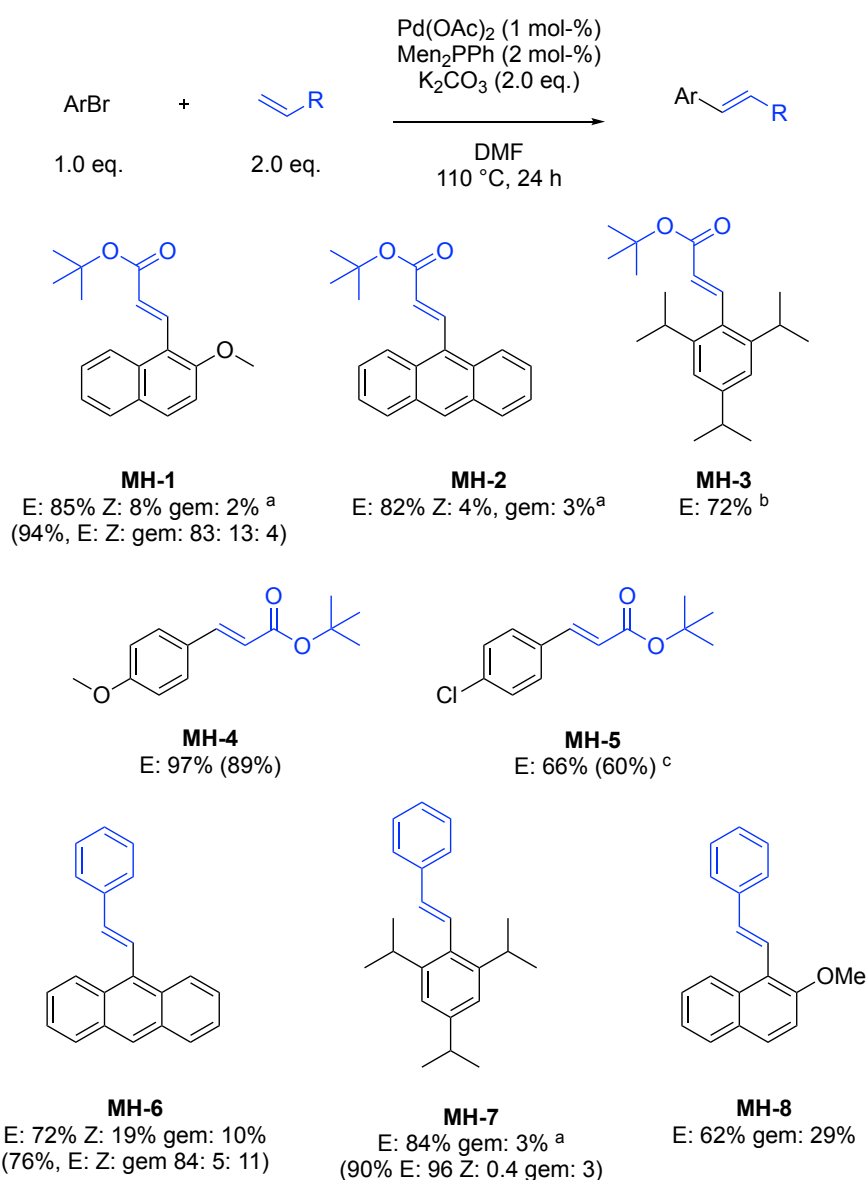
**Scheme 43.** Results of the Negishi coupling and C-O coupling using **L2** and benchmark ligands. Analytical yields (mol-%) were determined by <sup>1</sup>H-qNMR analysis using an internal standard.



## 2.7.2 (Aryl)dimethylphosphines in Catalytic Coupling Reactions: Investigation on Substrate Scopes

### Substrate Scope: L2 in the Mizoroki-Heck Coupling

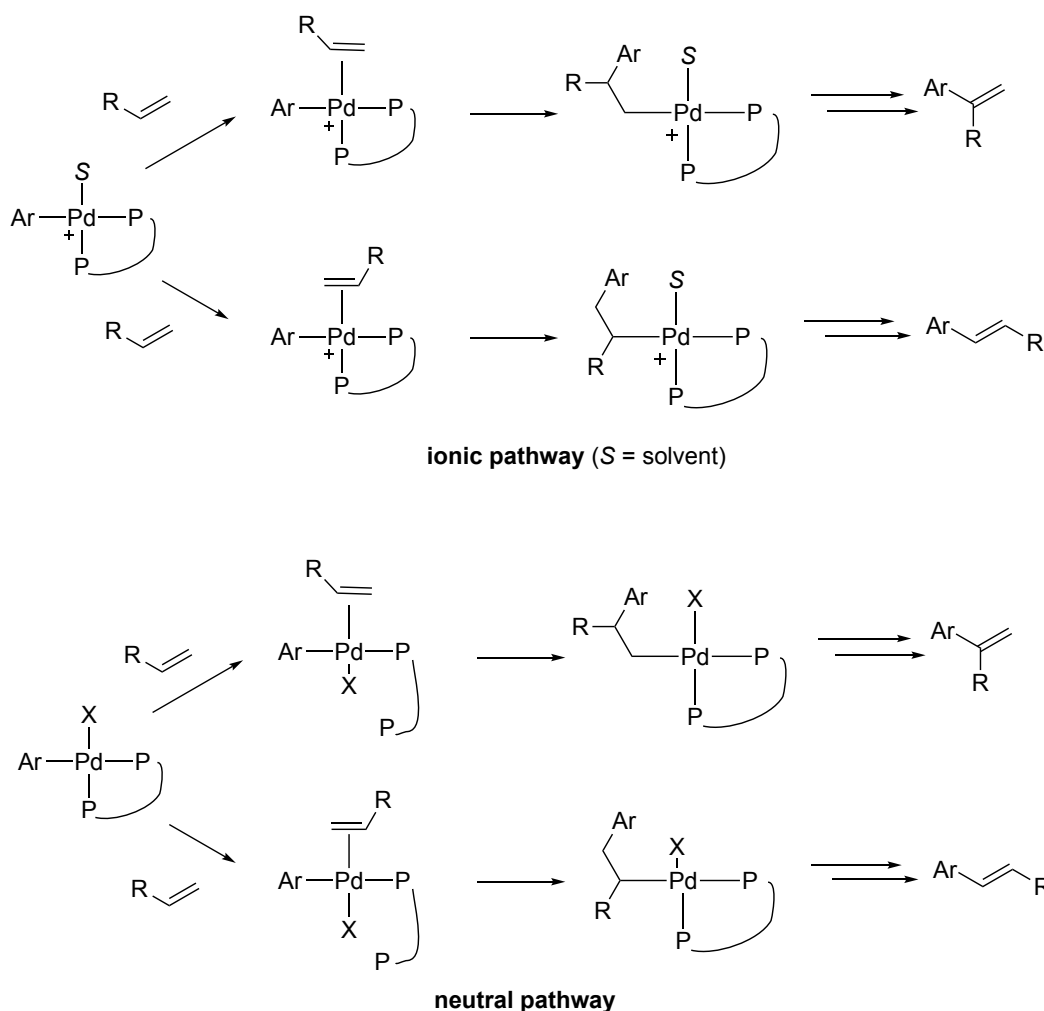
Dimethyl(phenyl)phosphine **L2** gave promising results in the model Mizoroki-Heck coupling of bromobenzene and methyl acrylate (see section 0.1). Its applicability to further substrate combinations was therefore assessed. Scheme 44 shows the results in case of combining sterically hindered or unactivated aryl bromides with *t*-butyl acrylate or styrene as alkene coupling partners, with the analytical yields of *Z*-, *E*- and *gem*-alkenes given below.



**Scheme 44.** Substrate scope of the Mizoroki-Heck coupling. Analytical yields (mol-%) are determined by <sup>1</sup>H-qNMR analysis using toluene or dibenzyl ether as internal standard. Isolated yields in brackets.

<sup>a)</sup> Average yields of two runs. <sup>b)</sup> The reaction was conducted at 150°C. <sup>c)</sup> 1.1 eq. of the alkene was used.

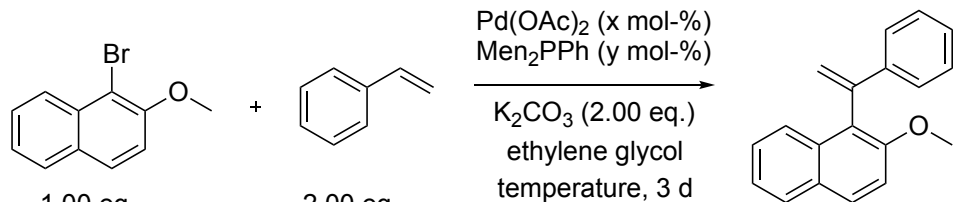
The ligand produced good to excellent yields using sterically hindered aryl bromides and *tert*-butyl acrylate (**MH-1-3**). However, *E*-selectivity was relatively low. Generally, *E*-, *Z*- and regioselectivity seems to decrease with increasing sterical bulk of the aryl bromide. Unactivated aryl bromides (**MH-3-4**) were also coupled in moderate to excellent yields. For 1-bromo-4-chlorobenzene, the excess of alkene had to be lowered to give a selective result. Otherwise, a considerable amount of divinylated product was observed. As for styrene as coupling partner, sterically hindered aryl bromides gave excellent yields, but low *E:Z:gem* selectivity (**MH5-7**). Surprisingly, in all three cases, the geminal (branched) alkene was produced as by-product in considerable amount. In the case of **MH-7**, the ratio of regioisomers *E:gem* was even 2:1, with geminal alkene produced in 29% analytical yield. A such high ratio of  $\alpha$ -arylation of an alkene is odd for the Mizoroki-Heck coupling, which typically selectively results in *E*-alkenes. The amount of  $\alpha$ -arylation in the Mizoroki-Heck coupling is usually determined by the type of mechanism which is prevalent (scheme 45).<sup>117</sup>



**Scheme 45.** Ionic vs. neutral pathway of the Mizoroki-Heck reaction leading to geminal or *E*-alkenes with a bisphosphine ligand.<sup>117</sup>

In case of the ionic mechanism, which is favored by aryl triflates or when using halide scavengers, electron-rich alkenes, bisphosphine ligands and polar solvents, a cationic Pd(II) complex is formed as intermediate.<sup>117</sup> This intermediate is more sensitive towards electronic factors, resulting in orientation of the charge-deficient  $\alpha$ -carbon towards the aryl moiety, which leads to the branched alkene as major product. On the other hand, the neutral intermediate, which is prevalent with the coupling of electron-deficient alkenes, is more sensitive towards steric factors, leading to the linear alkene as major product. The high amount of formed geminal alkene especially for substrate **MH-7** seems odd because the favorable conditions for an ionic pathway are not given. There are, however, some examples in the literature where a high amount of branched alkene is reported when coupling sterically hindered aryl bromides.<sup>118</sup> So far, mainly bisphosphines have been reported as ligand for  $\alpha$ -regioselectivity in the Mizoroki-Heck coupling.<sup>119</sup> It therefore became of interest to improve the unexpected regioselectivity seen with the use of monophosphine ligand **L2** by changing the reaction conditions in such a manner that the ionic pathway would be favored. Hereby, a selective  $\alpha$ -arylation leading to the branched alkene was envisaged. According to literature reports, the ionic pathway is preferred when using polar, hydrogen-bond donor solvents such as ionic liquid or ethylene glycol. Supposedly, these help abstract halide to form the cationic Pd(II) complex.<sup>120</sup> Therefore, the coupling of 1-bromo-2-methoxynaphthalene and styrene was repeated in ethylene glycol as solvent (table 26).

**Table 26.** Attempts for the  $\alpha$ -arylation of styrene with 1-bromo-2-methoxy naphthalene.



entry	Pd(OAc) <sub>2</sub> (x mol-%)	Men <sub>2</sub> PPh (y mol-%)	temperature	yield /% <sup>a</sup>	E /% <sup>a</sup>
1	1	2	110°C	8	15
2	2	4	145°C	5	8

a) Analytical yields (mol-%) calculated by <sup>1</sup>H-qNMR analysis using an internal standard.

This condition resulted in a much lower yield, while still maintaining an *E:gem* ratio of roughly 2:1 (entry 1). Raising the catalyst loading and temperature (entry 2) led to even lower yields,

which is possibly explained by polymerization. It was thus decided not to follow the quest towards  $\alpha$ -regioselectivity any further.

The reactivity of aryl chlorides in the Pd(OAc)<sub>2</sub>/Men<sub>2</sub>PPh catalyst system was also assessed for the Mizoroki-Heck coupling (table 27).

**Table 27.** Mizoroki-Heck coupling of aryl chlorides using the Pd(OAc)<sub>2</sub>/Men<sub>2</sub>PPh catalyst system.

entry	substrate	additive	yield /% <sup>a</sup>
1	PhCl	-	trace
2	PhCl	TBAB (0.5 eq.)	trace
3	4-OMePhCl	-	10

a) Analytical yields (mol-%) calculated by <sup>1</sup>H-qNMR analysis using an internal standard.

The coupling of chlorobenzene gave only trace amounts of desired target material (entry 1). Addition of tetrabutylammonium bromide<sup>121</sup> as additive did not lead to any change (entry 2). Surprisingly, electron-rich aryl chloride 4-chloroanisole was a slightly better substrate, however still affording very low yield (entry 3). Generally, the findings show that aryl chlorides are not suitable substrates for the Pd(OAc)<sub>2</sub>/Men<sub>2</sub>PPh catalyst system under typical reaction conditions.

### On the Type of Catalytic System When Using L2 in the Mizoroki-Heck Reaction

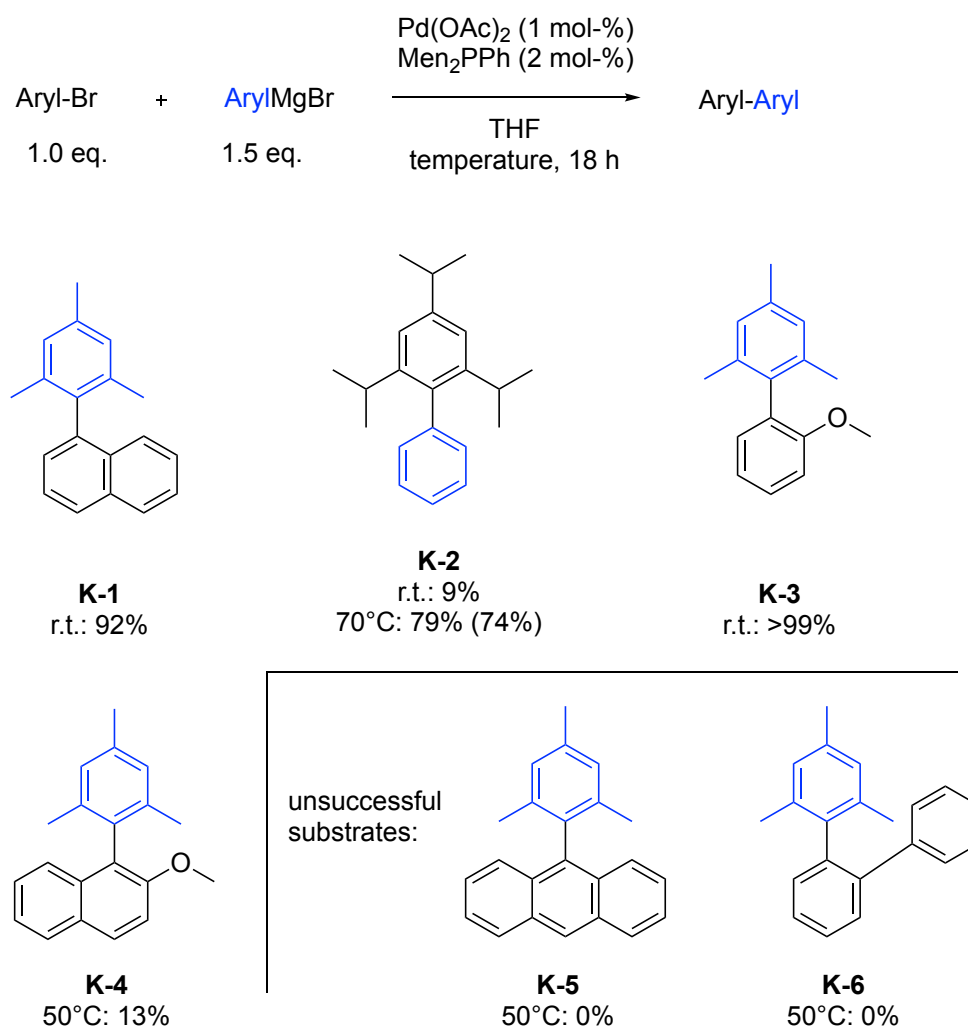
Mizoroki-Heck reactions are thought to follow one of four mechanisms depending on the catalytic system and reaction conditions employed. Beletskaya and Cheprakov defined type 1 as the “classic” Mizoroki-Heck coupling, where typical substrates are aryl iodides or activated aryl bromides and ancillary ligands are not necessary.<sup>122</sup> Typical ligands in this type of catalytic system are simple anionic species such as acetate or chloride. With type 2 catalytic systems, on the other hand, ligands usually only play a supporting role rather than forming defined oxidative addition complex. This type of catalytic system typically employs aryl bromides and activated aryl chlorides as substrates and is defined by its lacking robustness: A slight change of reaction conditions or substrate leads to worse catalytic performance. The type 3 catalytic system, on the other hand, is truly ligand-accelerated and tolerates unactivated aryl chlorides and bromides as substrates. The type 4 catalytic system, which leads to geminal alkenes, shall be neglected

here as it is not of importance at this point. The reaction conditions used in this work, namely DMF as polar coordinating solvent and a relatively high reaction temperature of 110 °C support the assumption that the  $\text{Men}_2\text{PPh}/\text{Pd}(\text{OAc})_2$  catalytic system can be described as type 2, with the ligand not fulfilling an activating function with defined oxidative addition complexes, but rather a supporting function without contributing to a defined catalytically active palladium(0) species. This assumption is moreover supported by the substrate scope, which was limited to unactivated aryl bromides, but failed for aryl chlorides (except for unactivated *tert*-butyl(*E*)-3-(4-chlorophenyl)acrylate, which was formed from 4-chloro-1-bromo benzene and afforded doubly vinylated product under standard conditions).<sup>122</sup>

Arguments for a type 3 catalytic system and thus a truly accelerating function of the ligand would be the robustness of the catalytic system – for type 2 systems, a slight change to reaction conditions, for example substrate combinations, can be detrimental for the outcome of the reaction and therefore usually requires further tuning of the reaction conditions. Furthermore, a clear difference in performance was shown when using no ligand (see table 16, entry 4), thus indicating that ligand choice does play a role for these conditions. Tuning the reaction conditions to those typically employed for type 3 catalytic systems could be beneficial to reach a better tolerance for aryl chlorides as substrates.

## Substrate Scope: L2 in the Kumada-Corriu Coupling

Due to the promising ligand qualities of dimethyl(phenyl)phosphine **L2**, its substrate scope in the Kumada-Corriu coupling reaction was evaluated. As its use afforded good results in the coupling of phenylmagnesium bromide and 1-bromo-2-methoxynaphthalene, its efficacy in the synthesis of other sterically hindered biaryls, such as di-, tri- and tetra-*ortho*-substituted ones, was evaluated first (scheme 46).



**Scheme 46.** Substrate scope in the synthesis of di-, tri- and tetra-*ortho*-substituted biaryls for the Kumada-Corriu coupling using dimethyl(phenyl)phosphine (**L2**). Analytical yields (mol-%) calculated by  $^1\text{H}$ -qNMR analysis using an internal standard. Isolated yields are given in brackets.

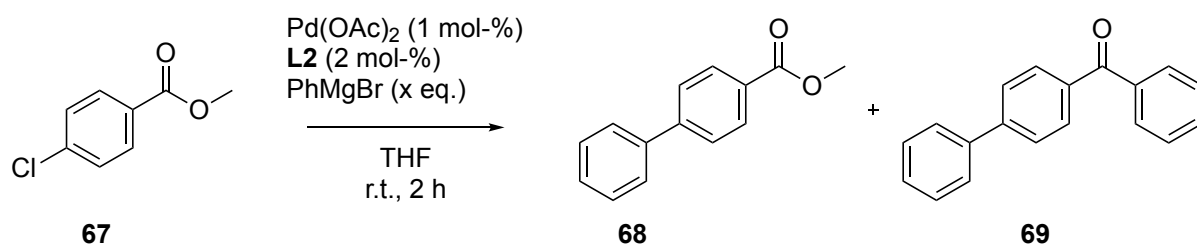
The formation of tri-*ortho*-substituted substrates worked out excellently with mesitylmagnesiumbromide as nucleophile (**K-1** and **K-3**) at room temperature. As a comparison, **K-3** was obtained by Kumada-Corriu coupling by Organ *et al.* using the well-established NHC complex PEPPSI-IPr at 50 °C in a yield of 86%.<sup>123</sup> This somewhat demonstrates a competitiveness of ligand **L2** with benchmark ligands. Mesitylmagnesiumbromide is sterically hindered, but electron-rich due to  $\sigma$ -donation of the

three methyl groups, which makes it an easier substrate. On the contrary, with sterically hindered and electron-rich 1-bromo-2,4,6-triisopropylbenzene as electrophile and phenylmagnesium bromide as nucleophile, a successful coupling was only possible at elevated temperature (**K-2**). As for tetra-*ortho*-substituted substrates, the coupling of 2,4,6-mesitylmagnesiumbromide afforded low yields with 1-bromo-2-methoxynaphthalene as electrophile even with heating (**K-4**) and no target material with 9-bromoanthracene (**K-5**). *Ortho*-substituted aryl bromide 2-bromobiphenyl was also not a successful substrate (**K-6**). Apparently, a phenyl moiety in *ortho*-position of the aryl bromide is too much of a sterical hindrance. Overall, the Kumada-Corriu coupling towards tri-*ortho*-substituted biaryls works well with **L2** as ligand.

### Screening of *Grignard*-sensitive Substrates

One of the issues with Kumada-Corriu couplings is their relatively low functional group tolerance due to the reactivity of the employed *Grignard* reagents as nucleophiles. Some groups have demonstrated the applicability of these couplings even with sensitive substrates, for example by using *Knochel*-type reagents<sup>124</sup>, low-temperature reactions<sup>12</sup> or a slow addition of *Grignard* reagents.<sup>125</sup> Using the latter strategy, the coupling of methyl 4-chlorobenzoate **67** and phenylmagnesium bromide was attempted using **L2** as ligand (table 28).

**Table 28.** Kumada-Corriu coupling of **67** and phenyl magnesium bromide using **L2**.



entry	PhMgBr /x eq.	<b>67</b> /% <sup>a</sup>	<b>68</b> /% <sup>a</sup>	<b>69</b> /% <sup>a</sup>	recovery /% <sup>a</sup>
1	1.50 <sup>b</sup>	16	31	6	55
2	1.10 <sup>c</sup>	35	28	4	72

a) Analytical yields (mol-%) and recoveries (mol-%) calculated by <sup>1</sup>H-qNMR analysis using an internal standard.

b) The *Grignard* solution was added over a period of 2 hours.

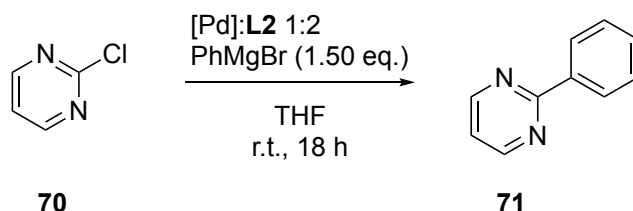
c) The *Grignard* solution was added over a period of 50 minutes.

For both entries, the *Grignard* solution was added slowly over a longer period of time (although addition time varied) to avoid side reactions. Evidently, lowering the amount of *Grignard*

reagent did not improve the yield of **68** substantially (entry 2), but recovery improved while conversion decreased. Thus, the fate of unrecovered material is explained by side reactions. Even though the aromatic region of the  $^1\text{H-NMR}$  spectrum indicates a plethora of side products, these cannot be clearly identified due to overlapping signals.

Nitrogen-containing heterocycles are another type of substrates that is typically not well tolerated in the Kumada-Corriu coupling reaction.<sup>125</sup> Thus, 1-chloropyrimidine **70** was also tested as substrate with **L2** as ligand (table 29).

**Table 29.** Kumada-Corriu coupling of **70** with phenyl magnesium bromide.



entry	[Pd] <sup>a</sup>	solvent	yield /% <sup>b</sup>	recovery /% <sup>b</sup>
1	1 mol-%	THF	18	34
2	2 mol-%	THF	20	28
3	1 mol-%	THF–toluene 3:4	18	27

*Grignard* reagent was added over a course of 20 – 30 minutes.

- a) Pd(OAc)<sub>2</sub> was used as Pd source.  
 b) Analytical yields (mol-%) and recoveries (mol-%) calculated by  $^1\text{H-qNMR}$  analysis using an internal standard.

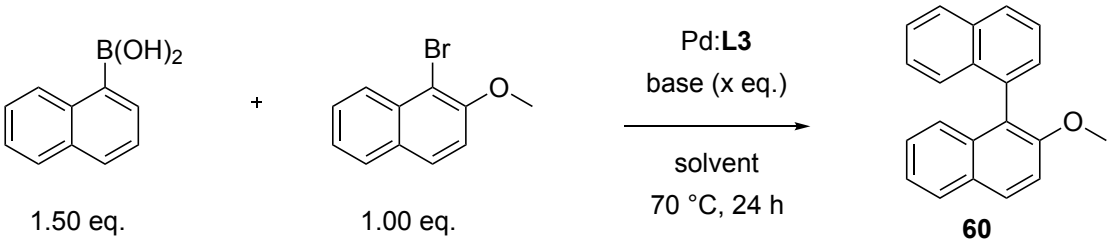
Yields and recoveries were relatively low and did not show any change when raising catalyst loading (entry 2) or using a less polar solvent (entry 3). Presumably, oxidative addition for aryl chlorides **67** and **70** is not fast enough to compete with side reactions of *Grignard* reagent and substrate when using **L2** as a ligand.



## Substrate Scope: L3 in Asymmetric and Sterically Hindered Suzuki-Miyaura Coupling Reactions

Given the overall satisfying performance of **L3** in the Suzuki-Miyaura couplings with aryl chlorides as well as aryl bromides and in the asymmetric Suzuki-Miyaura model reaction of 1-bromo-2-methoxynaphthalene and 1-naphthylboronic acid, this ligand was selected for a focused screening of reaction conditions of the latter to improve the yield. The reaction conditions were varied with respect to solvent, amount of base, and the palladium:ligand ratio (table 30).

**Table 30.** Screening of reaction conditions for the Suzuki-Miyaura coupling of 1-bromo-2-methoxynaphthalene and 1-naphthylboronic acid using (2-chlorophenyl)dimenthyl phosphine (**L3**) as ligand.



The reaction scheme shows the Suzuki-Miyaura coupling of 1-naphthylboronic acid (1.50 eq.) and 1-bromo-2-methoxynaphthalene (1.00 eq.) using Pd:L3 and base (x eq.) in a solvent at 70 °C for 24 h to yield product **60**.

entry	Pd:L <sup>a</sup>	base (x eq.)	solvent	yield /% <sup>b</sup>
1	1:2	K <sub>3</sub> PO <sub>4</sub> (2.00 eq.)	toluene	93
2	1:2	K <sub>3</sub> PO <sub>4</sub> (2.00 eq.)	1,4-dioxane	59
3	1:2	K <sub>2</sub> CO <sub>3</sub> (2.00 eq.)	toluene	60
4	1:2	K <sub>3</sub> PO <sub>4</sub> (3.00 eq.)	toluene	91
5	1:3	K <sub>3</sub> PO <sub>4</sub> (2.00 eq.)	toluene	87

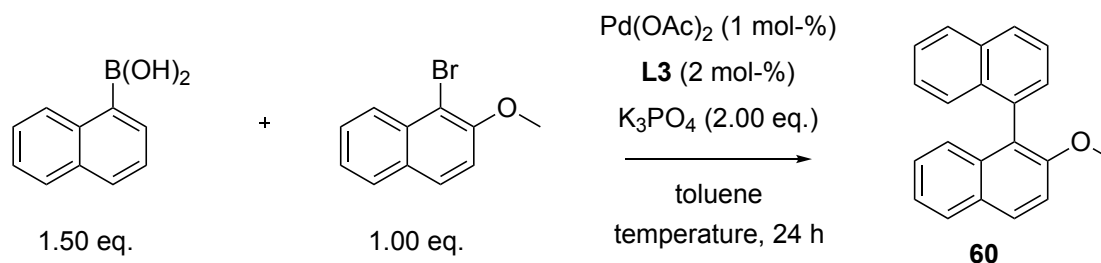
a) Pd:L ratio with 1 mol-% of Pd(OAc)<sub>2</sub> as Pd precursor.

b) Analytical yields (mol-%) calculated by <sup>1</sup>H-qNMR analysis using an internal standard.

As the aim was to reach a certain competitiveness with other “state of the art” ligands, palladium loading was reduced to 1 mol-% (as opposed to 2 mol-% in table 25) for the optimization. The best conditions were achieved using toluene as solvent and K<sub>3</sub>PO<sub>4</sub> as base (entry 1), reaching a near quantitative yield. Changing the solvent to 1,4-dioxane or changing the base to K<sub>2</sub>CO<sub>3</sub> drastically reduced the yield (entries 2 and 3). Employing a higher excess of base or lowering the palladium:ligand ratio did not affect the result within the limits of error (entries 4 and 5). With the much improved activity obtained, the reaction was now conducted at lower temperature. Besides the obvious advantages of lower temperatures such as a better substrate tolerance and less environmental impact, the aim was also to reach a better enantiomeric ratio

of the axially chiral coupling product, and general experience in asymmetric catalysis points to higher enantioselectivity at lower reaction temperature.<sup>126</sup> Table 31 describes the results of successively lowering the temperature to 50 °C (entry 2) and to room temperature (entry 3).

**Table 31.** Successive lowering of the reaction temperature for the asymmetric Suzuki-Miyaura coupling using **L3**.

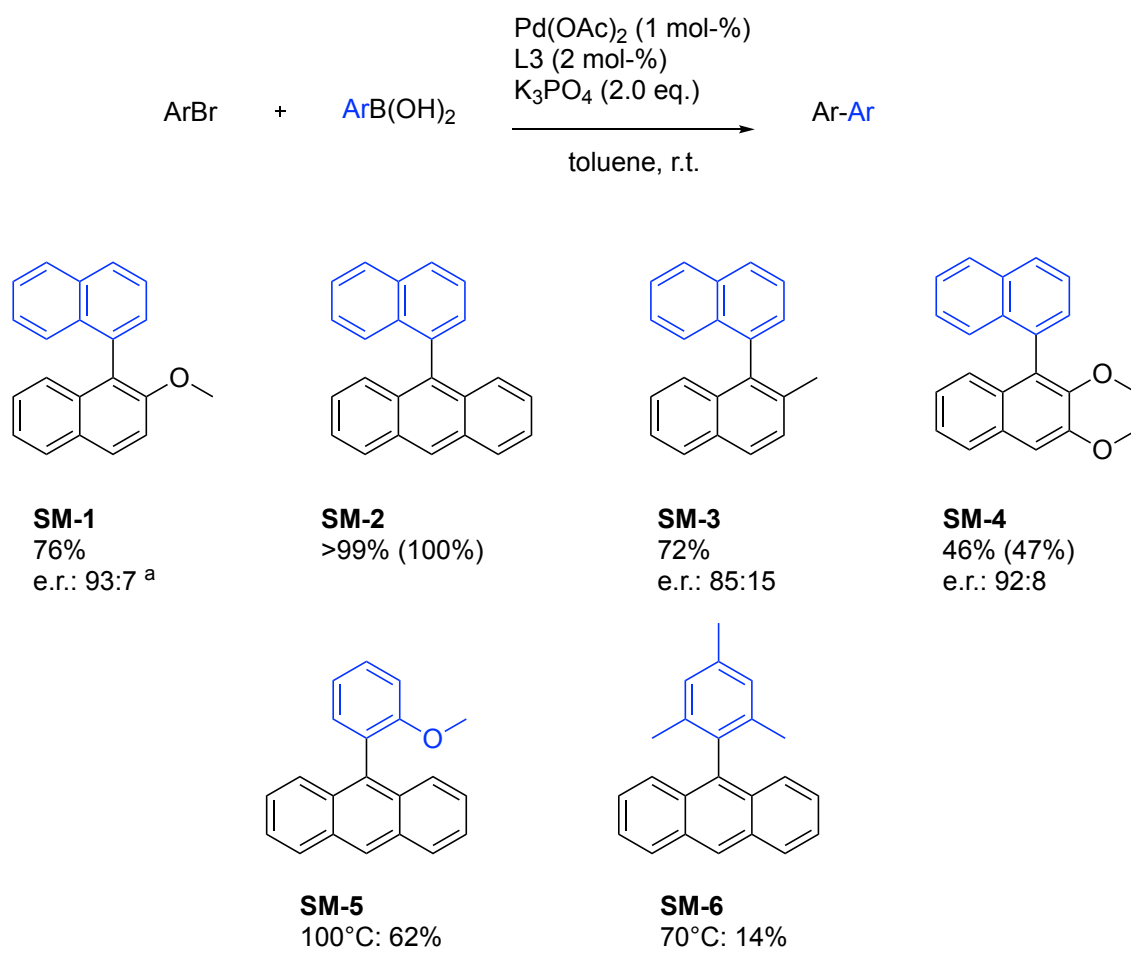


entry	temperature	yield /% <sup>a</sup>
1	70 °C	93
2	50 °C	89
3	r.t.	76

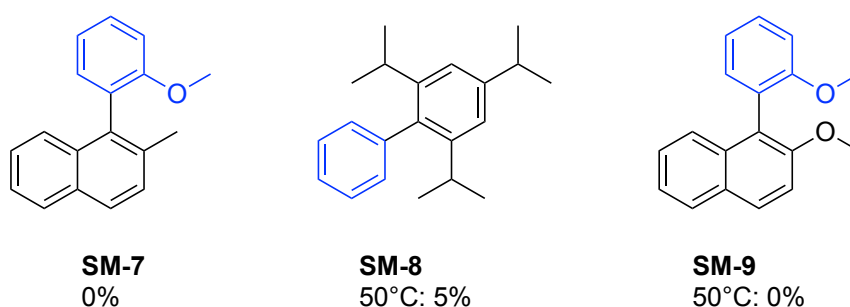
a) Analytical yields (mol-%) calculated by <sup>1</sup>H-qNMR analysis using an internal standard.

The reaction temperature was lowered to 50 °C without significant effect on the yield, and even when conducting the coupling at room temperature, the outcome was still satisfactory.

Due to these promising results, the testing of more sterically hindered was envisaged and, in case of chiral products, respective enantiomeric ratios were to be measured by chiral HPLC. Scheme 47 shows the substrate scope of the Suzuki-Miyaura coupling using ligand (2-chlorophenyl)dimenthyl phosphine **L3**.



unsuccessful substrates combinations:



**Scheme 47.** Substrate scope of the sterically hindered and asymmetric Suzuki-Miyaura coupling using **L3**. <sup>1</sup>H-qNMR yields (mol-%) using an internal standard. Isolated yields in brackets. Enantiomeric ratios are determined by chiral HPLC. a) The purified sample contained around 8 mol-% dibenzyl ether.

With 1-naphthylboronic acid, sterically hindered aryl bromides were coupled in moderate to excellent yields (**SM1-4**) comparable to other reported ligands.<sup>127</sup> For example, the synthesis of **SM-2** was achieved quantitatively by Korb *et al.* at higher temperatures (70 °C) with a

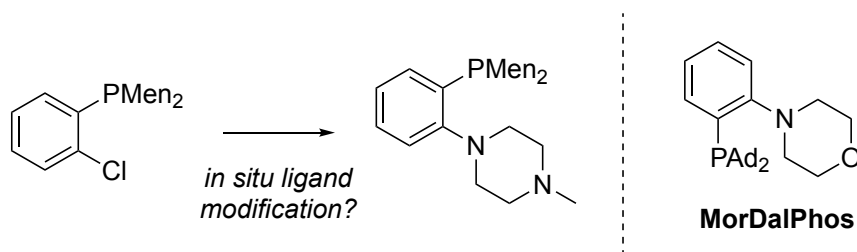
ferrocene-based ligand, however using a lower catalyst loading.<sup>128</sup> With the optimized conditions at room temperature, rather high enantiomeric ratios were obtained (compare **SM-1**, **SM-3** and **SM-4**). These substantial enantiomeric enrichments demonstrate the utility of the dimethylphosphino ligand motif in asymmetric cross-coupling reactions. In reactions of 2-methoxyphenylboronic acid and mesitylboronic acid, however, most substrates failed (**SM-7** and **SM-9**) or required heating to obtain moderate to low yields (**SM-5** and **SM-6**). The coupling of sterically hindered 1-bromo-2,4,6-triisopropylbenzene and phenylboronic acid was unsuccessful at slightly elevated temperatures (**SM-8**), probably due to steric demand of the aryl bromide. With regards to the fact that even the use of benchmark ligand SPhos needs a higher catalyst loading and high temperatures, further optimization of the conditions with respect to temperature and catalyst loading could be attempted.<sup>5</sup> Generally speaking, **L3** exhibits promising activity in the sterically hindered and asymmetric Suzuki-Miyaura coupling.

## 2.8 *In situ* Ligand Modification of L2 and L3

### 2.8.1 *Investigations on In Situ Ligand Modification of L3*

Initial promising catalysis results<sup>77</sup> of ligand **L3** had shown higher activity than expected and prompted a more detailed investigation of its fate during catalysis. As a hypothesis, it was assumed that not **L3** was the catalytically active species, but rather that ligand might be susceptible to *in situ* modification by substitution of the chlorine moiety. Besides the obvious quest to further explore **L3**'s mechanism of action, such an *in situ* modification of ligands could be a useful synthetic approach as it could enable simple diversification of ligand structures based on a single ligand precursor.

**L3** exhibited excellent results in the amination of aryl chlorides (see section 2.7.1), and so the assumption was that an *in situ* amination of the ligand leads to a *Stradiotto*-like (1-aminoaryl)phosphine ligand of the *MorDalPhos* type (scheme 48) which could be the actual catalytically active species.<sup>129</sup>



**Scheme 48.** Proposed *in situ* ligand modification to result in a *Stradiotto*-like *P,N*-ligand

The fate of the ligand was examined by  $^{31}\text{P}$ -NMR analysis of the crude reaction mixture of a  $\text{PdCl}_2(\text{MeCN})_2/\mathbf{L3}$ -catalyzed amination reaction, as shown in figure 14.

It is evident that the ligand stayed widely intact during the catalysis, except for minor amounts of oxidized ligand ( $\delta_P$  48.11) and a minor signal of a new, unknown species at  $\delta_P$  -22.12. For a further enrichment and identification of the new component, the catalysis was repeated with 50 mol-% catalyst loading. These conditions gave rise to another new signal at  $\delta_P$  -9 as judged by  $^{31}\text{P}$ -NMR analysis, and this time, no signal at  $\delta_P$  -22.12 was observed.

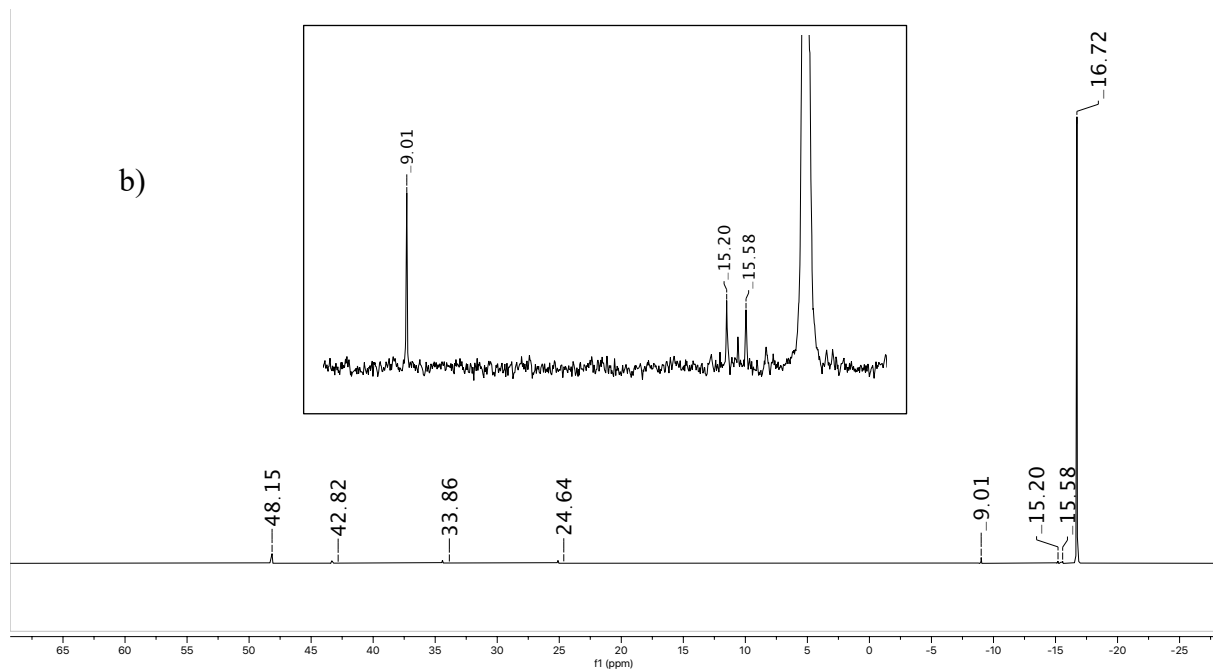
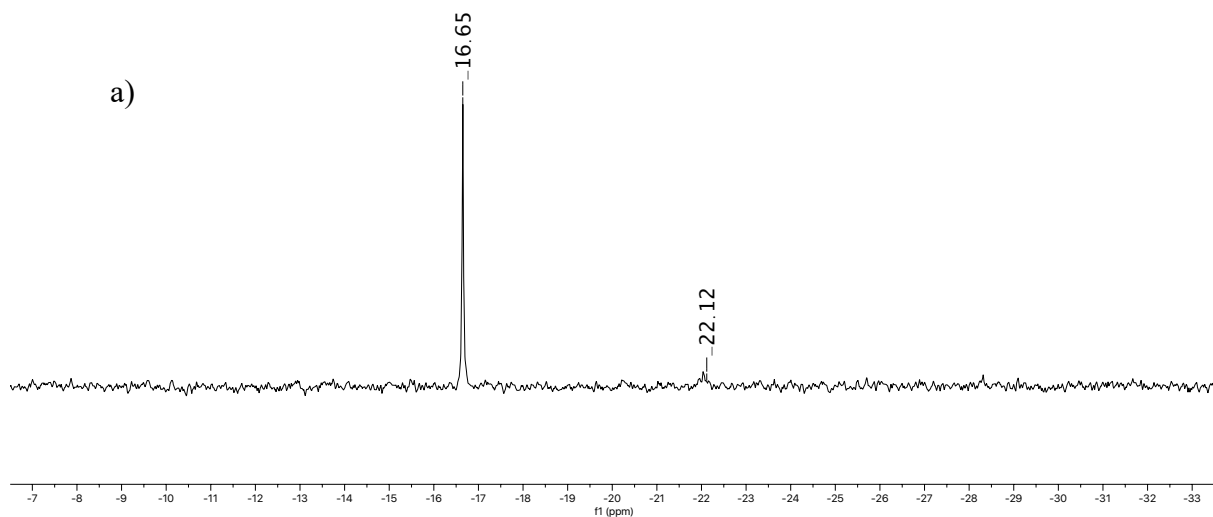
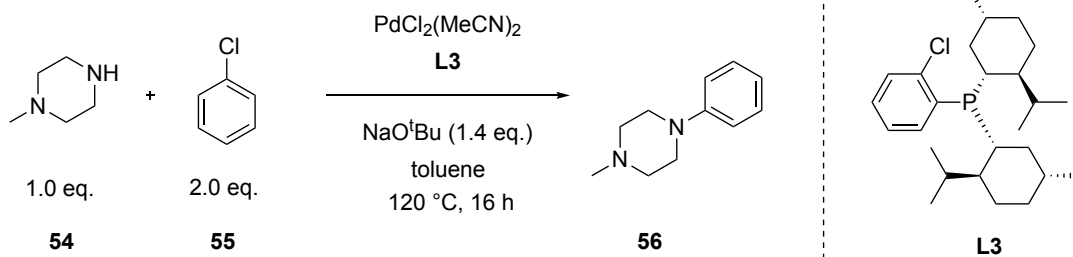


**Figure 14.** Excerpts of the  $^{31}\text{P}$ -NMR spectra of **L3**-catalyzed Buchwald-Hartwig amination of **55**. a)  $\text{PdCl}_2(\text{MeCN})_2$  (2 mol-%), **L3** (4 mol-%), scale: 1.00 mmol. b)  $\text{PdCl}_2(\text{MeCN})_2$ : 50 mol-%, **L3**: 1.00 eq, scale: 0.20 mmol.

Following the assumption that **L3** might be *in situ* modified to afford an *ortho*-aminated ligand, stoichiometric amounts of the ligand, amine and base were heated with catalytic amounts of  $\text{PdCl}_2(\text{MeCN})_2$  and the crude material was analyzed by  $^{31}\text{P}$ -NMR analysis. This time, the  $^{31}\text{P}$ -NMR spectrum gave rise to the signal at  $\delta_P$  -9.01 at significant intensity (figure 15). However, GC-MS analysis and synthesis of reference material proved that this signal does not stem from aminated ligand, but dehalogenated ligand **L2**. Because of these findings, dimethyl(phenyl)phosphine (**L2**) was included in the catalytic investigations on (aryl)dimethylphosphines, as described earlier in this work.

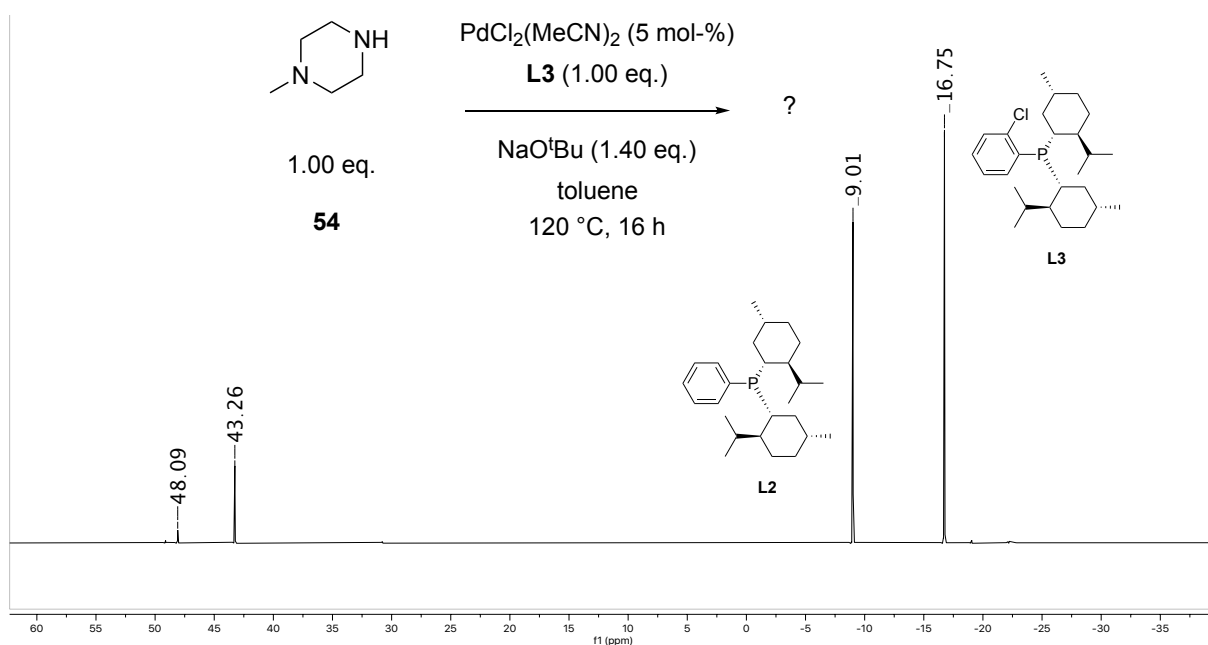


**Figure 15.** Excerpt of the  $^{31}\text{P}$ -NMR spectrum of the reaction mixture with **54**, base, **L3** and catalytic amounts of  $\text{PdCl}_2(\text{MeCN})_2$ , scale: 1.0 mmol. The signals at  $\delta_P$  43.26 and  $\delta_P$  48.09 stem from oxidized ligands **L2** and **L3**, respectively.

### 2.8.2 *Investigation of In Situ Modification of L2*

While investigating dimethyl(phenyl)phosphine **L2** in the palladium-catalyzed amination of chlorobenzene with *N*-methylpiperazine, qNMR samples were analyzed by  $^{31}\text{P}$ -NMR spectroscopy as well, driven by curiosity.<sup>102</sup> This revealed degradation of the ligand over the course of the reaction: As seen in figure 16a, after three hours of reaction time, the  $^{31}\text{P}$ -NMR spectrum gives rise to a signal at  $\delta_P$  -22.06 (as seen when studying the *in situ* functionalization of **L3**, section 2.8.1).

After stirring overnight, **L2** ( $\delta_P$  8.85) has completely degraded, and a set of signals in the chemical shift area of  $\delta_P$  -22 – -24 appears in the  $^{31}\text{P}$ -NMR spectrum (figure 16b). These signals are not in the chemical shift area typically observed for ligand palladium complexes or ligand oxide (which would appear downfield-shifted from the ligand signal). Thus, it is assumed that **L2** is modified *in situ* over the course of the reaction to generate new species. Notably, the amination reaction is already finished after three hours, thus a contribution of the newly formed species to the catalytic activity seems unlikely.



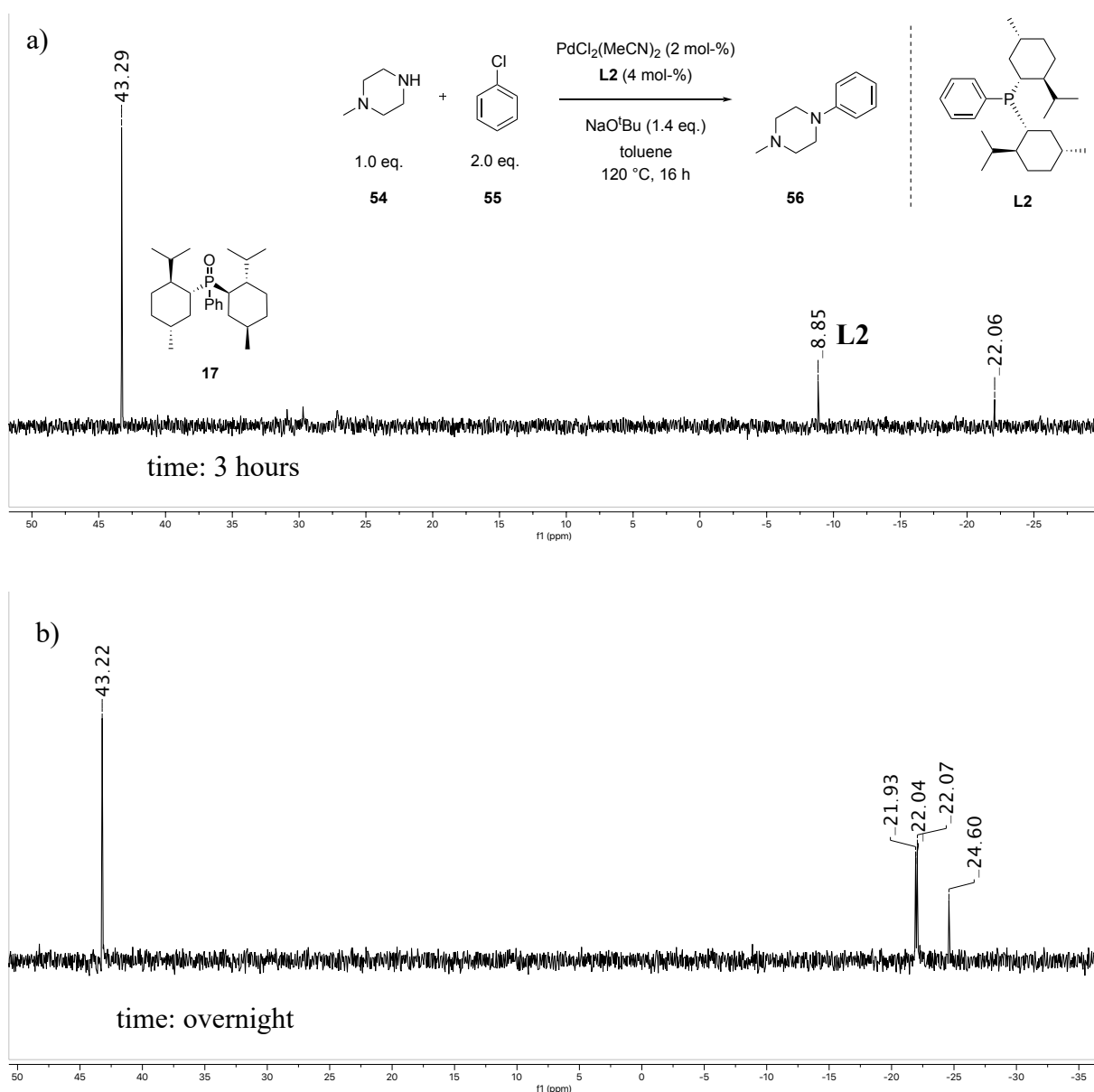


**Figure 16.** Excerpts of the  $^{31}\text{P}$ -NMR spectrum of the coupling of **54** and **55** using **L2** after 3 hours and overnight (scale: 1.0 mmol).

A further experiment involved heating chlorobenzene and base with catalytic amounts of Pd precursor and **L2** in toluene while monitoring the reaction by  $^{31}\text{P}$ -NMR sampling. The reaction was performed at a higher scale than before for a better detection of by-products in the  $^{31}\text{P}$ -NMR spectrum. Figure 17 shows the  $^{31}\text{P}$ -NMR spectra after designated reaction times. After two hours, the aforementioned signals in the area of  $\delta_P$  -21 –  $\delta_P$  -23 appear. After four hours, ligand **L2** is almost completely consumed, now giving rise to a new signal at  $\delta_P$  -16. After 5.5 hours, complete conversion of **L2** took place, with the new signal at  $\delta_P$  -16 as the major component in the  $^{31}\text{P}$ -NMR spectrum. The chemical shift of the new species is the same as halogenated ligand **L3**, but this could be coincidental since a conversion of **L2** to **L3** under the

given condition appears unlikely. All in all, these findings show that **L2** is not subjected to a clean *in situ* functionalization, but a rather complex degradation, presumably by undirected cyclometallation and subsequent modification which could actually hamper catalysis. Such cyclometallation reactions of ligands and subsequent modifications during catalysis has long been described in the literature.<sup>11,130, 131</sup>

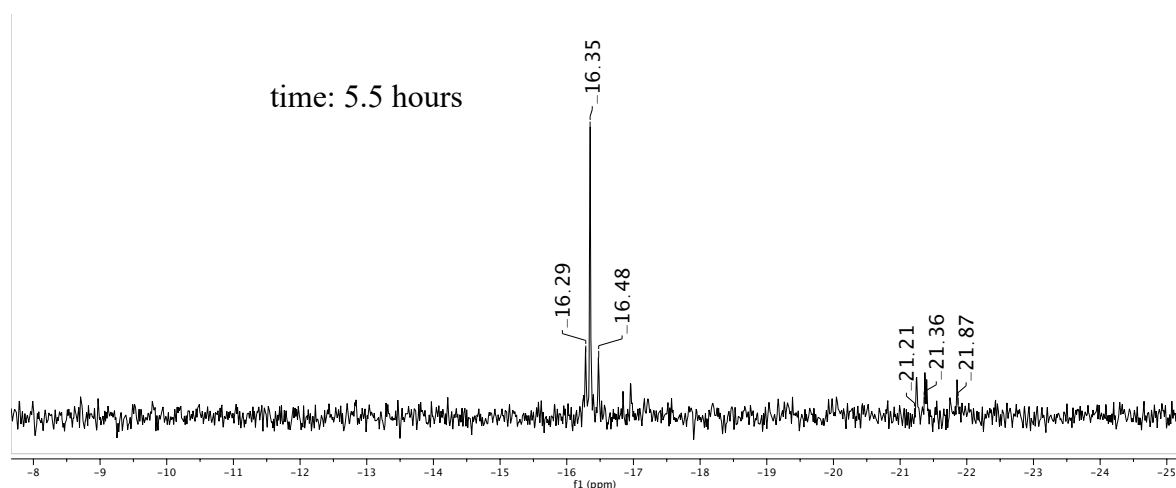
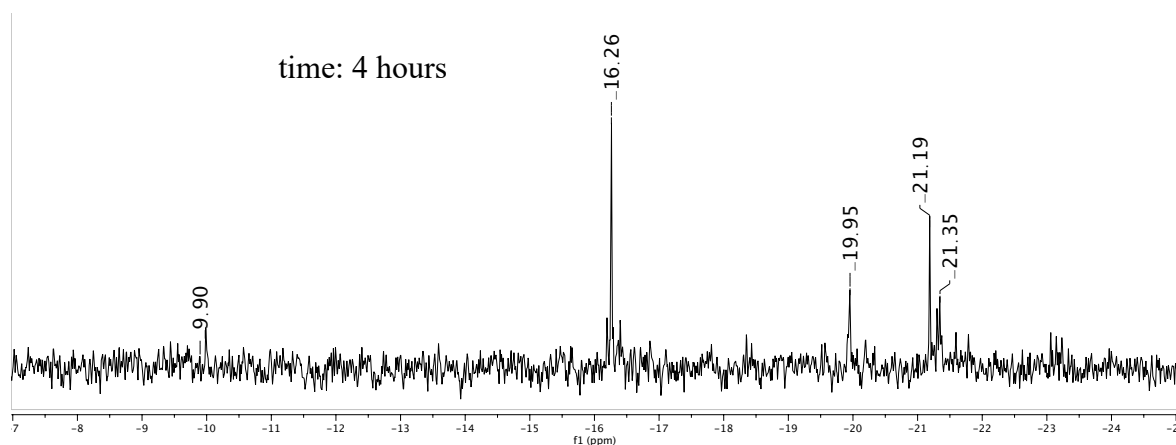
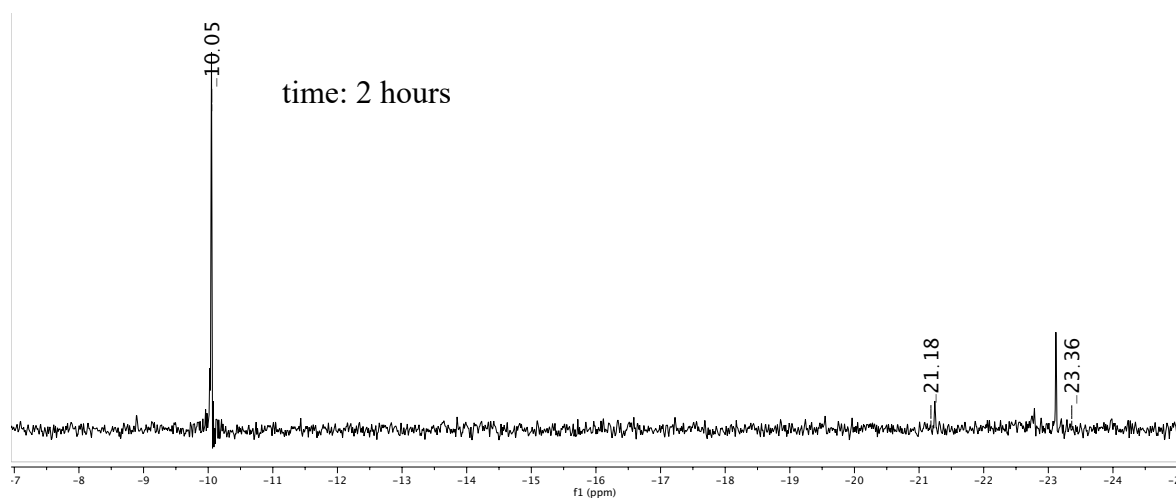
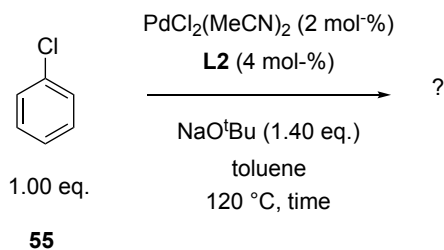
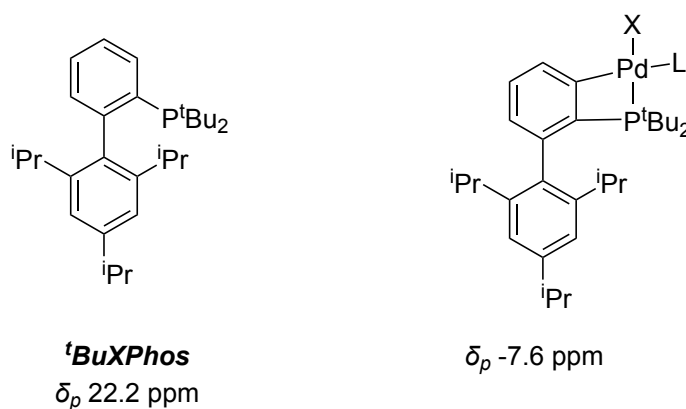


**Figure 17.** Reaction of **55** with catalytic amounts of Pd precursor and **L2**:  $^{31}\text{P}$ -NMR spectra of the reaction mixtures after the designated reaction times (scale: 2.5 mmol).

As for **L3**, the following fate in the palladium-catalyzed amination reaction of chlorobenzene is assumed: During the catalytic reaction, a small amount of ligand is dehalogenated and converted to **L2**. This might contribute to a better catalytic activity. The formed **L2** is then degrading fast to catalytically inactive species, and is thus withdrawn from the catalytic cycle. However, the benefits of **L3** in catalysis cannot completely be explained by *in situ* conversion to **L2**: Especially its performance in Suzuki-Miyaura couplings is better than that of **L2** (see section 2.7.1). In fact, given the relative stability of **L3** in the palladium-catalyzed amination of chlorobenzene compared to **L2** (compare figures 14 and 16), the chloro substituent at *ortho*-position to phosphorus could even prevent cyclometallation reactions and thus degradation of **L3** during the course of the catalytic reaction. A similar observation was made for *Buchwald's* dialkylbiaryl phosphine ligands, where the formation of a four-membered palladacycle was observed during a palladium-catalyzed amination of aryl bromide with <sup>t</sup>BuXPhos as ligand (scheme 49).<sup>132</sup> It is therefore suggested that the *ortho*-methoxy substituent incorporated into the structure of various dialkylbiaryl phosphine ligands prevents cyclometallation and therefore contributes to ligand stability.<sup>2</sup>



**Scheme 49.** <sup>t</sup>BuXPhos (left) and a stable four-membered palladacycle identified as degradant (right).<sup>132</sup>

## 2.9 Conclusion and Outlook

### 2.9.1 The Dimethylphosphino Structural Motif and its Application in Catalysis

In conclusion, the incorporation of the dimethylphosphino donor motif into ligands and ligand precursors was demonstrated *via*

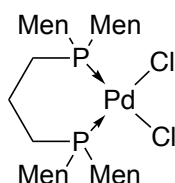
- a direct modification starting from  $\text{Men}_2\text{POH}$  (**4**) and
- reaction of  $\text{Men}_2\text{PCl}$  (**3**) with ligand precursors.

Both approaches demonstrate the utility of dimethylphosphine *P*-oxide as an air-stable platform chemical for ligands containing the dimethylphosphino donor motif.

In the assessment of the dimethylphosphino donor motif in ligands in transition-metal catalyzed cross-coupling reactions, most notably its ability to induce asymmetry in Suzuki-Miyaura coupling reactions was demonstrated in this work. Among the tested ligands **L1-L4**, especially (2-chlorophenyl)dimethylphosphine **L3** succeeded in inducing high enantiomeric excesses (exceeding 80% ee) in asymmetric biaryl coupling reactions. Although the substrate scope should be expanded in the future, these results are remarkable in view of the limited success previously achieved with dimethylphosphanyl ligands in asymmetric catalysis<sup>70,72,133</sup>. Generally, (monoaryl)dimethylphosphines performed better than their biaryl analogs, which seems to contrast *Buchwald's* findings using dialkylbiaryl phosphines and could be a result of the steric congestion surrounding the bulky menthyl groups. There are still questions concerning what exactly causes the superior performance of some ligands which are not yet sufficiently answered. Especially the functionality of *ortho*-chlorine present in **L3** was not yet explored in sufficient detail. The possibility that this ligand could be subjected to *in situ* modification during the catalytic process, which leads to the actual catalytically active species, seems rather unlikely because apart from minor amounts of dehalogenated ligand **L2**, no modification of this ligand was observed during catalysis. In fact, the *ortho*-chlorine present in **L3** seemed to cause superior performance to its dehalogenated equivalent **L2** in some instances. An explanation for this could be stabilizing interactions of the chlorine lone pairs with Pd in ligand-palladium complexes. This was also suggested by Pramic *et al.* in their study of Suzuki-Miyaura couplings with  $\text{P}(\text{C}_6\text{H}_5)(2\text{-C}_6\text{H}_4\text{Cl})_2$  as ligand,<sup>81</sup> however they did not investigate further on this assumption. Syntheses of the oxidative addition complexes of **L1-L5** and X-Ray crystallographic studies could give further insight into their modes of action, which could help with future ligand design. Especially the (monoaryl)dimethylphosphine structural motif offers further potential for structural diversification of ligands at the aryl moiety.

When comparing the tested couplings, it is apparent that ligands exhibiting an aryl substitution in *ortho*-position to phosphorus (**L1**, **L3** and **L4**) are promising ligands in Suzuki-Miyaura couplings, while dimethyl(phenyl)phosphine (**L2**) gave better results in Kumada-Corriu and Mizoroki-Heck couplings. This suggests that for the latter, stabilizing arene-Pd (or the suggested chloro-Pd) interactions might not be of importance in the catalytic cycle.

The applicability of bisphosphine palladium(II) complex **27** in catalytic reactions has so far not been explored, but could be an interesting task for the future (scheme 50).



**27**

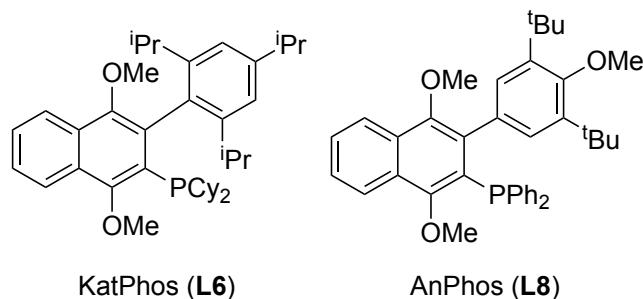
**Scheme 50.** Bisphosphine palladium(II) complex **27** as potential catalyst for asymmetric catalysis.

Since (aryl)dimethyl monophosphine ligands showed promising results in asymmetric catalysis, bisphosphine **23** could be even more beneficial, since chelating bisphosphine ligands are privileged structures for inducing high enantiomeric excesses.

### **3 Synthesis of Benzoannulated Ligands of the Buchwald Type and Their Application in Catalysis**

### 3.1 New Variations of the Dialkylbiaryl Phosphine Ligand type: KatPhos, AnPhos and CyAnPhos

Previously, ligands KatPhos (**L6**) and AnPhos (**L8**) have become available in our group (scheme 51).<sup>78</sup> These ligand structures are a variation of the *Buchwald* dialkylbiaryl phosphine ligand type, exhibiting a benzoannulation of the phosphine-containing aryl moiety.



**Scheme 51.** Benzoannulated ligands of the *Buchwald* type: KatPhos and AnPhos.

This phenyl-naphthyl dialkyl phosphine structural motif has been reported in the literature (see section 1.1 of this work), but direct analogs of their *Buchwald* derivatives have not been synthesized. Thus, the influence of a benzoannulated ligand motif on catalytic activity (compared to *Buchwald*'s dialkylbiaryl phosphine ligands) has not been assessed yet. Such an assessment is enabled by the novel ligand KatPhos, which is a direct analog of *Buchwald* ligand BrettPhos.

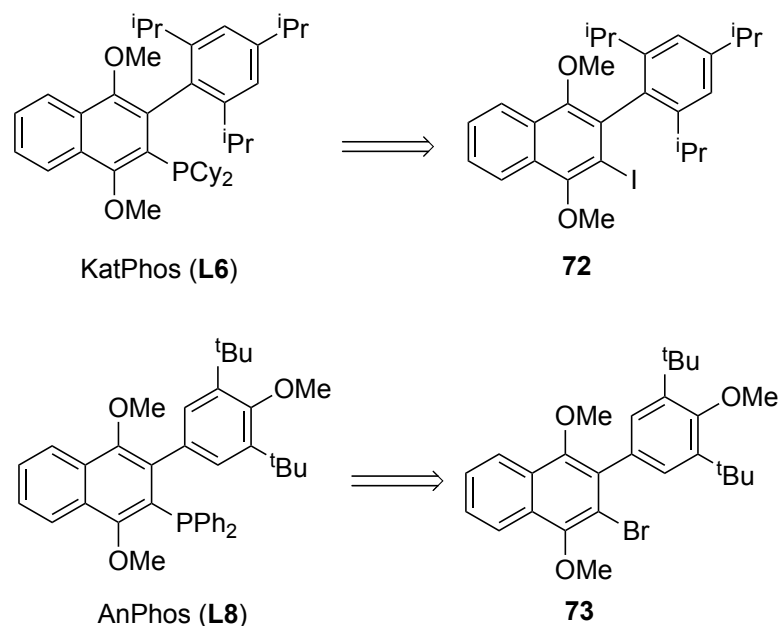
Moreover, AnPhos (**L8**) exhibits a further variation of the dialkylbiaryl phosphine ligand type on the aryl' moiety, namely dispersive *tert*-butyl groups in *meta*-aryl' position instead of the usual *ortho* position. The influence of this substitution pattern has been studied in other cases in the literature. For instance, Doyle and co-workers found that aryldialkyl phosphine ligands bearing *meta*-substitution at the aryl moiety performed better in nickel-catalyzed cross-coupling reactions than their *ortho*-substituted counterparts.<sup>134</sup> They elaborated that the former enable a relatively low sterical hindrance around the metal center, while still providing remote sterical crowding, which is beneficial specifically in nickel-catalyzed cross-couplings.

As far as dialkylbiaryl phosphine ligands are concerned, *ortho*-aryl' substitution usually prevents cyclometallation of ligands and thus enhances their activity in catalysis.<sup>2</sup> The effects of a *meta*-aryl' substituted equivalent have so far not been studied, but could be an intriguing scaffold for ligand design.



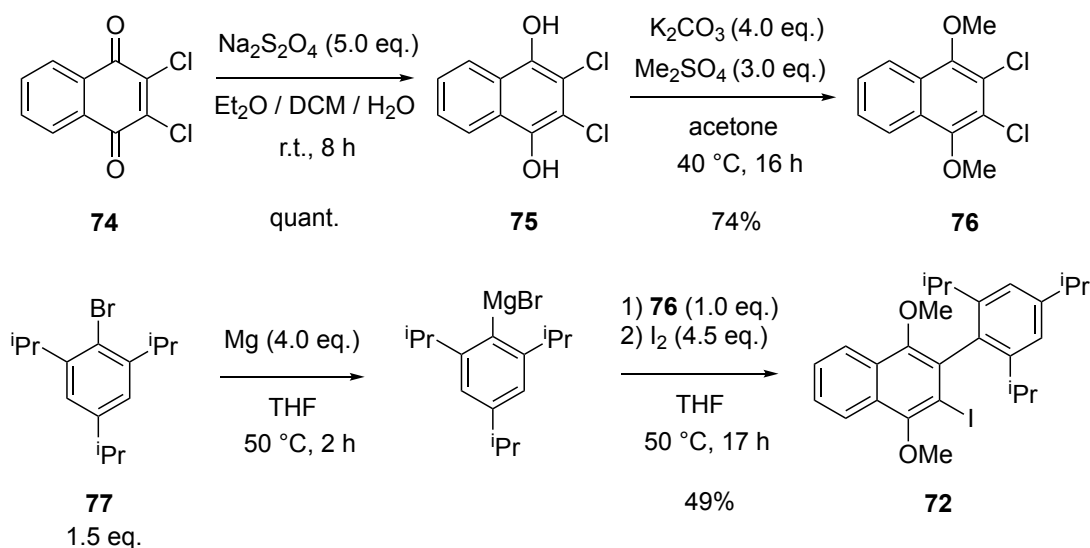
### 3.1.1 Previously Established Ligand Syntheses

The benzoannulated ligand precursors **72** and **73** (scheme 52) offer easy synthetic access starting from naphthoquinone derivatives, which was realized in an earlier work in our group.<sup>78</sup>



**Scheme 52.** Retrosynthetic analysis of *KatPhos* and *AnPhos*.

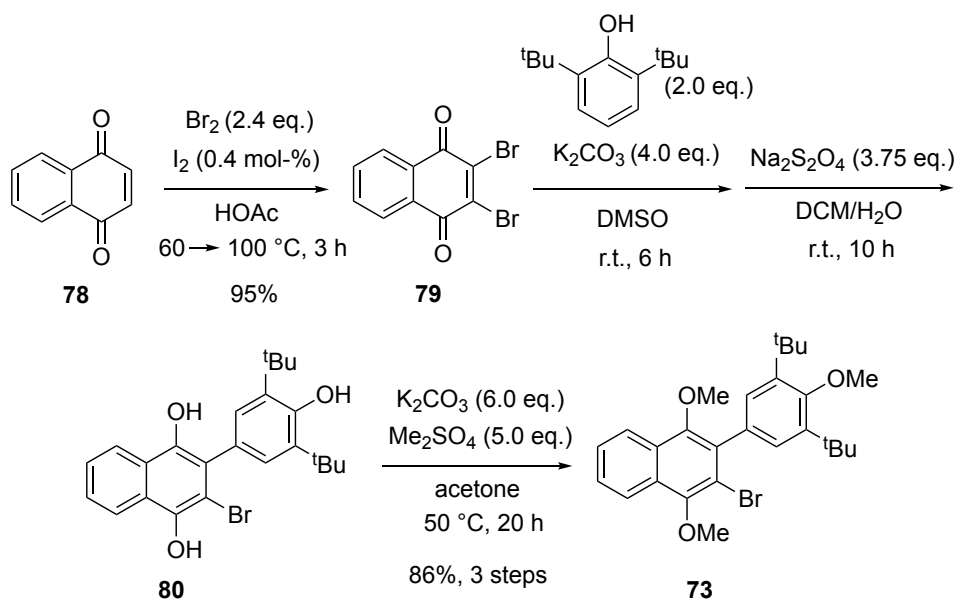
Scheme 53 shows the synthesis of the precursor **72** for the benzoannulated ligand *KatPhos* (**L6**) starting from 2,3-dichloronaphthoquinone **74**.<sup>78</sup>



**Scheme 53.** Three-step synthesis of **72**.

Reduction of **74** by sodium dithionite afforded 1,4-dihydroxy-2,3-dichloro naphthalene **75** in quantitative yield. Methylation then gave **76**, which was subjected to an aryne *Grignard* addition to result in precursor **72** after iodine quench (overall yield over three steps: 36%).

Ligand AnPhos (**L8**) can be synthesized from precursor **73** (scheme 54), which was synthesized in a four-step synthesis starting from **78**. Bromination was performed according to a literature procedure to give **79** in near quantitative yield.<sup>135</sup> The subsequent addition elimination reaction with 2,6-di-*tert*-butyl phenol was also performed according to an existing literature procedure.<sup>136</sup> Direct reduction of the reaction mixture afforded **80**, which was directly methylated to afford precursor **73** in 86% yield in three steps.

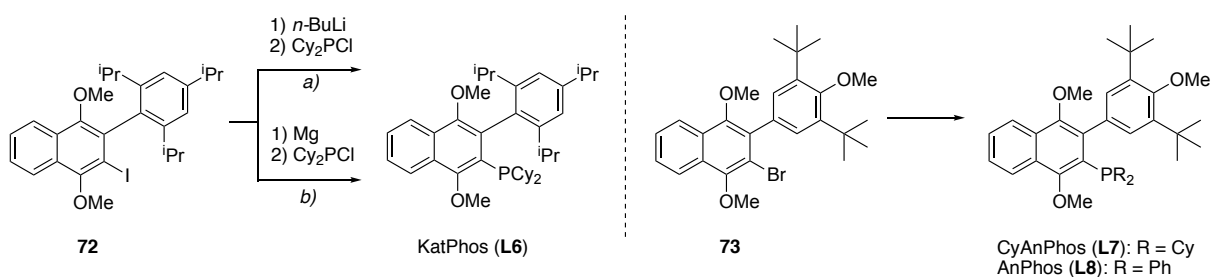


**Scheme 54.** Four-step synthesis of **73**.

### 3.1.2 *Aim of this Work*

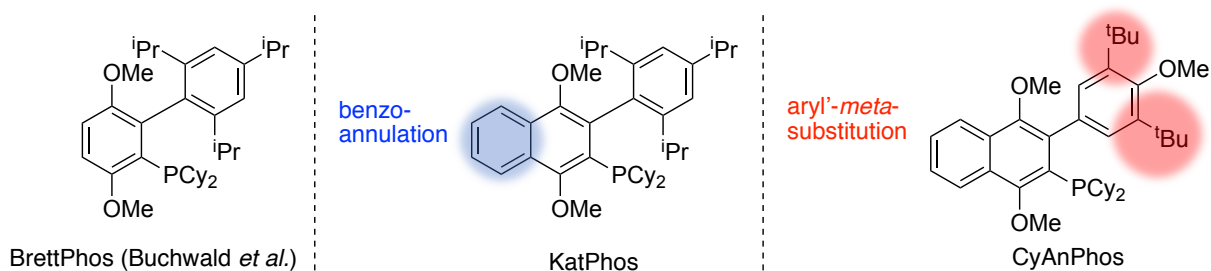
Starting from precursors **72** and **73**, an optimized synthesis for the hitherto only low yielding procedures to access benzoannulated ligands KatPhos (**L6**) and AnPhos (**L8**) was envisaged. Furthermore, for a direct comparison of the *meta*-aryl' substitution to the usual *ortho*-aryl' substitution in catalysis, the synthesis of CyAnPhos (**L7**), a dicyclohexylphosphino analog of **L8**, was envisaged.

These syntheses can either be achieved by lithiation and subsequent ClPCy<sub>2</sub> quench strategy (pathway a, scheme 55) or generation of *Grignard* reagent with subsequent ClPCy<sub>2</sub> quench (pathway b).



**Scheme 55.** Benzoannulated dialkylbiaryl phosphine ligands studied in this work

With ligands **L6-L8** at hand, further investigation of their properties in catalysis is then envisaged. A direct comparison of established *Buchwald* ligand BrettPhos with its benzoannulated derivative **L6** offers information about the influence of a benzoannulation of the phosphine-containing aryl moiety in *Buchwald* ligands. Moreover, comparison of the performance of **L6** to **L7** will give insight into the functionality of the *meta*-aryl' substitution compared to the usual *ortho*-substitution, and whether they could lead to new interesting activities (scheme 56).



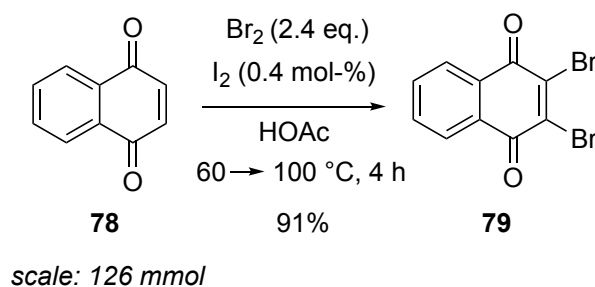
**Scheme 56.** Distinct structural features of BrettPhos, KatPhos and CyAnPhos.

## 3.2 Syntheses of ligands KatPhos, CyAnPhos and AnPhos

### 3.2.1 *Synthesis of the Ligand Precursors*

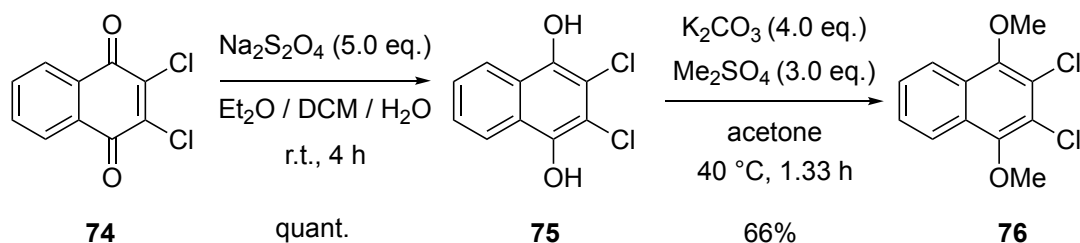
#### Syntheses of the Naphthoquinone Precursors

The synthesis of the naphthoquinone precursors for the benzoannulated ligands had already been achieved in previous works (see section 3.1), but was altered and improved at some points. The bromination of 1,4-naphthoquinone was performed according to a procedure by Inoue *et al.*<sup>135</sup> and further-scaled up with excellent yield (scheme 57).



**Scheme 57.** Scale-up of the bromination of naphthoquinone **79**.

The synthesis of **75** was further optimized by reducing the equivalents of reductant  $\text{Na}_2\text{S}_2\text{O}_4$  used and the amount of solvent. The optimized procedure afforded **75** in quantitative yield. As for the subsequent methylation, the reaction time was drastically reduced to 1.33 hours after monitoring by TLC had confirmed complete consumption of starting material. This led to a slightly lower yield of **76** as before, however still satisfying considering the much shorter reaction time (scheme 58).



**Scheme 58.** Two-step synthesis of **76**.

Earlier, oxidation of starting material **75** was assumed to be the main cause for diminished yields in the methylation reaction, but analysis of the crude  $^1\text{H-NMR}$  spectrum also showed presence of methylated and presumably dehalogenated by-products (see figure 18).

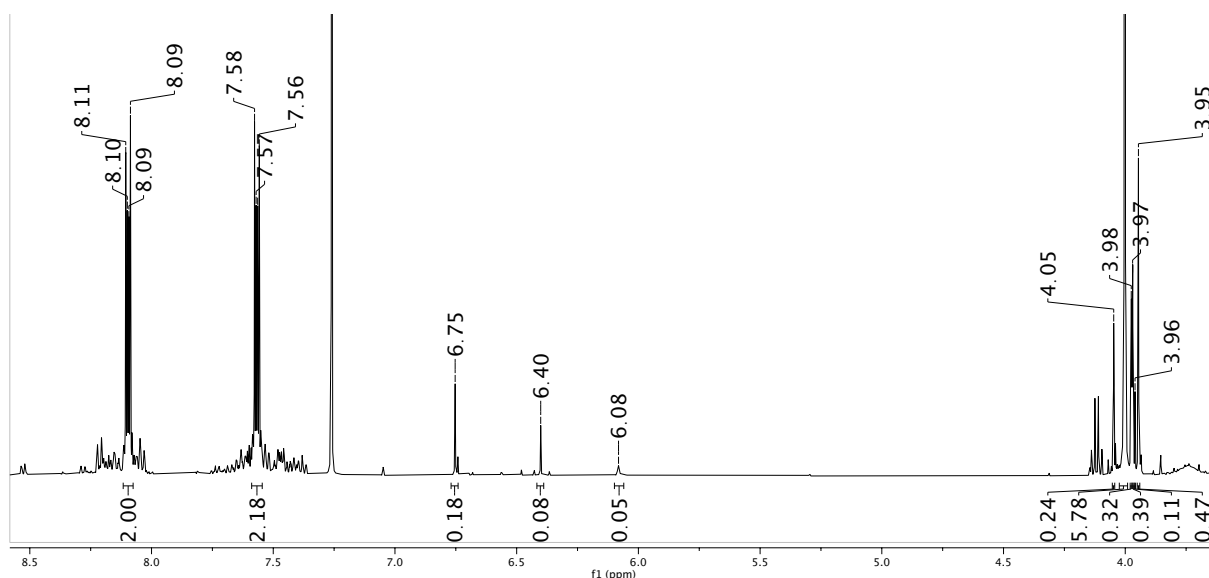
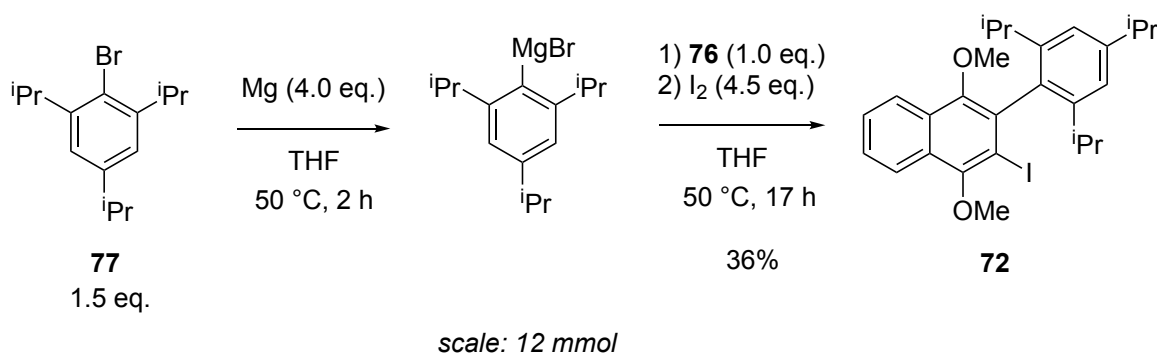


**Figure 18.** Excerpt of the  $^1\text{H}$ -NMR spectrum of crude **76**. The signals at  $\delta_{\text{H}}$  6.75, 6.40 and 6.08 ppm and the signals in the methoxy area indicate dehalogenated (and presumably partly methylated) by-products.

### Synthesis of Phenyl-Naphthyl Precursor **72**

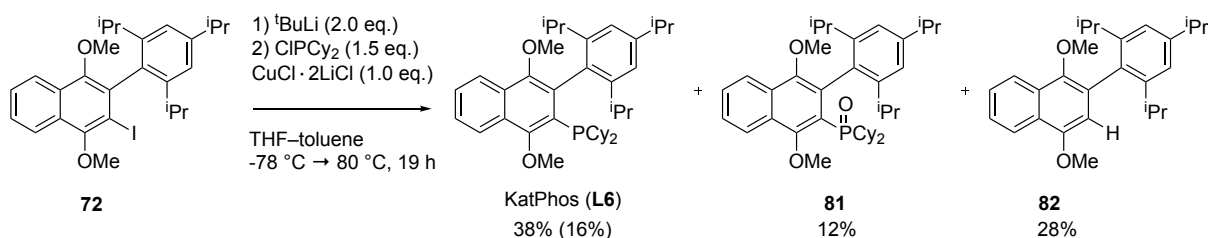
The preparation of ligand precursor **72** was optimized with respect to purification. Precipitation or crystallization from the crude mixture was hampered when scaling up the reaction, leading to diminished yields or impure product. Column chromatography and subsequent hexane wash afforded **72** in moderate yield, but good purity (scheme 59).



**Scheme 59.** Synthesis of ligand precursor **72**.

### 3.2.2 *Optimization of the KatPhos Synthesis*

As mentioned before, KatPhos was synthesized in an earlier work,<sup>78</sup> however in a low yield (scheme 60).



**Scheme 60.** Previously achieved synthesis of KatPhos using <sup>t</sup>BuLi and stoichiometric amounts of copper-salt. Analytical yields (mol-%) determined by <sup>1</sup>H-qNMR analysis of the crude material after work-up. Yields in brackets are isolated yields.

As scheme 60 shows, the synthesis using <sup>t</sup>BuLi and stoichiometric amounts of copper salt suffered from a low recovery rate (78%) after work-up. Presumably, this is due to the formation of a ligand copper complex during the reaction. A work-up using a conc. aq. NH<sub>3</sub> solution fails to deliver a complete decomplexation of the formed copper complex, and its low solubility leads to a loss of yield. Furthermore, loss of yield is attributed to oxidation of the target material in solution during work-up and during isolation by column chromatography.

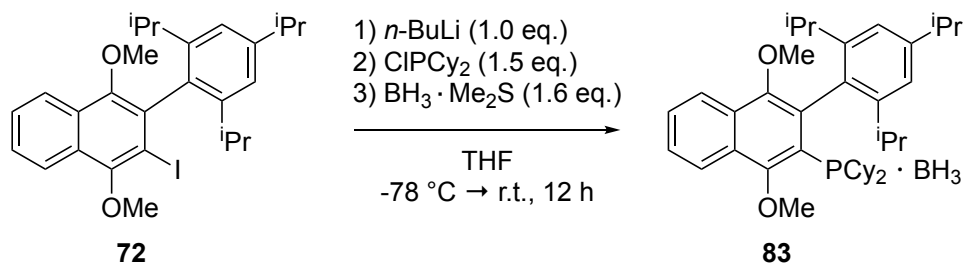
Thus, the objective was to develop a reliable method for synthesis optimization by qNMR of the crude reaction mixture, so as not to lose information during work-up, and to find an efficient method for isolating the pure ligand, preferably by crystallization.

For an easy qNMR analysis devoid of overlapping signals, <sup>31</sup>P-qNMR analysis of the reaction mixture was envisaged. <sup>31</sup>P quantitative NMR spectroscopy is commonly used in analytical chemistry, for example in lignin analysis. For a precise result, it should be noted that spin lattice relaxation times (*T*<sub>1</sub>) are quite long for <sup>31</sup>P nuclei, and thus a long pulse delay should be chosen in order to ensure complete relaxation of all nuclei.<sup>137</sup> *T*<sub>1</sub> can also vary depending on the solvent and composition of the analyzed mixture.<sup>138</sup>

For KatPhos, a further problem with <sup>31</sup>P-NMR analysis was the similar chemical shift of dicyclohexylphosphine oxide, which is formed as by-product by hydrolysis of excess chloro dicyclohexylphosphine, and oxidized target material. To circumvent this problem, scavenging the target material with BH<sub>3</sub>·Me<sub>2</sub>S was envisaged. It was assumed that the ligand copper complex formed during the reaction would be displaced by borane.

Table 32 shows the optimization of pulse delays of a preliminary experiment of the KatPhos synthesis after borane scavenging. To test the precision and correctness of the quantitative  $^{31}\text{P}$ -NMR analysis, recoveries based on  $\text{ClPCy}_2$  were calculated. It is apparent that recoveries decrease with increasing relaxation delay. A relaxation delay of at least 40 seconds seems to be necessary for a precise and correct analysis.

**Table 32.** Optimization of relaxation delay



entry	relaxation delay	recovery /% <sup>a</sup>
1	20s	121
2	30s	113
3	40s	108

a) Recoveries (mol-%) based on  $\text{ClPCy}_2$  determined by  $^{31}\text{P}$ -qNMR analysis using an internal standard.

An exemplary spectrum is depicted in figure 19, which shows the  $^{31}\text{P}$ -NMR spectrum of table 32, entry 3. The components of the reaction mixture were assigned by comparison with literature NMR data or known data from previous works.

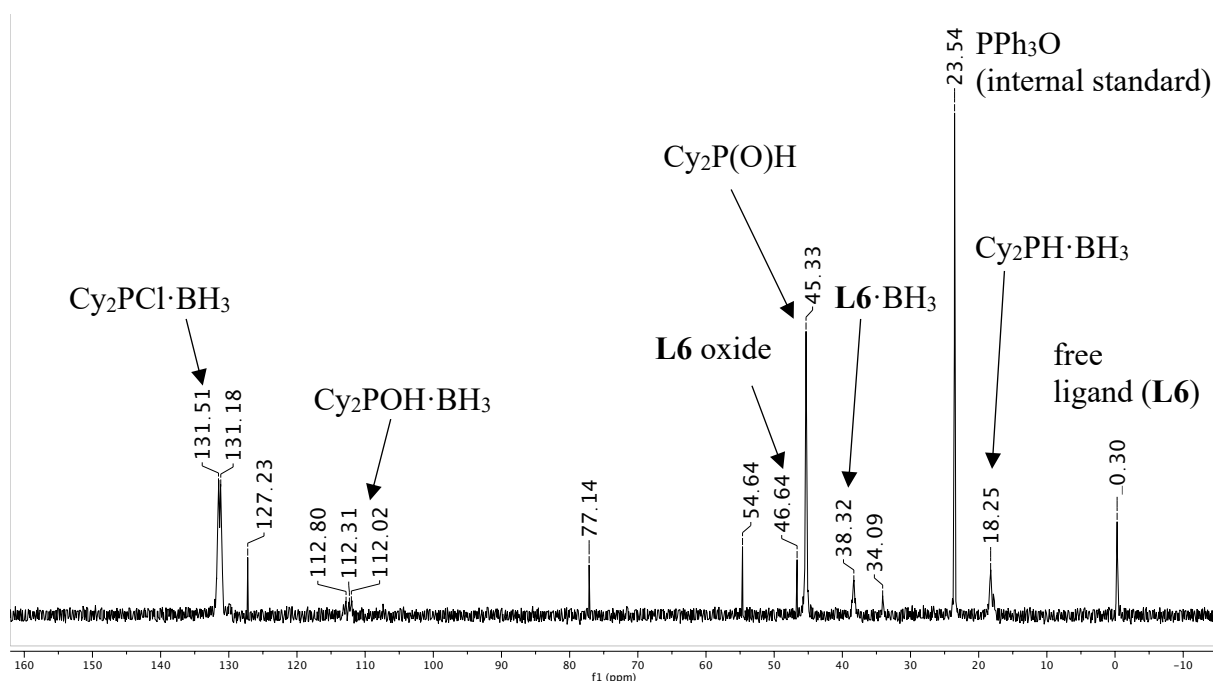
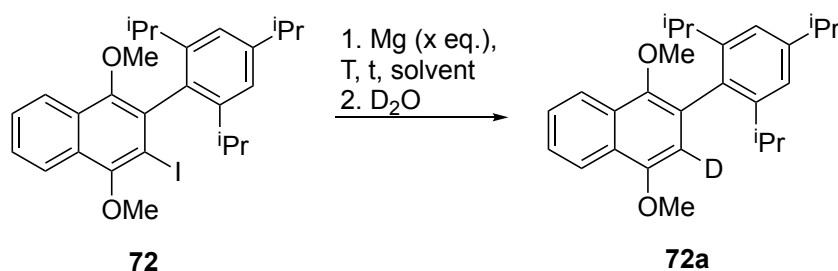


**Figure 19.** Exemplary spectrum of the *KatPhos* synthesis optimization (table 32, entry 3). Assignments to compounds are based on literature data<sup>139,140,141</sup> or previous works.<sup>78</sup>

Starting from precursor **72**, formation of *Grignard* species was first optimized by quenching reaction mixtures with D<sub>2</sub>O and analyzing the crude material with <sup>2</sup>H-qNMR spectroscopy (table 33).<sup>i</sup>

**Table 33.** Optimization of *Grignard* formation by D<sub>2</sub>O quench experiments.



entry	Mg (x eq.)	solvent	t /h	T / °C	yield /% <sup>a</sup>
1	3.8	THF	3	80	66
2	3.8	THF–toluene 3:7	3	100	61
3	3.8	THF	2	60	76

For all experiments, magnesium turnings were activated by heating with 1,2-dibromoethane at 80 °C in THF for 30 min before addition of **72**.

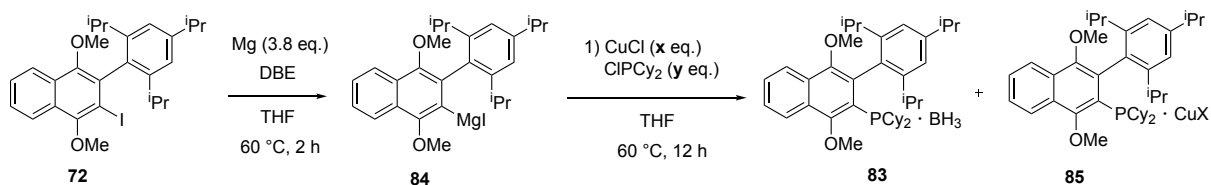
a) Analytical yield (mol-%) determined by <sup>2</sup>H-qNMR analysis using an internal standard.

<sup>i</sup> These optimizations were part of a student's research project in our group supervised by Philippe Klein.



The experiments show that elevated temperatures of 80 °C (entry 1) or 100 °C (entry 2) were not beneficial for *Grignard* formation, which could be attributed to side reactions such as demethylation (however, the less polar solvent composition in entry 2 could also be detrimental). The <sup>2</sup>H-qNMR yield improved considerably by lowering the reaction temperature to 60 °C in THF (entry 3). These conditions were then applied to the optimization of the subsequent phosphination reaction by <sup>31</sup>P-qNMR analysis (table 34), with slightly changed conditions (activation of magnesium with 1,2-dibromoethane at 60 °C instead of 80 °C).<sup>i</sup>

**Table 34.** Optimization reactions for the phosphination of Grignard reagent **84** with ClPCy<sub>2</sub>.



entry	CuCl (x eq.)	ClPCy <sub>2</sub> (y eq.)	<b>83</b> /% <sup>a</sup>	<b>85</b> /% <sup>a</sup>	Σ /% <sup>a</sup>
1	0.5	1.5	-	45	45
2	1.0	1.5	-	73	73
3	1.0	1.2	10	87	97
4	1.0	1.0	24	80	104

a) Analytical yields (mol-%) determined by <sup>31</sup>P-qNMR using an internal standard. Yields are based on **72**.

As seen in table 34, copper complex **85** stayed widely intact under these conditions and was only partly displaced by borane in entries 3 and 4. Employing a substoichiometric amount of CuCl (entry 1) was not beneficial. Raising the amount of copper(I) chloride to an equimolar amount afforded a considerably higher qNMR yield (entry 2). The yield improved further when lowering the amount of phosphine to 1.2 equivalents (entry 3) and was not negatively affected by using an even lower, equimolar amount of phosphine (entry 4). Comparison with crude <sup>1</sup>H-NMR of entry 4 also confirmed no major signals besides the ones stemming from **83** and **85**. In order to check the accuracy of the results, the recovery of phosphorus components (based on ClPCy<sub>2</sub>) was calculated for each entry of table 34. The results are listed in table 35.

<sup>i</sup> On a sidenote, despite a <sup>2</sup>H-NMR yield of only 74% of **72a** in the preliminary *Grignard* optimization experiments, little to no starting material **72** was observed in the crude <sup>1</sup>H-NMR spectra of all phosphination experiments. This might be attributed to the slightly changed reaction conditions for the *Grignard* formation.

**Table 35.** Quantification of phosphorus components seen in the  $^{31}\text{P}$ -qNMR spectra of table 34.

					$\text{C}_2\text{PH} \cdot \text{BH}_3$ ( <b>P</b> <sub>1</sub> )	$\text{C}_2\text{POH} \cdot \text{BH}_3$ ( <b>P</b> <sub>3</sub> )	$\text{C}_2\text{P}(\text{O})\text{H}$ ( <b>P</b> <sub>2</sub> )	$\text{C}_2\text{PCI} \cdot \text{BH}_3$ ( <b>P</b> <sub>4</sub> )		
	<b>L6</b>	<b>81</b>	<b>83</b>	<b>85</b>						
# <sup>a</sup>	<b>L6</b>	<b>81</b>	<b>83</b>	<b>85</b>	<b>P</b> <sub>1</sub>	<b>P</b> <sub>2</sub>	<b>P</b> <sub>3</sub>	<b>P</b> <sub>4</sub>	n.d.	$\Sigma$
	/% <sup>b</sup>	/% <sup>b</sup>	/% <sup>b</sup>	/% <sup>b</sup>	/% <sup>b</sup>	/% <sup>b</sup>	/% <sup>b</sup>	/% <sup>b</sup>	/% <sup>b</sup>	/% <sup>b</sup>
1	-	14	1.5	30	-	34	48	4.6	6.5	139
2	-	-	-	48.5	-	24	31.5	8.6	9.3	122
3	-	0.8	8.3	72.5	-	4.9	6.3	-	-	93
4	-	-	24.3	79.5	-	10.8	-	-	-	115

n.d.: unknown phosphorus species

a) Entry numbers of table 34.

b) Molar ratios (mol-%) based on  $\text{ClPCy}_2$  determined by  $^{31}\text{P}$ -qNMR using an internal standard.

It is evident that generally, recoveries are too high for most of the experiments, which questions the accuracy and comparability of the results. Notably, integrals of  $^{31}\text{P}$  nuclei are not only influenced by the  $T_1$  value of a nucleus, but also the Nuclear Overhauser effect (NOE), which can enhance sensitivity of decoupled  $^{31}\text{P}$  NMR spectra due to partial saturation of neighboring  $^1\text{H}$  nuclei.<sup>142</sup> When comparing the results of table 35, it is obvious that with a higher ratio of dicyclohexylphosphine oxide (**P**<sub>2</sub>) present in the mixture, recovery rates are generally higher. It seems plausible that the NOE is particularly pronounced for compounds bearing protons directly connected to phosphorus, thus enhancing integrals disproportionately. For borane complex **83** and copper complex **85**, such a trend cannot be found, and so the results are still seen as somewhat comparable, especially because the crude  $^1\text{H}$ -NMR spectra generally correlate with the respective  $^{31}\text{P}$ -qNMR results. However, it cannot be ruled out that other factors than the presence of dicyclohexylphosphine oxide have an influence on the NOE or on spin lattice relaxation times, and thus an accurate integration of the  $^{31}\text{P}$ -NMR spectra, as well. As another reaction mode, halogen-lithium exchange of the aryl iodide, followed by phosphination, was attempted (table 36).

**Table 36.** Optimization reactions for the synthesis of **83** via halogen-lithium exchange.

entry	x eq.	ClPCy <sub>2</sub> (y eq)	CuCl (z eq)	conc.	<b>83</b> /% <sup>a</sup>	<b>81</b> /% <sup>a</sup>	<b>85</b> /% <sup>a</sup>	<b>L6</b> /% <sup>a</sup>
1	1.0	1.5	-	0.1 M	33	-	-	-
2	1.0	1.5	-	0.2 M	18	-	-	-
3	1.0	1.5	1.0	0.2 M	-	-	37	-
4 <sup>b</sup>	1.0	1.5	-	0.2 M	19	-	-	-
5	1.3	1.0	-	0.1 M	32	2	-	7

a) Analytical yields (mol-%) determined by <sup>31</sup>P-qNMR using an internal standard. Yields are based on **72**.

b) The ClPCy<sub>2</sub> – solution was cooled to -60°C before addition to the aryl lithium solution.

Variation of the nominal concentration resulted in slightly better results for a lower concentration (entries 1 and 2). Addition of a stoichiometric amount of copper(I) chloride significantly improved the <sup>31</sup>P-qNMR yield (entry 3). Changing the reaction mode by cooling down the ClPCy<sub>2</sub> solution to -60°C before adding it to the aryl lithium solution, did not affect the yield at all (compare entries 2 and 4). As the aryl lithium species could undergo side reactions such as butylation, a slight excess of aryl lithium species was used (entry 5). This improved the yield slightly, but not considerably. Notably, in case when CuCl was used as additive, almost no borane adduct was formed, as observed before.

Again, the recovery of phosphorus components for the phosphinations *via* halogen-lithium exchange (based on ClPCy<sub>2</sub>) were calculated for each experiment and the results are listed in table 37.

**Table 37.** Quantification of phosphorus components seen in the  $^{31}\text{P}$ -qNMR spectra of table 36.

# <sup>a</sup>	Ligand Structures				Species		Species		n.d.	$\Sigma$
	L6	81	83	85	$\text{Cy}_2\text{PH} \cdot \text{BH}_3$ ( $\text{P}_1$ )	$\text{Cy}_2\text{P(O)H}$ ( $\text{P}_2$ )	$\text{Cy}_2\text{POH} \cdot \text{BH}_3$ ( $\text{P}_3$ )	$\text{Cy}_2\text{PCl} \cdot \text{BH}_3$ ( $\text{P}_4$ )		
	L6	81	83	85	$\text{P}_1$	$\text{P}_2$	$\text{P}_3$	$\text{P}_4$		
	/% <sup>b</sup>	/% <sup>b</sup>	/% <sup>b</sup>	/% <sup>b</sup>	/% <sup>b</sup>	/% <sup>b</sup>	/% <sup>b</sup>	/% <sup>b</sup>	/% <sup>b</sup>	/% <sup>b</sup>
1	-	-	22.7	-	6.1	41.6	10.6	32	10	112
2	-	-	11.8	-	8.3	64.8	10.6	22.5	7.9	126
3	-	-	3.6	22.2	5.6	63.2	9.6	21	3.8	129
4	-	-	12.8	-	4.2	60.7	6.9	39.1	6.4	130
5	6.9	1.6	32	-	2	37.5	11.2	11.2	16.2	119

n.d.: unknown phosphorus species

a) Entry numbers of table 36.

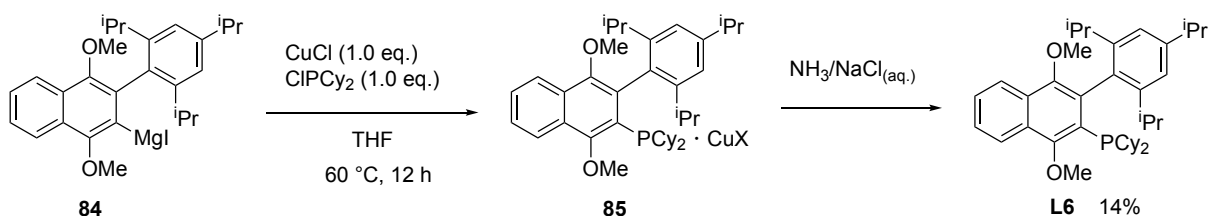
b) Molar ratios (mol-%) based on  $\text{ClPCy}_2$  determined by  $^{31}\text{P}$ -qNMR using an internal standard.

Again, recoveries are too high for all of the experiments, but somewhat comparable for entries 2-4. As observed before in table 35, recovery rates are generally higher with a higher content of  $\text{Cy}_2\text{P(O)H}$  ( $\text{P}_2$ ), although this trend is not observable when comparing entries 2-4. Again, other factors could contribute to the NOE or spin lattice relaxation times.

### Isolation of KatPhos

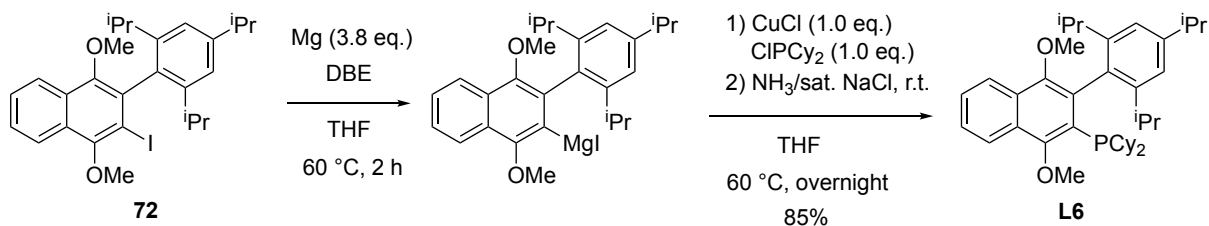
With the best conditions at hand, an optimized purification procedure for the isolation of KatPhos was now envisaged. Isolation as a borane adduct was considered, but dismissed due to incomplete conversion of the copper complex to borane adduct. Due to the stability and low solubility of the copper complex, purification by precipitation of **85** and subsequent treatment with a solution of  $\text{NH}_3$ /sat. aq. NaCl to release the free ligand was envisaged.<sup>15</sup> Crystallization from THF/hexanes afforded pure copper complex, however in insufficient yield (scheme 62), which was even further reduced after  $\text{NH}_3$ /sat. aq. NaCl wash (the loss of yield during decomplexation is probably due to the very small scale).

Obtaining crystals of copper complex **85** suitable for X-ray analysis failed due to decomposition of the material. Thus, the structure and composition of **85** could not be confirmed, however upon decomposition, the material adapted a purple color, which indicates iodide as counter-anion.



**Scheme 62.** Isolation of copper complex **85** and subsequent decomplexation.

Due to the unsuccessful efforts to purify the copper complex, direct decomplexation of the quenched reaction mixture was preferred when performing the reaction on a millimolar scale (scheme 63). This was done according to a protocol developed by Buchwald and co-workers<sup>15</sup> for the work-up of their ligand AlPhos which involved diluting the reaction mixture with solvent and an aqueous solution of  $\text{NH}_3/\text{sat. NaCl}$  and stirring the resulting mixture at room temperature for 30 minutes before work-up. This method of decomplexation was successful, showing no signal for **85** in the crude  $^{31}\text{P}$ -NMR spectrum. The best isolated yield was achieved by purification of the crude material by filtration over a short silica column to retain dicyclohexylphosphine oxide, which was formed as by-product, and subsequent precipitation with MeOH from EtOAc. This procedure delivered **L6** in sufficient yield and purity (containing 6.7 wt-% of **72**).



**Scheme 63.** Synthesis of *KatPhos* on the millimolar scale (**L6**) (best isolated yield).

Performing the reaction on the millimolar scale, however, could not reproduce the results of the small scale optimization reliably, as the reaction was not completed. This was observed when monitoring the reaction by TLC, which still showed minor amounts of hydrodehalogenated starting material and starting material **72** as by-products after the designated reaction time. However, when the reaction did not proceed any further after stirring for three more hours, it was decided to stop the reaction to avoid side reactions such as demethylation.

It is to be noted that other runs on the millimolar scale afforded lower isolated yields (up to 32% isolated yield after purification by trituration with MeOH and another crystallization from MeOH/EtOAc). This is attributed partly to the less optimal purification conditions, but also to a lack of reproducibility in the *Grignard* formation. It should therefore be considered to put

further efforts into the optimization of the *Grignard* formation on a larger scale for a better and more reproducible result.

The structure of **L6** was confirmed by X-ray crystallography after growing suitable crystals by diffusion crystallization from THF/MeOH (figure 20).

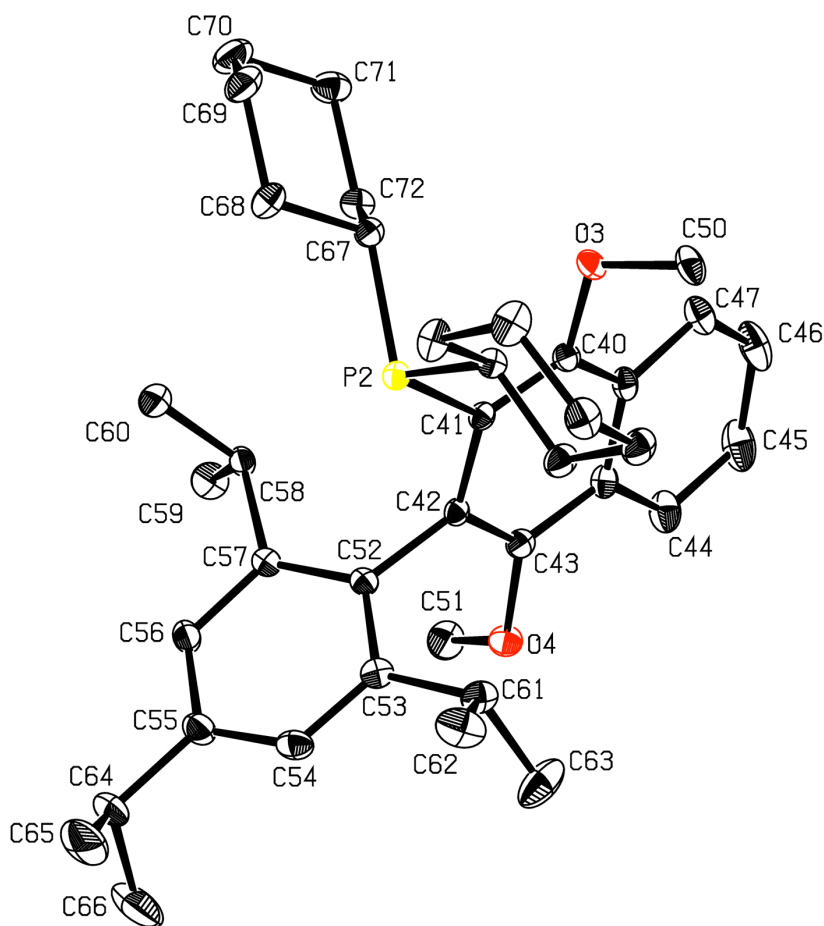


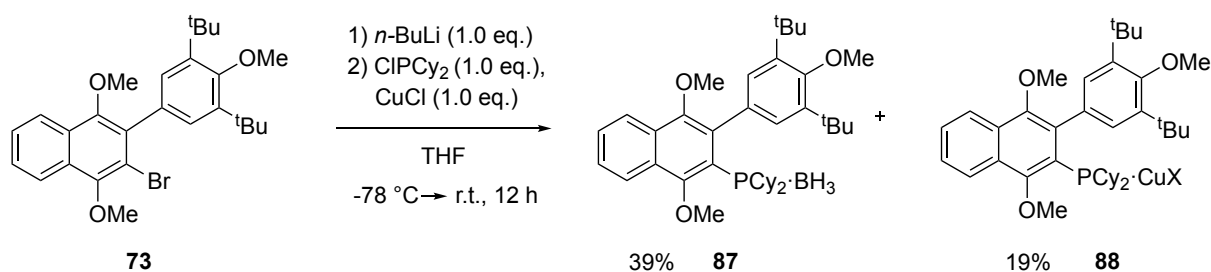
**Figure 20.** Solid-state molecular structure of **L6**. Ellipsoids are shown at 50% probability. Hydrogens are omitted for clarity. One unit cell features two molecules of **L6**. For clarity, only one molecule of the smallest unit cell is shown.

The compound crystallized as triclinic crystals belonging to the P-1 space group. One unit cell consists of two molecules of **L6**. Hydrogen bonding interactions are observed between the cyclohexyl group and the methoxy oxygen (in *ortho*-position to phosphorus, C72-H72A $\cdots$ O3). This was also reported in the crystal structure of BrettPhos.<sup>143</sup> Notably, the two methoxy groups face away from the plane that is defined by the naphthalene scaffold. This is contradictory to the crystal structure reported for BrettPhos, where the methoxy groups are in plane with the phosphorus-containing arene moiety, facing away from the neighboring dicyclohexylphosphine and aryl' substituents.<sup>143</sup> For KatPhos, the steric congestion caused by the benzoannulation

might force the methoxy substituents to face away from the plane. This indicates different steric properties of the two ligands and therefore interesting effects in catalysis.

### 3.2.3 Optimization of the CyAnPhos Synthesis

As for the synthesis of CyAnPhos, a lithiation and subsequent phosphination was attempted (scheme 64), but leading only to a moderate yield.



**Scheme 64.** Synthesis of CyAnPhos via lithiation route. Analytical yields (mol-%) determined by <sup>31</sup>P-qNMR using an internal standard.

The best conditions of the KatPhos synthesis were also tested, however not leading to a quantitative yield (table 38, entry 1). Thus, the reaction temperature was raised to 80 °C, leading to a near quantitative yield (entry 2).

**Table 38.** Synthesis of CyAnPhos starting from Grignard reagent.

entry	temperature	87 /% <sup>a</sup>	88 /% <sup>a</sup>
1	60 °C	65	19
2	80 °C	75	21

a) Analytical yields (mol-%) determined by <sup>31</sup>P-qNMR using an internal standard.

Unlike with the synthesis of KatPhos, the CyAnPhos copper complex is mostly, but not quantitatively displaced by borane using the same conditions. Figure 21 shows the crude <sup>31</sup>P-NMR of entry 1 (table 38) after the standard borane scavenging procedure and after heating the crude mixture with BH<sub>3</sub>·Me<sub>2</sub>S at 60 °C overnight, which led to almost complete formation of the borane adduct.

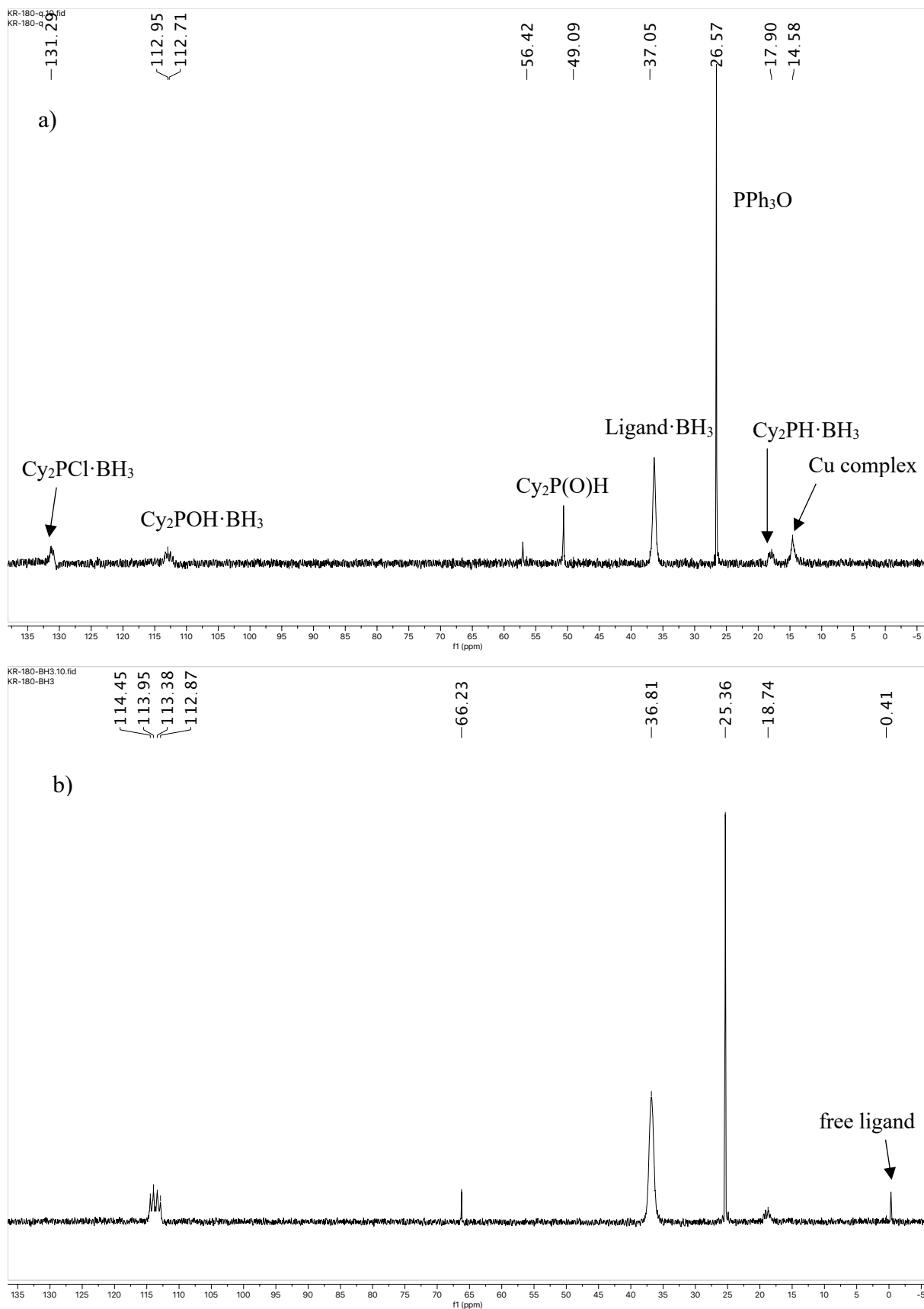
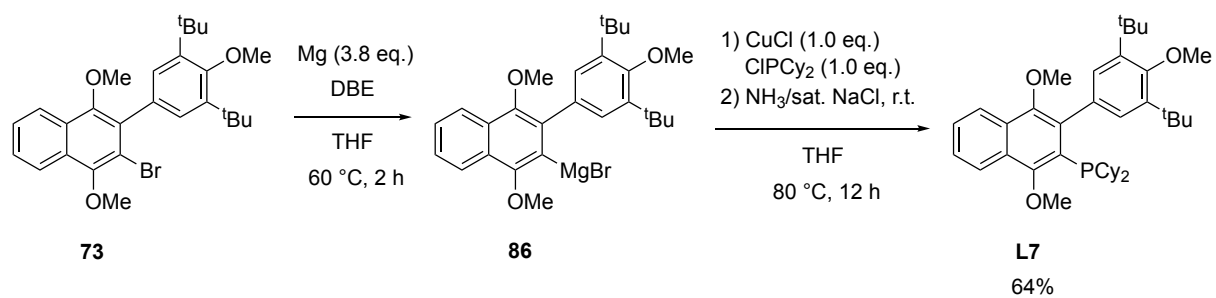


**Figure 21.** Excerpt of the  $^{31}\text{P}$ -NMR spectrum of entry 1, table 38. a) Crude material. b) Crude material after heating with  $\text{BH}_3\cdot\text{Me}_2\text{S}$  in THF at 60 °C overnight.



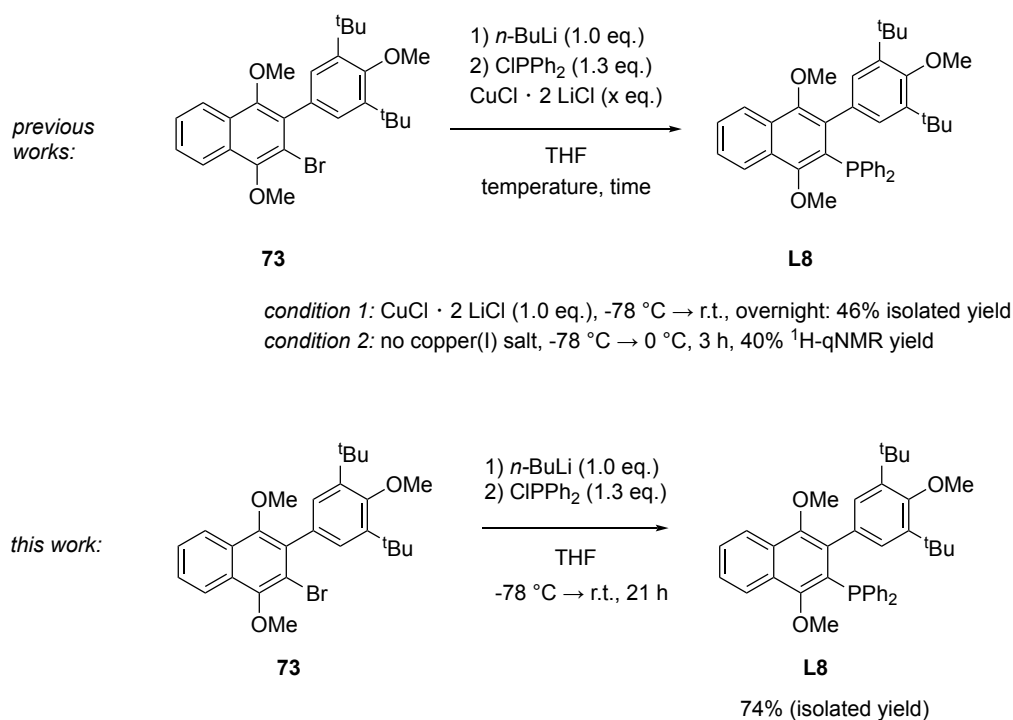
Isolation of the CyAnPhos borane adduct by column chromatography failed, and thus it was decided to use  $\text{NH}_3/\text{sat. aq. NaCl}$  decomplexation. Free ligand **L6** was obtained in 64% yield after recrystallization from hot acetone (scheme 65).



*Scheme 65. Synthesis of CyAnPhos (L7).*

### 3.2.4 Optimization of the AnPhos Synthesis

In previous works, the synthesis of AnPhos (**L8**) had been achieved in a moderate yield of 46% after column chromatography (scheme 66).<sup>78</sup> When revisiting antecedent optimization experiments, it became obvious that moderate yields (40% <sup>1</sup>H-qNMR yield) were achieved for this reaction even without the use of copper(I) salt. Following this realization, a reaction with the same condition was set up again, this time choosing a longer reaction time and a higher reaction temperature. This led to an improved synthesis of **L8** in 74% isolated yield. The purification method was also improved by choosing precipitation instead of column chromatography.



**Scheme 66.** Optimized synthesis of AnPhos (**L8**).

### 3.2.5 General Remarks on the Applicability of <sup>31</sup>P-qNMRs

As seen in the results of the optimization for the KatPhos and CyAnPhos ligand synthesis, recovery values of the <sup>31</sup>P quantitative NMR analysis varied from experiment to experiment, leading to questionable results. As mentioned before, integrals in <sup>31</sup>P-NMR spectra are not only influenced by the  $T_1$  value of a nucleus, but also the Nuclear Overhauser effect (NOE), which enhances sensitivity of decoupled <sup>31</sup>P NMR spectra due to partial saturation of neighboring <sup>1</sup>H nuclei.<sup>142</sup>

Presumably, the fluctuating recovery values are due to the changing composition of the analyte solution, which can influence the  $T_1$  value of  $^{31}\text{P}$  nuclei and leads to unequal signal responses as a result of environment-specific NOEs. To suppress NOE enhancement, inverse gated decoupling is often used in analytical chemistry.<sup>138,137</sup>

Thus, inverse gated decoupling should be applied in the  $^{31}\text{P}$ -qNMR reaction optimization to deliver more accurate results. Furthermore, relaxation delays could be optimized for each experiment. This, however, would come with the cost of long measuring times which is often not feasible in practice.

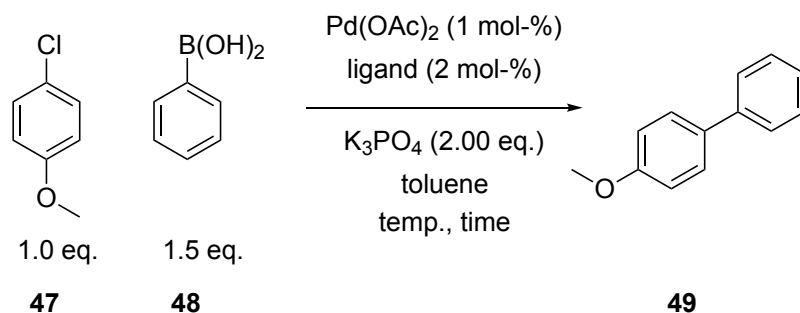
### 3.3 Catalytic Test Reactions Employing Benzoannulated Ligands of the Buchwald Type

#### 3.3.1 *KatPhos* and *CyAnPhos* in Suzuki-Miyaura Coupling Reactions

##### The Coupling of 4-Chloroanisole and Phenylboronic Acid as a Model Reaction

As a first catalytic test reaction, the benzoannulated ligands were tested in the Suzuki-Miyaura coupling of 4-chloroanisole and phenylboronic acid using reaction conditions adapted from Buchwald and co-workers.<sup>1</sup> The screened conditions along with their <sup>1</sup>H-qNMR yields are listed in table 39.

**Table 39.** First catalytic test reactions for the Suzuki-Miyaura coupling of 4-chloroanisole and phenylboronic acid using *CyAnPhos* and *KatPhos*.



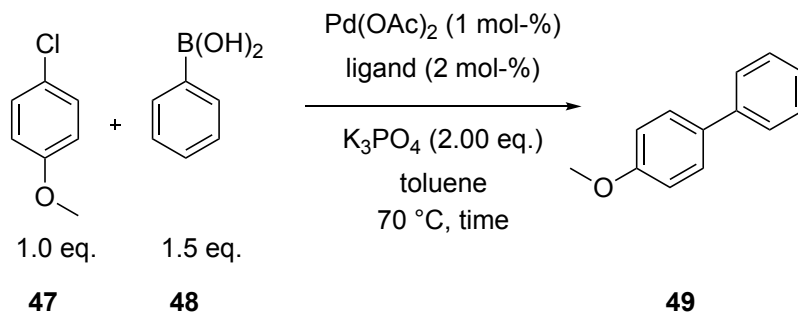
entry	ligand	temperature	time	yield /% <sup>a</sup>
1	<i>CyAnPhos</i>	100 °C	3 d	91
2	<i>CyAnPhos</i>	100 °C	1 h	93
3	<i>KatPhos</i>	100 °C	1 h	100
4	<i>CyAnPhos</i>	r.t.	23 h	trace
5	<i>CyAnPhos</i>	50 °C	23 h	4
6	<i>CyAnPhos</i>	70 °C	24 h	47

a) Reactions were conducted using an internal standard (tetradecane) and analytical yields (mol-%) were determined by direct sampling from the reaction mixture and subsequent <sup>1</sup>H-qNMR analysis.

At first, the reaction was conducted at 100 °C, but both ligands showed comparable, near quantitative results (entries 2 and 3) already after one hour (with *KatPhos* showing slightly better results). In the case of *CyAnPhos*, even after 3 days, the reaction did not progress any further (compare entries 1 and 2). For a better comparison, the reaction temperature was lowered (entries 4-6). At lower temperatures, *CyAnPhos* delivered unsatisfying results, and so 70 °C was chosen as ideal temperature for comparing the performance of different ligands.

Table 40 shows the performance of KatPhos, CyAnPhos compared to benchmark ligands BrettPhos and SPhos. For each reaction, a sample was taken after 100 minutes and 24 hours, respectively, and the reaction progress analyzed by <sup>1</sup>H-qNMR.

**Table 40.** Comparison of benzoannulated ligands and Buchwald ligands in the Suzuki-Miyaura coupling of 4-chloroanisole and phenylboronic acid at 70 °C.



entry	ligand	yield at 100 min /% <sup>a</sup>	yield at 24 h /% <sup>a</sup>
1	CyAnPhos	20	47
2	KatPhos	63	96
3	BrettPhos	56	98
4	SPhos	81	81

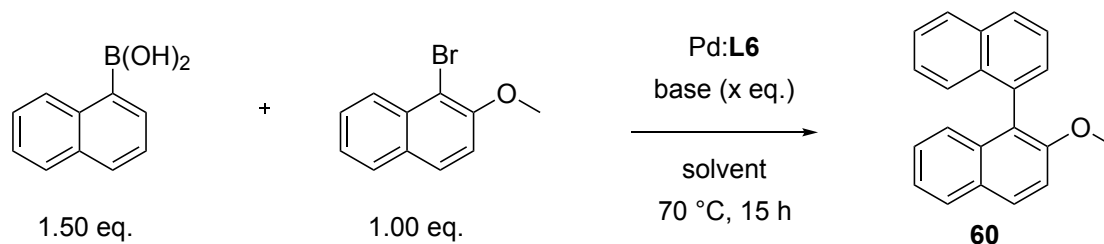
a) Reactions were conducted using an internal standard (tetradecane) and yields (mol-%) were determined by direct sampling from the reaction mixture and subsequent <sup>1</sup>H-qNMR analysis.

With CyAnPhos as ligand (entry 1), the reaction progressed rather slowly. Even though after 100 minutes, a small amount (20%) of target material had already been formed, the reaction did not proceed at the same rate, as the yield was only 47% after 24 hours. The use of KatPhos showed much better results (entry 2). Compared to BrettPhos (entry 3), the yield was slightly higher after 100 minutes, but results were comparable after 24 hours. The use of benchmark ligand SPhos showed by far the best result after 100 minutes, but did not show any further progress after that (entry 4). Overall, KatPhos turned out to be a competitive, but not superior ligand with its direct *Buchwald* analogue BrettPhos in this coupling. The use of CyAnPhos is clearly of disadvantage here.

### Substrate Scope: KatPhos and the Suzuki-Miyaura Coupling

As KatPhos seemed to show promising results in the Suzuki-Miyaura test reaction similar to BrettPhos, its substrate scope was tested in sterically demanding Suzuki-Miyaura coupling reactions. As such, the coupling of 1-bromo-2-methoxynaphthalene and 1-naphthylboronic acid was tested (see table 41).

**Table 41.** Screening of reaction conditions for sterically hindered substrates using KatPhos (**L6**)



entry	base (x eq)	solvent	L:Pd <sup>a)</sup>	yield /% <sup>b)</sup>
1	K <sub>3</sub> PO <sub>4</sub> (2.00 eq.)	toluene	1:2	32
2	K <sub>3</sub> PO <sub>4</sub> (2.00 eq.)	toluene	1:1	22
3	K <sub>3</sub> PO <sub>4</sub> (2.00 eq.)	toluene	1:3	32
4	K <sub>3</sub> PO <sub>4</sub> (3.00 eq.)	toluene	1:2	36
5	K <sub>3</sub> PO <sub>4</sub> (2.00 eq.)	1,4-dioxane	1:2	38
6	K <sub>3</sub> PO <sub>4</sub> (3.00 eq.)	1,4-dioxane	1:2	67

a) Pd(OAc)<sub>2</sub> (1 mol-%) was used as Pd precursor.

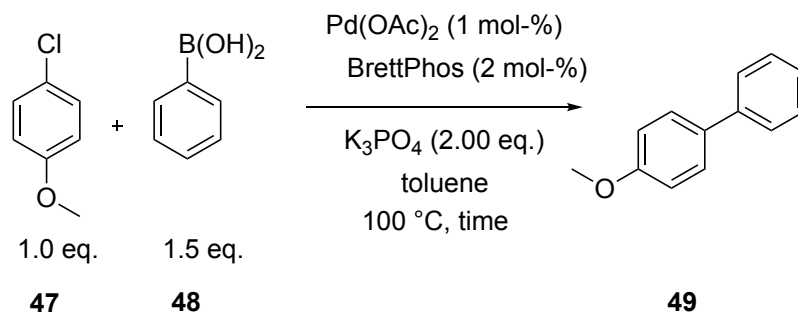
b) Analytical yields (mol-%) determined by <sup>1</sup>H-qNMR analysis using an internal standard.

The standard conditions<sup>1</sup> only resulted in a low yield (entry 1), so further optimization efforts were undertaken. Variation of L:Pd ratio did not offer any advantage (entries 2 and 3). A slight improvement in yield was reached by increasing the amount of base (entry 4) and changing the solvent to more polar 1,4-dioxane<sup>144</sup> (entry 5). Combining the latter variations led to a significant improvement in yield (entry 6). However, the screening of reaction conditions for sterically hindered substrates was left at this point because the yield was still not satisfying.

### Side Note on the Reproducibility of Suzuki-Miyaura Couplings

On a side note, differing results from a colleague conducting the same catalytic reaction motivated the conduction of Pd(OAc)<sub>2</sub>/BrettPhos-catalyzed coupling of phenyl boronic acid and 4-chloroanisole under two different parameters: Firstly, weighing in the inorganic base in a glovebox, and secondly, weighing in the inorganic base (stored in a Schlenk flask outside of the glovebox) on the bench (table 42).

**Table 42.** Results for the Pd(OAc)<sub>2</sub>/BrettPhos-catalyzed Suzuki-Miyaura coupling of 4-chloroanisole and phenylboronic acid under different parameters.



entry	time	yield /% <sup>a</sup>	comment
1	5 h	89	K <sub>3</sub> PO <sub>4</sub> added in the glovebox
2	1 h	98	K <sub>3</sub> PO <sub>4</sub> stored in a Schlenk flask under argon, but weighed in on the bench

a) Analytical yields (mol-%) determined by <sup>1</sup>H-qNMR analysis using an internal standard.

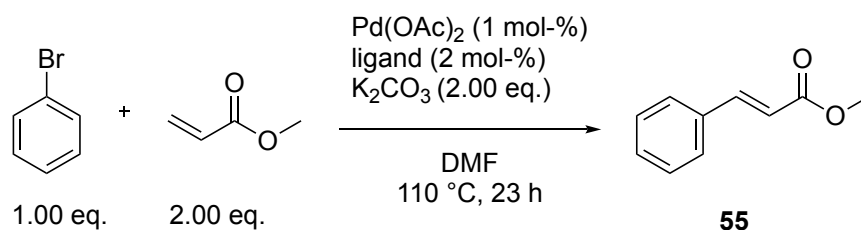
As shown in table 42, even after 5 hours of reaction time, the yield of **49** in entry 1 was still considerably lower than for entry 2, which was conducted with base weighed in on the bench. In conclusion, conditions under perfect water exclusion might not always be the most beneficial for the Suzuki-Miyaura coupling. Assumedly, trace amounts of water might improve solubility of the inorganic base. Similar observations have already been made in C-N couplings.<sup>145</sup> These findings should be taken into consideration when discussing reproducibility issues of cross-coupling reactions.

### 3.3.2 *KatPhos* and *CyAnPhos* in the Mizoroki-Heck Reaction

#### The Coupling of Bromobenzene and Methyl Acrylate as a Model Reaction

In another catalytic test reaction, the ligands were evaluated in a Mizoroki-Heck coupling with bromobenzene and methyl acrylate (table 43).

**Table 43.** Ligand screening in the Mizoroki-Heck reaction of bromo benzene and methyl acrylate.



entry	ligand	time	yield /% <sup>a</sup>
1	SPhos	23	40
2	BrettPhos	23	29
3	CyAnPhos	18	21
4	KatPhos	23	>99

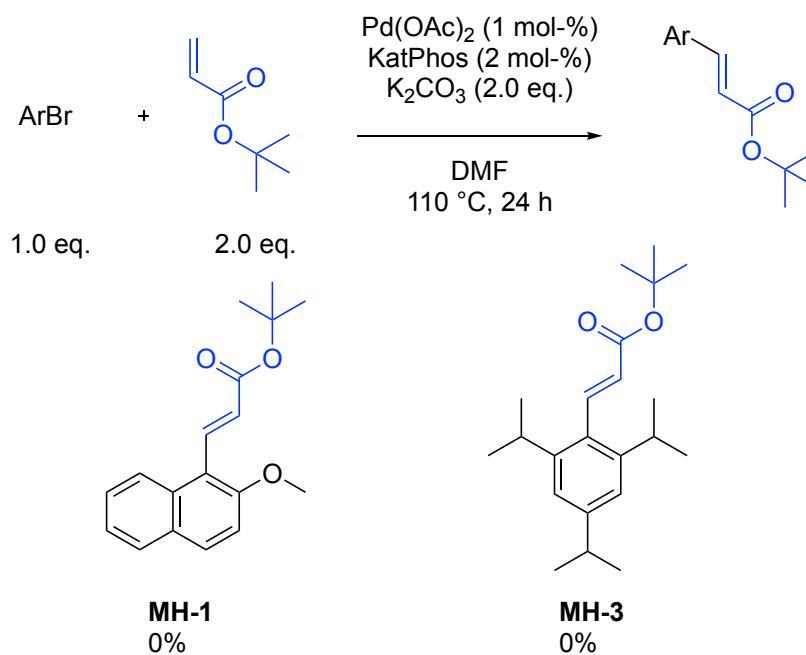
a) Analytical yields (mol-%) determined by <sup>1</sup>H-qNMR analysis using an internal standard.

When looking at entries 1-3, the observed trend of section 2.7.1 seems to continue: Ligands exhibiting a biaryl (both naphthyl-phenyl or phenyl-phenyl) motif perform rather poorly, indicating that the aryl' moiety is not of significant importance in the Mizoroki-Heck coupling. It should be noted that the reaction time with the use of CyAnPhos (entry 3) was shorter, so an exact comparability might not be given. Surprisingly, for KatPhos, this observation was not confirmed, as it afforded target material in excellent yield and outperformed its *Buchwald*-analogue BrettPhos by far (entry 4).



### Substrate Scope: KatPhos and the Mizoroki-Heck Reaction

Due to the excellent results of KatPhos in the *Mizoroki-Heck* coupling, a further investigation in its substrate scope was conducted with sterically hindered aryl bromides and *tert*-butyl acrylate as substrates (scheme 67).



**Scheme 67.** Failed substrates in Mizoroki-Heck couplings using KatPhos as ligand.

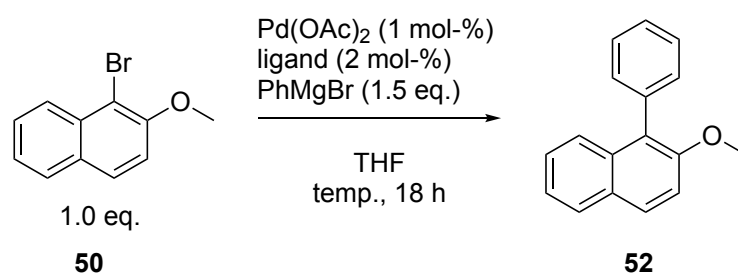
As none of the tested substrates were successful, a further investigation of the substrate scope was dismissed.

### 3.3.3 *Further Tests in Cross-Coupling Reactions*

#### **Kumada-Corriu Cross Coupling of 1-Bromo-2-methoxynaphthalene and Phenylmagnesium Bromide**

The ligands were further evaluated in the Pd-catalyzed Kumada-Corriu coupling of 1-bromo-2-methoxy naphthalene and phenylmagnesium bromide. The results of the ligand screening are presented in table 44.

**Table 44.** Ligand screening in the Kumada-Corriu coupling of 1-bromo-2-methoxynaphthalene and phenylmagnesium bromide.



entry	ligand	temperature	yield /% <sup>a</sup>
1	SPhos	70 °C	88
2	BrettPhos	70 °C	45
3	CyAnPhos	70 °C	84
4	KatPhos	70 °C	77
5	SPhos	r.t.	86
6	BrettPhos	r.t.	5
7	CyAnPhos	r.t.	70
8	KatPhos	r.t.	10

a) Analytical yields (mol-%) determined by <sup>1</sup>H-qNMR analysis using an internal standard.

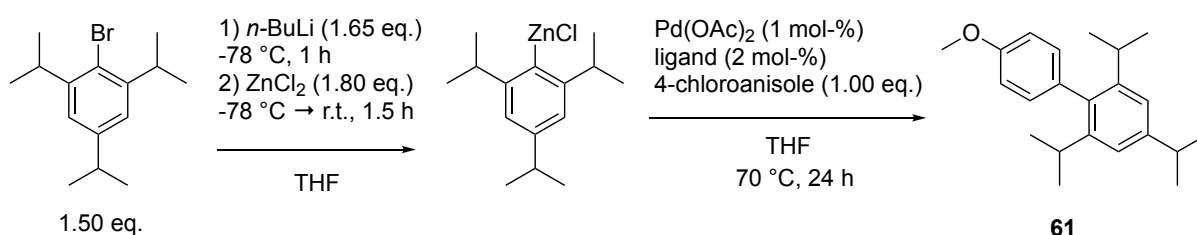
When conducting the coupling at elevated temperature (entries 1-4), CyAnPhos showed very good results (entry 3) comparable to benchmark ligand SPhos (entry 1). The use of KatPhos resulted in a slightly lower yield than CyAnPhos (entry 4). BrettPhos, on the other hand, showed poor results (entry 2). Next, the performance of the ligands at room temperature was evaluated. While the performance of SPhos was equally good at room temperature (entry 5), the use of CyAnPhos afforded a considerably lower yield, but still satisfying (entry 7). The performance of BrettPhos and KatPhos, on the other hand, dropped considerably to afford almost no product (entries 6 and 8). At higher temperatures, again, the activity of BrettPhos and its benzoannulated derivative KatPhos vary considerably. Combined with the results from the Mizoroki-

Heck coupling, this indicates that the benzoannulation might contribute to a better ligand activity at higher temperatures. In this coupling, the aryl'-*meta*-substitution of CyAnPhos seems to be of benefit.

### KatPhos and CyAnPhos in the Negishi Coupling of 2,4,6-Triisopropylphenylzinc Chloride and 4-Chloroanisole

The ligands were furthermore screened in the Negishi coupling of 2,4,6-triisopropylphenylzinc chloride and 4-chloroanisole (table 45) based on a procedure reported in the literature.<sup>13</sup>

**Table 45.** Ligand screening in the Negishi coupling test reaction.



entry	ligand	yield /% <sup>a</sup>
1	SPhos	80
2	BrettPhos	51
3	CyAnPhos	10
4	KatPhos	69

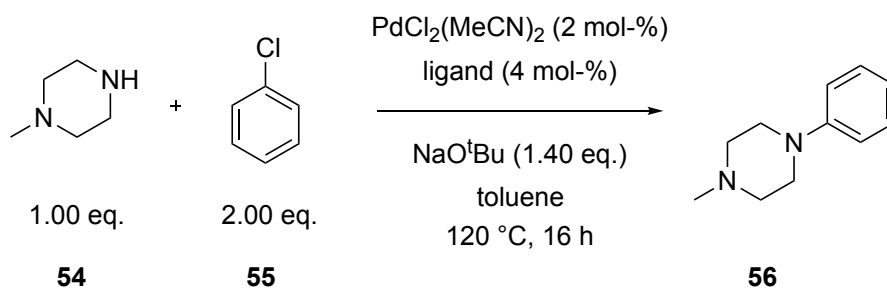
a) Analytical yields (mol-%) determined by <sup>1</sup>H-qNMR analysis using an internal standard.

Buchwald ligand SPhos, which is typically employed in the Negishi coupling, performed excellently (entry 1), whereas BrettPhos only showed a moderate result (entry 2). The use of CyAnPhos (entry 3) gave poor yields. KatPhos, on the other hand, performed well (entry 4), again indicating an advantage of the benzoannulated structural motif. The performance of KatPhos in the Negishi coupling was not further investigated, as its result in the model coupling still lags behind compared to benchmark ligand SPhos. A further tuning of reaction conditions for enhanced catalytic activity might be beneficial.

### KatPhos and CyAnPhos in the Buchwald-Hartwig Amination of *N*-Methylpiperazine and Chlorobenzene

The ligands were screened in a Buchwald-Hartwig amination following a protocol by Reddy et al. (table 46).<sup>109</sup>

**Table 46.** Ligand screening in the Buchwald-Hartwig amination reaction of *N*-methylpiperazine and chlorobenzene.

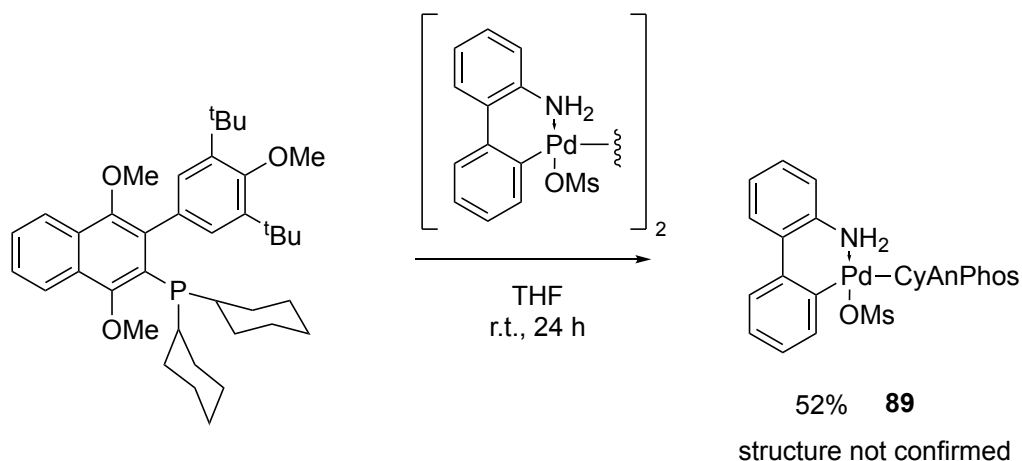


entry	ligand	yield /% <sup>a</sup>
1	CyAnPhos	37
2	KatPhos	6
3	BrettPhos	66

a) Analytical yields (mol-%) determined by <sup>1</sup>H-qNMR analysis using an internal standard.

It is evident that BrettPhos, a ligand typically employed in amination reactions, delivered the best result in this protocol (entry 3). CyAnPhos afforded a considerably lower yield (entry 1), while KatPhos performed very poorly (entry 2). This implies that the benzoannulated structural motif might be of disadvantage with these conditions, while the *meta*-substituted aryl' moiety might be slightly beneficial. An interesting addition to this screening could be the corresponding dialkylbiarylphosphine ligand with *meta*-aryl'-substitution.

Notably, the conditions employed are not typical *Buchwald* conditions, which explains the moderate, but not excellent performance of BrettPhos. The precatalyst system is an important factor for a successful cross-coupling reaction, and for typical palladium precatalysts like  $\text{PdCl}_2(\text{MeCN})_2$  or  $\text{Pd}(\text{OAc})_2$ , the metal center has to disassociate from the ligand and the Pd(II) species must be reduced to Pd(0) before entering the catalytic cycle. To circumvent these issues, Buchwald and co-workers developed a variety of pre-ligated Pd precatalysts which proved useful in C-N coupling reactions.<sup>2,17</sup> Therefore, the synthesis of a CyAnPhos ligated 2-aminobiphenyl palladium methane sulfonate was attempted according to an altered literature procedure by Buchwald and co-workers<sup>17</sup> (scheme 68).



**Scheme 68.** Attempted synthesis of a CyAnPhos ligated 2-aminobiphenyl palladium methanesulfonate preligand **89**.

The reaction was monitored by  $^{31}\text{P}$ -NMR. After 1.5 hours of reaction time, analysis of the reaction mixture showed complete conversion of the ligand (figure 22). The main species gave rise to a broad signal at  $\delta_P$  43.94. Besides, two minor signals are observed at  $\delta_P$  38.99 and  $\delta_P$  57.65. Adding pentane to the reaction mixture after 24 hours precipitated a colorless solid, which after  $^{31}\text{P}$ -NMR analysis gave rise to only a single peak at  $\delta_P$  58.59, which is a considerable downfield shift compared to the free ligand ( $\delta_P$  -0.14).

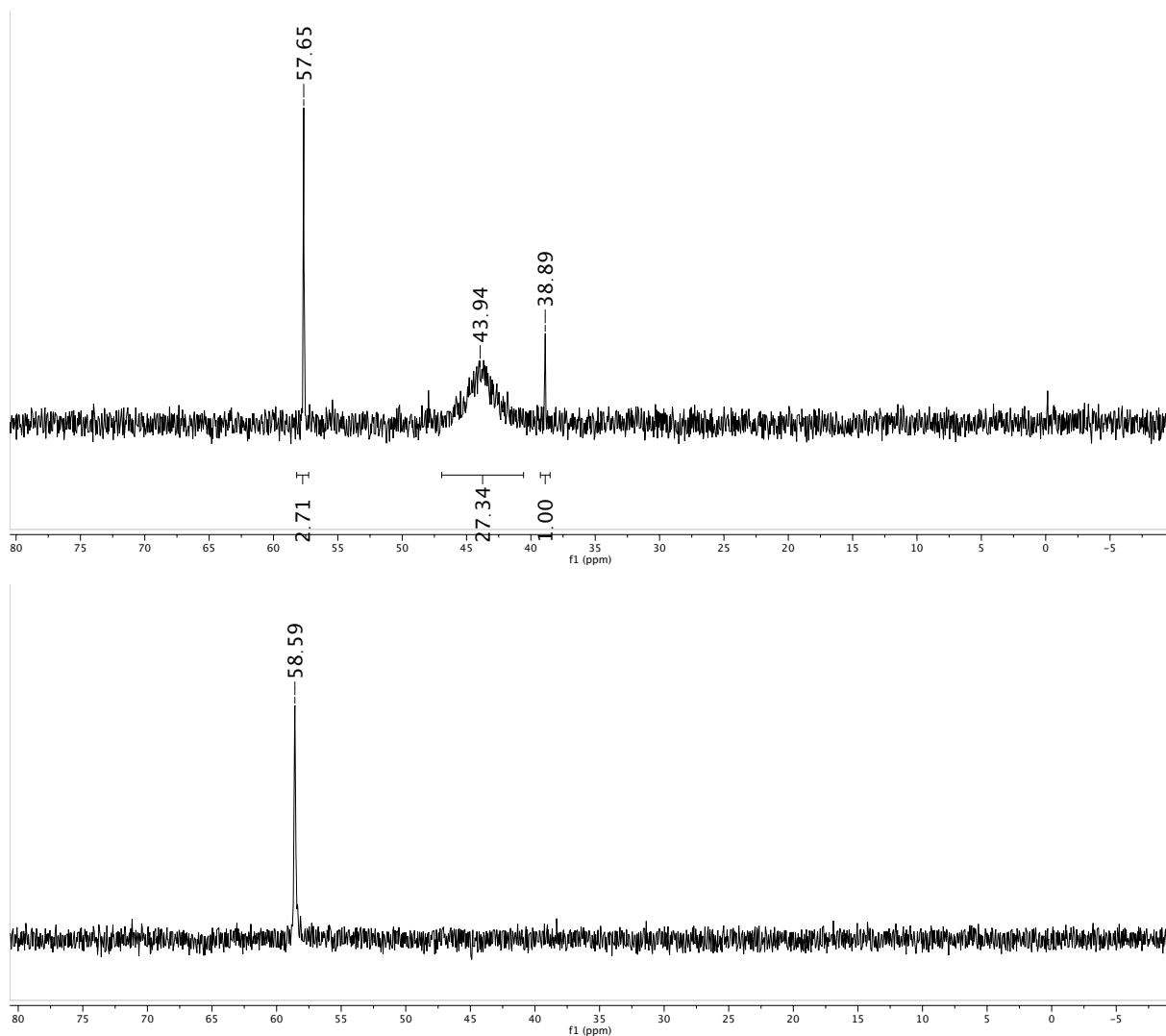


**Figure 22.**  $^{31}\text{P}$ -NMR analysis of a) the reaction mixture after 1.5 hours and b) precipitated product after 24 hours of reaction time.

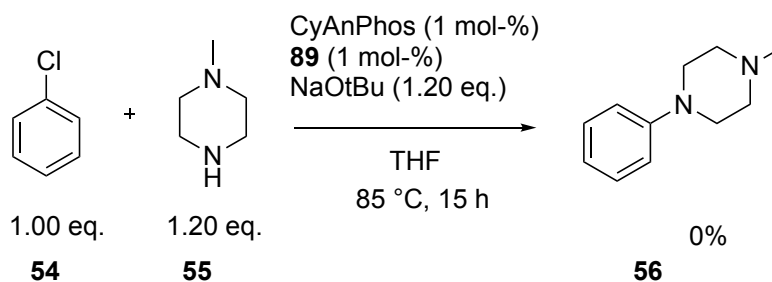
Analysis of the  $^1\text{H}$ -NMR spectrum was puzzling, as only two methoxy group signals instead of three were observed in the expected chemical shift area and no signals for methanesulfonic acid anion were observed. Apart from this observation, the signals matched those expected for the target complex, and no signal in other chemical shift ranges was observed which could stem from the third methoxy group.

This phenomenon is unfathomable, as a demethylation under the employed reaction conditions seems unfeasible. An elemental analysis was conducted for further elucidation of the identity of the formed solid (table 47).

**Table 47.** Elemental analysis for compound **89**.

element	%-content (calcd.)	%-content (first analysis)	%-content (second analysis)
C	64.22	68.83	68.83
H	7.05	7.28	7.18
N	1.44	1.62	1.64
S	3.30	0.44	0.20

The results of the elemental analysis lead to the assumption that a different species than the desired one was formed. While the H and N contents seem to agree with the calculated ones within the limits of error, the C content is considerably higher, whereas the S content is considerably lower. A plausible structure which takes into consideration a) the elemental analysis and b) the lacking  $^1\text{H-NMR}$  signals cannot be defined. Before considering a further elucidation of the structure, the model coupling of chlorobenzene and *N*-methyl piperazine was conducted according to *Buchwald* conditions<sup>17</sup> (scheme 69) to test if its use bears an advantage over the formerly applied conditions (table 46). As the coupling failed, a further elucidation of the structure of the obtained complex was dismissed and it was decided to best leave the case unsolved.<sup>146</sup>

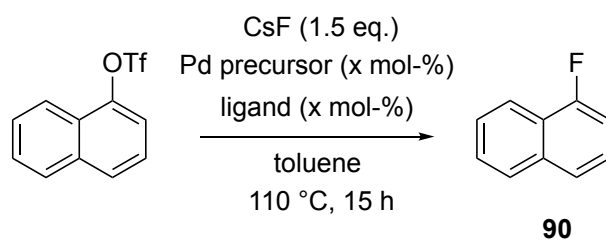


**Scheme 69.** Failed *Buchwald-Hartwig* coupling of chlorobenzene and *N*-methyl piperazine using **89** as *Pd* precursor.

### KatPhos and AnPhos in the Pd-Catalyzed Fluorination of 1-Naphthyl Triflate

Benzoannulated ligands KatPhos (**L6**) and AnPhos (**L8**) were furthermore tested in the Pd-catalyzed fluorination of 1-naphthyl triflate, which was performed based on an altered procedure by *Buchwald* and co-workers (table 48).<sup>15</sup> *Buchwald* ligand BrettPhos was used for a direct comparison. It is to be noted that *Buchwald* and co-workers prefer to use the AlPhos ligand for this procedure, however when starting their efforts in Pd-catalyzed fluorination, BrettPhos and <sup>t</sup>BuBrettPhos were used, so BrettPhos is still a viable ligand for comparison in this coupling.<sup>147</sup>

**Table 48.** Ligand screening for the Pd-catalyzed fluorination of aryl triflates.



entry	Pd precursor	ligand	yield /% <sup>a</sup>	conversion /% <sup>a</sup>
1	Pd(OAc) <sub>2</sub> (2 mol-%)	KatPhos (3 mol-%)	0	8
2	Pd(OAc) <sub>2</sub> (2 mol-%)	BrettPhos (3 mol-%)	0	37
3	[(allyl)PdCl] <sub>2</sub> (2.5 mol-%)	KatPhos (7.5 mol-%)	<5	27
4	[(allyl)PdCl] <sub>2</sub> (2.5 mol-%)	BrettPhos (7.5 mol-%)	23	84
5	[(allyl)PdCl] <sub>2</sub> (2.5 mol-%)	AnPhos (7.5 mol-%)	0	5

a) Analytical yields (mol-%) and conversions (mol-%) determined by <sup>19</sup>F-qNMR analysis using an internal standard.

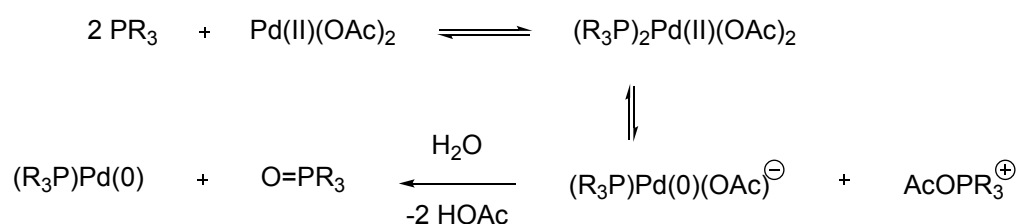
At first, the fluorinations were conducted with Pd(OAc)<sub>2</sub> as palladium precursor. This coupling was unsuccessful for KatPhos (entry 1) and even for BrettPhos (entry 2), which had been used in the literature model reaction. This result indicated that Pd(OAc)<sub>2</sub> is not suitable as Pd precursor. In fact, Buchwald and co-workers reported best results with [(cinnamyl)PdCl]<sub>2</sub>. Assuming that [(allyl)PdCl]<sub>2</sub> could perform similarly, this was instead employed as palladium precursor (entries 3-5). The use of BrettPhos gave low yield (entry 4), which was in accordance to its performance described in the literature. In comparison, its benzoannulated version KatPhos performed poorer (entry 3) and the use of AnPhos resulted in no product at all (entry 5). As for the conversions, BrettPhos also showed an almost complete conversion (entry 4), whereas KatPhos only gave low conversion (entry 3). By-products of the reaction were identified by GC-MS analysis and are mainly binaphthyl ether and 1-chloronaphthalene (for entries 3-5).



### 3.4 Evaluation of KatPhos and CyAnPhos in BrettPhos-Typical Couplings

#### 3.4.1 Arylation of Primary Amines

As a further investigation of the properties of CyAnPhos and KatPhos in catalysis, their performance in BrettPhos-typical couplings was compared directly with benchmark ligand BrettPhos. As such, it was tested in the arylation of primary amines. Since the *Buchwald* type palladium precatalysts were not available in the case KatPhos and CyAnPhos, the Pd(II) water activation protocol developed by Buchwald and co-workers was used for a better catalyst activation (scheme 70).<sup>111</sup>



**Scheme 70.** Mechanism of the water-mediated catalyst preactivation as reported by Buchwald and co-workers.

As model reaction, the coupling of 4-chloroanisole and aniline was chosen. The reactions were stopped after two hours of reaction time and the crude material analyzed by <sup>1</sup>H-qNMR (table 49).

**Table 49.** Ligand screening in the arylation of primary amines.

entry	ligand	yield /% <sup>a</sup>
1	BrettPhos	47
2	KatPhos	65
3	CyAnPhos	13

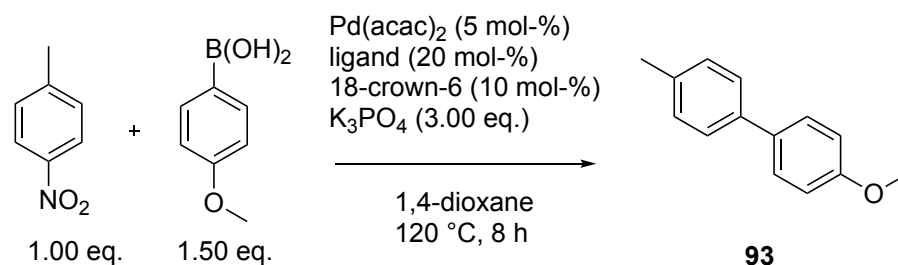
a) Analytical yields (mol-%) determined by <sup>1</sup>H-qNMR analysis using an internal standard.

In this coupling, the use of KatPhos (entry 2) was considerably more beneficial compared to BrettPhos (entry 1). CyAnPhos, on the other hand, afforded only low yields (entry 3).

### 3.4.2 *Denitrative Suzuki-Miyaura Coupling of Nitroarenes*

BrettPhos has also demonstrated wide applicability in denitrative transformations, such as Pd catalyzed hydrogenation reactions, intramolecular C-H arylation, alkylation and alkenylations.<sup>148</sup> In 2017, Nakao and co-workers reported the denitrative *Suzuki-Miyaura* coupling of nitroarenes with BrettPhos as ligand.<sup>149</sup> As model reaction, the coupling of 4-nitrotoluene and 4-methoxyphenylboronic acid was chosen for a comparison between the performance of BrettPhos and its benzoannulated derivative KatPhos (table 50).

**Table 50.** Ligand screening in the denitrative *Suzuki-Miyaura* coupling of 4-nitrotoluene and 4-methoxyphenylboronic acid.



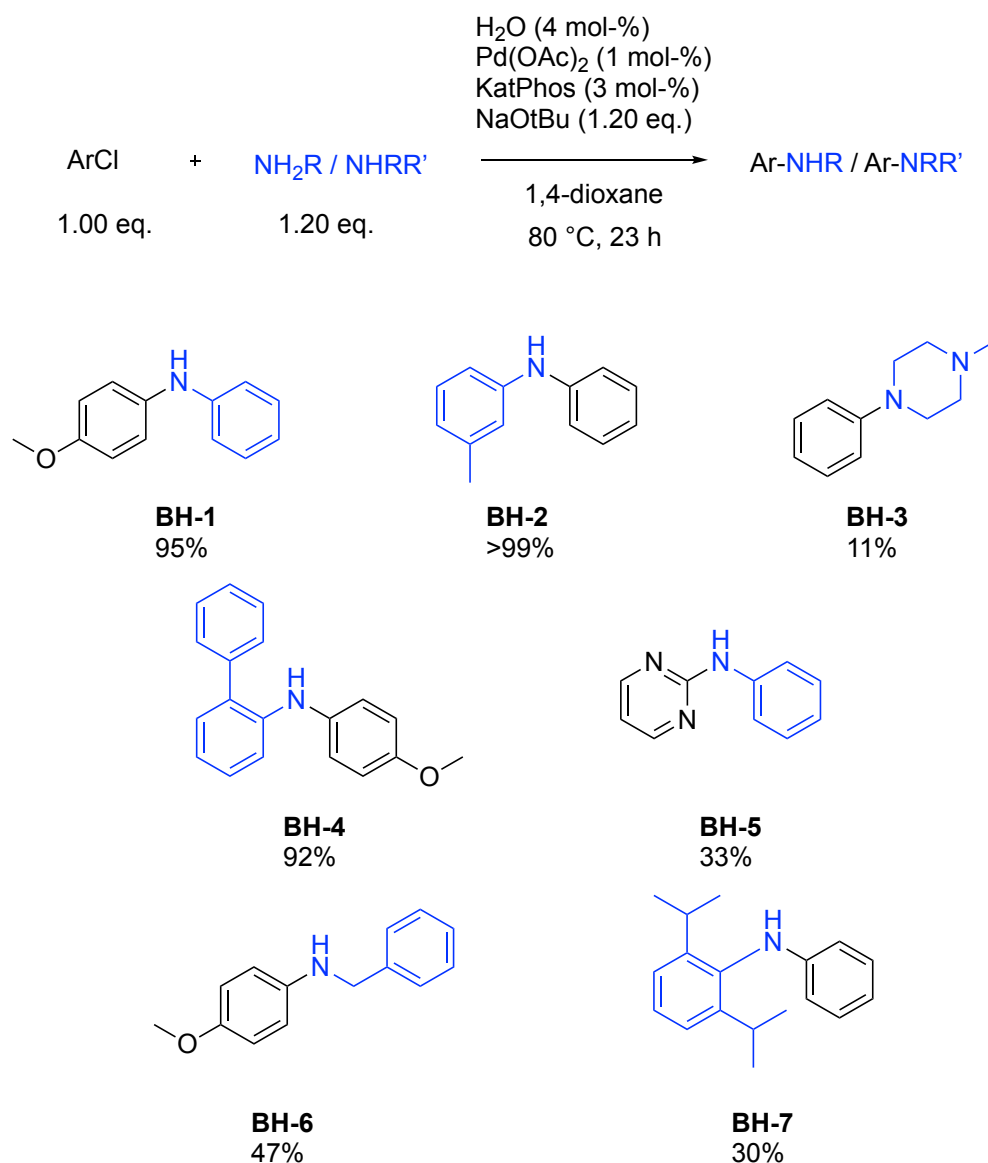
entry	ligand	yield /% <sup>a</sup>	conversion /% <sup>a</sup>
1	BrettPhos	42	47
2	KatPhos	10	19

a) Analytical yields (mol-%) determined by <sup>1</sup>H-qNMR analysis using an internal standard.

It is evident that after 8 hours, the use of KatPhos resulted in a very low yield and low conversion (entry 2) compared to BrettPhos. The benzoannulated structural motif, in this case, seems not beneficial. This finding is contradictory to the *Suzuki-Miyaura* couplings of aryl chlorides (see section 3.5.1), where the two ligands showed comparable performance.

### 3.4.3 Evaluations of the Substrate Scope in the Arylation of Primary and Secondary Amines using KatPhos as Ligand

Due to the promising results for the arylation of primary amines using *Buchwald* conditions (see section 3.5.1 of this work), the substrate scope for KatPhos as ligand for both primary and secondary amines was further investigated (scheme 71).



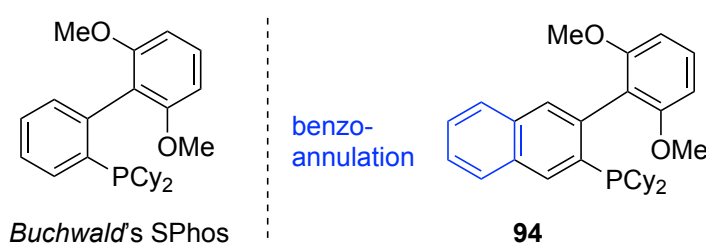
**Scheme 71.** Substrate scope for the amination of aryl chlorides using KatPhos. Analytical yields (mol-%) determined by  $^1\text{H-qNMR}$  analysis using an internal standard.

Deactivated aryl chlorides as well as unactivated ones were aminated in quantitative yield (**BH-1** and **BH-2**). The coupling of secondary amine *N*-methylpiperazine and chlorobenzene resulted in poor yields (**BH-3**), thus indicating that KatPhos, like BrettPhos, might preferably be used in the coupling of primary amines.<sup>2</sup> Sterically hindered aryl amines with a phenyl moiety in

*ortho*-position were coupled successfully (**BH-4**), but more sterically encumbered amine 2,6-diisopropyl aniline resulted only in low yields (**BH-7**). Benzyl amine and deactivated 4-chloroanisole gave moderate yield (**BH-6**). Heterocyclic substrate 2-chloropyrimidine resulted in a low yield as well (**BH-5**). Presumably, 2-chloropyrimidine is not stable under the very basic reaction conditions. Generally speaking, the coupling of simple primary aryl amines and activated or unactivated aryl chlorides was accomplished in excellent yields, but limitations were seen in the coupling of more sterically hindered or heterocyclic substrates.

### 3.5 Conclusion and Outlook

Effective syntheses of ligands **L6-L8** have been developed, however  $^{31}\text{P}$ -qNMR analysis turned out not to be a very reliable method for reaction optimization towards those targets. Compared to biaryldialkyl monophosphine ligands, the benzoannulated derivative KatPhos showed similar or superior performance in catalysis. In the model Mizoroki-Heck coupling, KatPhos showed a superior performance to BrettPhos, but attempts to widen the substrate scope were unsuccessful. The Kumada-Corriu and Negishi couplings, both at elevated temperature, benefitted from a benzoannulation, although in both cases Buchwald ligand SPhos was still superior. The synthesis of a benzoannulated SPhos derivative could therefore be considered for assessment in these couplings (scheme 72).



**Scheme 72.** Proposed synthesis of benzoannulated SPhos derivative **94** for assessing in Kumada-Corriu and Negishi couplings.

However, synthetically, the phenyl-naphthyl precursor for such a ligand would not be easily accessible from naphthoquinone derivatives as for ligands **L6-L8**. In the cases of Mizoroki-Heck, Kumada-Corriu and Negishi couplings, it was assumed that the benzoannulation could contribute to a higher stability of the catalytically active species at elevated temperature. This trend, however, did not continue for the denitrative Suzuki-Miyaura couplings and the fluorination of naphthyl triflates. When comparing BrettPhos und KatPhos in a Buchwald-Hartwig coupling with *Buchwald* conditions, the benzoannulation was superior in the model coupling reaction. Exploration of the substrate scope showed some limitations for heterocyclic and sterically hindered substrates, for which a further improvement of reaction conditions is needed. A *meta,meta*-disubstitution in the phenyl group of the phenyl-naphthyl phosphane ligand backbone mostly led to inferior catalytic performance. However, in the *Kumada-Corriu* coupling, this structural motif proved beneficial. A further investigation into the substrate scope of CyAnPhos in the Kumada-Corriu coupling could therefore be worthwhile. Interestingly, when comparing to results obtained in the screenings of (aryl)dimenthylphosphine ligands, monoaryl

dimenthylphosphine ligand **L2** performed best in this coupling. This leads to the assumption that the *meta,meta*-substitution of CyAnPhos is not a beneficial addition, but rather the Kumada-Corriu coupling does not necessarily require the biaryl ligand motif for a successful catalytic reaction. As for AnPhos (**L8**), its applicability in catalysis was only rarely assessed in this work and a screening in catalytic test reactions could be worthwhile in future research endeavors to access more data points that correlate ligand structure to catalytic activity.

## 4 Experimental Part

## 4.1 Materials and Methods

### 4.1.1 *Chemicals and Reagents*

All solvents and chemicals were obtained commercial suppliers, and were used without further purification unless otherwise specified. Solvents for purification and reaction work-up were bought technical grade and distilled before use. Solvents for air- and moisture-sensitive reactions were dried by filtration over aluminum oxide (Sigma Aldrich, neutral, Brockmann I), degassed by purging with argon for at least 15 minutes and stored over molecular sieve (3 Å or 4 Å) under argon. DMF, MeOH and 1,4-dioxane for catalytic reactions were purchased in 'extra-dry' quality from ACROS Organics™ (Fisher Scientific).

Inorganic bases were ground and dried for two days at 150°C in an oven and stored in a Schlenk tube under argon or in the glovebox. Molecular sieves were dried in vacuum ( $10^{-2}$  mbar) with a heat gun.

Celite™ 545 (flux-calcinated, Fisher Scientific) was used as filtration aid if mentioned.

$\text{PdCl}_2(\text{MeCN})_2$  and  $\text{NiCl}_2(\text{dme})$  were synthesized according to literature procedures and stored under argon in a Schlenk flask or in the glovebox.<sup>150, 151</sup>

### 4.1.2 *Working Techniques*

**Air- and moisture sensitive reactions:** Air- and moisture sensitive reactions were performed using Argon 4.6 as inert gas with standard Schlenk techniques.

**Flash column chromatography:** Flash column chromatography was performed on silica gel 60 (Acros, 35 – 70 µm). Compressed air (0.1 – 0.3 bar) was used for flash elution.

**Thin-layer chromatography:** TLC was performed on silica-coated glass plates (Merck, silica gel 60 F<sub>254</sub>). Detection was realized by UV light ( $\lambda = 254$  nm) and staining with Mostain solution (prepared from 10.0 g  $(\text{NH}_4)_6[\text{Mo}_7\text{O}_{24}] \cdot 4 \text{H}_2\text{O}$ , 200 mg  $\text{Ce}(\text{SO}_4)_2 \cdot 4 \text{H}_2\text{O}$  and 190 mL of water by slow addition of 12 mL conc.  $\text{H}_2\text{SO}_4$  with stirring) and heating.

**Heating/Cooling:** Reactions were heated in an oil bath containing silicon oil (Gruessing, silicon oil M100) or an aluminum block. Temperatures were controlled by digital thermometers. Cooling was achieved by ice/water (0 °C), ice/EtOH (-20 °C), dry ice/acetone



(-78 °C) or liquid N<sub>2</sub>/ethyl acetate (-78 °C) mixture. Reaction temperatures for temperatures below 0 °C were checked by analog thermometer.

#### 4.1.3 *Analytical Techniques*

**NMR spectrometry:** NMR spectrometric measurements were performed at 300 K on Bruker AVHD-300, AVHD-400 or AVHD-500 spectrometers. For <sup>1</sup>H-NMR measurements, a relaxation delay (d1) of 20s was generally used. Chemical shifts  $\delta$  are reported in parts per million (ppm) and calibrated to the residual proton signal of the deuterated solvent or TMS (<sup>1</sup>H), the <sup>13</sup>C signal of the deuterated solvent (<sup>13</sup>C), or to the external standard H<sub>3</sub>PO<sub>4</sub> (85%, <sup>31</sup>P). Multiplicities are assigned as follows: s – singulet, d – dublet, t- triplet, p – pentet, hept – heptett, m – multiplet – or combinations thereof. Table 51 shows the residual chemical shifts of the deuterated solvents used for referencing.

**Table 51.** *Residual signals of deuterated solvents.*

solvent	<sup>1</sup> H residual signal	<sup>13</sup> C signal
	$\delta_H$	$\delta_C$
C <sub>6</sub> D <sub>6</sub>	7.16	128.06
CDCl <sub>3</sub>	7.26	77.16
CD <sub>2</sub> Cl <sub>2</sub>	5.32	53.84

**GC-MS:** GC-MS measurements were recorded on an Agilent Technologies 7890B gas chromatograph with a HP-5ms UI Columns (dimensions: 30 m × 0.25 m × 0.25  $\mu$ m) by Agilent coupled to an Agilent Technologies 5977A mass spectrometer and an Agilent Technologies 7693 Autosampler using helium as carrier gas (flow rate: 1.8 mL/min). The applied methods are listed in table 52.

**Table 52.** *Methods for GC-MS analysis.*

method	T <sub>start</sub>	T <sub>end</sub> /°C	t /min
StandardHT	r.t.	250	24
StdHTlong	r.t.	250 <sup>a</sup>	27

a) Isocratic elution during the last 3 minutes

For the analysis of compounds with a molecular weight  $< 500 \text{ g} \cdot \text{mol}^{-1}$ , the method “StandardHT” was used. For the analysis of compounds with a molecular weight  $> 500 \text{ g} \cdot \text{mol}^{-1}$ , the method “StdHTlong” was used.

**Chiral HPLC analysis:** Chiral HPLC measurements were performed on an Agilent instrument (1260 Infinity Standard Autosampler, 1260 Infinity quaternary pump, 1290 Infinity multicolumn thermostat, 1260 Infinity diode array detector). The stationary phase was a ChiralCel® OJ column (packing composition: cellulose tris (4-methylbenzoate) coated on  $10 \mu\text{m}$  silicagel,  $250 \times 4.6 \text{ mm}$ ). As mobile phase, isohexane/isopropanol mixtures (analytical reagent grade) were used.

**Elementary analysis:** Elementary analysis was performed by the staff of the CRC microanalytic laboratory at TU München.

**High-resolution mass spectrometry (HR-MS):** HR-MS measurements were performed by the staff of the central analytic laboratories of the department of chemistry at TU München. EI-HR-MS were recorded on a DFS high resolution mass spectrometer (EI, 70 eV) (Thermo Fisher Scientific).

**X-Ray diffraction:** Single crystals were measured by Philippe Klein (AK Hintermann) or Christian Jandl at the central analytic laboratories at CRC (TU München). The crystals were measured on a single crystal X-ray diffractometer (CMOS detector, Photon 100) an IMS microsource with  $MoK_{\alpha}$  radiation ( $\lambda = 0.71073 \text{ \AA}$ ) and a Helios optic using the APEX3 software package. The structures were solved by Philippe Klein using the SHELXL and SHELXLE software packages.

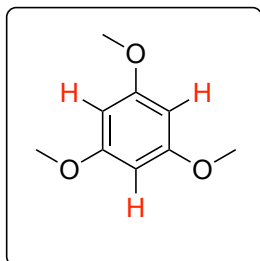
**qNMR analysis:**

$^1\text{H}$ -qNMR:

*Preparation of samples:* Generally, samples for  $^1\text{H}$ -qNMR analysis were prepared by addition of internal standard (weighed in on a balance or added by  $\mu\text{L}$  syringe) to the crude material. A minimum amount of solvent (typically  $\text{CH}_2\text{Cl}_2$ ) was added to the mixture until all material had

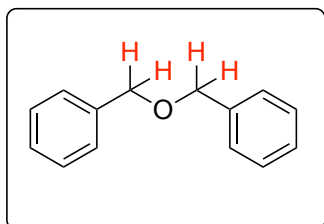
completely dissolved. Then, an aliquot of the solution was added to an NMR tube charged with deuterated solvent (typically ~300  $\mu\text{L}$ ).

*Analysis:* Quantitative analysis was performed by comparing the integral of the internal standard's signal to the integral of the analyzed substance's signal with respect to the number of protons inducing the signal. The internal standards used in this work are listed below.



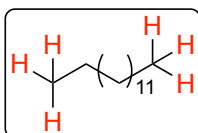
**1,3,5-trimethoxybenzene**

$\text{CDCl}_3$ :  $\delta_H$  6.08 (s, 3H)



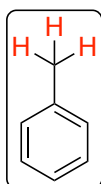
**dibenzylether**

$\text{CDCl}_3$ :  $\delta_H$  4.55 (s, 4H)



**tetradecane**

$\text{CDCl}_3$ :  $\delta_H$  0.85 (t, 6H)



**toluene**

$\text{CDCl}_3$ :  $\delta_H$  2.34 (s, 3H).

<sup>31</sup>P-qNMR:

**Table 53.** Typically used parameters for <sup>31</sup>P-qNMR measurements and processing.

<b>measurement parameters</b>	
sw:	300 ppm
o1p:	100 ppm
d1:	40s
<b>processing parameters</b>	
zero filling	128k
<b>internal standard</b>	
$\delta_P$ (PPh <sub>3</sub> O)	27.0 ppm (CDCl <sub>3</sub> )

<sup>19</sup>F-qNMR:

**Table 54.** Typically used parameters for <sup>19</sup>F-qNMR measurements and processing.

<b>measurement parameters</b>	
sw:	150 ppm
o1p:	-125 ppm
d1:	15s
<b>internal standard</b>	
$\delta_F$ (C <sub>6</sub> F <sub>6</sub> )	-163.01 (C <sub>6</sub> D <sub>6</sub> )

## 4.2 Synthetic Procedures

### 4.2.1 General Procedures

#### **GP-1: Attempted arylation of dimethylphosphine oxide.**

Adapted from Stankevic *et al.*<sup>88</sup>

To an oven-dried Schlenk tube under argon, copper(I) iodide (19.0 mg, 100  $\mu$ mol, 10 mol-%), ligand (20 mol-%) and iodobenzene (0.22 mL, 2.00 mmol, 2.00 eq.) were added sequentially. After 5 minutes, dry solvent (5 mL) and Men<sub>2</sub>POH (327 mg, 1.00 mmol, 1.00 eq.) were added and the solution was stirred at room temperature for seven minutes before freshly dried and crushed base (2.00 mmol, 2.00 eq.) was added. The resulting suspension was stirred at 110 °C for 24 hours. After the reaction mixture had come to room temperature, it was filtered over a plug of Celite and eluted with CH<sub>2</sub>Cl<sub>2</sub> (3  $\times$  15 mL). When DMF was used as solvent, the filtrate was washed with H<sub>2</sub>O (2 $\times$ ), sat. aq. NaCl (2 $\times$ ) and dried (MgSO<sub>4</sub>). The solvent was evaporated *in vacuo*. The crude material was analyzed by <sup>1</sup>H- and <sup>31</sup>P-NMR spectroscopy.

#### **GP-2: Brønsted acid catalyzed enantioselective Friedel-Crafts alkylation of 1-phenyl indole with *trans*-1,2-dibenzoyl ethylene.**

An oven-dried Schlenk tube was charged with 1-phenyl indole (38.7 mg, 20.0  $\mu$ mol, 1.00 eq.), *trans*-1,2-dibenzoyl ethylene (47.3 mg, 20.0  $\mu$ mol, 1.00 eq.) and phosphinic acid (0.04 mmol, 20 mol-%). After evacuating and backfilling with argon (3 $\times$ ), the mixture was stirred at the given temperature for the given time, and the reaction was monitored by TLC. After addition of sat. aq. NaHCO<sub>3</sub> (1 $\times$ ) and extraction of the aqueous phase with CH<sub>2</sub>Cl<sub>2</sub> (2 $\times$ ), the combined organic phases were washed with sat. aq. NaCl (1 $\times$ ), dried (MgSO<sub>4</sub>), filtered and the solvent evaporated *in vacuo*. The crude material was analyzed by <sup>1</sup>H-NMR spectroscopy.

Adapted procedure, for NMR reference data see Jaisankar *et al.*<sup>103</sup>

#### **GP-3: Pd-Catalyzed dimerization of phenyl ethyne.**

An oven-dried Schlenk flask was charged with PdCl<sub>2</sub>(Men<sub>2</sub>POH)<sub>2</sub> (41.5 mg, 0.05 mmol, 5 mol-%) and NaOAc (164 mg, 2.00 mmol, 2.00 eq.) and evacuated and back-filled with argon (3 $\times$ ). Toluene (25 mL) was added and the resulting mixture was stirred for 12 minutes. Subsequently, phenyl acetylene (110  $\mu$ L, 1.00 mmol, 1.00 eq.) was added, the flask was sealed and then stirred at the designated temperature for 18 hours. After the mixture had cooled to room temperature, it was diluted with EtOAc (25 mL) and washed with sat. aq. NaCl (3  $\times$  25 mL). The organic

phase was then dried ( $\text{MgSO}_4$ ), filtered and the solvent evacuated *in vacuo*. The crude material was analyzed by  $^1\text{H}$ -qNMR spectroscopy using dibenzyl ether as internal standard.

Adapted procedure, for NMR reference data see Morales-Serna and co-workers.<sup>106</sup>

#### **GP-4: Pd-Catalyzed [2+1] cycloaddition of phenyl acetylene to norbornadiene.**

$\text{Pd}(\text{OAc})_2$  (11.2 mg, 0.05 mmol, 5 mol-%) and dimethylphosphine oxide (32.7 mg, 100  $\mu\text{mol}$ , 10 mol-%) were added to an oven-dried Schlenk tube. The tube was evacuated and back-filled with argon (3 $\times$ ) and toluene (2 mL) was added. The resulting mixture was stirred at room temperature for 30 minutes before norbornadiene (203  $\mu\text{L}$ , 2.00 mmol, 2.00 eq.) in toluene (1 mL) and phenyl acetylene (110  $\mu\text{L}$ , 1.00 mmol, 1.00 eq.) in toluene (2 mL) were added sequentially. The resulting dark mixture was stirred at room temperature for 20 hours. After 20 hours, dibenzyl ether was added to the stirred solution as internal standard and an aliquot of the mixture was analyzed by  $^1\text{H}$ -qNMR spectroscopy.

Adapted procedure, for NMR reference data see Buono *et al.*<sup>107</sup>

#### **GP-5: Pd-Catalyzed Suzuki-Miyaura couplings.**

**GP-5-A:** An oven dried Schlenk tube was charged with Pd species (2 mol-%) or  $\text{Pd}(\text{OAc})_2$  (2 mol-%) and ligand (4 mol-%), phenylboronic acid (183 mg, 1.50 mmol, 1.50 eq.),  $\text{K}_2\text{CO}_3$  (415 mg, 3.00 mmol, 3.00 eq.) and aryl halide (if solid). The Schlenk tube was sealed with a septum and then evacuated and backfilled with argon (3 $\times$ ). Then, aryl halide (if liquid) and THF (3.0 mL) was added. The flask was sealed with a glass plug and PTFE sleeve and then stirred at 70  $^\circ\text{C}$  for 24 hours. After the reaction mixture had come to room temperature, it was diluted with  $\text{Et}_2\text{O}$  and filtered over a plug of celite, further eluting with  $\text{Et}_2\text{O}$ . After removing the solvent on a rotary evaporator, the crude compound was analyzed by  $^1\text{H}$ -qNMR using an internal standard (dibenzyl ether).

**GP-5-B:** An oven-dried Schlenk tube was charged with Pd species (1 mol-%), ligand (x mol-%), phenylboronic acid (183 mg, 1.46 mmol, 1.50 eq.) and  $\text{K}_3\text{PO}_4$  (425 mg, 1.94 mmol, 2.00 eq.) and the tube was evacuated and back-filled with argon (3 $\times$ ). Then, toluene (2 mL) and 4-chloroanisole (125  $\mu\text{L}$ , 1.03 mmol, 1.00 eq.) were added *via* septum, the flask was sealed with a glass plug and PTFE sleeve and heated at 70  $^\circ\text{C}$  for 24 hours. After the mixture had come to room temperature, it was diluted with  $\text{Et}_2\text{O}$ , filtered over a plug of celite and eluted with  $\text{Et}_2\text{O}$ . After removing the solvent on a rotary evaporator, the crude compound was analyzed by  $^1\text{H}$ -qNMR spectroscopy using an internal standard (dibenzyl ether).

**GP-5-C:** An oven-dried Schlenk tube was charged with Pd species (1 mol-%), ligand (x mol-%), phenyl boronic acid (183 mg, 1.46 mmol, 1.50 eq.) and K<sub>3</sub>PO<sub>4</sub> (425 mg, 1.94 mmol, 2.00 eq.) and the tube was evacuated and back-filled with argon (3×). Then, toluene (2 mL), 4-chloroanisole (125 μL, 1.03 mmol, 1.00 eq.) and internal standard tetradecane (45 μL, 173 μmol) were added *via* septum, and the flask was heated at 70 °C for 24 hours. An aliquot of the reaction mixture (0.1 mL) was used after 100 minutes and 24 hours of reaction time for <sup>1</sup>H-qNMR sampling.

For isolation, the crude material was purified by flash chromatography (SiO<sub>2</sub>; Hex–EtOAc 50:1) and washed with cold methanol.

### **GP-6: Mizoroki-Heck couplings.**

#### **GP-6-A: Mizoroki-Heck coupling of bromobenzene and methyl acrylate.**

An oven-dried Schlenk tube was charged with Pd(OAc)<sub>2</sub> (1.12 mg, 5 μmol, 1 mol-%), ligand (2 mol-%) and K<sub>2</sub>CO<sub>3</sub> (138 mg, 1.00 mmol, 2.00 eq.). After the flask had been evacuated and back-filled with argon (3×), DMF (1 mL), bromobenzene (53 μL, 500 μmol, 1.00 eq.) and methyl acrylate (84 μL, 1.00 mmol, 2.00 eq.) were added sequentially. The tube was then sealed and the mixture was stirred at 110 °C for 23 hours. After the solution had come to room temperature, internal standard toluene was added *via* microsyringe. H<sub>2</sub>O (3 mL) was then added and the resulting solution was extracted once with Et<sub>2</sub>O (3 mL). The organic phase was separated and an aliquot (0.25 mL) was used for <sup>1</sup>H-qNMR analysis.

#### **GP-6-B: Substrate scope for the Mizoroki-Heck coupling.**

An oven-dried Schlenk tube was charged with Pd(OAc)<sub>2</sub> (2.25 mg, 0.01 mmol, 1 mol-%), **L2** (7.73 mg, 0.02 mmol, 2 mol-%), aryl halide (1.00 mmol, 1.00 eq., if solid) and K<sub>2</sub>CO<sub>3</sub> (276 mg, 2.00 mmol, 2.00 eq.). The Schlenk tube was then evacuated and back-filled with argon (3×). Then, aryl halide (1.00 mmol, 1.00 eq., if liquid) and *tert*-butylacrylate (290 μL, 2.00 mmol, 2.00 eq.) or styrene (230 μL, 2.00 mmol, 2.00 eq.) was added, the flask was sealed and the mixture was stirred at 110 °C for 24 hours. After the solution had cooled to room temperature, it was filtered over a plug of celite and the filtrate eluted with Et<sub>2</sub>O. The filtrate was washed with water (2×), sat. aq. NaCl (1×), dried (MgSO<sub>4</sub>) and filtered. The solvent was removed on a rotary evaporator and the residue was analyzed by <sup>1</sup>H-qNMR spectroscopy using dibenzyl ether or toluene as internal standard. The crude material was purified by flash chromatography.

**GP-7: Kumada-Corriu coupling of phenylmagnesium bromide and 1-bromo-2-methoxynaphthalene.**

To an oven-dried Schlenk tube, Pd(OAc)<sub>2</sub> (2.25 mg, 0.01 mmol, 1 mol-%), ligand (2 mol-%) and aryl halide (1.00 mmol, 1.00 eq.) was added and the Schlenk tube was evacuated and back-filled with argon (3×). After addition of dry and degassed THF, arylmagnesiumbromide (~1 M solution in THF, 1.50 mmol, 1.50 eq.) was added (final nominal concentration of aryl halide: 0.33 M) and the resulting reaction was stirred at the designated temperature for 18 hours. Then, either a 1 M solution of aq. HCl (12 mL) or sat. aq. NH<sub>4</sub>Cl (2 mL) and H<sub>2</sub>O (10 mL) was added at room temperature. The aqueous phase was extracted with CH<sub>2</sub>Cl<sub>2</sub> (3×15 mL) and the combined organic phases were washed with sat. aq. NaCl (15 mL). The combined organic phases were dried (MgSO<sub>4</sub>), filtered and the solvent removed on a rotary evaporator. The crude material was analyzed by <sup>1</sup>H-qNMR spectroscopy using dibenzyl ether as internal standard and, if specified, purified by column chromatography.

**GP-8: Ni-Catalyzed demethoxylative coupling of 2-methoxynaphthalene and phenylmagnesium bromide.**

**GP-8-A: Procedure in THF.** In a glovebox, an oven-dried Schlenk tube was charged with NiCl<sub>2</sub>(dme) (5.49 mg, 0.025 mmol, 5 mol-%) and **L2** (19.3 mg, 0.05 mmol, 10 mol-%). Outside of the glovebox, 2-methoxynaphthalene (79.1 mg, 500 μmol, 1.00 eq.) and THF (0.3 mL) was added. Subsequently, phenylmagnesium bromide (0.53 M, 1.4 mL, 0.75 mmol, 1.5 eq.) was added dropwise to the stirred solution. The mixture was heated to 60 °C for 21 hours. After it had cooled to room temperature, sat. aq. NH<sub>4</sub>Cl (1 mL) and water (5 mL) was added. The aqueous phase was extracted with EtOAc (3×) and the combined organic phases were washed with sat. aq. NaCl (1×), dried (MgSO<sub>4</sub>) and the solvent removed under reduced pressure. The crude material was analyzed by <sup>1</sup>H-qNMR spectroscopy using 1,3,5-trimethoxybenzene as internal standard.

**GP-8-B: Procedure in THF/toluene.**

To an oven-dried Schlenk tube was added 2-methoxynaphthalene (79.1 mg, 500 μmol, 1.00 eq.) and after introduction to the glovebox, NiCl<sub>2</sub>(dme) (5.49 mg, 0.025 mmol, 5 mol-%) and ligand (10 mol-%) was added. Outside of the glovebox, toluene (0.8 mL) and phenylmagnesium bromide (0.91 M, 0.82 mL, 0.75 mmol, 1.50 eq.) were added sequentially and the solution was stirred at room temperature for 14 hours. Work-up and analysis proceeded as described in GP-8-A.



### GP-9-A: Buchwald-Hartwig aminations.

Adapted from Reddy *et al.*<sup>109</sup>

An oven-dried Schlenk tube was charged Pd species (2 mol-%) or PdCl<sub>2</sub>(MeCN)<sub>2</sub> (2 mol-%) and ligand (4 mol-%) and NaO<sup>t</sup>Bu (135 mg, 1.40 mmol, 1.40 eq.) and evacuated and backfilled with argon (3×). Chlorobenzene (203 μL, 2.00 mmol, 2.00 eq.), *N*-methylpiperazine (111 μL, 100 mg, 1.00 eq.) and toluene (4 mL) were added through a septum. The septum was exchanged with a glass plug and PTFE sleeve under a counterflow of argon, and the resulting mixture was stirred at 120 °C for 16 h. After letting the reaction mixture cool to room temperature, the mixture was diluted with DCM (15 mL), transferred to an Erlenmeyer flask and dried (MgSO<sub>4</sub>). The mixture was filtered over a plug of celite, eluting with DCM (2 × 15 mL) and the solvent evaporated under reduced pressure (700 mbar, 20 min). The crude mixture was analyzed by <sup>1</sup>H-qNMR spectroscopy using an internal standard (1,1,2,2-tetrachloroethane or 1,3,5-trimethoxybenzene). For isolation, the crude product was purified by flash chromatography (SiO<sub>2</sub>; MeOH–DCM 1:20).

### GP-9-B: Buchwald-Hartwig amination with Pd(II) preactivation.

An oven-dried Schlenk tube was charged with PdCl<sub>2</sub>(MeCN)<sub>2</sub> (2.59 mg, 0.01 mmol, 2 mol-%), L2 (7.73 mg, 0.02 mmol, 4 mol-%) and NaO<sup>t</sup>Bu (7.69 mg, 0.08 mmol, 16 mol-%) and toluene (1 mL) in the glovebox. The flask was sealed and heated to 120 °C for one hour outside of the glovebox. After the solution had cooled to room temperature, NaO<sup>t</sup>Bu (67.3 mg, 700 μmol, 1.40 eq.) was added under a counter-flow of argon, and chlorobenzene (101 μL, 1.00 mmol, 2.00 eq.) and *N*-methylpiperazine (55 μL, 500 μmol, 1.00 eq.) were added through a septum. The inner walls of the tube were rinsed with toluene (1 mL), the flask was sealed and heated to 60 °C for 17 hours. Work-up proceeded as described in GP-9-A.

### GP-10: Negishi-coupling of 2,4,6-triisopropylphenyl zinc chloride and 4-chloroanisole.

Adapted literature procedure.<sup>13</sup>

To an oven-dried Schlenk tube under argon was added bromo-2,4,6-triisopropylbenzene (425 mg, 1.50 mmol, 1.50 eq.) and THF (2 mL). The flask was cooled to -78 °C (N<sub>2</sub>/EtOAc) and *n*-BuLi (1.6 M solution in hexanes, 1.0 mL, 1.65 mmol, 1.65 eq.) was added dropwise to the stirred solution, and the resulting mixture was stirred at this temperature for one hour. Dry ZnCl<sub>2</sub> (245 mg, 1.8 mmol, 1.8 eq.) was added under a counterflow of argon and the solution was stirred at -78 °C for 30 minutes before it was warmed to room temperature over the course of 1 hour. Pd(OAc)<sub>2</sub> (2.25 mg, 0.01 mmol, 1 mol-%), ligand (2 mol-%) and 4-chloroanisole (125 μL, 1.03 mmol, 1.00 eq.) was added and the walls of the Schlenk tube were rinsed with

THF (1 mL). The solution was heated to 70 °C for 20 hours. After cooling to room temperature, the mixture was quenched with H<sub>2</sub>O (1 mL) and transferred to a separatory funnel. The aqueous phase was extracted with Et<sub>2</sub>O (4×) and the combined organic phases washed with sat. aq. NaCl (1×), dried (MgSO<sub>4</sub>), filtered and the solvent evaporated under reduced pressure. The crude material was analyzed by <sup>1</sup>H-qNMR spectroscopy using an internal standard (dibenzyl ether).

#### **GP-10: Asymmetric Suzuki-Miyaura coupling.**

To a screw cap vial equipped with a magnetic stirring bar was added Pd(OAc)<sub>2</sub> (1.12 mg, 0.005 mmol, 1 mol-%), **L3** (x mol-%), aryl halide (0.5 mmol, 1.00 eq.), aryl boronic acid (0.75 mmol, 1.50 eq.) and base (x eq.). The vial was sealed and solvent (1 mL) was added. The reaction mixture was stirred for 24 hours at the designated temperature. After cooling to room temperature, the mixture was filtered over a pad of celite, further eluting with Et<sub>2</sub>O. The solvent was evacuated *in vacuo* and the crude material was analyzed by <sup>1</sup>H-qNMR using an internal standard (dibenzyl ether). The crude material was purified by flash chromatography and pure target material was analyzed by chiral HPLC.

#### **GP-11: Buchwald-Hartwig aminations with H<sub>2</sub>O-preactivation.**

Adapted from Fors *et al.*<sup>111</sup>

Pd(OAc)<sub>2</sub> (1 mol-%) and ligand (3 mol-%) were added to a screw cap vial and the tube was evacuated and back-filled with argon (3×). Then, 1,4-dioxane (0.25 mL for a 0.5 mmol scale) H<sub>2</sub>O (4 mol-%) was added over a septum and the solution was stirred at 80 °C for two minutes. After the solution had cooled to room temperature, it was transferred to an oven-dried Schlenk tube charged with NaO<sup>t</sup>Bu (1.20 eq.), aryl chloride (1.00 eq.), amine (1.20 eq.) and dioxane (final nominal concentration of aryl chloride: 1M) *via* syringe. The resulting solution was heated at 80 °C for the designated time and brought to room temperature. It was diluted with EtOAc, washed with H<sub>2</sub>O (1×) and sat. aq. NaCl (1×). The organic phase was dried (MgSO<sub>4</sub>), filtered and the solvent removed *in vacuo*. The crude material was analyzed by <sup>1</sup>H-qNMR spectroscopy using dibenzyl ether as internal standard and, if specified, the product was isolated by flash chromatography.

#### **GP-12: Denitrative Suzuki-Miyaura coupling of nitroarenes.**

Adapted from Yadav *et al.*<sup>149</sup>

An oven-dried Schlenk tube was charged with Pd(acac)<sub>2</sub> (4.51 mg, 15.0 μmol, 5 mol-%), ligand (20 mol-%), 18-crown-6 (7.93 mg, 30.0 μmol, 10 mol-%), K<sub>3</sub>PO<sub>4</sub> (191 mg, 900 μmol,

2.90 eq.), 4-methoxyphenylboronic acid (68.4 mg, 450  $\mu\text{mol}$ , 1.50 eq.) and 4-nitrotoluene (42.2 mg, 310  $\mu\text{mol}$ , 1.00 eq.). The tube was evacuated and back-filled with argon (3 $\times$ ) and dry dioxane (1.5 mL) was added over a septum. The Schlenk tube was sealed and heated to 120  $^{\circ}\text{C}$  for 8 hours. After the reaction mixture had cooled to room temperature, it was diluted with  $\text{CH}_2\text{Cl}_2$  and filtered over a pad of Celite (eluting with additional  $\text{CH}_2\text{Cl}_2$ ). The solvent was removed under reduced pressure and the residue analyzed by  $^1\text{H}$ -qNMR spectroscopy with dibenzyl ether as internal standard.

### **GP-13: Pd-catalyzed fluorination of 1-naphthyl triflate.**

Adapted from Sather *et al.*<sup>15</sup>

A Schlenk tube was dried in vacuum by heat-gun and introduced into the glovebox, where CsF (1.50 eq.) were weighed in. Outside of the glovebox, Pd precursor (x mol-%), ligand (y mol-%), 1-naphthyl triflate (1.00 eq.) and toluene (final nominal concentration of naphthyl triflate: 0.1 M) were added under a counterflow of argon. The Schlenk tube was sealed and heated to 110  $^{\circ}\text{C}$  for the designated reaction time. After the solution had cooled to room temperature, internal standard ( $\text{C}_6\text{F}_6$ ) was added and the mixture was stirred at room temperature for 5 minutes. An aliquot ( $\sim 300 \mu\text{L}$ ) of the mixture was removed by syringe and added to an NMR tube containing  $\text{C}_6\text{D}_6$  ( $\sim 200 \mu\text{L}$ ) by filtering through a pad of cotton in a pasteur pipette for  $^{19}\text{F}$ -qNMR analysis.

### **Kinetic study of the Kumada-Corriu coupling of 1-bromo-2-methoxynaphthalene and phenylmagnesiumbromide using SPhos and $\text{Men}_2\text{PPh}$ as ligands.**

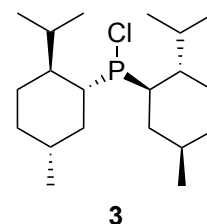
An oven-dried Schlenk tube was charged with  $\text{Pd}(\text{OAc})_2$  (2.25 mg, 0.01 mmol, 1 mol-%), ligand (2 mol-%), a defined amount of internal standard (1,2,4,5-tetramethylbenzene) and 1-bromo-2-methoxynaphthalene (237 mg, 1.00 mmol, 1.00 eq.) and evacuated and back-filled with argon (3 $\times$ ). THF (dry and degassed) was added, followed by freshly titrated phenylmagnesiumbromide in THF ( $c = 0.9 \text{ M}$ , 0.63 mL, 1.50 eq.) in one portion with stirring solution (total amount of solvent: 3 mL). An aliquot of the sample ( $\sim 0.1 \text{ mL}$ ) was removed by syringe after 30 minutes, 1 hour, 1.5 hours, 2.5 hours and 4.5 hours.

*Work-up of the samples:* The sample was quenched in a vial filled with sat. aq.  $\text{NH}_4\text{Cl}-\text{H}_2\text{O}$  (1:1, 2 mL) and EtOAc (2 mL). The vial was closed and shaken vigorously. Then, it was opened, the organic phase was separated and added to a new vial, and washed with sat. aq. NaCl (1 mL), again under vigorous shaking of the closed vial. The organic phase was separated again and transferred into a headspace vial equipped with a stirring bar. A small amount of  $\text{MgSO}_4$

was added and the vial was sealed. A cannula connected to a vacuum pump was pushed through the septum and the solvent was removed under vacuum under continuous stirring (the vial was placed in a water bath to ensure faster evaporation). The residue was combined with  $\text{CDCl}_3$  (0.7 mL) and the suspension was stirred for 5 minutes. The solution was transferred into an NMR tube by filtering through a pad of cotton in a Pasteur pipette, and the sample was analyzed by  $^1\text{H}$ -qNMR spectroscopy.

#### 4.2.2 *Synthesis Procedures*

**Chlorodimethylphosphine (3).** Dimethylphosphine oxide (**4**; 7.00 g, 21.4 mmol, 1.00 eq.) was added to a Schlenk flask and the flask was evacuated and backfilled with argon (3×). Freshly degassed hexanes (140 mL) were added to the flask through a septum. PCl<sub>3</sub> (3.70 mL, 42.8 mmol, 2.00 eq.) was slowly added to the stirred solution at room temperature, and the mixture was stirred for 3 h. The solvent and excess PCl<sub>3</sub> was removed in high vacuum into a liquid N<sub>2</sub> cooling trap. The residual colorless solid was redissolved in degassed hexanes (20 mL), and a colorless, insoluble precipitate was left at the bottom of the flask. The supernatant solution was transferred via cannula into another Schlenk flask, and the solvent was again removed in vacuo to give colorless solid (7.15 g, 97%). The material was stored in a glovebox.



**<sup>1</sup>H-NMR (300 MHz, C<sub>6</sub>D<sub>6</sub>):** δ 0.60–1.09 (m, 16H), 0.82 (d, *J* = 6.6 Hz, 3H), 0.84 (d, *J* = 6.9 Hz, 3H), 1.11–1.51 (m, 4H), 1.53–1.75 (m, 8H), 1.87 (br. d, *J* = 11.0, 1H), 2.14 (td, *J* = 12.4, 3.2 Hz, 1H), 2.58–2.72 (m, 1H), 2.73–2.86 (m, 1H).

**<sup>13</sup>C{<sup>1</sup>H} -NMR (101 MHz, C<sub>6</sub>D<sub>6</sub>):** δ 15.52, 16.26, 21.68, 22.19, 22.99 (2C), 25.43 (br, 2C), 27.73 (d, *J*<sub>P-C</sub> = 21.8 Hz), 28.89 (d, *J*<sub>P-C</sub> = 8.1 Hz), 33.51 (2C), 34.52–36.10 (m, 4C), 40.44 (d, *J*<sub>P-C</sub> = 37.2 Hz), 42.00 (d, *J*<sub>P-C</sub> = 40.9 Hz), 43.61 (d, *J*<sub>P-C</sub> = 3.8 Hz), 48.64 (d, *J*<sub>P-C</sub> = 18.4 Hz).

**<sup>31</sup>P{<sup>1</sup>H} -NMR (122 MHz, C<sub>6</sub>D<sub>6</sub>):** δ 122.7.

Known compound. CAS 75992-49-3.

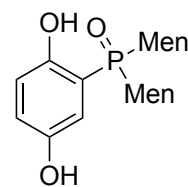
***cis/trans*-PtCl<sub>2</sub>(MeCN)<sub>2</sub> (29).** Adapted from Hartley *et al.*<sup>99</sup>

A Schlenk flask was charged with PtCl<sub>2</sub> (450 mg, 1.69 mmol) and evacuated and back-filled with argon (3×). Then, dry and degassed MeCN (23 mL) was added and the resulting suspension was heated at 80 °C for 4 hours. The hot suspension was filtered, rinsing with a small amount of MeCN. The cooled filtrate was then evaporated *in vacuo* until a pale yellow solid precipitated. The solid was filtered off and dried *in vacuo* to afford **29** (328 mg, 56%) as pale yellow solid. The filtrate was left in the refrigerator (4 °C) overnight, and a further crop of yellow solid precipitated, which was again filtered and washed with a small amount of Et<sub>2</sub>O to afford **32** (143 mg, 80% yield in total) as pale yellow-green solid (*cis/trans* mixture, 4.4:1).

**<sup>1</sup>H-NMR (500 MHz, CD<sub>2</sub>Cl<sub>2</sub>)** δ 2.54 (s, *trans*-isomer), 2.49 (s, *cis*-isomer).

Known compound. CAS 13869-38-0. The analytical data is in accordance with the literature.<sup>152</sup>

**(2,5-Dihydroxyphenyl)-1-yl-dimethylphosphine oxide (10).** A Schlenk tube was charged with *p*-benzoquinone (270 mg, 2.50 mmol, 1.00 eq.), dimethylphosphine oxide (**4**; 816 mg, 2.50 mmol, 1.00 eq.) and *p*TsOH·H<sub>2</sub>O (23.8 mg, 125 μmol, 5 mol-%) and then evacuated and back-filled with argon



**10**

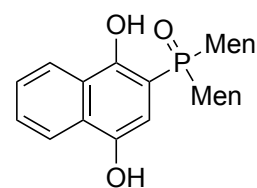
for 22 h. After the reaction mixture had cooled to room temperature, it was diluted with water (5 mL) and CH<sub>2</sub>Cl<sub>2</sub> (10 mL) and transferred to a separatory funnel. The aqueous phase was extracted with CH<sub>2</sub>Cl<sub>2</sub> (2 × 20 mL) and the combined organic phases were washed with half-sat. aq. Na<sub>2</sub>S<sub>2</sub>O<sub>3</sub> (10 mL), water (2 × 10 mL), sat. aq. NaCl (10 mL) and dried (MgSO<sub>4</sub>). After filtration, the solvent was evaporated *in vacuo* and the crude product recrystallized from hot EtOAc to afford off-white solid (670 mg, 62%).

**<sup>1</sup>H-NMR (400 MHz, CDCl<sub>3</sub>):** δ 0.37 (d, *J* = 6.7 Hz, 3H), 0.77 (d, *J* = 5.4 Hz, 3H), 0.79 (d, *J* = 5.4 Hz, 3H), 0.81 – 0.84 (m, 1H), 0.87 (d, *J* = 6.7 Hz, 3H), 0.94 (d, *J* = 6.5 Hz, 3H), 0.98 (d, *J* = 5.7 Hz, 3H), 1.01 – 1.06 (m, 1H), 1.06 – 1.29 (m, 4H), 1.33 – 1.54 (m, 3H), 1.68 – 1.90 (m, 8H), 2.02 – 2.21 (m, 2H), 2.68 (sept·d, *J* = 2.0, 6.5 Hz, 1H), 4.83 (br s, 1 H, ArOH), 6.67 (dd, *J* = 3.0, 11.5 Hz, 1H), 6.77 (dd, *J* = 4.5, 8.9 Hz, 1H), 6.88 (dd, *J* = 2.9, 8.9 Hz, 1H), 11.29 (s, 1H).

**<sup>31</sup>P{<sup>1</sup>H}-NMR (162 MHz, CDCl<sub>3</sub>):** δ 58.11.

**HR-MS (EI, *m/z*):** Calcd. for C<sub>26</sub>H<sub>43</sub>O<sub>3</sub>P<sup>+</sup> ([M]<sup>+</sup>), 434.2944; found, 434.2936.

**(1,4-Dihydroxynaphthalen-2-yl)dimethylphosphine oxide (12).** An oven-dried Schlenk tube was charged with naphthoquinone (158 mg, 1.00 mmol, 1.0 eq.), *p*TsOH (11.4 mg, 60 μmol, 6 mol-%), and dimethylphosphine oxide (**4**; 327 mg, 1.00 mmol, 1.0 eq.) and evacuated and back-filled with argon (3×). Then, DMF (2 mL) was



crude

**12**

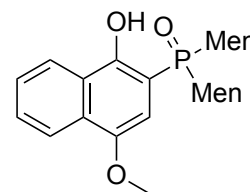
added and the mixture was stirred at 80 °C for two days. After addition of EtOAc and a half-sat. aq. Na<sub>2</sub>S<sub>2</sub>O<sub>3</sub>, the phases were separated in a separatory funnel. The aqueous phase was extracted with EtOAc (1 ×), and the combined organic phases washed with a half-sat. aq. Na<sub>2</sub>S<sub>2</sub>O<sub>3</sub> (1×), water (1×) and sat. aq. NaCl (1×). The combined organic phases were dried (MgSO<sub>4</sub>) and the solvent evaporated *in vacuo*. The residue was recrystallized from hot EtOAc–hexanes to afford a slushy mass which shrunk upon filtration and drying *in vacuo* to afford white solid (160 mg, 33%).

**<sup>31</sup>P{<sup>1</sup>H}-NMR (162 MHz, C<sub>6</sub>D<sub>6</sub>):** δ 57.50.

**HR-MS (EI, *m/z*):** calcd for C<sub>30</sub>H<sub>45</sub>O<sub>3</sub>P<sup>+</sup> ([M]<sup>+</sup>), 484.3101, found, 484.3115.

**(1-Hydroxy-4-methoxynaphthalen-2-yl)dimenthylphosphine oxide**

**(13)**. An oven-dried Schlenk tube was charged with naphthoquinone (160 mg, 1.01 mmol, 1.00 eq.) and *p*TsOH·H<sub>2</sub>O (11.5 mg, 60 mmol, 6 mol-%) and evacuated and backfilled with argon (3×). After addition of DMF (2 mL), the solution was stirred at 80 °C for 24 h. After cooling to RT, the reaction mixture was diluted with EtOAc and transferred to a



**13**

separating funnel. The organic phase was washed with a half-saturated solution of Na<sub>2</sub>SO<sub>3</sub> (2×) and the aqueous phase re-extracted with EtOAc (1×). The combined organic phases were washed with sat. aq. NaCl, dried (MgSO<sub>4</sub>) and filtered. After removing the solvent on a rotary evaporator, the crude (1,4-dihydroxynaphthalen-2-yl)dimenthylphosphine oxide (**14**) was directly employed in the subsequent methylation reaction. In a 50 mL Schlenk flask under argon, dry and ground K<sub>2</sub>CO<sub>3</sub> (415 mg, 3.00 mmol, 3.0 eq.), degassed acetone (4 mL) and Me<sub>2</sub>SO<sub>4</sub> (0.4 mL, 4.00 mmol, 4.0 eq.) was added under a counter-flow of argon. Crude **14** was added and the reaction mixture was stirred at room temperature for 2.5 h. A conc aq NH<sub>4</sub>OH solution (2 mL) was added and the solution was stirred at room temperature for 2 h to quench remaining Me<sub>2</sub>SO<sub>4</sub>. Water was added and the aqueous phase was extracted with EtOAc (2×) and the combined organic phases were washed with H<sub>2</sub>O (1×) and sat. aq. NaCl (1×), dried (MgSO<sub>4</sub>) and filtered. The solvent was removed in vacuo and the crude compound purified by CC (SiO<sub>2</sub>; EtOAc–hexanes 1:20) to afford **13** (226 mg, 45%, 2 steps) as orange solid.

**<sup>1</sup>H-NMR (400 MHz, CDCl<sub>3</sub>):** δ 0.38 (d, *J* = 6.7 Hz, 3H), 0.68 (d, *J* = 6.9 Hz, 3H), 0.7–1.45 (m, 6H), 0.72 (d, *J* = 6.8 Hz, 3H), 0.88 (d, *J* = 6.7 Hz, 3H), 0.94 (d, *J* = 6.4 Hz, 3H), 1.01 (d, *J* = 5.9 Hz, 3H), 1.45–2.02 (m, 10H), 2.16–2.29 (m, 2H), 2.80 (sept, *J* = 6.8 Hz, 1H), 3.94 (s, 3 H), 6.44 (d, *J*<sub>P-H</sub> = 10.4 Hz, 1H), 7.51–7.63 (m, 2H), 8.17 (d, *J* = 7.9 Hz, 1H), 8.33 (d, *J* = 7.6 Hz, 1H), 12.31 (s, OH).

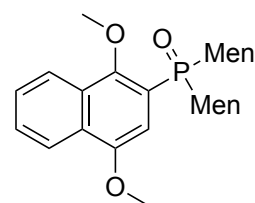
**<sup>13</sup>C-NMR (101 MHz, CDCl<sub>3</sub>):** δ 15.81, 15.99, 21.40, 21.66, 22.92, 23.00, 24.68 (d, *J*<sub>P-C</sub> = 11.4 Hz), 24.87 (d, *J*<sub>P-C</sub> = 12.5 Hz), 27.17 (d, *J*<sub>P-C</sub> = 3.6 Hz), 28.17 (d, *J*<sub>P-C</sub> = 2.0 Hz), 33.14 (d, *J*<sub>P-C</sub> = 12.3 Hz), 33.21 (d, *J*<sub>P-C</sub> = 12.9 Hz), 33.43 (d, *J*<sub>P-C</sub> = 3.1 Hz), 34.23 (d, *J*<sub>P-C</sub> = 1.2 Hz), 34.68 (d, *J*<sub>P-C</sub> = 1.7 Hz), 36.80 (d, *J*<sub>P-C</sub> = 0.8 Hz), 37.04 (d, *J*<sub>P-C</sub> = 64.0 Hz), 40.66 (d, *J*<sub>P-C</sub> = 62.5 Hz), 42.74 (d, *J*<sub>P-C</sub> = 3.6 Hz), 43.58 (d, *J*<sub>P-C</sub> = 3.2 Hz), 55.91, 102.19 (d, *J*<sub>P-C</sub> = 83.6 Hz), 102.90 (d, *J*<sub>P-C</sub> = 11.3 Hz), 121.47, 123.22 (d, *J*<sub>P-C</sub> = 1.0 Hz), 126.12, 126.38, 127.90, 128.35 (d, *J*<sub>P-C</sub> = 2.0 Hz), 146.72 (d, *J*<sub>P-C</sub> = 13.0 Hz), 155.67.

**<sup>31</sup>P{<sup>1</sup>H}-NMR (162 MHz, CDCl<sub>3</sub>):** δ 59.5.

**HR-MS (EI, *m/z*):** calcd for C<sub>31</sub>H<sub>47</sub>O<sub>3</sub>P<sup>+</sup> ([M]<sup>+</sup>), 498.3263, found 498.3286.

**1,4-Dimethoxynaphthalene-2-yl-dimethylphosphine oxide (14).**

1,4-Naphthoquinone (79.1 mg, 500  $\mu$ mol, 1.00 eq.), dimethylphosphine oxide (**4**; 163 mg, 500  $\mu$ mol, 1.00 eq.) and *p*-TsOH $\cdot$ H<sub>2</sub>O (5.70 mg, 0.03 mmol, 6 mol-%) were added to a Schlenk

**14**

tube and the tube was evacuated and back-filled with argon (3  $\times$ ). Then, dry DMF (1 mL) was added and the resulting solution was stirred at 80  $^{\circ}$ C for 24 h. The reaction mixture was then brought to room temperature, and K<sub>2</sub>CO<sub>3</sub> (610 mg, 4.41 mmol, 8.80 eq.) and methyl iodide (160  $\mu$ L, 2.57 mmol, 5.14 eq.) were added sequentially under a positive stream of argon. The tube was sealed with a glass plug and PTFE sleeve and the reaction mixture was heated at 50  $^{\circ}$ C for 17 h, after which TLC analysis confirmed completion of the reaction. After letting the reaction mixture cool to room temperature, 10% aq NH<sub>3</sub> (4 mL) was added. The reaction mixture was diluted with EtOAc (5 mL) and H<sub>2</sub>O (2 mL) and transferred to a separatory funnel. The organic layer was separated and the aqueous layer was extracted with EtOAc (2  $\times$  8 mL). The combined organic phases were washed with H<sub>2</sub>O (10 mL) and sat. aq. NaCl (10 mL) and then dried (Na<sub>2</sub>SO<sub>4</sub>), filtered and the solvent removed on a rotary evaporator. The crude material was purified by CC (SiO<sub>2</sub>; EtOAc–hexanes 1:4) to afford **14** in 79% yield, which still contained about 1 mol-% of **4** and some other unidentified impurities. Analytical purity was reached by trituration with cold MeOH to afford colorless solid (173 mg, 67%).

**<sup>1</sup>H-NMR (300 MHz, CDCl<sub>3</sub>)**  $\delta$  0.46 (d,  $J$  = 6.7 Hz, 3H), 0.55 – 0.85 (m, 1H), 0.71 (d,  $J$  = 6.8 Hz, 3H), 0.82 (d,  $J$  = 6.5 Hz, 3H), 0.83 (d,  $J$  = 7.0 Hz, 3H), 0.90 (d,  $J$  = 6.8 Hz, 3H), 1.01 (d,  $J$  = 5.8 Hz, 3H), 0.96 – 1.38 (m, 9H), 1.46 – 1.96 (m, 7H), 2.19 (dtd,  $J$  = 13.3, 10.3, 2.4 Hz, 1H), 2.43 – 2.55 (m, 1H), 3.28 – 3.39 (m, 1H), 4.01 (s, 3H), 4.04 (s, 3H), 6.95 (d,  $^3J_P$  = 10.4 Hz, 1H), 7.55 – 7.60 (m, 3H), 8.06 – 8.16 (m, 1H), 8.22 – 8.33 (m, 1H).

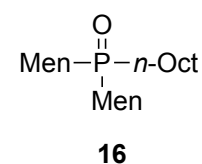
**APT-<sup>13</sup>C NMR (75 MHz, CDCl<sub>3</sub>):**  $\delta$  16.17 (CH<sub>3</sub>), 16.46 (CH<sub>3</sub>), 21.53 (CH<sub>3</sub>), 21.61 (CH<sub>3</sub>), 22.78 (d,  $J_{P-C}$  = 1.0 Hz, CH<sub>3</sub>), 22.99 (d,  $J_{P-C}$  = 0.7 Hz, CH<sub>3</sub>), 24.95 (d,  $J_{P-C}$  = 12.4 Hz, CH<sub>2</sub>), 25.04 (d,  $J_{P-C}$  = 11.4 Hz, CH<sub>2</sub>), 27.59 (d,  $J_{P-C}$  = 1.7 Hz, CH), 27.83 (d,  $J_{P-C}$  = 3.4 Hz, CH), 32.86 (d,  $J_{P-C}$  = 13.8 Hz, CH), 33.46 (d,  $J_{P-C}$  = 12.6 Hz, CH), 34.52 (d,  $J_{P-C}$  = 1.3 Hz, CH<sub>2</sub>), 34.57 (d,  $J_{P-C}$  = 1.7 Hz, CH<sub>2</sub>), 34.77 (d,  $J_{P-C}$  = 2.9 Hz, CH<sub>2</sub>), 36.63 (CH<sub>2</sub>), 38.15 (d,  $J_{P-C}$  = 65.5 Hz, CH), 39.27 (d,  $J_{P-C}$  = 65.0 Hz, CH), 42.78 (d,  $J_{P-C}$  = 3.7 Hz, CH), 43.29 (d,  $J_{P-C}$  = 3.5 Hz, CH), 55.81 (CH<sub>3</sub>), 63.56 (d,  $J_{P-C}$  = 1.2 Hz, CH<sub>3</sub>), 105.54 (d,  $J_{P-C}$  = 8.5 Hz, CH), 121.39 (d,  $J_{P-C}$  = 75.8 Hz, C), 122.50 (CH), 123.26 (d,  $J_{P-C}$  = 0.9 Hz, CH), 126.49 (CH), 126.91 (CH), 128.34 (d,  $J_{P-C}$  = 2.1 Hz, C), 128.62 (d,  $J_{P-C}$  = 8.3 Hz, C), 150.49 (d,  $J_{P-C}$  = 11.6 Hz, C), 153.23 (C).

**<sup>31</sup>P{<sup>1</sup>H}-NMR (122 MHz, CDCl<sub>3</sub>):**  $\delta$  46.6.

**HRMS (EI,  $m/z$ ):** calcd for C<sub>32</sub>H<sub>49</sub>O<sub>3</sub>P<sup>+</sup> ([M]<sup>+</sup>), 512.3414; found, 512.3414.



**Dimethyl(*n*-octyl)phosphine oxide (16).** An oven-dried Schlenk tube was charged with dimethylphosphine oxide (163 mg, 500  $\mu$ mol, 1.00 eq.) and dissolved in dry THF (2.0 mL). The solution was cooled to 0 °C (ice bath) and *n*-BuLi (1.6 M in hexanes, 0.31 mL, 500  $\mu$ mol, 1.00 eq.) was added



dropwise. The resulting solution was stirred at 0°C for 4 min before the ice bath was removed and the mixture was stirred at room temperature for 1 hour. Then, 1-bromooctane (86  $\mu$ L, 500  $\mu$ mol, 1.00 eq.) was added dropwise at room temperature. The reaction mixture was stirred at room temperature for 18 h and then transferred to a separatory funnel and diluted with H<sub>2</sub>O-sat. aq. NaCl (5 mL) and EtOAc (5 mL). The organic phase was separated and the aqueous phase was extracted again with EtOAc (2  $\times$  5 mL). The combined organic phases were washed with sat. aq. NaCl (5 mL), dried (MgSO<sub>4</sub>) and filtered. The solvent was removed under reduced pressure and the oily residue was purified by a short column chromatography, eluting with EtOAc-hexanes (1:4), then MeOH-DCM (1:20), to afford colorless oil (199 mg, 91%).

**<sup>1</sup>H-NMR (CDCl<sub>3</sub>, 400 MHz):**  $\delta$  = 0.70–1.20 (m, 6H), 0.83 (d,  $J$  = 6.9 Hz, 3H), 0.85 (d,  $J$  = 6.8 Hz, 3H), 0.88 (t,  $J$  = 7.1 Hz, 3H), 0.91 (d,  $J$  = 6.7 Hz, 6H), 0.92 (d,  $J$  = 6.4 Hz, 3 H), 0.97 (d,  $J$  = 6.8 Hz, 3H), 1.19–1.42 (m, 12H), 1.49–1.93 (m, 14H), 2.19 (sept,  $J$   $\approx$  6.5 Hz, 1H), 2.72 (sept·d,  $J$  = 6.8, 1.9 Hz, 1H).

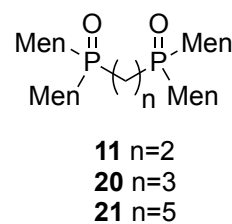
**<sup>13</sup>C{<sup>1</sup>H}-NMR (101 MHz, CDCl<sub>3</sub>):**  $\delta$  14.11, 16.02, 16.16, 21.65, 21.75, 22.09 (d,  $J_{\text{P-C}}$  = 4.3 Hz), 22.67, 22.71, 22.79, 25.14 (d,  $J_{\text{P-C}}$  = 11.3 Hz), 25.20 (d,  $J_{\text{P-C}}$  = 11.4 Hz), 25.47 (d,  $J_{\text{P-C}}$  = 58.5 Hz), 28.00 (d,  $J_{\text{P-C}}$  = 1.7 Hz), 28.68 (d,  $J_{\text{P-C}}$  = 2.3 Hz), 29.11, 29.12, 31.58 (d,  $J$  = 12.9 Hz), 31.84, 33.28 (d,  $J_{\text{P-C}}$  = 12.3 Hz), 33.48 (d,  $J_{\text{P-C}}$  = 11.4 Hz), 34.52 (d,  $J_{\text{P-C}}$  = 1.1 Hz), 34.68 (d,  $J_{\text{P-C}}$  = 1.2 Hz), 35.55 (d,  $J_{\text{P-C}}$  = 2.9 Hz), 36.54, 39.82 (d,  $J_{\text{P-C}}$  = 59.0 Hz), 41.10 (d,  $J_{\text{P-C}}$  = 59.7 Hz), 43.42 (d,  $J_{\text{P-C}}$  = 2.5 Hz), 44.09 (d,  $J_{\text{P-C}}$  = 3.4 Hz).

**<sup>31</sup>P{<sup>1</sup>H}-NMR (162 MHz, CDCl<sub>3</sub>):**  $\delta$  52.5.

**HR-MS (EI, *m/z*):** calcd for C<sub>28</sub>H<sub>55</sub>OP<sup>+</sup> ([M]<sup>+</sup>), 438.3985, found 438.3992.

#### GP-14: Synthesis of alkane-1,*n*-diyl bis(dimethyl)phosphine oxides 10, 20, 21.

*Small scale:* Dimethylphosphine oxide (**4**; 327 mg, 1.00 mmol, 2.00 eq.) was dissolved in dry THF (5.0 mL) in an oven-dried Schlenk tube under argon atmosphere. The solution was cooled to 0 °C (ice bath) and *n*-butyl lithium (625  $\mu$ L, 1.00 mmol, 2.00 eq., 1.6 M solution in hexanes) was added dropwise. The solution was stirred at RT for 1 hour, then cooled to 0 °C again and 1,*n*-dihalo-alkane (1.00 eq.) was added dropwise *via* microsyringe. The ice bath was



removed and the solution was first stirred at room temperature for 1 hour before it was heated to 65 °C for 23 h. The reaction was quenched by adding a 1 M solution of HCl (5 mL) and transferred to a separatory funnel. The mixture was extracted with DCM or hexanes (2 × 15 mL), and the combined organic phases were washed with H<sub>2</sub>O (10 mL) and sat. aq. NaCl (10 mL), dried (MgSO<sub>4</sub>) and filtered. The solvent was removed in a rotary evaporator.

### **Ethane-1,2-diylbis(dimethylphosphine oxide) 11.**

1. Small scale synthesis performed by co-workers<sup>77</sup> according to GP-14 using 1,2-dichloroethane (39 μL, 500 μmol, 1.00 eq.). After drying in high vacuum, **11** was obtained as a colorless solid (339 mg, 100%; ca. 95% purity as calculated by <sup>31</sup>P NMR area integration). A sample for analysis was recrystallized from pentane at -25 °C.

#### *2. Larger scale synthesis:*

An oven-dried Schlenk tube was charged with dimethyl phosphine oxide (**4**; 1.31 g, 4.00 mmol, 2.00 eq.) and evacuated and back-filled with argon. Then, dry THF (10 mL) was added over a septum. The stirred solution was cooled to 0°C (ice/water bath) and *n*-BuLi (1.6 M in hexane, 2.5 mL, 4.00 mmol, 2.00 eq.) was added dropwise. The ice bath was removed and the reaction mixture was stirred at room temperature for 1 hour before 1,2-dichloro ethane (160 μL, 2.00 mmol, 1.00 eq.) was added at room temperature. The solution was stirred for a further hour at room temperature and then at 60°C for 24 hours. After the mixture had come to room temperature, it was quenched by sat. aq. NH<sub>4</sub>Cl (5 mL). The mixture was transferred to a separatory funnel, diluted with H<sub>2</sub>O and the aqueous phase was extracted with Et<sub>2</sub>O:hexane (2:1, 3×). The combined organic phases were washed with sat. aq. NaCl (1×), dried (MgSO<sub>4</sub>), filtered and the solvents evaporated *in vacuo* to afford crude **11** in quantitative yield (1.38 g). The crude material was considered pure enough to be used in further reactions.

**<sup>1</sup>H-NMR (400 MHz, CDCl<sub>3</sub>):** δ 0.64–1.17 (m, 10H), 0.85 (d, *J* = 6.8 Hz, 6H), 0.87 (d, *J* = 6.8 Hz, 6H), 0.91 (d, *J* = 6.4 Hz, 6H), 0.92 (d, *J* = 6.2 Hz, 6H), 0.93 (d, *J* = 6.9 Hz, 6H), 0.98 (d, *J* = 6.8 Hz, 6H), 1.21–1.40 (m, 6H), 1.52–1.80 (m, 16H), 1.83–1.98 (m, 4H), 2.05 (m, 4H), 2.18 (sept·d, *J* = 6.7, 2.0 Hz, 2H), 2.77 (sept·d, *J* = 6.8, 2.3 Hz, 2H).

**APT-<sup>13</sup>C NMR (101 MHz, CDCl<sub>3</sub>):** δ 16.19 (CH<sub>3</sub>), 16.30 (CH<sub>3</sub>), 17.67 (dd, <sup>1</sup>*J*<sub>P-C</sub> = 75.2, <sup>2</sup>*J*<sub>P-C</sub> = 23.4 Hz, CH<sub>2</sub>), 21.85 (CH<sub>3</sub>), 21.88 (CH<sub>3</sub>), 22.77 (CH<sub>3</sub>), 22.81 (CH<sub>3</sub>), 25.19–25.40 (2 x m, CH<sub>2</sub>), 28.26 (CH), 28.99 (CH), 33.42 (*t*, *J*<sub>P-C</sub> = 6.3 Hz, CH), 33.63 (*t*, *J*<sub>P-C</sub> = 5.8 Hz, CH), 34.64 (CH<sub>2</sub>), 34.70 (CH<sub>2</sub>), 35.76 (CH<sub>2</sub>), 36.62 (CH<sub>2</sub>), 39.97 (d, *J*<sub>P-C</sub> = 59.4 Hz, CH), 41.35 (d, *J*<sub>P-C</sub> = 59.9 Hz, CH), 43.72 (CH), 44.43 (*t*, *J*<sub>P-C</sub> = 1.6 Hz, CH).

**<sup>31</sup>P{<sup>1</sup>H} -NMR (162 MHz, CDCl<sub>3</sub>):** δ 52.8.

**HR-MS (EI,  $m/z$ ):** calcd for  $C_{39}H_{73}O_2P_2^+$  ( $[M - C_3H_7]^+$ ), 635.5080, found 635.5064.

**Propane-1,3-diylbis(dimethylphosphine oxide) 20.**

1. Small scale synthesis according to GP-14, using 1,3-dichloro-propane (48  $\mu$ L, 500  $\mu$ mol, 1.00 eq.). The crude material was purified by filtration over a short silica column, elution with EtOAc–hexanes (1:1, 2  $\times$  15 mL) and then MeOH–DCM (1:20, 3  $\times$  15 mL) to afford **20** (219 mg, 63%) as colorless solid.

2. *Larger scale synthesis:* Larger scale synthesis: Dimethylphosphine oxide (**4**; 1.31 g, 4.01 mmol, 1.99 eq.) was dissolved in dry THF (10 mL) in an oven-dried Schlenk tube under argon atmosphere. The solution was cooled to 0°C (ice bath) and *n*-BuLi (2.5 mL, 4.00 mmol, 2.00 eq., 1.6 M solution in hexanes) was added dropwise. The solution was stirred at room temperature for 1 h, then 1,3-dichloropropane (192 mL, 2.02 mmol, 1.00 eq.) was added dropwise *via* microsyringe. The solution was first stirred at room temperature for 1 h, then heated to 60 °C for 24 h. The reaction was quenched by adding sat. aq.  $NH_4Cl$  (5 mL) and transferred to a separatory funnel. The mixture was extracted with  $Et_2O$ –hexanes (3  $\times$  30 mL), and the combined organic phases were washed with sat. aq. NaCl, dried ( $MgSO_4$ ), filtered and evaporated to afford crude **20** (1.45 g) in quantitative yield. This was considered pure enough for further reactions. For analytical purposes, a portion of the crude material was purified by filtration over a short column ( $SiO_2$ ) with EtOAc.

**$^1H$ -NMR (300 MHz,  $CDCl_3$ ):**  $\delta$  0.76–1.39 (m, 16H), 0.83 (d,  $J = 6.8$  Hz, 6H), 0.86 (d,  $J = 6.8$  Hz, 6H), 0.91 (d,  $J = 6.3$  Hz, 12H), 0.93 (d,  $J = 6.3$  Hz, 6 H), 0.97 (d,  $J = 6.9$  Hz, 6H), 1.45–1.97 (m, 24H), 2.01–2.17(m, 2H), 2.24 (sept·m,  $J \approx 6.7$  Hz, 2H), 2.72 (sept·d,  $J = 6.8$ , 2.0 Hz, 2H).

**APT- $^{13}C$  NMR (101 MHz,  $CDCl_3$ ):**  $\delta$  15.49 (t,  $J_{P-C} = 3.0$  Hz,  $CH_2$ ), 15.88 ( $CH_3$ ), 15.97 ( $CH_3$ ), 21.57 (2  $CH_3$ ), 22.50 ( $CH_3$ ), 22.59 ( $CH_3$ ), 24.95 (d,  $J_{P-C} = 11.8$  Hz, 2  $CH_2$ ), 27.09 (dd,  $J_{P-C} = 57.6$ , 10.5 Hz,  $CH_2$ ), 27.77 (CH), 28.58 (CH), 33.12 (d,  $J = 13.0$  Hz, CH), 33.27 (d,  $J_{P-C} = 12.0$  Hz, CH), 34.28 ( $CH_2$ ), 34.35 ( $CH_2$ ), 35.69 ( $CH_2$ ), 36.31 ( $CH_2$ ), 39.44 (d,  $J_{P-C} = 58.8$  Hz, CH), 41.31(d,  $J_{P-C} = 59.1$  Hz, CH), 43.10 (CH), 43.66 (CH).

**$^{31}P\{^1H\}$  NMR (122 MHz,  $CDCl_3$ ):**  $\delta$  52.4.

**HR-MS (EI,  $m/z$ ):** calcd for  $C_{43}H_{82}O_2P_2^+$  ( $[M]^+$ ), 692.5785, found 692.5785.

**Pentane-1,5-diylbis(dimethylphosphine oxide) (21).**

1. Small scale synthesis according to GP-14, with 1,5-dibromo-pentane (68  $\mu$ L, 500  $\mu$ mol, 1.00 eq.). The crude material was purified by filtration over a short column ( $SiO_2$ ), eluting with

EtOAc–hexanes (1:4), then MeOH–DCM (1:20) to afford **21** (346 mg, 96%) as colourless, amorphous solid.

## 2. Larger scale synthesis:

To an oven-dried Schlenk tube, dimethylphosphine oxide (**4**; 1.31 g, 4.00 mmol, 2.00 eq.) was added and the tube was evacuated and back-filled with argon (3×). Then, dry THF was added over a septum and the stirred solution was cooled to 0°C (ice/water bath). Over a septum, *n*-BuLi (1.24 M in hexane, 3.2 mL, 4.00 mmol, 2.00 eq.) was added dropwise over a period of 5 minutes. The ice bath was then removed and the solution was stirred at room temperature for 1 hour. Then, 1,5-dibromopentane (271 μL, 2.00 mmol, 1.00 eq.) was added dropwise while cooling with a water bath. The reaction was stirred at room temperature for 3 days and then quenched by adding a sat. aq. NH<sub>4</sub>Cl solution (4 mL). The mixture was diluted with H<sub>2</sub>O and the aqueous phase extracted with Et<sub>2</sub>O:hexanes (2:1, 3×). The combined organic phases were washed with sat. aq. NaCl (1×), dried (MgSO<sub>4</sub>) and the solvents were removed *in vacuo* to afford crude **21** in quantitative yield (1.61 g).

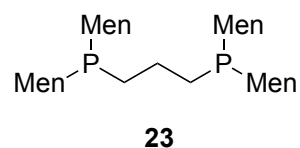
**<sup>1</sup>H-NMR (400 MHz, CDCl<sub>3</sub>):** δ 0.80–1.00 (m, 4H), 0.83 (d, *J* = 6.8 Hz, 6 H), 0.85 (d, *J* = 6.8 Hz, 6H), 0.91 (d, *J* = 6.7 Hz, 12H), 0.92 (d, *J* = 6.4 Hz, 6H), 0.97 (d, *J* = 6.8 Hz, 6H), 1.01–1.20 (m, 6H), 1.21–1.38 (m, 6H), 1.46–1.96 (m, 30H), 2.20 (sept, *J* = 6.5 Hz, 2H), 2.74 (sept·d, *J* = 6.7, 1.8 Hz, 2H).

**APT-<sup>13</sup>C NMR (101 MHz, CDCl<sub>3</sub>):** δ 16.03 (CH<sub>3</sub>), 16.18 (CH<sub>3</sub>), 21.73 (CH<sub>3</sub>), 21.80 (CH<sub>3</sub>), 22.04 (d, *J*<sub>P-C</sub> = 4.1 Hz, CH<sub>2</sub>), 22.72 (CH<sub>3</sub>), 22.80 (CH<sub>3</sub>), 25.10–25.27 (m, 2 x CH<sub>2</sub>), 25.49 (d, *J*<sub>P-C</sub> = 58.2 Hz, CH<sub>2</sub>), 28.00 (d, *J*<sub>P-C</sub> = 1.5 Hz, CH), 28.73 (d, *J* = 2.1 Hz, CH), 33.30 (d, *J*<sub>P-C</sub> = 12.4 Hz, CH), 33.51 (d, *J*<sub>P-C</sub> = 11.4 Hz, CH), 33.71 (t, *J*<sub>P-C</sub> = 12.6 Hz, CH<sub>2</sub>), 34.54 (CH<sub>2</sub>), 34.65 (CH<sub>2</sub>), 35.71 (d, *J*<sub>P-C</sub> = 2.7 Hz, CH<sub>2</sub>), 36.58 (CH<sub>2</sub>), 39.77 (d, *J*<sub>P-C</sub> = 58.9 Hz, CH), 41.31 (d, *J*<sub>P-C</sub> = 59.6 Hz, CH), 43.48 (d, *J*<sub>P-C</sub> = 2.5 Hz, CH), 44.09 (d, *J*<sub>P-C</sub> = 3.4 Hz, CH).

**<sup>31</sup>P{<sup>1</sup>H} -NMR (162 MHz, CDCl<sub>3</sub>):** δ 52.3.

**HR-MS (EI, *m/z*):** calcd for C<sub>45</sub>H<sub>86</sub>O<sub>2</sub>P<sub>2</sub><sup>+</sup> ([M]<sup>+</sup>), 720.6098, found 720.6116.

**1,3-Bis(dimethylphosphaneyl)propane (23).** Crude propane-1,3-diyl-bismenthyl-phosphineoxide **20** (679 mg, 1.00 mmol, 1.00 eq.) was added to a 250 mL Schlenk flask and the flask was evacuated and



back-filled with argon (3×). Sequentially, dry and degassed toluene (20 mL) and NEt<sub>3</sub> (0.83 mL, 6.00 mmol, 6.00 eq.) were then added through a septum. The flask was cooled to 0 °C with an ice bath and HSiCl<sub>3</sub> (0.6 mL, 6.00 mmol, 6.00 eq.) was added dropwise to the stirred solution. After replacing the septum with a glass plug with Teflon collar, the ice bath was removed and

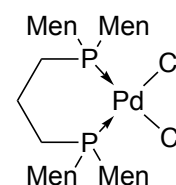
the solution was heated at 60 °C in an oil bath for 26 h. The oil bath was then removed and exchanged with an ice bath again. Then, degassed aq 6 M NaOH (15 mL) was added dropwise to the cooled reaction mixture under argon. After stirring the resulting solution overnight, the organic phase was transferred into another Schlenk flask and the aqueous phase was once again extracted with degassed toluene (8 mL) under Schlenk conditions. The combined organic phases were dried (Na<sub>2</sub>SO<sub>4</sub>), filtered through a plug of Celite under argon and the solvent was removed *in vacuo*. When <sup>31</sup>P-NMR analysis confirmed almost complete conversion of starting material to **23**, the crude product was used in the next step without further purification. The crude material could be recrystallized under argon from hot MeOH–EtOAc (12:10) to obtain analytically pure material.

**<sup>1</sup>H-NMR (400 MHz, C<sub>6</sub>D<sub>6</sub>):** δ 0.75–1.40 (m, 12H), 0.87 (d, *J* = 6.9 Hz, 6H), 0.94 (d *J* = 6.4 Hz, 18H), 1.02 (d, *J* = 7.0 Hz, 6H), 1.02 (d, *J* = 6.9 Hz, 6H), 1.49–1.61 (m, 4H), 1.66–1.91 (m, 14H), 2.04 (br. t, *J* ≈ 14 Hz, 4H), 2.81 (sext·d, *J* = 6.7, 2.7 Hz, 2H), 3.14 (sext, *J* = 6.5 Hz, 2H).

**<sup>31</sup>P{<sup>1</sup>H}-NMR (162 MHz, C<sub>6</sub>D<sub>6</sub>):** δ –27.9.

**(1,3-Bis(dimethylphosphaneyl)propane-κ<sup>2</sup>P,P')palladium(II) chloride**

**(27).** To crude 1,3-Bis(dimethylphosphaneyl)propane **23** was added degassed toluene (6 mL) and PdCl<sub>2</sub>(MeCN)<sub>2</sub> (259 mg, 1.00 mmol, 1.00 eq.) in a Schlenk flask under argon and the resulting solution was stirred at 80 °C



**27**

for 16 h. The solution was then cooled to room temperature and the solvent was removed *in vacuo*. The yellow-orange residue was washed with hexanes (8 mL) and then dissolved in DCM (10 mL), leaving an insoluble red residue which was filtrated off and washed with DCM several times. The filtrate was removed on a rotary evaporator to afford propane-1,3-diyl-bismenthyl-phosphine palladium dichloride **27** (333 mg, 40%) as a yellow solid which still contained minor impurities as judged by <sup>31</sup>P NMR analysis. The solid was further purified by washing with hexanes (4 mL) and dried in vacuum to afford **27** (250 mg, 30%) yellow solid. Crystals for an X-ray structure determination were obtained from dissolving the material in DCM and overlaying with hexanes.

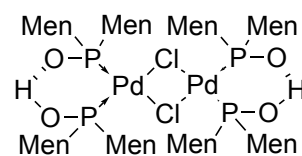
**<sup>1</sup>H-NMR (400 MHz, CD<sub>2</sub>Cl<sub>2</sub>):** broadened signals: δ 0.68–1.27 (m, 8H), 0.91 (d, *J* = 5.9 Hz, 12H), 0.93 (d, *J* = 5.7 Hz, 12H), 0.97 (d, *J* = 6.4 Hz, 6H), 1.03 (d, *J* = 6.2 Hz, 6H), 1.28–1.86 (m, 22H), 1.87–2.33 (m, 8H), 2.46–2.60 (m, 6H), 2.66 (br. sept, *J* ≈ 6.2 Hz, 2H).

**<sup>13</sup>C{<sup>1</sup>H}-NMR (101 MHz, CD<sub>2</sub>Cl<sub>2</sub>):** δ 17.37, 19.14, 19.59–19.98 (m), 21.08, 22.18, 22.52 (2 x), 23.32, 24.67 (d, *J*<sub>P-C</sub> = 6.1 Hz), 26.84 (d, *J*<sub>P-C</sub> = 9.3 Hz), 29.10 (d, *J*<sub>P-C</sub> = 3.9 Hz), 31.06 (d,

$J_{P-C} = 6.1$  Hz), 31.63, 31.96 (d,  $J_{P-C} = 13.1$  Hz), 34.33 (d,  $J_{P-C} = 11.3$  Hz), 34.71, 37.16, 39.99, 40.37 (d,  $J_{P-C} = 25.8$  Hz), 41.48 (d,  $J_{P-C} = 17.8$  Hz), 43.40, 46.05 (d,  $J_{P-C} = 4.5$  Hz).

$^{31}\text{P}\{^1\text{H}\}$ -NMR (162 MHz,  $\text{CD}_2\text{Cl}_2$ ):  $\delta$  23.4 (s).

$[\{(\text{Men}_2\text{P}-\text{O}-\text{H}-\text{O}-\text{PMen}_2-\kappa^2P,P')\text{Pd}\}_2(\mu\text{-Cl})_2]$  (**30**). A plug of basic aluminum oxide ( $\varnothing = 5$  cm;  $h = 0.5$  cm) on a sintered glass frit was charged with  $(\text{Men}_2\text{POH})_2\text{PdCl}_2$  (101.1 mg, 121.8  $\mu\text{mol}$ , 1.00 eq.) dissolved in toluene (6 mL). After 5 min, the plug was eluted



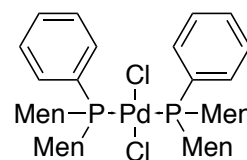
**30**

with toluene ( $2 \times 15$  mL) and the solvent was evaporated *in vacuo*. Hexanes ( $2 \times$ ) was added to the oily residue and the solvent evaporated again to remove residual toluene. After drying in high vacuum, a yellow powder was obtained (50.6 mg, 52%).

$^1\text{H}$ -NMR (400 MHz,  $\text{C}_6\text{D}_6$ ): integrals for major at 80 mol % abundance (integrals of aliphatic area approximated):  $\delta$  0.77–1.31 (m, 88H), 1.33–1.62 (m, 14H), 1.64–1.84 (m, 12H), 1.84–2.12 (m, 12H), 2.20 (br. m, 4H), 2.30–2.41 (m, 4H), 2.53–2.69 (m, 8H), 2.77–2.91 (m, 6H), 3.08 (sept,  $J = 6.7$  Hz, 4H), 15.20 (s, 2H).

$^{31}\text{P}\{^1\text{H}\}$ -NMR (162 MHz,  $\text{C}_6\text{D}_6$ ):  $\delta$  109.4 (s, linewidth 128 Hz).

**Bis(dimethyl(phenyl)phosphine)palladium(II) chloride (32)**. An oven-dried Schlenk tube was charged with  $\text{PdCl}_2$  (22.9 mg, 129  $\mu\text{mol}$ , 1.00 eq.) and then transferred to the glovebox, where it was charged with dimethyl(phenyl)phosphine (100 mg, 259  $\mu\text{mol}$ , 2.00 eq.). Outside of the glovebox, dry and degassed MeCN (4 mL) was added *via* septum, the



**32**

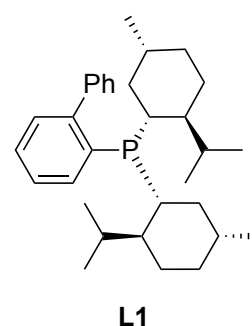
tube was sealed and the resulting yellow mixture was stirred at 70 °C for 17 hours. After the reaction mixture had come to room temperature, the solvent was evacuated *in vacuo* and the residue was washed with hexanes to afford 38% (46.4 mg) of bis(dimethyl(phenyl)phosphine)palladium(II) chloride.

$^1\text{H}$ -NMR (400 MHz,  $\text{CD}_2\text{Cl}_2$ ): signals for both rotamers:  $\delta$  0.13 (t,  $J = 11.4$  Hz, 1H), 0.43 – 0.55 (m, 2H), 0.55 (d,  $J = 6.6$  Hz, 6H), 0.76 (d,  $J = 6.6$  Hz, 6H), 0.80 (d,  $J = 6.7$  Hz, 6H), 0.88 (d,  $J = 6.4$  Hz, 6H), 0.92 (d,  $J = 6.5$  Hz, 6H), 0.99 – 1.28 (m, 14H), 1.14 (d,  $J = 6.5$  Hz, 6H), 1.33 – 1.49 (m, 8H), 1.53 – 1.62 (m, 3H), 1.65 – 1.89 (m, 13H), 2.15 – 2.30 (m, 2H), 2.35 – 2.52 (m, 5H), 3.25 (t,  $J = 11.6$  Hz, 2H), 3.40 – 3.49 (m, 2H), 7.32 – 7.51 (m, 6H), 7.61 (br s, 2H), 8.21 (br s, 2H).

$^{31}\text{P}\{^1\text{H}\}$ -NMR (162 MHz,  $\text{CD}_2\text{Cl}_2$ )  $\delta$  25.64.

**<sup>13</sup>C-APT-NMR (101 MHz, CD<sub>2</sub>Cl<sub>2</sub>):** signals for both rotamers:  $\delta$  17.37 (CH/CH<sub>3</sub>), 19.08 (CH/CH<sub>3</sub>), 22.02 (CH/CH<sub>3</sub>), 22.91 (CH/CH<sub>3</sub>), 23.15 (CH/CH<sub>3</sub>), 23.29 (CH/CH<sub>3</sub>), 26.21(CH<sub>2</sub>), 26.47 (CH<sub>2</sub>), 28.03 (CH), 29.31 (CH), 33.88 (CH), 34.35 (CH), 35.45 (CH<sub>2</sub>), 35.64 (CH<sub>2</sub>), 35.88 (CH<sub>2</sub>), 37.73 (t, CH), 38.23 (CH<sub>2</sub>), 44.79 (CH), 47.47 (CH), 126.89 (CH), 127.76 (C), 130.45 (CH), 132.89 (CH, br s), 138.55 (CH, br s).

**MenJohnPhos (L1).** To a dried-up Schlenk flask, 2-bromobiphenyl (933 mg, 4.00 mmol, 1.00 eq.) and THF (11 mL) was added under argon atmosphere. The stirred solution was cooled to  $-78^{\circ}\text{C}$  (dry ice/acetone bath) and *n*-butyl lithium (1.6 M in hexane, 2.76 mL, 4.40 mmol, 1.10 eq.) was added dropwise. After stirring the solution at  $-78^{\circ}\text{C}$  for one hour, chlorodimethylphosphine (**3**; 1.66 g, 4.80 mmol, 1.20 eq.) in THF (2.90 mL) was added to the reaction mixture and it was stirred at  $-$



$-78^{\circ}\text{C}$  for one hour before it was slowly warmed to room temperature overnight. Then, sat. aq. NH<sub>4</sub>Cl (10 mL) was added and the mixture was extracted with MTBE (2  $\times$  40 mL). The combined organic phases were washed with sat. aq. NaCl (40 mL), dried (MgSO<sub>4</sub>) and filtered. The solvent was evaporated *in vacuo* and the resulting yellowish solid was recrystallized from hot MeOH–EtOAc (2:1) to afford **L1** (910 mg, 49%) as a white solid.

**<sup>1</sup>H-NMR (400 MHz, CDCl<sub>3</sub>):**  $\delta$  0.35–1.70 (m, 16 H), 0.38 (d,  $J$  = 6.6 Hz, 3 H), 0.48 (d,  $J$  = 6.9 Hz, 3 H), 0.51 (d,  $J$  = 6.8 Hz, 3 H), 0.80 (d,  $J$  = 6.5 Hz, 3 H), 0.85 (d,  $J$  = 6.9 Hz, 3 H), 0.92 (d,  $J$  = 6.5 Hz, 3 H), 1.70–1.80 (m, 2 H), 1.94 (m,  $J$  = 9.4, 6.7, 2.6 Hz, 1 H), 2.19 (m,  $J$  = 11.7, 4.1 Hz, 1 H), 7.20–7.24 (m, 1 H), 7.26–7.42 (m, 1 H), 7.71 (dt,  $J$  = 7.4, 1.9 Hz, 1 H).

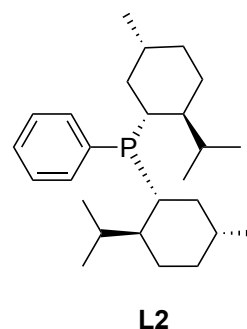
**<sup>13</sup>C{<sup>1</sup>H}-NMR (100 MHz, CDCl<sub>3</sub>):**  $\delta$  14.78, 15.71, 21.80, 21.82, 22.75, 23.09, 25.08 (d,  $J_{\text{P-C}}$  = 7.8 Hz), 25.51 (d,  $J_{\text{P-C}}$  = 11.2 Hz), 26.97 (d,  $J_{\text{P-C}}$  = 19.5 Hz), 28.20 (d,  $J_{\text{P-C}}$  = 10.4 Hz), 33.59, 33.80 (d,  $J_{\text{P-C}}$  = 6.0 Hz), 34.82, 34.78 (d,  $J_{\text{P-C}}$  = 19.4 Hz), 34.92, 36.06 (d,  $J_{\text{P-C}}$  = 22.9 Hz), 37.75 (d,  $J_{\text{P-C}}$  = 7.5 Hz), 38.26 (d,  $J_{\text{P-C}}$  = 3.2 Hz), 42.75 (d,  $J_{\text{P-C}}$  = 10.9 Hz), 49.07 (d,  $J_{\text{P-C}}$  = 23.3 Hz), 125.34, 126.48, 127.51, 127.94, 130.29 (d,  $J_{\text{P-C}}$  = 4.6 Hz), 130.85 (d,  $J_{\text{P-C}}$  = 5.4 Hz), 134.56 (d,  $J_{\text{P-C}}$  = 28.1 Hz), 135.21 (d,  $J_{\text{P-C}}$  = 2.9 Hz), 143.07 (d,  $J_{\text{P-C}}$  = 4.7 Hz), 148.00 (d,  $J_{\text{P-C}}$  = 27.7 Hz).

**<sup>31</sup>P{<sup>1</sup>H}-NMR (162 MHz, CDCl<sub>3</sub>):**  $\delta$   $-22.2$  (s).

**HR-MS (EI, *m/z*):** calcd for C<sub>23</sub>H<sub>47</sub>P<sup>+</sup> ([M]<sup>+</sup>), 462.3410; found, 462.3390.

### Dimethyl(phenyl)phosphine (L2).

<sup>1</sup>H-qNMR experiment for reaction monitoring: An oven-dried Schlenk tube was charged with Men<sub>2</sub>PCl (**3**; 127.5 mg, 500 μmol, 1.00 eq.) in a glovebox and the flask was sealed. Outside of the glovebox, internal standard naphthalene (25.6 mg, 200 μmol) and dry and degassed THF (1.5 mL) were added under a positive stream of argon and the mixture was cooled to 0°C (ice/water bath). Then, phenyl lithium (1.5 M solution in dibutyl ether, 0.4 mL, 600 μmol, 1.20 eq.) was added dropwise over a septum to the stirred solution. The resulting solution was stirred for 1.5 hours at room temperature. Then, the ice bath was removed and the reaction mixture was further stirred at room temperature. After a total of 2.5 hours of reaction time, an aliquot of the reaction mixture was removed by syringe and added to an NMR tube under argon, which was charged with degassed C<sub>6</sub>D<sub>6</sub>. The reaction mixture was then analyzed by <sup>1</sup>H-qNMR as soon as possible, indicating formation of **L2** (94% <sup>1</sup>H-qNMR yield).



*Synthesis:* An oven-dried Schlenk tube was charged with chlorodimethylphosphine (**3**; 862 mg, 2.50 mmol, 1.00 eq.) in a glovebox. Outside of the glovebox, THF (7.5 mL) was then added through a septum and the reaction mixture was cooled to 0 °C. with an ice bath. Phenyl lithium (1.5 M solution in dibutyl ether, 2.0 mL, 3.0 mmol, 1.20 eq.) was then added dropwise and the resulting solution was stirred at 0°C for 15 min. The ice bath was then removed and the reaction mixture was stirred at room temperature for 2 h before it was quenched with degassed water (10 mL). Under argon, degassed EtOAc was then added to the biphasic mixture and the organic phase was transferred to another Schlenk tube *via* syringe. The aqueous phase was again extracted with EtOAc (2 × 5 mL) and the combined organic phases were dried (Na<sub>2</sub>SO<sub>4</sub>). After filtering off the drying agent, the solvent was removed under high vacuum (10<sup>-2</sup> mbar) until a yellow, oily residue remained. Degassed acetone (0.5 mL) was added to the residue and the compound was left to crystallize at -25 °C overnight. The colorless crystals were then filtered off under argon at -30 °C (MeOH/ice bath) and washed with cold, degassed acetone (0.4 mL). The solids were dried in high vacuum to afford dimethylphenylphosphine (747 mg, 1.93 mmol, 77%) as a colorless solid which was stored in the glovebox.

<sup>1</sup>H-NMR (400 MHz, C<sub>6</sub>D<sub>6</sub>): δ 0.45 (d, *J* = 6.7 Hz, 3H), 0.48–0.59 (m, 1H), 0.80–1.18 (m, 7H), 0.83 (d, *J* = 6.8, 3H), 0.85 (d, *J* = 6.3 Hz, 3H), 0.97 (dd, *J* = 7.1, 0.8 Hz, 3H), 0.97 (d, *J* = 6.4 Hz, 3H), 1.03 (d, *J* = 6.8 Hz, 3H), 1.23–1.90 (m, 8H), 1.92–2.03 (m, 2H), 2.23 (dddd, *J* = 11.9, 10.6, 6.2, 3.4 Hz, 1H), 3.31 (sept·d, *J* = 7.0, 2.9 Hz, 1H), 7.06–7.15 (m, 3H), 7.59–7.65 (m, 2H).

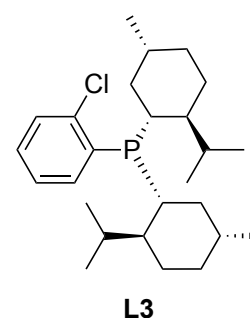


**$^{13}\text{C}\{^1\text{H}\}$ -NMR (101 MHz,  $\text{C}_6\text{D}_6$ ):**  $\delta$  15.32 (d,  $J_{\text{P-C}} = 1.5$  Hz), 16.28, 21.57, 22.44, 23.00, 23.33, 25.64 (d,  $J_{\text{P-C}} = 7.2$  Hz), 25.87 (d,  $J_{\text{P-C}} = 11.1$  Hz), 27.78 (d,  $J_{\text{P-C}} = 22.4$  Hz), 28.35 (d,  $J_{\text{P-C}} = 11.4$  Hz), 33.33 (d,  $J_{\text{P-C}} = 17.7$  Hz), 33.91, 34.07 (d,  $J_{\text{P-C}} = 6.1$  Hz), 35.33, 35.40, 36.39 (d,  $J_{\text{P-C}} = 19.9$  Hz), 37.79 (d,  $J_{\text{P-C}} = 3.5$  Hz), 38.07 (d,  $J_{\text{P-C}} = 6.8$  Hz), 43.98 (d,  $J_{\text{P-C}} = 9.0$  Hz), 50.46 (d,  $J_{\text{P-C}} = 23.2$  Hz), 127.72, 128.64 (d,  $J_{\text{P-C}} = 1.0$  Hz), 135.00 (d,  $J_{\text{P-C}} = 19.3$  Hz), 137.11 (d,  $J_{\text{P-C}} = 22.3$  Hz).

**$^{31}\text{P}\{^1\text{H}\}$ -NMR (162 MHz,  $\text{C}_6\text{D}_6$ ):**  $\delta$  -10.1.

**HR-MS (EI):** Calcd for  $\text{C}_{26}\text{H}_{43}\text{P}_1^+$  ( $[\text{M}]^+$ ), 386.3097, found 386.3097.

**(2-Chlorophenyl)dimenthylphosphine (L3).** An oven-dried Schlenk flask under argon atmosphere was charged with 1-bromo-2-chlorobenzene (0.48 mL, 4.12 mmol, 1.01 eq.) and dry and degassed THF (10 mL). After cooling to  $-78$  °C (acetone–dry ice bath), *n*-BuLi (1.6 M in hexane, 2.6 mL, 1.02 eq.) was added dropwise to the stirred solution. After stirring the resulting solution for 1 h at  $-78$  °C, chlorodimenthylphosphine (**3**; 345 mg, 4.08 mmol, 1.00 eq.) in THF (4 mL) was added dropwise. The resulting solution was stirred for one hour at  $-78$  °C, and then slowly warmed to room temperature over the course of 16 h. After adding sat. aq.  $\text{NH}_4\text{Cl}$  (12 mL), the mixture was transferred to a separatory funnel and the aqueous phase was extracted with EtOAc ( $2 \times 20$  mL). The combined organic phases were washed with sat. aq. NaCl (20 mL), dried ( $\text{MgSO}_4$ ), filtered and the solvent evaporated in vacuum. The crude material was triturated with MeOH and the flask ultrasonicated until off-white solids had formed. The solids were filtered off and washed with a minimum amount of cold MeOH. Drying in high vacuum gave **L3** (640 mg, 37%) as colorless solid.

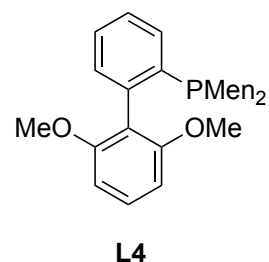


**$^1\text{H}$ -NMR (400 MHz,  $\text{CDCl}_3$ ):**  $\delta$  0.25 (d,  $J = 6.6$  Hz, 3H), 0.57–1.11 (m, 7H), 0.78 (d,  $J = 6.8$  Hz, 3H), 0.80 (d,  $J = 6.5$  Hz, 3H), 0.82 (d,  $J = 6.9$  Hz, 3H), 0.89 (dd,  $J = 6.9, 1.0$  Hz, 3H), 0.96 (d,  $J = 6.6$  Hz, 3H), 1.20–1.37 (m, 2H), 1.42–1.54 (m, 1H), 1.57–1.85 (m, 8H), 2.09 (dddd,  $J = 12.1, 11.1, 4.5, 3.6$  Hz, 1H), 3.05 (octett·d,  $J = 6.9, 2.6$  Hz, 1H), 7.18–7.25 (m, 2H), 7.34–7.43 (m, 1H), 7.56–7.63 (m, 1H).

**$^{31}\text{P}\{^1\text{H}\}$ -NMR (162 MHz,  $\text{CDCl}_3$ ):**  $\delta$  -16.9 (s). ESI-MS ( $m/z$ ): 420.15 ( $[\text{M} - \text{H}]^+$ , 5%), 385.19 ( $[\text{M} - \text{Cl}]^+$ , 100%).

**HR-MS (EI,  $m/z$ ):** calcd for  $\text{C}_{26}\text{H}_{42}\text{ClP}^+$  ( $[\text{M}]^+$ ) 420.2707, found 420.2749.

**MenSPhos (L4).** To an oven-dried Schlenk tube, magnesium granules (26.8 mg, 1.12 mmol, 1.12 eq.) and 2-bromo-2',6'-dimethoxybiphenyl (**34**; 293 mg, 1.00 mmol, 1.00 eq.) was added and the Schlenk tube was evacuated and back-filled with argon (3 ×). Then, dry and degassed THF (2.0 mL) and DBE (4 μL) was added and the mixture was stirred at



80 °C for 19 h. After cooling the mixture to room temperature, CuCl (4.95 mg, 0.05 mmol, 5 mol-%) and chlorodimethylphosphine (345 mg, 1.00 mmol, 1.00 eq.) in THF (0.5 mL) were added sequentially. The reaction mixture was stirred at room temperature for 3 days and for 5 more hours at 60 °C, after which the reaction was quenched by adding sat. aq. NH<sub>4</sub>Cl (2 mL) and H<sub>2</sub>O (3 mL). The mixture was transferred into a separatory funnel and extracted with Et<sub>2</sub>O (3 × 10 mL). The combined organic phases were washed with H<sub>2</sub>O (20 mL) and sat. aq. NaCl (30 mL). The combined organic phases were dried (MgSO<sub>4</sub>), filtered and the solvent was removed on a rotary evaporator. After recrystallization from hot MeOH–EtOAc (9:1), **L4** was obtained as a colorless solid (155 mg, 30%).

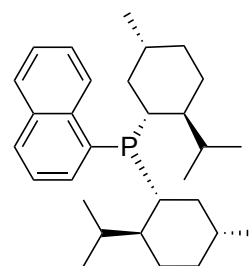
**<sup>1</sup>H-NMR (400 MHz, C<sub>6</sub>D<sub>6</sub>):** δ 0.65–1.20 (m, 5H), 0.72 (d, *J* = 6.8 Hz, 3H), 0.79 (dd, *J* = 6.8, 0.4 Hz, 3H), 0.81 (d, *J* = 7.0 Hz, 3H), 0.83 (d, *J* = 6.5 Hz, 3H), 0.97 (d, *J* = 6.4 Hz, 3H), 0.98 (d, *J* = 6.9 Hz, 3H), 1.26–1.90 (m, 11H), 2.21 (td, *J* = 11.5, 2.8 Hz, 1H), 2.27–2.40 (m, 2H), 2.72 (sept·d, *J* = 6.9, 2.6 Hz, 1H), 3.33 (s, 3H), 3.41 (s, 3H), 6.38 (d, *J* = 8.3 Hz, 1H), 6.44 (d, *J* = 8.3 Hz, 1H), 7.12–7.22 (m, 3H, overlap with residual solvent signal), 7.26–7.30 (m, 1 H), 7.83 (dt, *J* = 7.4, 1.6 Hz, 1H).

**<sup>13</sup>C{<sup>1</sup>H}-NMR (76 MHz, C<sub>6</sub>D<sub>6</sub>):** δ 15.73 (d, *J*<sub>P-C</sub> = 0.9 Hz, CH<sub>3</sub>), 16.17 (CH<sub>3</sub>), 22.13 (CH<sub>3</sub>), 22.60 (CH<sub>3</sub>), 23.06 (CH<sub>3</sub>), 23.23 (CH<sub>3</sub>), 26.07 (d, *J*<sub>P-C</sub> = 8.6 Hz, CH<sub>2</sub>), 26.22 (d, *J*<sub>P-C</sub> = 9.5 Hz, CH<sub>2</sub>), 27.56 (d, *J*<sub>P-C</sub> = 44.1 Hz, CH), 27.58 (CH), 34.38 (d, *J*<sub>P-C</sub> = 2.1 Hz, CH), 34.45 (CH), 35.48 (CH<sub>2</sub>), 35.58 (d, *J*<sub>P-C</sub> = 26.1 Hz, CH), 35.62 (CH<sub>2</sub>), 36.86 (d, *J*<sub>P-C</sub> = 21.8 Hz, CH), 39.01 (d, *J*<sub>P-C</sub> = 1.5 Hz, CH<sub>2</sub>), 40.40 (d, *J*<sub>P-C</sub> = 2.5 Hz, CH<sub>2</sub>), 44.16 (d, *J*<sub>P-C</sub> = 18.1 Hz, CH), 47.73 (d, *J*<sub>P-C</sub> = 21.4 Hz, CH), 54.93 (CH<sub>3</sub>), 55.45 (d, *J*<sub>P-C</sub> = 0.8 Hz, CH<sub>3</sub>), 103.94 (CH), 104.24 (CH), 120.95 (d, *J*<sub>P-C</sub> = 5.5 Hz, C), 126.38 (CH), 128.35 (CH, overlap with solvent signal), 128.85 (CH), 132.23 (d, *J*<sub>P-C</sub> = 6.0 Hz, CH), 133.32 (d, *J*<sub>P-C</sub> = 1.5 Hz, CH), 138.82, (d, *J*<sub>P-C</sub> = 26.2 Hz, C), 141.90, (d, *J*<sub>P-C</sub> = 32.4 Hz, C), 158.20 (d, *J*<sub>P-C</sub> = 0.8 Hz, C), 158.58 (d, *J*<sub>P-C</sub> = 0.8 Hz, C).

**<sup>31</sup>P{<sup>1</sup>H}-NMR (162 MHz, C<sub>6</sub>D<sub>6</sub>):** δ –21.1 (s).

**HR-MS (EI):** Calcd for C<sub>34</sub>H<sub>51</sub>O<sub>2</sub>P<sup>+</sup> ([M]<sup>+</sup>), 522.3622, found 522.3614.

**Dimethyl(1-naphthyl)phosphine (L5).** An oven-dried Schlenk tube was dried by heat gun and back-filled and evacuated with argon (3 ×). It was then charged with 1-bromonaphthalene (280 μL, 2.00 mmol, 2.00 eq.) and THF (2.5 mL) and cooled to -78 °C (acetone/dry ice). Then, *n*-BuLi (1.6 M in hexane, 1.25 mL, 2.00 mmol, 2.00 eq.) was added dropwise and the solution was stirred at -78 °C for 100 min before adding Men<sub>2</sub>PCl (**3**; 345 mg, 1.00 mmol, 1.00 eq.) in THF



**L5**

(1 mL) dropwise. The resulting solution was stirred at -78 °C for a further 2 hours before it was slowly brought to room temperature and then quenched by addition of H<sub>2</sub>O (5 mL). It was then extracted with EtOAc (3 × 8 mL) and the combined organic phases were washed with sat. aq. NaCl (8 mL), dried (MgSO<sub>4</sub>) and filtered. The solvent was removed on a rotary evaporator and the crude product was triturated with a small amount of MeOH, filtered and washed with MeOH to afford **L5** (237 mg, 54%) as off-white solid.

**<sup>1</sup>H-NMR (400 MHz, C<sub>6</sub>D<sub>6</sub>):** δ 0.30 (d, *J* = 6.7 Hz, 3H), 0.70 (d, *J* = 6.8 Hz, 3H), 0.73 – 1.06 (m, 5H), 0.83 (d, *J* = 6.5 Hz, 3H), 0.87 (d, *J* = 6.9 Hz, 3H), 1.00 (d, *J* = 6.5 Hz, 3H), 1.06 (d, *J* = 6.8 Hz, 3H), 1.16 – 1.68 (m, 8H), 1.74 (d, *J* = 12.7 Hz, 1H), 1.83 – 2.03 (m, 3H), 2.10 (d, *J* = 12.8 Hz, 1H), 2.29 – 2.44 (m, 1H), 3.44 (sept-d, *J* = 6.9, 2.5 Hz, 1H), 7.21 – 7.28 (m, 1H), 7.55 – 7.69 (m, 2H), 7.63 (dd, *J* = 13.3, 8.1 Hz, 2H), 7.83 (dd, *J* = 7.4, 2.8 Hz, 1H), 9.21 – 9.32 (m, 1H).

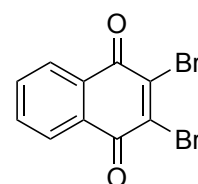
**<sup>31</sup>P{<sup>1</sup>H} -NMR (162 MHz, C<sub>6</sub>D<sub>6</sub>):** δ -28.68.

**<sup>13</sup>C{<sup>1</sup>H}-NMR (75 MHz, CDCl<sub>3</sub>)** δ 15.45, 15.84, 21.41, 22.13, 22.81, 23.25, 25.37, 25.47, 25.55, 25.70, 27.97, 28.01, 28.16, 28.24, 33.57, 34.02, 34.11, 34.61, 34.83, 35.26, 35.92, 36.18, 38.28, 38.37, 42.96, 49.99, 50.29, 124.16, 125.54, 125.57, 125.59, 125.63, 127.05, 127.45, 128.52, 128.54, 128.93, 133.56, 133.73, 133.77, 133.80, 133.89, 137.11, 137.44. Complicated signal-splitting due to C-P coupling.

### **2,3-Dibromo-1,4-naphthoquinone (79).**

The synthesis was performed according to Inoue *et al.*<sup>135</sup>

A 2-neck flask which was equipped with a stirring bar and connected to a wash-bottle filled with Na<sub>2</sub>SO<sub>3</sub> solution was charged with 1,4-naphthoquinone (20.0 g, 126 mmol, 1.00 eq.), HOAc (320 mL), Br<sub>2</sub> (15.5 mL, 303 mmol, 2.40 eq.) and I<sub>2</sub> (128 mg, 5.06 mmol, 0.4 mol-%). The stirred solution was then heated to 60 °C for 2 hours and then to 100 °C for



**79**

1.5 hours before it was brought to room temperature. The formed solids were filtered, washed with MeOH and dried *in vacuo* to afford **79** (35.5 g, 91%).

**<sup>1</sup>H-NMR (500 MHz, CDCl<sub>3</sub>):**  $\delta$  7.69 – 7.84 (m, 2H), 8.15 – 8.24 (m, 2H).

**<sup>13</sup>C{<sup>1</sup>H}-NMR (101 MHz, CDCl<sub>3</sub>):**  $\delta$  128.39, 130.92, 134.69, 142.73, 176.00.

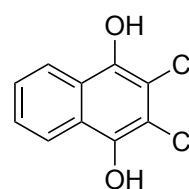
**TLC:**  $R_f$  = 0.31 (SiO<sub>2</sub>; hexanes:EtOAc 20:1) [UV, Mostain]

Known compound. CAS: 13243-65-7.

The analytical data is in accordance with the literature.<sup>153</sup>

### 2,3-Dichloro-1,4-dihydroxynaphthalene (**75**).

*Small scale synthesis:* A round bottom flask was charged with 2,3-dichloro-1,4-naphthoquinone (**74**; 7.00 g, 30.8 mmol, 1.00 eq.), Et<sub>2</sub>O (100 mL) and CH<sub>2</sub>Cl<sub>2</sub> (100 mL). Then, a solution of Na<sub>2</sub>S<sub>2</sub>O<sub>4</sub> (86 wt.-% purity, 31.2 g, 154 mmol, 5.00 eq.) in H<sub>2</sub>O (200 mL) was added and the resulting two-phase mixture was stirred vigorously at room temperature for 4 hours, after which



**75**

TLC analysis confirmed complete formation of target material. Then, the organic solvent was evaporated *in vacuo* and the aqueous phase was extracted with EtOAc (2 × 50 mL). The combined organic phases were washed with H<sub>2</sub>O (80 mL) and sat. aq. NaCl (100 mL), dried (MgSO<sub>4</sub>) and filtered. The solvent was removed on a rotary evaporator to afford **73** in quantitative yield.

*Larger scale synthesis:* A round bottom flask was charged with 2,3-dichloro-1,4-naphthoquinone (**74**; 20.0 g, 88.0 mmol, 1.00 eq.), CH<sub>2</sub>Cl<sub>2</sub> (275 mL) and Et<sub>2</sub>O (275 mL). Then, Na<sub>2</sub>S<sub>2</sub>O<sub>4</sub> (86 wt.-% purity, 89.8 g, 440 mmol, 5.00 eq.) in H<sub>2</sub>O (550 mL) was added and the two-phase mixture was stirred vigorously at room temperature for 20 hours. The organic solvent was then removed on a rotary evaporator and the aqueous phase extracted with EtOAc (3×). The combined organic phases were washed with H<sub>2</sub>O (1×), sat. aq. NaCl (1×), dried (MgSO<sub>4</sub>), filtered and the solvent evaporated *in vacuo* to afford **75** (19.45 g, 96%) as pale pink solid.

**<sup>1</sup>H-NMR (500 MHz, CDCl<sub>3</sub>):**  $\delta$  5.70 (s, 2H), 7.48 – 7.61 (m, 2H), 8.14 – 8.21 (m, 2H).

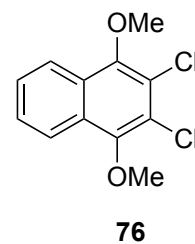
**<sup>13</sup>C{<sup>1</sup>H}-NMR (101 MHz, CDCl<sub>3</sub>):**  $\delta$  111.28, 122.22, 123.29, 127.15, 142.24.

**TLC:**  $R_f$  = 0.57 (SiO<sub>2</sub>; hexanes:EtOAc 3:1) [UV, Mostain]

Known compound. CAS: 7474-86-4. The analytical data is in accordance with the literature.

### 2,3-dichloro-1,4-dimethoxy-naphthalene (746).

An oven-dried Schlenk flask was evacuated and back-filled with argon (3×), charged with degassed acetone (125 mL). Then, dried and crushed K<sub>2</sub>CO<sub>3</sub> (12.0 g, 87.2 mmol, 4.00 eq.) was added portionwise under a positive pressure of argon so that a well-stirred suspension was formed. Me<sub>2</sub>SO<sub>4</sub> (6.2 mL, 65.2 mmol, 3.00 eq.) and 2,3-dichloro-1,4-dimethoxynaphthalene (**73**; 5.00 g, 21.8 mmol, 1.00 eq.) were then subsequently added (the latter portionwise) under water-bath cooling. The mixture was then heated to 40 °C for 1.5 hours, after which TLC confirmed complete consumption of starting material. After the reaction mixture had cooled to room temperature, conc. aq. NH<sub>3</sub> (20 mL) was added to destroy any remaining Me<sub>2</sub>SO<sub>4</sub> and the mixture was stirred overnight. It was then filtered over a pad of cotton, diluted with water and extracted with EtOAc (2×). The combined organic phases were washed with H<sub>2</sub>O (1×) and sat. aq. NaCl (1×), dried (MgSO<sub>4</sub>) and the solvent evaporated *in vacuo*. The residue was then purified by column chromatography (SiO<sub>2</sub>; hexanes–EtOAc 20:1) to afford **76** (3.7 g, 66%) as off-white solid.



**<sup>1</sup>H-NMR (500 MHz, CDCl<sub>3</sub>):** δ 4.01 (s, 6H), 7.54 – 7.61 (m, 2H), 8.07 – 8.14 (m, 2H).

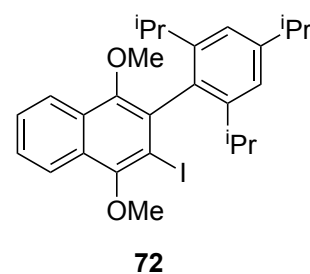
**<sup>13</sup>C{<sup>1</sup>H}-NMR (75 MHz, CDCl<sub>3</sub>):** δ 61.61, 122.50, 123.16, 127.43, 127.78, 149.84.

**TLC:** *R*<sub>f</sub> = 0.79 (SiO<sub>2</sub>; hexanes-EtOAc 3:1) [UV, Mostain].

Known substance, CAS 41245-40-3. The analytical data is in accordance with the literature.<sup>155</sup>

### 2-Iodo-1,4-dimethoxy-3-(2,4,6-triisopropylphenyl)naphthalene (72).

An oven-dried 250 mL Schlenk flask was charged with Mg turnings (1.14 g, 46.8 mmol, 4.00 eq.), evacuated and back-filled with argon (3×) and dried by heat-gun (2×). Then, dry THF (12 mL) and a granule of I<sub>2</sub> were added. Then, 1-bromo-2,4,6-triisopropyl benzene (4.97 g, 17.6 mmol, 1.50 eq.) was added dropwise and slowly *via* syringe, while the reaction was initiated by heat gun. After fading of the purple iodine colour had indicated initiation of the *Grignard* reaction, the remaining 1-bromo-2,4,6-triisopropyl benzene was added dropwise under stirring, and the syringe was rinsed with dry THF (2 mL). The reaction mixture was then heated to 50°C in an oil bath for 2 hours. Then, **76** (3.00 g, 11.7 mmol, 1.00 eq.) was added dropwise at this temperature over a period of 20 minutes. The mixture was stirred at 50°C for 17 hours. After the reaction had cooled to room temperature, the flask was placed in an ice bath and iodine (13.4 g, 52.7 mmol, 4.50 eq.) was added under a positive pressure of argon. The ice bath was removed and the mixture was stirred at room



temperature for 45 minutes. The solution was then diluted with EtOAc and remaining Mg turnings were filtered off. The organic phase was then washed with half-sat. aq. Na<sub>2</sub>SO<sub>3</sub> solution (2×) and the combined aqueous phases re-extracted with EtOAc (2×). The combined organic phases were then washed with sat. aq. NaCl (1×), dried (MgSO<sub>4</sub>) and the solvent evaporated *in vacuo*. The crude material was purified by column chromatography (SiO<sub>2</sub>; hexanes–toluene 20:1 → 4:1) and then washed with cold hexanes to afford **72** (2.14 g, 35%) as pale yellow solid.

**<sup>1</sup>H-NMR (400 MHz, CDCl<sub>3</sub>):** δ 1.11 (d, *J* = 6.8 Hz, 6H), 1.21 (d, *J* = 6.8 Hz, 6H), 1.33 (d, *J* = 6.8 Hz, 6H), 2.44 (p, *J* = 6.8 Hz, 2H), 2.99 (p, *J* = 6.9 Hz, 1H), 3.61 (s, 3H), 3.99 (s, 3H), 7.09 (s, 2H), 7.53 – 7.61 (m, 2H), 8.08 – 8.19 (m, 2H).

**<sup>13</sup>C{<sup>1</sup>H}-NMR (75 MHz, CDCl<sub>3</sub>)** δ 24.27, 24.56, 24.98, 31.13, 34.33, 61.54, 61.72, 97.72, 121.23, 123.03, 123.63, 126.73, 127.86, 133.88, 135.61, 146.35, 148.95, 150.20, 153.18, 129.10.

**HR-MS (EI):** Calcd for C<sub>27</sub>H<sub>33</sub>IO<sub>2</sub><sup>+</sup> ([M]<sup>+</sup>) 516.1520, found 516.1495.

#### **GP-15. General Procedure for the screening of reaction conditions for the synthesis of **83**.**

**A: Via Grignard reagent:** An oven-dried Schlenk tube was charged with Mg turnings (35.3 mg, 1.47 mmol, 3.80 eq.), evacuated and back-filled with argon (3×) and dried by heatgun (2×). Then, dry and degassed THF (0.5 mL) and 1,2-dibromoethane (1 drop) was added. The stirred mixture was heated to 60°C for 30 minutes and then cooled to room temperature. Then, precursor **72** (200 mg, 387 μmol, 1.00 eq.) and dry and degassed THF (1.4 mL) was added under a positive pressure of argon. The resulting mixture was stirred at 60 °C for 2 hours. After it had come to room temperature, the resulting *Grignard* solution was transferred to a second, oven-dried Schlenk tube which was charged with CuCl (*x* eq.) under argon. The first flask was rinsed with THF (0.5 mL) and the solution transferred once more. Then, ClPCy<sub>2</sub> (128 μL, 581 μmol, 1.50 eq.) in dry and degassed THF (0.5 mL) was added to the stirred *Grignard* solution at room temperature. The resulting mixture was stirred at 60 °C overnight and then brought to room temperature. After addition of BH<sub>3</sub>·Me<sub>2</sub>S (94% purity, 60 μL, 1.60 eq.) over a septum, the mixture was stirred at room temperature for a further hour. Then, a degassed solution of citric acid in H<sub>2</sub>O (2 mL) was added, resulting in gas evolution. After gas evolution had ceased, a defined amount of internal standard (triphenylphosphine oxide) and THF (3 mL) were added under a positive flow of argon. After sufficient stirring, an aliquot of the mixture (~0.4 mL) was removed by syringe, added to an NMR tube charged with C<sub>6</sub>D<sub>6</sub> (0.2 mL) and argon and analyzed by <sup>31</sup>P-qNMR.

**B: Via Aryllithium:** An oven-dried Schlenk tube was evacuated and back-filled with argon (3×) and dried once more by heat gun. Then, precursor **72** (x eq.) and THF (x mL) was added under counter-flow of argon. The stirred solution was cooled to -78°C and *n*-BuLi (x eq., 16 M solution in hexane) was added. The mixture was stirred at -78 °C for 1.5 hours. Then, if indicated, CuCl (x eq.) and ClPCy<sub>2</sub> (128 μL, 581 μmol 1.50 eq.) in THF (0.5 mL) were added subsequently and the resulting solution was slowly warmed to room temperature overnight. Then, BH<sub>3</sub>·Me<sub>2</sub>S (94% purity, 60 μL, 1.60 eq.) was added over a septum und the resulting solution was stirred for 1 – 2 hours at room temperature. The reaction was then quenched with degassed sat. aq. NaCl (1.5 mL) and a defined amount of internal standard (triphenylphosphine oxide) was added. <sup>31</sup>P-qNMR sampling was performed analogically to **GP-15-A**.

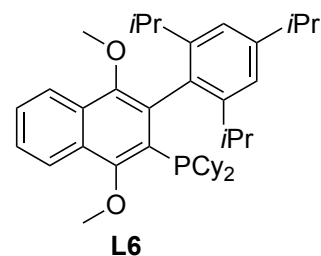
**KatPhos copper halide complex (85).** An oven-dried Schlenk tube was charged with Mg turnings (35.3 mg, 147 mmol, 3.80 eq.), evacuated and back-filled with argon (3×) and dried by heatgun (2×). Dry and degassed THF (0.5 mL) and 1,2-dibromoethane (1 drop). The tube was sealed and heated to 60 °C for 30 minutes. After 30 minutes, the mixture was cooled to room temperature and 2-iodo-1,4-dimethoxy-3-(2,4,6-triisopropylphenyl)naphthalene **72** (200 mg, 387 μmol, 1.00 eq.) in dry and degassed THF (1.4 mL) was added dropwise and the resulting mixture was stirred at 60 °C for 2 hours. The resulting *Grignard* solution was separated from excess magnesium turnings by syringe and the solution added to a new, oven-dried Schlenk tube under argon charged with CuCl (38.8 mg, 387 μmol, 1.00 eq.). The first flask was rinsed once with dry and degassed THF (0.5 mL) and the solution transferred once more. Then, chloro(dicyclohexyl)phosphine (1.13 M solution in THF, 0.34 mL, 1.00 eq.) was added and the resulting solution was stirred at 60 °C for 16 hours. After letting the reaction mixture come to room temperature, BH<sub>3</sub>·Me<sub>2</sub>S (94% purity, 60 μL, 1.60 eq.) was added and the solution stirred at room temperature for one hour. Then, a solution of citric acid in H<sub>2</sub>O (2 mL) was added, resulting in gas evolution. After gas evolution had ceased, internal standard (triphenylphosphine oxide, 39.8 mg) and THF (3 mL) was added. After qNMR sampling, the 2-phased mixture was transferred to a separatory funnel, diluted with H<sub>2</sub>O (2 mL) and extracted with Et<sub>2</sub>O (4×). The combined organic phases were washed with sat. aq. NaCl (1×), dried (MgSO<sub>4</sub>), filtered and the solvent evaporated *in vacuo*. The resulting white solid was triturated with a minimum amount of Et<sub>2</sub>O and filtered to afford a white solid. Further recrystallization from THF–hexanes (1:3) afforded 61 mg of **85** (counteranion not confirmed) as a white solid.

**<sup>1</sup>H-NMR (400 MHz, C<sub>6</sub>D<sub>6</sub>):** δ 1.11 – 1.02 (m, 6H, *Cy*-H), 1.17 (d, *J* = 6.6 Hz, 6H, *iPr*-H), 1.37 – 1.30 (m, 2H, *Cy*-H), 1.57 – 1.48 (m, 2H, *Cy*-H), 1.61 (d, *J* = 6.9 Hz + m, 16H, *Cy*-H + *iPr*-

H), 1.71 – 1.64 (m, 4H, *Cy*-H), 2.10 (d,  $J = 13.1$  Hz, 2H, *Cy*-H), 2.40 – 2.29 (m, 2H, *Cy*-H), 2.66 (hept,  $J = 6.7$  Hz, 2H, *iPr*-H), 3.15 (s + m, 4H, O-CH<sub>3</sub> + *iPr*-H), 3.54 (s, 3H, O-CH<sub>3</sub>), 7.32 – 7.18 (m, 2H, *nap*-H), 7.46 (s, 2H, *aryl*-H), 7.82 (d,  $J = 8.3$  Hz, 1H, *nap*-H), 8.00 (d,  $J = 8.6$  Hz, 1H, *nap*-H).

<sup>31</sup>P{<sup>1</sup>H} -NMR (162 MHz, C<sub>6</sub>D<sub>6</sub>):  $\delta$  13.55.

**KatPhos (L6).** An oven-dried Schlenk tube was charged with Mg turnings (179 mg, 7.36 mmol, 3.80 eq.), evacuated and back-filled with argon (3 $\times$ ) and dried by heat gun (2 $\times$ ). Then, THF (2.2 mL) and 1,2 dibromo ethane (2 drops) were added under a positive stream of argon and the suspension was heated to 60 °C for 30 minutes. After



it had cooled to room temperature, precursor **72** (1.00 g, 1.94 mmol, 1.00 eq.) in dried and degassed THF (7.5 mL) was added slowly and dropwise. The resulting mixture was then heated to 60 °C for 2 hours, after which TLC analysis confirmed full conversion to *Grignard* reagent. A second Schlenk tube under argon was charged with CuCl (192 mg, 1.94 mmol, 1.00 eq.) and the *Grignard* solution was transferred to the second Schlenk tube *via* syringe. The first flask was rinsed once more with THF (0.5 mL) and transferred once more. Then, ClPCy<sub>2</sub> (0.43 mL, 1.94 mmol, 1.00 eq.) in THF (1.5 mL) was added to the stirred solution at room temperature (rinsing once more with 0.5 mL THF). The solution was heated to 60 °C overnight, then brought to room temperature and quenched with NH<sub>4</sub>OH/sat. aq. NaCl (2:1, 3 mL). The mixture was transferred to an Erlenmeyer flask, diluted with both Et<sub>2</sub>O (50 mL) and NH<sub>4</sub>OH/sat. aq. NaCl (2:1, 10 mL) and stirred at room temperature for one hour. The mixture was then transferred to a separatory funnel and the organic phase separated. The aqueous phase was extracted with Et<sub>2</sub>O (2 $\times$ ) and the combined organic phases washed with NH<sub>4</sub>OH/sat. aq. NaCl (until the blue color of the aqueous phase had faded), H<sub>2</sub>O (1 $\times$ ) and sat. aq. NaCl (1 $\times$ ). The combined organic phases were then dried (MgSO<sub>4</sub>), filtered and the solvent was removed on a rotary evaporator. The oily residue was dissolved again in a minimum amount of Et<sub>2</sub>O and filtered over a short path SiO<sub>2</sub> column, eluting with Et<sub>2</sub>O. After removing the solvent *in vacuo*, the residue was triturated with a minimum amount of cold MeOH and ultrasonicated until solids had formed, which were filtered off and washed again with MeOH to afford **L6** (971 mg, 85%) as off-white solid (containing 6.7 wt-% of **72**). For analytical purposes, the material was recrystallized from EtOAc/MeOH.

<sup>1</sup>H-NMR (300 MHz, C<sub>6</sub>D<sub>6</sub>):  $\delta$  1.07 – 1.48 (m, 10H), 1.29 (d,  $J = 6.9$  Hz, 6H), 1.32 (d,  $J = 6.6$  Hz, 6H), 1.55 (d,  $J = 6.7$  Hz, 6H), 1.60 – 1.83 (m, 8H), 2.02 – 2.12 (m, 2H), 2.36 – 2.54 (m,



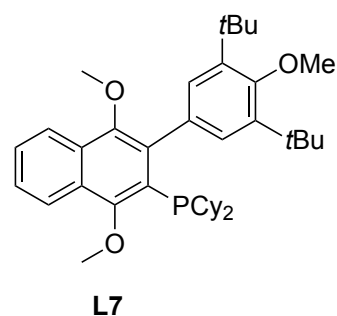
2H), 2.75 – 2.98 (2 hept, 3H), 3.33 (s, 3H), 3.69 (s, 3H), 7.21 – 7.35 (m, 4H), 7.97 (d,  $J = 7.2$  Hz, 1H), 8.12 (d,  $J = 8.3$  Hz, 1H).

$^{31}\text{P}\{^1\text{H}\}$ -NMR (122 MHz,  $\text{C}_6\text{D}_6$ ):  $\delta$  -0.16.

$^{13}\text{C}\{^1\text{H}\}$ -NMR (101 MHz,  $\text{C}_6\text{D}_6$ ):  $\delta$  24.36, 25.57, 25.87, 25.91, 26.85, 27.83, 27.96, 28.04, 28.13, 31.22, 31.24, 31.74, 31.86, 32.86, 33.09, 34.62, 37.58, 37.75, 61.19, 62.89, 121.22, 123.90, 124.08, 125.80, 126.76, 131.00, 147.49, 148.35.

HR-MS (EI,  $m/z$ ): calcd for  $\text{C}_{39}\text{H}_{55}\text{O}_2\text{P}^+$  ( $[\text{M}]^+$ ) 586.3934, found 586.3934.

**CyAnPhos (L7).** An oven-dried Schlenk flask was charged with Mg turnings (184 mg, 7.60 mmol, 3.80 eq.), dried by heat gun (2 $\times$ ) and evacuated and back-filled with argon (3 $\times$ ). Then, dry and degassed THF (2 mL) and 1,2-dibromo ethane (2 drops) were added under a positive stream of argon. The flask was sealed and heated to 60 °C for 20 minutes. Then, precursor **73** (971 mg,



2.00 mmol, 1.00 eq.) in THF (8 mL) was added dropwise to the stirred suspension and the resulting mixture was heated to 70 °C for 23 hours until TLC monitoring had confirmed complete conversion of **73**. Then, the solution was cooled to r.t. and transferred to a second oven-dried Schlenk tube charged with CuCl (198 mg, 2.00 mmol, 1.00 eq.), rinsing the first flask with THF (1 mL) and transferring the solution once more. ClPCy<sub>2</sub> (0.44 mL, 2.00 mmol, 1.00 eq.) in THF (1.9 mL) was then added, the flask was sealed and heated to 80 °C for 22 hours. After the solution had cooled to room temperature, it was transferred to an Erlenmeyer flask and diluted with Et<sub>2</sub>O (40 mL) and NH<sub>4</sub>OH–sat. aq. NaCl (2:1, 60 mL). The resulting two-phase mixture was stirred at room temperature for 30 minutes and then transferred to a separatory funnel. The organic phase was separated and the aqueous phase was then extracted with Et<sub>2</sub>O (2 $\times$ ). The combined organic phases were washed with NH<sub>4</sub>OH/sat. aq. NaCl (2:1) until the aqueous phase showed no blue color anymore. The combined organic phases were then washed with sat. aq. NaCl (1  $\times$  50 mL), dried (MgSO<sub>4</sub>) and filtered. The solvent was evaporated *in vacuo* and the crude material was recrystallized from hot acetone to afford **L7** (747 mg, 64%) as white solid.

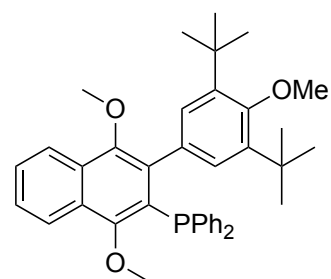
$^1\text{H}$ -NMR (400 MHz,  $\text{C}_6\text{D}_6$ ):  $\delta$  1.14 – 1.48 (m, 10H), 1.54 – 1.79 (m, 8H), 1.59 (s, 18H), 1.83 – 2.02 (m, 2H), 2.20 – 2.36 (m, 2H), 3.35 (s, 3H), 3.55 (s, 3H), 3.84 (s, 3H), 7.29 – 7.37 (m, 2H), 7.39 (s, 2H), 8.14 (d,  $J = 9.4$  Hz, 1H), 8.21 – 8.28 (m, 1H).

$^{31}\text{P}\{^1\text{H}\}$ -NMR (162 MHz,  $\text{C}_6\text{D}_6$ ):  $\delta$  -0.14.

$^{13}\text{C}\{^1\text{H}\}$ -NMR (101 MHz,  $\text{C}_6\text{D}_6$ ):  $\delta$  26.88, 27.22, 27.39 (d,  $J = 7.0$  Hz), 31.74 (d,  $J = 10.9$  Hz), 32.60, 33.29, 33.55, 35.42 (d,  $J = 16.3$  Hz), 36.00, 61.11, 62.42 (d,  $J = 3.1$  Hz), 64.53, 123.72, 126.08, 127.01, 130.14, 130.90, 133.95, 142.32, 150.51, 158.97. Complicated signal-splitting due to C-P coupling.

**HR-MS (EI,  $m/z$ ):** calcd for  $\text{C}_{39}\text{H}_{55}\text{O}_3\text{P}^+$  ( $[\text{M}]^+$ ) 602.3883, found 602.3858.

**AnPhos (L8).** An oven-dried Schlenk tube was dried by heat gun (2 $\times$ ) and evacuated and back-filled with argon (3 $\times$ ). Precursor **73** (400 mg, 824  $\mu\text{mol}$ , 1.00 eq.) and dry and degassed THF (2 mL) was then added under a positive pressure of argon. The resulting solution was cooled to  $-78$   $^\circ\text{C}$  ( $\text{N}_2$ /ethyl acetate) and *n*-BuLi (1.6 M in hexane, 0.51 mL, 824  $\mu\text{mol}$ , 1.00 eq.) was added dropwise. After the resulting solution had stirred at this temperature for one



**L8**

hour,  $\text{Ph}_2\text{PCl}$  (198  $\mu\text{L}$ , 1.07 mmol, 1.30 eq.) was added *via* microsyringe and the reaction mixture was slowly warmed to room temperature overnight. After 21 hours, the reaction was quenched by  $\text{H}_2\text{O}$  (2 mL) and the solution was transferred to a separatory funnel. The aqueous phase was extracted with  $\text{Et}_2\text{O}$  (3 $\times$ ) and the combined organic phases washed with sat. aq.  $\text{NaCl}$  (1 $\times$ ), dried ( $\text{Mg}_2\text{SO}_4$ ), filtered and the solvent removed on a rotary evaporator. The residue was then dissolved in a minimum amount of  $\text{EtOAc}$  and precipitated with  $\text{MeOH}$ . The precipitation process was completed overnight in the freezer ( $-20$   $^\circ\text{C}$ ), and then the formed solids were filtered and washed with  $\text{MeOH}$  to afford **L8** (358 mg, 74%) as off-white solid (containing 4 wt-% of hydrodehalogenated starting material).

$^1\text{H}$ -NMR (400 MHz,  $\text{C}_6\text{D}_6$ ):  $\delta$  1.43 (s, 18H), 3.13 (s, 3H), 3.34 (s, 3H), 3.48 (s, 3H), 6.99 (d,  $J = 6.0$  Hz, 6H), 7.24 – 7.39 (m, 4H), 7.46 (td,  $J = 7.5, 2.0$  Hz, 4H), 8.05 (d,  $J = 8.0$  Hz, 1H), 8.27 (d,  $J = 8.7$  Hz, 1H).

$^{31}\text{P}\{^1\text{H}\}$ -NMR (162 MHz,  $\text{C}_6\text{D}_6$ ):  $\delta$  -11.60.

$^{13}\text{C}\{^1\text{H}\}$ -NMR (101 MHz,  $\text{C}_6\text{D}_6$ )  $\delta$  32.39, 35.88, 60.99, 61.91 (d,  $J_{\text{PC}} = 1.4$  Hz), 64.27, 123.64 (d,  $J_{\text{PC}} = 2.9$  Hz), 126.33, 127.40, 129.27, 129.88 (d,  $J_{\text{PC}} = 3.5$  Hz), 131.28, 132.72 (d,  $J_{\text{PC}} = 7.8$  Hz), 133.68 (d,  $J_{\text{PC}} = 21.2$  Hz), 138.61 (d,  $J_{\text{PC}} = 14.2$  Hz), 142.33, 150.74 (d,  $J_{\text{PC}} = 7.0$  Hz), 157.43, 158.88.

**HR-MS (EI,  $m/z$ ):** calcd for  $\text{C}_{39}\text{H}_{43}\text{O}_3\text{P}^+$  ( $[\text{M}]^+$ ) 590.2944, found 590.2941.

**CyAnPhos ligated (2-aminobiphenyl)palladium(II) methanesulfonate precatalyst complex (84).**

The synthetic procedure was adapted from Buchwald and co-workers.<sup>17</sup>

An oven dried Schlenk tube was charged with L7 (100 mg, 170  $\mu\text{mol}$ , 1.00 eq.) and  $\mu\text{-OMs}$  dimer (62.9 mg, 85.0  $\mu\text{mol}$ , 0.50 eq.) and evacuated and back-filled with argon (3 x). Then, THF (1 mL) was added and the solution was stirred at room temperature for 23 hours. Then, the Schlenk tube was opened to air and pentane (4 mL) was added, causing white solids to precipitate. The Schlenk tube was left in the refrigerator (4  $^{\circ}\text{C}$ ) for a few days to complete precipitation. The colorless solid was then filtered, and washed with pentane to afford **84** (84.3 mg, 52%, structure not confirmed) as colorless solid.

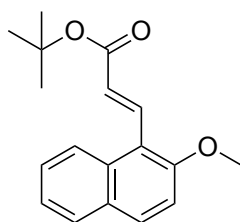
**$^1\text{H-NMR}$  (400 MHz,  $\text{CDCl}_3$ ):**  $\delta$  0.91 – 1.18 (m, 7H), 1.43 (s, 33H), 3.37 (s, 3H), 3.70 (s, 3H), 4.81 (s, 2H), 6.98 (td,  $J = 7.4, 1.5$  Hz, 1H), 7.05 – 7.10 (m, 1H), 7.11 – 7.21 (m, 5H), 7.26 – 7.31 (m, 1H, overlap with deuterated solvent), 7.38 – 7.53 (m, 4H), 7.89 (d,  $J = 8.2$  Hz, 1H), 8.49 (d,  $J = 8.2$  Hz, 1H).

**$^{31}\text{P}\{^1\text{H}\}\text{-NMR}$  (162 MHz,  $\text{CDCl}_3$ ):**  $\delta$  58.59.

#### 4.2.3 Analytical Data of Cross-Coupling Products

##### ***tert*-Butyl (*E*)-3-(2-methoxynaphthalen-1-yl)acrylate (MH-1).**

Synthesis according to GP-6-B. Isolation by flash chromatography ( $\text{SiO}_2$ ; hexane–EtOAc 100:1  $\rightarrow$  50:1).

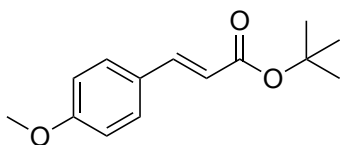


**MH-1**

**$^1\text{H-NMR}$  (500 MHz,  $\text{CDCl}_3$ ):** *major (E)-isomer:*  $\delta$  1.58 (s, 9H), 4.00 (s, 3H), 6.66 (d,  $J = 16.2$  Hz, 1H), 7.28 (d,  $J = 9.1$  Hz, 1H), 7.35 – 7.40 (m, 1H), 7.47 – 7.55 (m, 1H), 7.78 (d,  $J = 8.5$  Hz, 1H), 7.84 (d,  $J = 9.0$  Hz, 1H), 8.20 (d,  $J = 9.7$  Hz, 1H), 8.25 (d,  $J = 16.1$  Hz, 1H).

Known compound. CAS: 1309476-85-4. The analytical data is in accordance with the literature.<sup>156</sup>

***tert*-Butyl (*E*)-3-(4-methoxyphenyl)acrylate (MH-4).**



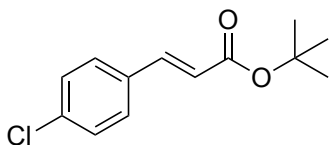
**MH-4**

Synthesis according to GP-6-B. Isolation by flash chromatography (SiO<sub>2</sub>; hexane–EtOAc 20:1).

**<sup>1</sup>H-NMR (500 MHz, CDCl<sub>3</sub>):**  $\delta$  1.53 (s, 9H), 3.83 (s, 3H), 6.24 (d,  $J$  = 15.9 Hz, 1H), 6.89 (d,  $J$  = 8.8 Hz, 2H), 7.45 (d,  $J$  = 8.8 Hz, 2H), 7.54 (d,  $J$  = 15.9 Hz, 1H).

Known compound. CAS: 53484-52-9. The analytical data is in accordance with the literature.<sup>156</sup>

***tert*-Butyl (*E*)-3-(4-chlorophenyl)acrylate (MH-5).**



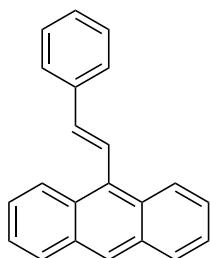
**MH-5**

Synthesis according to GP-6-B. Isolation by flash chromatography (SiO<sub>2</sub>; hexane).

**<sup>1</sup>H-NMR (500 MHz, CDCl<sub>3</sub>):**  $\delta$  1.53 (s, 9H), 6.34 (d,  $J$  = 16.1 Hz, 1H), 7.34 (d,  $J$  = 8.5 Hz, 2H), 7.43 (d,  $J$  = 8.5 Hz, 2H), 7.53 (d,  $J$  = 16.0 Hz, 1H).

Known compound. CAS: 125950-99-4. The analytical data is in accordance with the literature.<sup>157</sup>

**(*E*)-9-Styrylanthracene (MH-6).**



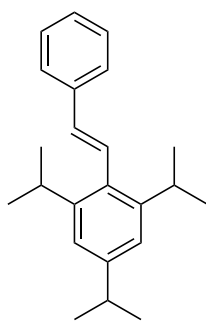
**MH-6**

Synthesis according to GP-6-B. Isolation by flash chromatography (SiO<sub>2</sub>; hexane).

**<sup>1</sup>H-NMR (500 MHz, CDCl<sub>3</sub>):** *major (E)-isomer:*  $\delta$  6.97 (d,  $J$  = 16.6 Hz, 1H), 7.34 – 7.40 (m, 1H), 7.42 – 7.51 (m, 6H), 7.69 (d,  $J$  = 6.9 Hz, 2H), 7.93 (d,  $J$  = 16.6 Hz, 1H), 7.98 – 8.06 (m, 2H), 8.33 – 8.39 (m, 2H), 8.42 (s, 1H).

Known compound. CAS: 42196-97-4. The analytical data is in agreement with the literature.<sup>158</sup>

**(E)-1,3,5-Triisopropyl-2-styrylbenzene (MH-7).**



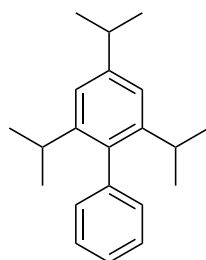
**MH-7**

Synthesis according to GP-6-B. Isolation by flash chromatography (SiO<sub>2</sub>; hexane).

**<sup>1</sup>H-NMR (500 MHz, CDCl<sub>3</sub>):** *major (E)-isomer:*  $\delta$  1.22 (d,  $J = 6.8$  Hz, 12H), 1.29 (d,  $J = 6.9$  Hz, 6H), 2.92 (hept,  $J = 6.9$  Hz, 1H), 3.29 (hept,  $J = 6.9$  Hz, 2H), 6.50 (d,  $J = 16.5$  Hz, 1H), 7.04 (s, 2H), 7.20 (d,  $J = 16.6$  Hz, 1H), 7.26 (s, 1H), 7.27 – 7.31 (m, 1H), 7.39 (t,  $J = 7.7$  Hz, 2H), 7.51 (d,  $J = 6.9$  Hz, 2H).

Known compound. CAS: 100103-94-4. The analytical data is in agreement with the literature.<sup>159</sup>

**2,4,6-Triisopropyl-1,1'-biphenyl (K-2).**



**K-2**

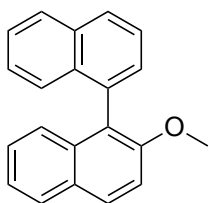
Synthesis according to GP-7. Isolation by column chromatography (SiO<sub>2</sub>; hexane).

**<sup>1</sup>H-NMR (400 MHz, CDCl<sub>3</sub>):**  $\delta$  1.08 (d,  $J = 6.9$  Hz, 12H), 1.31 (d,  $J = 6.9$  Hz, 6H), 2.60 (hept,  $J = 6.9$  Hz, 2H), 3.03 – 2.87 (m, 1H), 7.06 (s, 2H), 7.18 (d,  $J = 7.9$  Hz, 2H), 7.44 – 7.30 (m, 3H).

**<sup>13</sup>C{<sup>1</sup>H} -NMR (101 MHz, CDCl<sub>3</sub>):**  $\delta$  24.23, 24.36, 30.40, 34.41, 120.65, 126.52, 128.03, 129.96, 137.22, 141.02, 146.65, 147.96.

Known compound. CAS: 76804-34-7. The analytical data is in accordance with the literature.<sup>160</sup>

**2-Methoxy-1,1'binaphthalene (60/SM-1).**



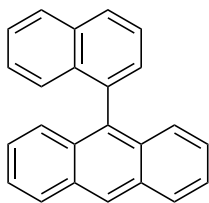
**60**

Synthesis according to GP-5 or GP-10. Isolation by column chromatography (SiO<sub>2</sub>; hexane–EtOAc 100:1).

**<sup>1</sup>H-NMR (500 MHz, CDCl<sub>3</sub>):**  $\delta$  3.76 (s, 3H), 7.13 – 7.18 (m, 1H), 7.20 – 7.25 (m, 1H), 7.27 – 7.39 (m, 4H), 7.41 – 7.49 (m, 3H), 7.62 (dd,  $J$  = 8.3, 6.9 Hz, 1H), 7.87 (d,  $J$  = 8.2 Hz, 1H), 7.95 (dd,  $J$  = 8.3, 5.0 Hz, 2H), 7.99 (d,  $J$  = 9.1 Hz, 1H).

Known compound. CAS 93603-10-2. The analytical data is in agreement with the literature.<sup>128</sup>

**9-(1-Naphthyl)anthracene (SM-2).**



**SM-2**

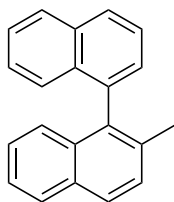
Synthesis according to GP-10. Isolation by column chromatography (hexane → hexane–EtOAc 20:1).

**<sup>1</sup>H NMR (400 MHz, CDCl<sub>3</sub>):**  $\delta$  7.07 (d,  $J$  = 8.5 Hz, 1H), 7.15 – 7.26 (m, 3H), 7.36 – 7.49 (m, 5H), 7.52 (d,  $J$  = 7.0 Hz, 1H), 7.65 – 7.73 (m, 1H), 8.00 (d,  $J$  = 8.3 Hz, 1H), 8.05 (d,  $J$  = 8.2 Hz, 1H), 8.10 (d,  $J$  = 8.5 Hz, 2H), 8.59 (s, 1H).

**<sup>13</sup>C{<sup>1</sup>H} -NMR (101 MHz, CDCl<sub>3</sub>):**  $\delta$  125.32, 125.63, 125.68, 126.10, 126.37, 126.69, 127.06, 128.23, 128.35, 128.53, 129.24, 131.13, 131.55, 133.64, 133.83, 135.08, 136.64.

Known compound. CAS 7424-70-6. The analytical data is in agreement with the literature.<sup>128</sup>

### 2-Methyl-1,1'-binaphthalene (SM-3).



**SM-3**

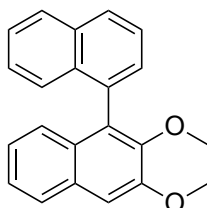
Synthesis according to GP-10. Isolation by column chromatography (hexane).

**<sup>1</sup>H-NMR (500 MHz, CDCl<sub>3</sub>):**  $\delta$  2.11 (s, 3H), 7.13 – 7.17 (m, 1H), 7.19 – 7.31 (m, 3H), 7.35 – 7.42 (m, 2H), 7.44 – 7.52 (m, 2H), 7.61 (dd,  $J = 8.3, 7.0$  Hz, 1H), 7.88 (dd,  $J = 8.4, 3.0$  Hz, 2H), 7.95 (d,  $J = 8.3$  Hz, 2H).

Known compound. CAS 69363-30-0. The analytical data is in accordance with the literature.<sup>128</sup>

### 2,3-Dimethoxy-1,1'-binaphthalene (SM-4).

Synthesis according to GP-10. Isolation by column chromatography (hexane–EtOAc 100:1).



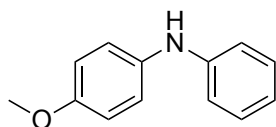
**SM-4**

**<sup>1</sup>H-NMR (500 MHz, CDCl<sub>3</sub>):**  $\delta$  3.53 (s, 3H), 4.07 (s, 3H), 7.04 – 7.14 (m, 2H), 7.26 – 7.30 (m, 1H), 7.31 (s, 1H), 7.33 – 7.40 (m, 2H), 7.43 – 7.51 (m, 2H), 7.61 (dd,  $J = 8.2, 7.0$  Hz, 1H), 7.79 (d,  $J = 8.3$  Hz, 1H), 7.94 (d,  $J = 8.2$  Hz, 1H), 7.96 (d,  $J = 8.2$  Hz, 1H).

Known compound. CAS 222555-03-5. The analytical data is in accordance with the literature.

161

### 4-Methoxy-*N*-phenylaniline (BH-1).



**BH-1**

Synthesis according to GP-11. Purification by column chromatography (SiO<sub>2</sub>; hexane–EtOAc 40:1).

**<sup>1</sup>H-NMR (400 MHz, CDCl<sub>3</sub>):**  $\delta$  3.81 (s, 3H), 5.49 (s, 1H), 6.80 – 6.94 (m, 5H), 7.08 (d,  $J = 8.9$  Hz, 2H), 7.22 (t,  $J = 7.9$  Hz, 2H).

$^{13}\text{C}\{^1\text{H}\}$  -NMR (101 MHz,  $\text{CDCl}_3$ ):  $\delta$  55.73, 114.82, 115.79, 119.71, 122.36, 127.94, 128.56, 129.45, 135.87, 145.32, 155.44.

Known compound. CAS 1208-86-2. The analytical data is in agreement with the literature.<sup>162</sup>



## **5 Appendix**

## 5.1 Glossary

(q)NMR	(quantitative) nuclear magnetic resonance
acac	acetylacetonate
Ad	adamantyl
aq.	aqueous (solution)
Ar	aryl
CC	column chromatography
Cy	cyclohexyl
d	days
d1	relaxation delay
DACH	diaminocyclohexane
DCM	dichloroethane
dme	dimethoxy ethane
DMF	dimethylformamide
e.r.	enantiomeric ratio
EI	electron ionization
<i>et al</i>	et alii
GC	gas chromatography
h	hours
HPLC	high performance liquid chromatography
HR	high resolution
Hz	Hertz
<i>i</i> Pr	isopropyl
<i>J</i>	coupling constant
<i>m</i>	meta
Me	methyl
Men	menthyl ( (1 <i>R</i> ,2 <i>S</i> ,5 <i>R</i> )-2-isopropyl-5-methyl-cyclohex-1-yl )
min	minutes
MS	mass spectrometry
<i>n</i> -Bu	<i>n</i> -butyl
<i>o</i>	ortho

o1p	center of spectrum
<i>p</i>	para
Ph	phenyl
ppm	parts per million
RT	room temperature
sat.	saturated
sw	spectral width
T	temperature
t	time
<i>t</i> Bu	tertiary butyl
Tf	trifluoromethane sulfonate
THF	tetrahydrofuran
TLC	thin layer chromatography
Ts	toluene sulfonate
UV	ultraviolet
wt.	weight

## 5.2 Crystallographic Data

### 5.2.1 *Sample and crystal Data for (1,3-Bis(dimethylphosphanyl)propane- $\kappa^2P,P'$ )palladium(II) Chloride (27)*

Identification code	ReiKa3 AP8780-100
Chemical Formula	C <sub>43</sub> H <sub>82</sub> Cl <sub>2</sub> P <sub>2</sub> Pd
Formula weight	838.38
Temperature	100(2) K
Wavelength	0.71073 Å
Crystal size	0.120 × 0.130 × 0.350 mm
Crystal habit	Clear yellow plate
Crystal system	Orthorhombic
Space group	P2(1)2(1)2(1)
Unit cell dimensions	a = 14.0238(9) Å b = 14.3605(10) Å c = 22.1564(14) Å
Volume	4462.1(5) Å <sup>3</sup>
Z	4
Density (calculated)	1.248 g/cm <sup>3</sup>
Absorption coefficient	0.635 mm <sup>-1</sup>
F(000)	1800

5.2.2 *Sample and crystal data for [ $\{(\text{Men}_2\text{P}-\text{O}-\text{H}-\text{O}-\text{PMen}_2-\kappa^2\text{P},\text{P}')\text{Pd}\}_2(\mu\text{-Cl})_2$ ]*  
**(30)**

Identification code	ReiKa7
Chemical Formula	$\text{C}_{92}\text{H}_{166}\text{Cl}_2\text{O}_4\text{P}_4\text{Pd}_2$
Formula weight	1743.82
Temperature	100(2) K
Wavelength	0.71073 Å
Crystal size	0.172 × 0.281 × 0.358 mm
Crystal habit	clear yellow fragment
Crystal system	triclinic
Space group	P1
Unit cell dimensions	a = 12.3896(16) Å b = 15.105(2) Å c = 15.259(2) Å
Volume	2333.6(5) Å <sup>3</sup>
Z	1
Density (calculated)	1.241 g/cm <sup>3</sup>
Absorption coefficient	0.557 mm <sup>-1</sup>
F(000)	936

### 5.2.3 *Sample and crystal data for KatPhos (L6)*

Identification code	ReiKa4
Chemical Formula	C <sub>39</sub> H <sub>55</sub> O <sub>2</sub> P
Formula weight	586.83
Temperature	100(2) K
Wavelength	0.71073 Å
Crystal size	0.042 × 0.085 × 0.120 mm
Crystal habit	clear colourless fragment
Crystal system	triclinic
Space group	P1
Unit cell dimensions	a = 10.918(4) Å b = 17.075(4) Å c = 19.651(6) Å
Volume	3461.(3) Å <sup>3</sup>
Z	2
Density (calculated)	1.135 g/cm <sup>3</sup>
Absorption coefficient	0.112 mm <sup>-1</sup>
F(000)	1280

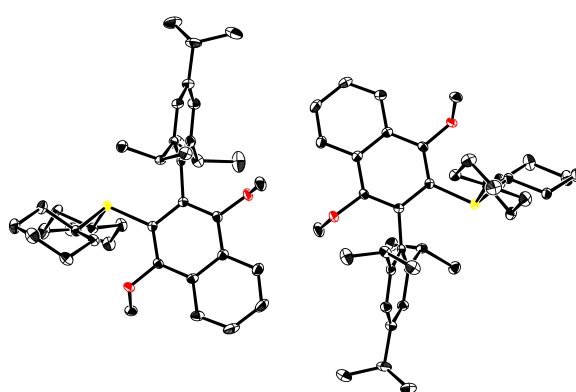


**Figure 21.** Solid-state molecular structure of **L6**. Ellipsoids are shown at 50% probability. Hydrogens are omitted for clarity.

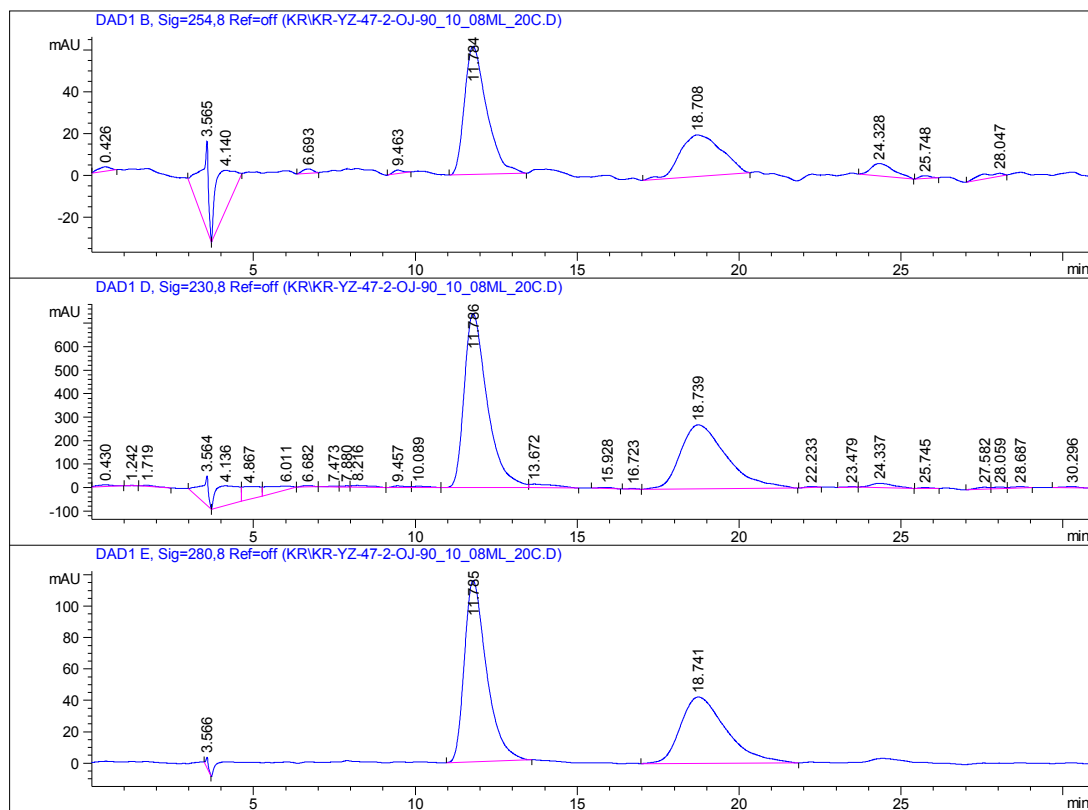
## 5.3 Chiral HPLC Chromatograms

### 5.3.1 Chromatograms for 2-Methoxy-binaphthyl

Exemplary chromatograms of the chiral HPLC analysis are presented in the following. Enantiomeric ratios were determined by comparing areas of both enantiomer peaks at  $\lambda = 280$  nm. Area percent reports for other wavelength are omitted.

#### **L1 (MenJohnPhos)**

Acq. Operator : SYSTEM  
 Sample Operator : SYSTEM  
 Acq. Instrument : Analytische HPLC Location : Vial 3  
 Injection Date : 12/16/2020 4:19:39 PM Inj. Volume : 5.000  $\mu$ l  
 Method : C:\CHEM82\1\METHODS\CD\_KATJA.M  
 Last changed : 12/16/2020 2:48:38 PM by SYSTEM  
 (modified after loading)  
 Sample Info : QJ, iso-hexane/iPrCH 90/10, 0.8 mL/min, 20 °C



Signal 3: DAD1 E, Sig=280,8 Ref=off

Peak #	Ret Time [min]	Type	Width [min]	Area [mAU*s]	Height [mAU]	Area %
1	3.566	BB	0.0752	33.16917	6.53520	0.3428
2	11.785	BB	0.7229	5506.60742	115.35451	56.9072
3	18.741	BB	1.3918	4136.69629	42.26605	42.7500

Total s : 9676.47289 164.15575

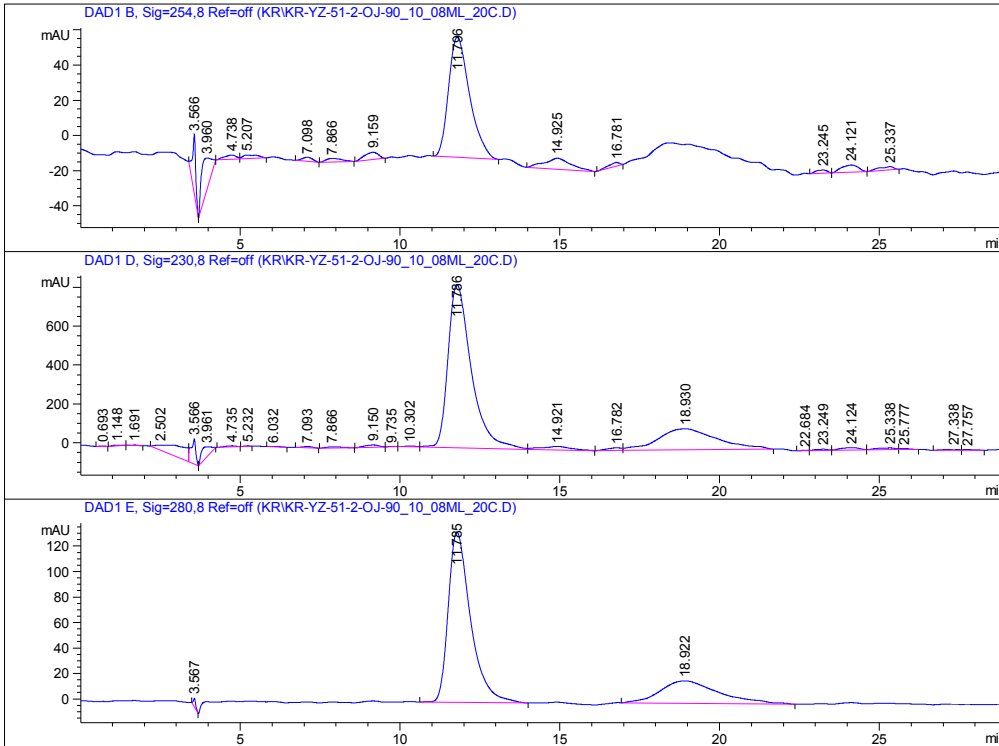
\*\*\* End of Report \*\*\*

# L3 (1-Chlorophenyl)dimenthylphosphine (Condition GP-5-A)

```

=====
Acq. Operator   : SYSTEM
Sample Operator : SYSTEM
Acq. Instrument : Analytische HPLC           Location : Vial 1
Injection Date  : 12/16/2020 3:16:59 PM
                                           Inj Volume : 5.000 µl

Method         : C:\Q-HEM82\1\METHODS\CD_KATJA.M
Last changed   : 12/16/2020 2:48:38 PM by SYSTEM
                (modified after loading)
Sample Info    : QJ, iso-hexane/iPrOH 90/10, 0.8 mL/min, 20 °C
    
```



Signal 3: DAD1 E, Sig=280,8 Ref=off

Peak #	Retention Time [min]	Type	Width [min]	Area [mAU*s]	Height [mAU]	Area %
1	3.567	BB	0.0778	35.52628	6.93428	0.4038
2	11.785	BB	0.7296	6506.12354	133.73264	73.9484
3	18.922	BB	1.5232	2256.54590	17.58403	25.6478

Totals : 8798.19571 158.25094

\*\*\* End of Report \*\*\*



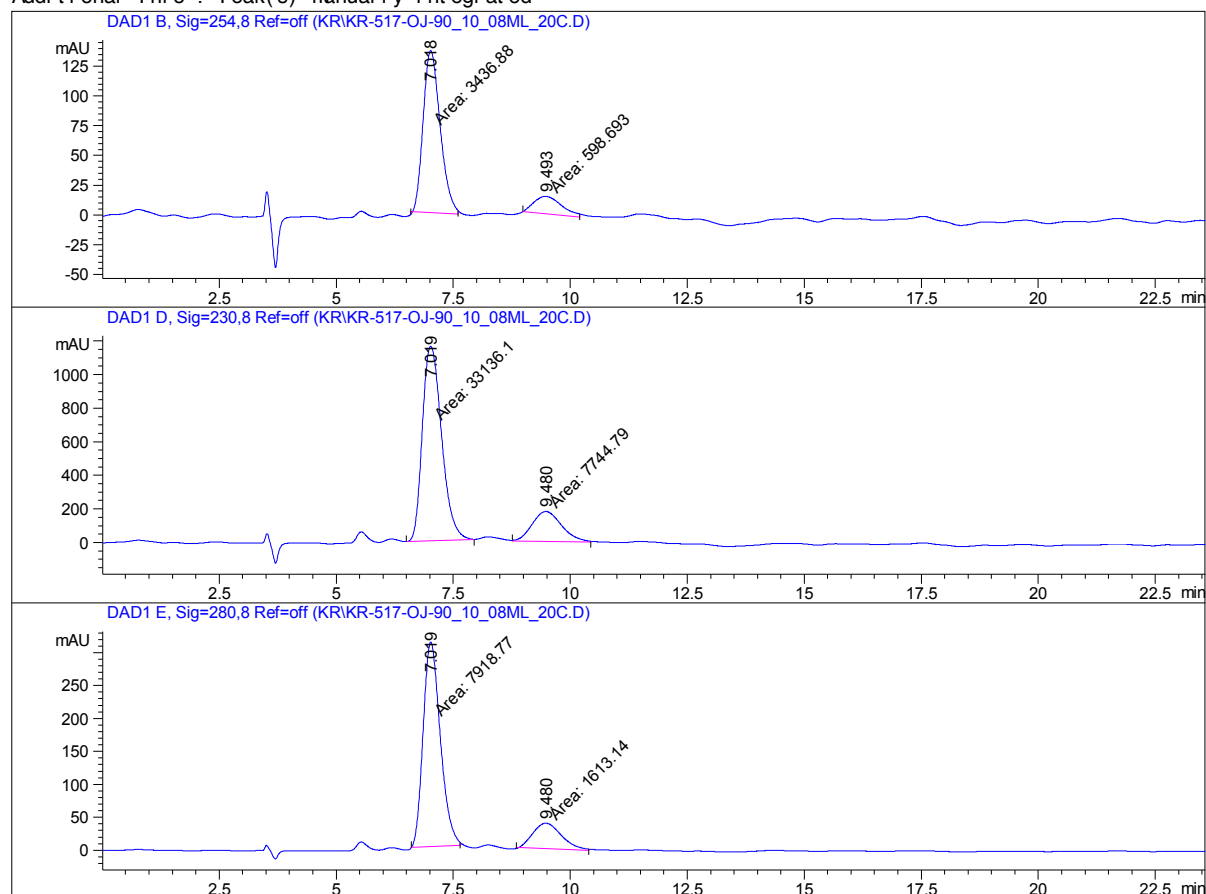
## 7.2.2 Chromatograms for 2-Methyl-binaphthyl

```

=====
Acq. Operator   : SYSTEM
Sample Operator : SYSTEM
Acq. Instrument : Analytische HPLC           Location : Vial 2
Injection Date  : 2/25/2021 2:41:13 PM      Inj Volume : 5.000 µl

Acq. Method     : C:\CHEM82\1\METHODS\CD_KATJA.M
Last changed    : 2/25/2021 1:36:18 PM by SYSTEM
                  (modified after Loading)
Analysis Method : C:\CHEM82\1\METHODS\CD_KATJA.M
Last changed    : 12/16/2020 4:52:36 PM by SYSTEM
Sample Info     : OJ, iso-hexane/iPrCH 90/10, 0.8 mL/min, 20 °C
  
```

Additional Info : Peak(s) manually integrated



Signal 3: DAD1 E, Sig=280,8 Ref=off

Peak #	Retention [min]	Type	Width [min]	Area [mAU*s]	Height [mAU]	Area %
1	7.019	MM T	0.4255	7918.76660	310.20303	83.0764
2	9.480	MM T	0.7012	1613.14172	38.34501	16.9236

Totals :                                    9531.90833    348.54804

\*\*\* End of Report \*\*\*



### 7.3 Exemplary $^1\text{H}$ -qNMR Analysis

Figure 22 shows an excerpt of an exemplary  $^1\text{H}$ -qNMR spectrum for the  $\text{Pd}(\text{OAc})_2/\text{MenSPhos}$  catalyzed *Suzuki-Miyaura* coupling of 4-chloro anisole **47** and phenyl boronic acid **48**.

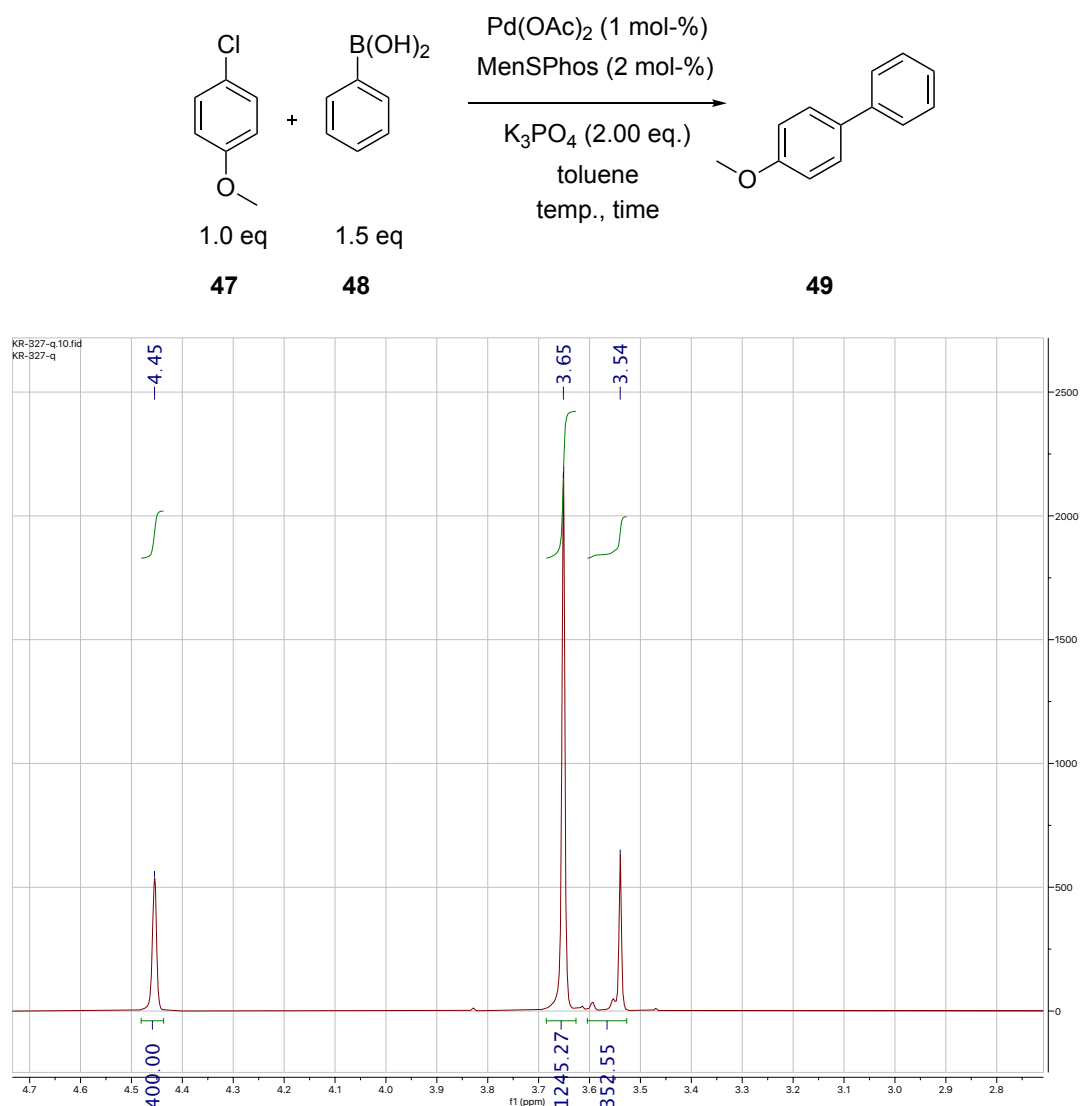


**Figure 22.** Excerpt of the  $^1\text{H}$ -NMR spectrum for the qNMR analysis of the  $\text{Pd}(\text{OAc})_2/\text{MenSPhos}$  catalyzed coupling of **47** and **48**.

The peak at  $\delta_{\text{H}} 4.45$  can be assigned to the 4 benzylic protons of internal standard dibenzyl ether, therefore its integral is set to 400 (integral values are multiplied by 100 for a more accurate analysis). The signal at  $\delta_{\text{H}} 3.65$  is assigned to the target material. The amount of target material present in the sample is calculated by the formula:

$$n_a = \frac{I_a}{N_{\text{prot}} \cdot 100} \cdot n_{\text{IS}} \quad (\text{eqn. 1})$$

where  $n_a$  = amount of the analyte /mmol,  $N_{\text{prot}}$  = number of analyte protons,  $I_a$  = integral of analyte peak and  $n_{\text{IS}}$  = amount of the internal standard /mmol.

In this case,  $N_{\text{prot}} = 3$  (corresponding to three methoxy protons of the target material) and  $n_{\text{IS}} = 209.8 \mu\text{mol}$ , which results in a calculated amount of target material  $n_a = 870 \mu\text{mol}$ .

## 7.4 References

- <sup>1</sup> D. W. Old, J. P. Wolfe, S. L. Buchwald, A Highly Active Catalyst for Palladium-Catalyzed Cross-Coupling Reactions: Room-Temperature Suzuki Couplings and Amination of Unactivated Aryl Chlorides, *J. Am. Chem. Soc.* **1998**, *120*, 9722-9723.
- <sup>2</sup> B. T. Ingoglia, C. C. Wagen, S. L. Buchwald, Biaryl monophosphine ligands in palladium-catalyzed C-N coupling: An updated User's guide, *Tetrahedron* **2019**, *75*, 4199-4211.
- <sup>3</sup> T. E. Barder, S. L. Buchwald, Rationale Behind the Resistance of Dialkylbiaryl Phosphines toward Oxidation by Molecular Oxygen, *J. Am. Chem. Soc.* **2007**, *129*, 5096-5101.
- <sup>4</sup> U. Christmann, R. Vilar, Monoligated Palladium Species as Catalysts in Cross-Coupling Reactions, *Angew. Chem. Int. Ed.* **2005**, *44*, 366-374.
- <sup>5</sup> S. D. Walker, T. E. Barder, J. R. Martinelli, S. L. Buchwald, A Rationally Designed Universal Catalyst for Suzuki-Miyaura Coupling Processes, *Angew. Chem. Int. Ed.* **2004**, *43*, 1871-1876.
- <sup>6</sup> J. P. Wolfe, R. A. Singer, B.; R. Martin; S. L. Buchwald, Palladium-Catalyzed Suzuki-Miyaura Cross-Coupling Reactions Employing Dialkylbiaryl Phosphine Ligands, *Acc. Chem. Res.* **2008**, *41*, 1461-1473.
- <sup>7</sup> J. F. Hartwig, Electronic Effects on Reductive Elimination To Form Carbon-Carbon and Carbon-Heteroatom Bonds from Palladium(II) Complexes, *Inorg. Chem.* **2007**, *46*, 1936-1947.
- <sup>8</sup> P. L. Arrechea, S. L. Buchwald, Biaryl Phosphine Based Pd(II) Amido Complexes: The Effect of Ligand Structure und Reductive Elimination. *J. Am. Chem. Soc.* **2016**, *138*, 12486-12493.
- <sup>9</sup> E. P. K. Olsen, P. L. Arrechea, S. L. Buchwald, Mechanistic Insight Leads to a Ligand Which Facilitates the Palladium-Catalyzed Formation of 2-(Hetero)Arylaminoxazoles and 4-(Hetero)Arylaminothiazoles, *Angew. Chem. Int. Ed.* **2017**, *56*, 10569-10572.
- <sup>10</sup> B. P. Fors, D. A. Watson, M. R. Biscoe, S. L. Buchwald, A Highly Active Catalyst for Pd-Catalyzed Amination Reactions: Cross-Coupling Reactions Using Aryl Mesylates and the Highly Selective Monoarylation of Primary Amines Using Aryl Chlorides, *J. Am. Chem. Soc.* **2008**, *130*, 13552-13554.
- <sup>11</sup> E. R. Strieter, S. L. Buchwald, Evidence for the Formation and Structure of Palladacycles during Pd-Catalyzed C-N Bond Formation with Catalysts Derived from Bulky Monophosphinobiaryl Ligands, *Angew. Chem. Int. Ed.* **2006**, *45*, 925-928.

- <sup>12</sup> R. Martin, S. L. Buchwald, Pd-Catalyzed Kumada-Corriu Cross-Coupling Reactions at Low Temperatures Allow the Use of Knochel-Type Reagents, *J. Am. Chem. Soc.* **2007**, *129*, 2844-3845.
- <sup>13</sup> J. E. Milne, S. L. Buchwald, An Extremely Active Catalyst for the Negishi Cross-Coupling Reaction, *J. Am. Chem. Soc.* **2004**, *126*, 13028-13032.
- <sup>14</sup> J. P. Wolfe, S. L. Buchwald, A Highly Active Catalyst for The Room-Temperature Amination and Suzuki Coupling of Aryl Chlorides, *Angew. Chem. Int. Ed.* **1999**, *38*, 2413-2416.
- <sup>15</sup> A. C. Sather, H. G. Lee, V. Y. De La Rosa, Y. Yang, P. Müller, S. L. Buchwald, A Fluorinated Ligand Enables Room-Temperature and Regioselective Pd-Catalyzed Fluorination of Aryl Triflates and Bromides, *J. Am. Chem. Soc.* **2015**, *41*, 13433-13438.
- <sup>16</sup> J. M. Dennis, N. A. White, R. Y. Liu, S. L. Buchwald, Breaking the Base Barrier: An Electron-Deficient Palladium Catalyst Enables the Use of a Common Soluble Base in C-N Coupling, *J. Am. Chem. Soc.* **2018**, *140*, 4721-4725.
- <sup>17</sup> N. C. Bruno, M. T. Tudge, S. L. Buchwald, Design and preparation of new palladium precatalysts for C-C and C-N cross-coupling reactions, *Chem. Sci.* **2013**, *4*, 916-920.
- <sup>18</sup> M. Su, S. L. Buchwald, A Bulky Biaryl Phosphine Ligand Allows for Palladium-Catalyzed Amidation of Five-Membered Heterocycles as Electrophiles, *Angew. Chem. Int. Ed.* **2012**, *51*, 4710-4713.
- <sup>19</sup> B. P. Fors, K. Dooleweerd, Q. Zeng, S. L. Buchwald, An Efficient System for the Pd-Catalyzed Cross-Coupling of Amides and Aryl Chlorides, *Tetrahedron* **2009**, *65*, 6576-6583.
- <sup>20</sup> N. Hoshiya, S. L. Buchwald, An Improved Synthesis of BrettPhos- and RockPhos-Type Biarylphosphine Ligands, *Adv. Synth. Catal.* **2012**, *354*, 2031-2037.
- <sup>21</sup> T. E. Barder, S. D. Walker, J. R. Martinelli, S. L. Buchwald, Catalysts for Suzuki-Miyaura Coupling Processes: Scope and Studies of the Effect of Ligand Structure, *J. Am. Chem. Soc.* **2005**, *127*, 4685-4696.
- <sup>22</sup> W. Tang, A. G. Capacci, X. Wei, W. Li, A. White, N. D. Patel, J. Savoie, J. J. Gao, S. Rodriguez, B. Qu, N. Haddad, B. Z. Lu, D. Krishnamurthy, N. K. Yee, C. H. Senanayake, A General and Special Catalyst for Suzuki-Miyaura Coupling Processes, *Angew. Chem. Int. Ed.* **2010**, *49*, 5879-5883.
- <sup>23</sup> S. Rodriguez, B. Qu, N. Haddad, D. C. Reeves, W. Tang, H. Lee, D. Krishnamurthy, C. H. Senanayake, Oxaphosphole-Based Monophosphorus Ligands for Palladium-Catalyzed Amination Reactions, *Adv. Synth. Catal.* **2011**, *353*, 533-537.

- <sup>24</sup> W. Tang, S. Keshipeddy, Y. Zhang, X. Wei, J. Savoie, N. D. Patel, N. K. Yee, C. H. Senanayake, Efficient Monophosphorus Ligands for Palladium-Catalyzed Miyaura Borylation, *Org. Lett.* **2011**, *13*, 1366-1369.
- <sup>25</sup> N. D. Patel, J. D. Sieber, S. Tcyrulnikov, B. J. Simmons, D. Rivalti, K. Duvvuri, Y. Zhang, D. A. Gao, K. R. Fandrick, N. Haddad, K. So Lao, H. P. R. Mangunuru, S. Biswas, B. Qu, N. Grinberg, S. Pennino, H. Lee, J. J. Song, B. F. Gupton, N. K. Garg, M. C. Kozlowski, C. H. Senanayake, Computationally Assisted Mechanistic Investigation and Development of Pd-Catalyzed Asymmetric Suzuki-Miyaura and Negishi Cross-Coupling Reactions for Tetra-ortho-Substituted Biaryl Synthesis, *ACS Catal.* **2018**, *8*, 10190-10209.
- <sup>26</sup> W. Tang, B. Qu, A. G. Capacci, S. Rodriguez, X. Wei, N. Haddad, B. Narayanan, S. Ma, N. Grinberg, N. K. Yee, D. Krishnamurthy, C. H. Senanayake, Novel, Tunable, and Efficient Chiral Bisdihydrobenzoxaphosphole Ligands for Asymmetric Hydrogenation, *Org. Lett.* **2010**, *12*, 176-179.
- <sup>27</sup> J. D. Laffoon, V. S. Chan, M. G. Fickes, B. Kotecki, A. R. Ickes, J. Henle, J. G. Napolitano, T. S. Franczyk, T. B. Dunn, D. M. Barnes, A. R. Haight, R. F. Henry, S. Shekhar, Pd-Catalyzed Cross-Coupling Reactions Promoted by Biaryl Phosphorinane Ligands, *ACS Catal.* **2019**, *9*, 11691-11708.
- <sup>28</sup> R. C. Smith, R. A. Woloszynek, W. Chen, T. Ren, J. D. Protasiewicz, Suzuki reactions catalyzed by palladium complexes bearing the bulky (2,6-dimesitylphenyl)dimethylphosphine, *Tetrahedron. Lett.* **2004**, *45*, 8327-8330.
- <sup>29</sup> M. Marín, J. J. Moreno, M. M. Alcaide, E. Álvarez, J. López-Serrano, J. Campos, M. C. Nicasio, E. Carmona, Evaluating stereoelectronic properties of bulky dialkylterphenyl phosphine ligands, *J. Organomet. Chem.* **2019**, *896*, 120-128.
- <sup>30</sup> R. J. Rama, C. Maya, M.C. Nicasio, Dialkylterphenyl Phosphine-Based Palladium Precatalysts for Efficient Aryl Amination of *N*-Nucleophiles, *Chem. Eur. J.* **2020**, *26*, 1064-1073.
- <sup>31</sup> L. Ortega-Moreno, M. Fernández-Espada, J. J. Moreno, C. Navarro-Gilabert, J. Campos, S. Conejero, J. López-Serrano, C. Maya, R. Peloso, E. Carmona, Synthesis, Properties, and Some Rhodium, Iridium, and Platinum Complexes of a Series of Bulky *m*-Terphenyl Phosphine Ligands, *Polyhedron* **2016**, *116*, 170-181.
- <sup>32</sup> E. Urnézius, J. D. Protasiewicz, Synthesis and Structural Characterization of New Hindered Aryl Phosphorus Centers (Aryl = 2,6-Dimesitylphenyl), *Main Group Chem.* **1996**, *1*, 369-372.

- <sup>33</sup> O. M. Demchuk, B. Yoruk, T. Blackburn, V. Snieckus, A Mixed Naphthyl-Phenyl Phosphine Ligand Motif for Suzuki, Heck, and Hydrodehalogenation Reactions, *Synlett* **2006**, *18*, 2908-2913.
- <sup>34</sup> O. M. Demchuk, K. Kielar, K. M. Pietrusiewicz, Rational design of novel ligands for environmentally benign cross-coupling reactions, *Pure Appl. Chem.* **2011**, *83*, 633-644.
- <sup>35</sup> O.M. Demchuk, K. Kaplon, L. Mazur, D. Strzelecka, K.M. Pietrusiewicz, Readily available catalysts for demanding Suzuki-Miyaura couplings under mild conditions, *Tetrahedron* **2016**, *72*, 6668-6677.
- <sup>36</sup> T. Achard, Advances in Homogeneous Catalysis Using Secondary Phosphine Oxides (SPOs): Pre-ligands for Metal Complexes, *CHIMIA* **2016**, *70*, 8-19.
- <sup>37</sup> A. Christiansen, C. Li, M. Garland, D. Selent, R. Ludwig, A. Spannenberg, W. Baumann, R. Franke, A. Börner, On the Tautomerism of Secondary Phosphine Oxides, *Eur. J. Org. Chem.* **2010**, 2733-2741.
- <sup>38</sup> D. Martin, D. Moraleda, T. Achard, L. Giordano, G. Buono, Assessment of the Electronic Properties of P ligands Stemming from Secondary Phosphine Oxides, *Chem. Eur. J.* **2011**, *17*, 12729-12740.
- <sup>39</sup> A. Gallen, A. Riera, X. Verdager, A. Grabulosa, Coordination chemistry and catalysis with secondary phosphine oxides, *Catal. Sci. Technol.* **2019**, *9*, 5504-5561.
- <sup>40</sup> P. W. N. M. van Leeuwen, C.F. Roobeek, R. L. Wife, J. H. G. Frijns, Platinum hydroformylation catalysts containing diphenylphosphine oxide ligands, *J.Chem. Soc., Chem. Commun.* **1986**, 31-33.
- <sup>41</sup> G. Y. Li, The First Phosphine Oxide Ligand Precursors for Transition Metal Catalyzed Cross-Coupling Reactions: C-C, C-N, and C-S Bond formation on Unactivated Aryl Chlorides, *Angew. Chem. Int. Ed.* **2001**, *40*, 1513-1516.
- <sup>42</sup> G.Y. Li, G. Zheng, A. F. Noonan, Highly Active, Air-Stable Versatile Palladium Catalysts for the C-C, C-N, and C-S Bond Formations via Cross-Coupling Reactions of Aryl Chlorides, *J. Org. Chem.* **2001**, *66*, 8677-8681.
- <sup>43</sup> C. Wolf, R. Lerebours, Use of Highly Active Palladium-Phosphinous Acid Catalysts in Stille, Heck, Amination, and Thiation Reactions of Chloroquinolines, *J. Org. Chem.* **2003**, *68*, 7077-7084.
- <sup>44</sup> L. Ackermann, R. Vicente, N. Hofmann, Air-Stable Secondary Phosphine Oxide as Preligand for Palladium-Catalyzed Intramolecular  $\alpha$ -Arylations with Chloroarenes, *Org. Lett.* **2009**, *11*, 4274-4276.

- <sup>45</sup> L. Ackermann, S. Barfüsser, C. Kornhaass, A. R. Kapdi, C-H Bond Arylations and Benzylations on Oxazol(in)es with a Palladium Catalyst of a Secondary Phosphine Oxide, *Org. Lett.* **2011**, *13*, 3082-3085.
- <sup>46</sup> L. Ackermann, H. K. Potukuchi, A. R. Kapdi, C. Schulzke, Kumada-Corriu Cross-Couplings with 2-Pyridyl Grignard Reagents, *Chem. Eur. J.* **2010**, *16*, 3300-3303.
- <sup>47</sup> L. Ackermann, R. Born, Modulare Diamino- und Dioxophosphanoxide und -chloride als Liganden in übergangsmetallkatalysierten C-C- und C-N-Kupplungen von Arylchloriden, *Angew. Chem.* **2005**, *117*, 2497-2500.
- <sup>48</sup> L. Ackermann, R. Born, J. H. Spitz, A. Althammer, C. J. Gschrei, Air-stable phosphine oxides as preligands for catalytic activation reactions of C-Cl, C-F, and C-H bonds, *Pure Appl. Chem.* **2009**, *78*, 209-214.
- <sup>49</sup> L. Ackermann, A. R. Kapdi, S. Fenner, C. Kornhaass, C. Schulzke, Well-Defined Air-Stable Palladium HASPO Complexes for Efficient Kumada-Corriu Cross-Couplings of (Hetero)Aryl or Alkenyl Tosylates, *Chem. Eur. J.* **2011**, *17*, 2965-2971.
- <sup>50</sup> W. S. Knowles, Asymmetric Hydrogenations – The Monsanto L-DOPA Process. In *Asymmetric Catalysis on Industrial Scale*. H. U. Blaser, E. Schmidt, Eds.; Wiley-VCH, 2004.
- <sup>51</sup> V. Caprio, J. M. J. Williams, Eds.; *Catalysis in Asymmetric Synthesis*, 2<sup>nd</sup> Ed.; Wiley-VCH, 2009.
- <sup>52</sup> J. A. Osborn, F. H. Jardine, J. F. Young, G. Wilkinson, The preparation and properties of tris(triphenylphosphine)halogenrhodium(I) and some reactions thereof including catalytic homogeneous hydrogenation of olefins and acetylenes and their derivatives, *J. Chem. Soc. A* **1966**, 1711-1732.
- <sup>53</sup> W. Tang, X. Zhang, Chiral Phosphorus Ligands for Enantioselective Hydrogenation, *Chem. Rev.* **2003**, *103*, 3029-3069.
- <sup>54</sup> L. Horner, H. Siegel, H. Büthe, Asymmetric Catalytic Hydrogenation with an Optically Active Phosphinerhodium Complex in Homogeneous Solution, *Angew Chem. Int. Ed. Engl.* **1968**, *7*, 942-942.
- <sup>55</sup> W. S. Knowles, M. J. Sabacky, Catalytic Asymmetric Hydrogenation employing a Soluble, Optically Active, Rhodium Complex, *Chem. Commun.* **1968**, 1445-1446.
- <sup>56</sup> T. P. Dang, H. B. Kagan, The Asymmetric Synthesis of Hydratropic Acid and Amino-acids by Homogeneous Catalytic Hydrogenation., *Chem. Commun.* **1971**, 481-481.
- <sup>57</sup> H. B. Kagan, T. P. Dang, Asymmetric Catalytic Reduction with Transition Metal Complexes. I. A Catalytic System of Rhodium(I) with (-)-2,3-O-Isopropylidene-2,3-



- dihydroxy-1,4-bis(diphenylphosphino)butane, a New Chiral Diphosphine, *J. Am. Chem. Soc.* **1972**, *94*, 6429-6433.
- <sup>58</sup> H. B. Kagan, N. Langlois, T. P. Dang, Reduction asymetrique catalysee par des complexes de metaux de transition IV. Synthese d'amines chirales au moyen d'un complexe de rhodium et d'isopropylidene dihydroxy-2,3 bis(diphenylphosphino)-1,4 butane (diop), *J. Organomet. Chem.* **1975**, *90*, 353-365.
- <sup>59</sup> F. Lagasse, H. B. Kagan, Chiral Monophosphines as Ligands for Asymmetric Organometallic Catalysis, *Chem. Pharm. Bull.* **2000**, *48*, 315-324.
- <sup>60</sup> Y. S. Jan, L. Wozniak, J. Pedroni, N. Cramer, Access to *P*- and Axially Chiral Biaryl Phosphine Oxides by Enantioselective Cp<sup>x</sup>Ir<sup>III</sup>-Catalyzed C-H Arylations, *Angew. Chem. Int. Ed.* **2018**, *57*, 12901-12905.
- <sup>61</sup> A. Togni, C. Breutel, A. Schnyder, F. Spindler, H. Landert, A. Tijani, A Novel Easily Accessible Chiral Ferrocenyldiphosphine for Highly Enantioselective Hydrogenation, Allylic Alkylation, and Hydroboration Reactions, *J. Am. Chem. Soc.* **1994**, *116*, 4062-4066.
- <sup>62</sup> W. Fu, W. Tang, Chiral Monophosphorus Ligands for Asymmetric Catalytic Reactions, *ACS Catal.* **2016**, *6*, 4814-4858.
- <sup>63</sup> R. Noyori, T. Ohkuma, M. Kitamura, H. Takaya, N. Sayo, H. Kumobayashi, S. Akutagawa, Asymmetric hydrogenation of .beta.-keto carboxylic esters. A practical, purely chemical access to .beta.-hydroxy esters in high enantiomeric purity. *J. Am. Chem. Soc.* **1987**, *109*, 5856-5858.
- <sup>64</sup> M. J. Burk, C<sub>2</sub>-Symmetric Bis(phospholanes) and Their Use in Highly Enantioselective Hydrogenation Reactions, *J. Am. Chem. Soc.* **1991**, *113*, 8518-8519.
- <sup>65</sup> B. D. Vineyard, W. S. Knowles, M. J. Sabacky, G. L. Bachmann, D.J. Weinkauff, Asymmetric Hydrogenation. Rhodium Chiral Bisphosphine Catalyst. *J. Am. Chem. Soc.* **1977**, *99*, 5946-5952.
- <sup>66</sup> W. S. Knowles, M. J. Sabacky, B. D. Vineyard, Catalytic Asymmetric Hydrogenation, *Chem. Comm.* **1972**, 10-11.
- <sup>67</sup> T. Saget, S. J. Lemouzy, N. Cramer, Chiral Monodentate Phosphines and Bulky Carboxylic Acids: Cooperative Effects in Palladium-Catalyzed Enantioselective C(sp<sup>3</sup>)-H Functionalization, *Angew. Chem. Int. Ed.* **2012**, *51*, 2238-2242.
- <sup>68</sup> T. Hayashi, Chiral Monodentate Phosphine Ligand MOP for Transition-Metal-Catalyzed Asymmetric Reactions, *Acc. Chem. Res.* **2000**, *33*, 354-362.
- <sup>69</sup> H. Oertling, A. Reckziegel, H. Surburg, H.-J. Bertram, Applications of Menthol in Synthetic Chemistry, *Chem. Rev.* **2007**, *107*, 2136-2164.

- <sup>70</sup> H. Brunner, M. Janura, Enantioselective Catalysis 113: New Menthylphosphane Ligands Differing in Steric and Electronic Properties. *Synthesis* **1998**, 45-55.
- <sup>71</sup> J. D. Morrison, R. E. Burnett, A. M. Aguiar, C. J. Morrow, C. Phillips, Asymmetric Homogeneous Hydrogenation with Rhodium(I) Complexes of Chiral Phosphines, *J. Am. Chem. Soc.* **1971**, *93*, 1301-1303.
- <sup>72</sup> B. Bogdanović, B. Henc, B. Meister, H. Pauling, G. Wilke, A Catalyzed Asymmetric Synthesis, *Angew. Chem. Int. Ed.* **1972**, *11*, 1023-1024.
- <sup>73</sup> S. Koller, J. Gatzka, K. M. Wong, P. Altmann, A. Pöthig, L. Hintermann, Stereochemistry of the Menthyl Grignard Reagent: Generation, Composition, Dynamics, and Reactions with Electrophiles, *J. Org. Chem.* **2018**, *83*, 15009-15028.
- <sup>74</sup> R. E. Black, R. F. Jordan, Synthesis and Reactivity of Palladium(II) Alkyl Complexes that Contain Phosphine-cyclopentanesulfonate Ligands. *Organometallics* **2017**, *36*, 3415-3428.
- <sup>75</sup> L. Hintermann, K.M. Wong, Rearrangement in Stereoretentive Syntheses of Menthyl Chloride from Menthol: Insight into Competing Reaction Pathways through Component Quantification Analysis, *Eur. J. Org. Chem.* **2017**, 5527-5535.
- <sup>76</sup> J. Gatzka, Master's Thesis, TU Munich **2016**, Bildung, Analyse und Reaktivität des Menthyl-Grignard-Reagenzes, und Anwendung in der Synthese enantiomerenreiner sekundärer Phosphinoxide.
- <sup>77</sup> C. Lossin, Master's Thesis, TU Munich **2018**, New Catalyst Systems: Dimethylphosphine Oxide as Ligand and Precursor for Chiral Ligands in Homogeneous Catalysis.
- <sup>78</sup> K. Reinhardt, Master's Thesis, TU Munich **2017**, New Syntheses of Chiral P-Menthylphosphane-Ligands and Syntheses of Benzo-annelated Ligands of the Buchwald Type.
- <sup>79</sup> H. W. Krause, A. Kinting, Herstellung von *P*-Chlordimethylphosphin, *J. prakt. Chem.* **1980**, *322*, 485-486.
- <sup>80</sup> G. Haegde, W. Kueckelhaus, J. Seega, G. Tossing, H. Kessler, R. Schuck, *Z. Naturforsch. B* **1985**, *40*, 1053-1063.
- <sup>81</sup> M. R. Pramick, S. M. Rosemeier, M. T. Beranek, S. B. Nickse, J. J. Stone, R. A. Stockland, Jr., S. M. Baldwin, M. E. Kastner, Coupling of Aryl Halides with Aryl Boronic Acids with P(C<sub>6</sub>H<sub>5</sub>)(2-C<sub>6</sub>H<sub>4</sub>Cl)<sub>2</sub> as the Supporting Ligand, *Organometallics* **2003**, *22*, 523-528.
- <sup>82</sup> A literature example reporting a 1-naphthyl (diphenyl)phosphine ligand in a Pd-catalyzed transformation: S. Zolezzi, S. A. Moya, G. Valdebenito, G. Abarca, J. Parada, P. Aguirre, Methoxycarbonylation of olefins catalyzed by palladium(II) complexes containing naphthyl (diphenyl)phosphine ligands, *Appl. Organometal. Chem.* **2014**, *28*, 364-371.

- <sup>83</sup> B. Xiong, R. Shen, M. Gotot, S.-F. Yin, L.-B. Han, Highly Selective 1,4- and 1,6-Addition of P(O)-H Compounds to *p*-Quinones: A Divergent Method for the Synthesis of *C*- and *O*-Phosphoryl Hydroquinone Derivatives, *Chem. Eur. J.* **2012**, *18*, 16902-16910.
- <sup>84</sup> J.-P. Wang, S.-Z. Nie, Z.-Y. Zhou, J.-J. Ye, J.-H. Wen, C.-Q. Zhao, Preparation of Optically Pure Tertiary Phosphine Oxides via the Addition of *P*-Stereogenic Secondary Phosphine Oxide to Activated Alkenes, *J. Org. Chem.* **2016**, *81*, 7644-7653.
- <sup>85</sup> a) S. W. McCombie, W. A. Metz, D. Nazareno, B. B. Shankar, J. Tagat, Generation and in Situ Acylation of Enaminone Anions: synthesis of 3-Carbethoxy-4(1H)-pyridinones and -4-pyrones and Related Compounds, *J. Org. Chem.* **1991**, *56*, 4963-4967. b) A. Jarrahpour, M. Zarei, DMF-dimethyl sulfate as a new reagent for the synthesis of  $\beta$ -lactams. *Tetrahedron Lett.* **2009**, *50*, 1568-1570.
- <sup>86</sup> GESTIS compound database: Entry for Me<sub>2</sub>SO<sub>4</sub>, <https://gestis.dguv.de/data?name=010580>, visited on July 19, 2021
- <sup>87</sup> GESTIS compound database: Entry for MeI, <https://gestis.dguv.de/data?name=028110>, visited on July 19, 2021
- <sup>88</sup> M. Stankevic, A. Wlodarczyk, Efficient copper(I)-catalyzed coupling of secondary phosphine oxides with aryl halides, *Tetrahedron* **2013**, *69*, 73-81.
- <sup>89</sup> a) X. Jin, K. Yamaguchi, N. Mizuno, Copper-Catalyzed Oxidative Cross-Coupling of H-Phosphonates and Amides to N-Acylphosphoramidates, *Org. Lett.* **2013**, *15*, 418-421. b) R. Curci, F. Di Furia, Oxidation of organophosphorus compounds—IV: Kinetics and mechanism of the oxidation of diarylphosphine oxides by *t*-butyl hydroperoxide, hydrogen peroxide and *p*-nitroperoxybenzoic acid in alkaline media, *Tetrahedron* **1972**, *28*, 3905-3913.
- <sup>90</sup> A.-X. Zhou, L.-L. Mao, G.-W. Wang, S.-D. Yang, A unique copper-catalyzed cross-coupling reaction by hydrogen (H<sub>2</sub>) removal for the stereoselective synthesis of 3-phosphoindoles, *Chem. Commun.* **2014**, *50*, 8529-8532.
- <sup>91</sup> C. Li, T. Chen, L.-B. Han, Iron-catalyzed clean dehydrogenative coupling of alcohols with P(O)-H compounds: a new protocol for ROH phosphorylation, *Dalton Trans.* **2016**, *45*, 14893-14897.
- <sup>92</sup> L. C. Baldwin, M. J. Fink, Synthesis of 1,2-bis[(diorgano)phosphino]ethanes via Michaelis-Arbuzov type rearrangements, *J. Org. Chem.* **2002**, *646*, 230-238.
- <sup>93</sup> H. Fritzsche, U. Hasserodt, F. Korte, Reduktion organischer Verbindungen des fünfwertigen Phosphors zu Phosphinen, II. Reduktion tertiärer Phosphinoxyde zu tertiären Phosphinen mit Trichlorsilan, *Chem. Ber.* **1965**, *98*, 171-174.

- <sup>94</sup> M.-L. Schirmer, S. Jopp, J. Holz, A. Spannenberg, T. Werner, Organocatalyzed Reduction of Tertiary Phosphine Oxides, *Adv. Synth. Catal.* **2016**, 358, 26-29.
- <sup>95</sup> E. Nicolas, A. Ohleier, F. D'Accriscio, A.-F. Pécharman, M. Demange, P. Ribagnac, J. Ballester, C. Gosmini, N. Mézailles, "(Diphosphine)Nickel"-Catalyzed Negishi Cross-Coupling: An Experimental and Theoretical Study, *Chem. Eur. J.* **2015**, 21, 7690-7694.
- <sup>96</sup> E. A. Standley, S. J. Smith, P. Müller, T. F. Jamison, A Broadly Applicable Strategy for Entry into Homogeneous Nickel(0) Catalysts from Air-Stable Nickel(II) Complexes, *Organometallics* **2014**, 33, 2012-2018.
- <sup>97</sup> I. M. Angulo, E. Bouwman, R. v. Gorkum, S. M. Lok, M. Lutz, A. L. Spek, New nickel-containing homogeneous hydrogenation catalysts: Structures of [Ni(*o*-MeO-dppol)Cl<sub>2</sub>] and [Ni(dcpe)Cl<sub>2</sub>] *J. Mol. Catal. A: Chem.* **2003**, 202, 97-103.
- <sup>98</sup> A. Pradal, S. Gladili, V. Michelet, P. Y. Toullec, Combinatorial Approach to Chiral Tris-ligated Carbophilic Platinum Complexes: Application to Asymmetric Catalysis, *Chem. Eur. J.* **2014**, 20, 7128-7135.
- <sup>99</sup> F. R. Hartley, S. G. Murray, C. A. McAuliffe, Monomeric Complexes of Palladium(II) and Platinum(II) with a Series of Open-Chain Tetrathioether Ligands Prepared from Complexes of Weak Donor Ligands, *Inorg. Chem.* **1979**, 18, 1394-1397.
- <sup>100</sup> a) D. Schmitz, V. A. Shubert, T. Betz, M. Schnell, Exploring the conformational landscape of menthol, menthone, and isomenthone: a microwave study, *Front. Chem.* **2015**, 3, 1-13. b) J. Härtner, U. M. Reinscheid, Conformational analysis of menthol diastereomers by NMR and DFT computation, *J. Mol. Struct.* **2008**, 872, 145-149.
- <sup>101</sup> J. P. Wolfe, R. A. Singer, B. H. Yang, S. L. Buchwald, Highly Active Palladium Catalysts for Suzuki Coupling Reactions, *J. Am. Chem. Soc.* **1999**, 121, 9550-9561.
- <sup>102</sup> K. Khrameshina, Bachelor's Thesis, TU Munich **2019**, Synthese von neuartigen, menthyl-basierten Liganden des *Buchwald*-Typs und Untersuchung ihrer Anwendung in der Katalyse.
- <sup>103</sup> S. Chatterjee, L. Hintermann, M. Mandal, A. Achari, S. Gupta, P. Jaisankar, Fiaud's Acid: A Bronsted Acid Catalyst for Enantioselective Friedel-Crafts Alkylation of Indoles with 2-Alkene-1,4-diones, *Org. Lett.* **2017**, 19, 3426-3429.
- <sup>104</sup> <https://de.climate-data.org/asien/indien/westbengalen/kalkutta-2826/> , visited on April 13, 2021
- <sup>105</sup> <https://de.climate-data.org/europa/deutschland/bayern/muenchen-6426/> , visited on April 13, 2021

- <sup>106</sup> R. E. Islas, J. Cárdenas, R. Gaviño, E. García-Ríos, L. Lomas-Romero, J. A. Morales-Serna, Phosphinito palladium(II) complexes as catalysts for the synthesis of 1,3-enynes, aromatic alkynes and ynones, *RSC Adv.* **2017**, *7*, 9780-9789.
- <sup>107</sup> J. Bigeault, L. Giordano, G. Buono, [2+1] Cycloadditions of Terminal Alkynes to Norbornene Derivatives Catalyzed by Palladium Complexes with Phosphinous Acid Ligands, *Angew. Chem.* **2005**, *117*, 4831-4835.
- <sup>108</sup> G. Y. Li, Highly Active, Air-Stable Palladium Catalysts for the C-C and C-S Bond-Forming Reactions of Vinyl and Aryl Chlorides: Use of Commercially Available [(*t*-Bu)<sub>2</sub>P(OH)]<sub>2</sub>PdCl<sub>2</sub>, [(*t*-Bu)<sub>2</sub>P(OH)PdCl<sub>2</sub>]<sub>2</sub>, and [[(*t*-Bu)<sub>2</sub>PO···H···OP(*t*-Bu)<sub>2</sub>]PdCl<sub>2</sub>]<sub>2</sub> as Catalysts, *J. Org. Chem.* **2002**, *67*, 3643-3650.
- <sup>109</sup> N. P. Reddy, M. Tanaka, Palladium-Catalyzed amination of aryl chlorides, *Tetrahedron* **1997**, *38*, 4807-4810.
- <sup>110</sup> V. Grushin, H. Alper, Alkali-induced disproportionation of palladium(II) tertiary phosphine complexes, [L<sub>2</sub>PdCl<sub>2</sub>], to LO and palladium(0). Key intermediates in the biphasic carbonylation of ArX catalyzed by [L<sub>2</sub>PdCl<sub>2</sub>], *Organometallics* **1993**, *12*, 1890-1901.
- <sup>111</sup> B. P. Fors, P. Krattiger, E. Strieter, S. L. Buchwald, Water-Mediated Catalyst Preactivation: An Efficient Protocol for C-N Cross-Coupling Reactions, *Org. Lett.* **2008**, *10*, 3505-3508.
- <sup>112</sup> A. Jutand, Mechanism of the Mizoroki-Heck Reaction when the Ligand is a Bulky and Electron-Rich Monophosphine. In: *The Mizoroki-Heck Reaction*, M. Oestreich, Ed., 2009, pp. 37-42.
- <sup>113</sup> J. W. Dankwardt, Nickel-Catalyzed Cross-Coupling of Aryl Grignard Reagents with Aromatic Alkyl Ethers: An Efficient Synthesis of Unsymmetrical Biaryls, *Angew. Chem. Int. Ed.* **2004**, *43*, 2428-2432.
- <sup>114</sup> P. Lahuerta, J. Latorre, R. Martínez-Mánez, F. Sanz, Orthometallation reactions of rhodium compounds containing orthohaloarylphosphines. V. Synthesis and reactivity of orthometallated rhodium(III) compounds. Crystal structure of RhCl(CO)[P(*o*-ClC<sub>6</sub>H<sub>4</sub>)Ph<sub>2</sub>]<sub>2</sub>. *J. Organomet. Chem.* **1988**, *356*, 355-366.
- <sup>115</sup> M. J. Burk, R. H. Crabtree, E. M. Holt, Halocarbon chelation in [Ir(cod)(η<sup>2</sup>-*o*-HalC<sub>6</sub>H<sub>4</sub>PPh<sub>2</sub>)]SbF<sub>6</sub> (Hal = Br, Cl): structural and chemical studies, *J. Organomet. Chem.* **1988**, *341*, 495-509.
- <sup>116</sup> S. Gowrisankar, H. Neumann, M. Beller, A Convenient and Practical Synthesis of Anisoles and Deuterated Anisoles by Palladium-Catalyzed Coupling Reactions of Aryl Bromides and Chlorides, *Chem. Eur. J.* **2012**, *18*, 2498-2502.

- <sup>117</sup> A. Jutand, Mechanism of the Mizoroki-Heck Reaction when the Catalytic Precursor is Pd(OAc)<sub>2</sub> Associated with Bisphosphine Ligands. In: *The Mizoroki-Heck reaction*, M. Oestreich, Ed., 2009, pp. 16-19.
- <sup>118</sup> K. Martina, F. Baricco, M. Caporaso, G. Berlier, G. Cravotto, Cyclodextrin-Grafted Silica-Supported Pd Nanoparticles: An Efficient and Versatile Catalyst for Ligand-Free C-C Coupling and Hydrogenation, *ChemCatChem* **2016**, *8*, 1176-1184.
- <sup>119</sup> I. P. Beletskaya, A. V. Cheprakov, Focus on Catalyst Development and Ligand Design. In: *The Mizoroki-Heck reaction*, M. Oestreich, Ed., 2009, pp. 80-81.
- <sup>120</sup> Some literature reports on the  $\alpha$ -arylation of olefins in ionic liquids or polar solvents: a) J. Mo, L. Xu, J. Xiao, Ionic Liquid-Promoted, Highly Regioselective Heck Arylation of Electron-Rich Olefins by Aryl Halides, *J. Am. Chem. Soc.* **2005**, *127*, 751-760. b) J. Mo, J. Xiao, The Heck-Reaction of Electron-Rich Olefins with Regiocontrol by Hydrogen-Bond Donors, *Angew. Chem. Int. Ed.* **2006**, *45*, 4152-4157. c) Z. Hyder, J. Ruan, J. Xiao, Hydrogen-Bond-Directed Catalysis: Faster, Regioselective and Cleaner Heck Arylation of Electron-Rich Olefins in Alcohols, *Chem. Eur. J.* **2008**, *14*, 5555-5566.
- <sup>121</sup> T. Jeffery, On the Efficiency of Tetraalkylammonium Salts in Heck Type Reactions, *Tetrahedron* **1996**, *52*, 10113.
- <sup>122</sup> I. P. Beletskaya, A. Cheprakov, Focus on Catalyst Development and Ligand Design. In: *The Mizoroki-Heck reaction*, M. Oestreich, Ed., 2009, pp. 51-132.
- <sup>123</sup> M. G. Organ, M. Abdel-Hadi, S. Avola, N. Hadei, J. Nasielski, C. J. O'Brien, C. Valente, Biaryls Made Easy: PEPPSI and the Kumada-Tamao-Corriu Reaction, *Chem. Eur. J.* **2007**, *13*, 150-157.
- <sup>124</sup> G. Manolikakes, P. Knochel, Radical Catalysis of Kumada Cross-Coupling Reactions Using Functionalized Grignard Reagents, *Angew. Chem. Int. Ed.* **2009**, *48*, 205-209.
- <sup>125</sup> X. Hua, J. Masson-Makdissi, R. J. Sullivan, S. G. Newman, Inherent vs Apparent Chemoselectivity in the Kumada-Corriu Cross-Coupling Reaction, *Org. Lett.* **2016**, *18*, 5312-5315.
- <sup>126</sup> P. J. Walsh, M. C. Kozlowski, *Fundamentals of Asymmetric Catalysis*, 2009, pp. 2-14.
- <sup>127</sup> Some examples of reported conditions with similar outcomes: a) Z. Zhou, H. Liang, W. Xia, H. Chen, Y. Zhang, X. He, S. Yu, R. Cao, L. Qiu, Synthesis of a class of binaphthyl monophosphine ligands with a naphthofuran skeleton and their applications in Suzuki-Miyaura coupling reactions, *New. J. Chem.* **2018**, *42*, 5967-5971. b) A. Ros, B. Estepa, A. Bermejo, E. Álvarez, R. Fernández, J. M. Lassaletta, Phosphino Hydrazones as Suitable Ligands in the Asymmetric Suzuki-Miyaura Cross-Coupling, *J. Org. Chem.* **2012**, *77*, 4740-

4750. c) Y. Liu, H. Peng, J. Yuan, M.-Q. Yan, X. Luo, Q.-G. Wu, S.-H. Liu, J. Chen, G.-A. Yu, An efficient indenyl-derived phosphine ligand for the Suzuki-Miyaura coupling of sterically hindered aryl halides, *Org. Biomol. Chem.* **2016**, *14*, 4664-4668.
- <sup>128</sup> M. Korb, D. Schaarschmidt, M. Grumbt, M. König, H. Lang, Evaluation of the Transferability of the „Flexible Steric Bulk“ Concept from N-Heterocyclic Carbenes to Planar Chiral Phosphiniferrocenes and their Electronic Modification, *Eur. J. Inorg. Chem.* **2020**, 2968-2982.
- <sup>129</sup> B. J. Tardiff, M. Stradiotto, Buchwald–Hartwig Amination of (Hetero)aryl Chlorides by Employing Mor-DalPhos under Aqueous and Solvent-Free Conditions, *Eur. J. Org. Chem.* **2012**, 3972-3977.
- <sup>130</sup> T. J. Maimone, P. J. Milner, T. Kinzel, Y. Zhang, M. K. Takase, S. L. Buchwald, Evidence for in Situ Catalyst Modification during the Pd-Catalyzed Conversion of Aryl Triflates to Aryl Fluorides, *J. Am. Chem. Soc.* **2011**, *133*, 18106-18109.
- <sup>131</sup> C. C. Wagen, B. T. Ingoglia, S. L. Buchwald, Unexpected Formation of Hexasubstituted Arenes through a 2-fold Palladium-Mediated Ligand Arylation, *J. Org. Chem.* **2019**, *84*, 12672-12679.
- <sup>132</sup> A. M. Allgeier, B. J. Shaw, T.-L. Hwang, J. E. Milne, J. S. Tedrow, C. N. Wilde, Characterization of Two Stable Degradants of Palladium <sup>t</sup>BuXPhos Catalyst and a Unique Dearomatization Reaction, *Organometallics* **2012**, *31*, 519-522.
- <sup>133</sup> A. Kinting, H.-W. Krause, Asymmetric Hydrogenation catalyzed by rhodium complexes of 2,3-bis(dimethylphosphino)maleic anhydride and 2,3-bis(dimethylphosphino)-*N*-phenylmaleimide, *J. Organomet. Chem.* **1986**, *302*, 259-264.
- <sup>134</sup> K. Wu, A. G. Doyle, Parameterization of phosphine ligands demonstrates enhancement of nickel catalysis via remote steric effects, *Nature Chem.* **2017**, *9*, 779-784.
- <sup>135</sup> A. Inoue, N. Kuroki, K. Konishi, Studies on the Utilization of 1,4-Naphthoquinone. VI Derivatives from Naphthoquinon-monoimine. *J. Syn. Org. Chem. Jpn.* **1958**, *16*, 607-609.
- <sup>136</sup> G. Wurm, Untersuchungen an 1,4-Naphthochinonen, 21. Mitt.: 2-(3,5-Di-*Tert*-Butyl-4-Hydroxyphenyl)-1,4-Naphthochinone als 5-Lipoxygenasehemmer, *Arch. Pharm.* **1991**, *324*, 491-495.
- <sup>137</sup> Y. Pu, S. Cao, A. J. Ragauskas, Application of quantitative <sup>31</sup>P-NMR biomass lignin and biofuel precursors characterization, *Energy Environ. Sci.* **2011**, *4*, 3154-3166., and references cited therein.
- <sup>138</sup> M. Weber, C. Hellriegel, A. Rueck. J. Wuethrich, P. Jenks, M. Obkircher, Method development in quantitative NMR towards metrologically traceable organic certified

- reference materials used as  $^{31}\text{P}$  qNMR standards, *Anal. Bioanal. Chem.* **2015**, *407*, 3115-3123.
- <sup>139</sup> M. Stankevic, K. M. Pietrusiewicz, The Synthesis and Reactivity of Phosphinous Acid-Boranes, *Synthesis* **2005**, *8*, 1279-1290.
- <sup>140</sup> M. Stankevic, G. Andrijewski, K. M. Pietrusiewicz, Direct Conversion of *sec*-Phosphine Oxides into Phosphinous Acid Boranes, *Synlett* **2004**, *2*, 311-315.
- <sup>141</sup> C. B. Provis-Evans, E. A. C. Emanuelsson, R. L. Webster, Rapid Metal-Free Formation of Free Phosphines from Phosphine Oxides, *Adv. Synth. Catal.* **2018**, *360*, 3999-4004.
- <sup>142</sup> R. van Sluis, G. S. Payne, M. O. Leach, Increased NOE Enhancement in  $^1\text{H}$  Decoupled  $^{31}\text{P}$  MRs, *Magnetic Resonance in Medicine* **1995**, *34*, 893-897.
- <sup>143</sup> A. G. Dikundwar, P. Chodon, S. P. Thomas, H. Bhutani, Supramolecular Chemistry of BrettPhos and BrettPhos Oxide: Breakup of Isostructurality via Order-Disorder Phase Transitions, *Cryst. Growth Des.* **2017**, *17*, 1982-1990.
- <sup>144</sup> Some literature reports using 1,4-dioxane as solvent in the palladium-catalyzed Suzuki-Miyaura coupling of sterically hindered substrates using phosphine or NHC ligands: a) J. Ruan, L. Shearer, J. Mo, J. Bacsá, A. Zanotti-Gerosa, F. Hancock, X. Wu, J. Xiao, [2.2]Paracyclophane-based monophosphine ligand for palladium-catalyzed cross-coupling reactions of aryl chlorides, *Org. Biomol. Chem.* **2009**, *7*, 3236-3242. b) L. Benhamou, C. Besnard, E. P. Kündig, Chiral PEPPSI Complexes: Synthesis, Characterization, and Application in Asymmetric Suzuki-Miyaura Coupling Reactions, *Organometallics* **2014**, *33*, 260-266. c) T. Tu, Z. Sun, W. Fang, M. Xu, Y. Zhu, Robust Acenaphthoimidazolylidene Palladium Complexes: Highly Efficient Catalysts for Suzuki-Miyaura Couplings with Sterically Hindered Substrates, *Org. Lett.* **2012**, *14*, 4250-4253.
- <sup>145</sup> A. S. Dallas, K. V. Gothelf, Effect of Water on the Palladium-Catalyzed Amidation of Aryl Bromides, *J. Org. Chem.* **2005**, *70*, 3321-3323.
- <sup>146</sup> R. Reiner. (Director). (1984). *This is Spinal Tap* [Film]. Spinal Tap Prod., Goldcrest Films International.
- <sup>147</sup> A. C. Sather, S. L. Buchwald, The Evolution of  $\text{Pd}^0/\text{Pd}^{\text{II}}$ -Catalyzed Aromatic Fluorination, *Acc. Chem. Res.* **2016**, *49*, 2146-2157.
- <sup>148</sup> K. Muto, T. Okita, J. Yamaguchi, Transition-Metal-Catalyzed Denitrative Coupling, *ACS Catal.* **2020**, *10*, 9856-9871., and references cited therein.
- <sup>149</sup> M. R. Yadav, M. Nagaoka, M. Kashiwara, R.-L. Zhong, T. Miyazaki, S. Sakaki, Y. Nakao, The Suzuki-Miyaura coupling of Nitroarenes, *J. Am. Chem. Soc.* **2017**, *139*, 9423-9426.



- <sup>150</sup> M. Rimodi, F. Ragaini, E. Gallo, F. Ferretti, P. Macchi, N. Casati, Unexpected isomerism in [Pd (2,9-dimethylphenanthroline) X 2]<sup>+</sup> (X = Cl, Br, I) complexes: a neutral and ionic form exist, *Dalton Trans.* **2012**, *41*, 3648-3658.
- <sup>151</sup> L. G. L. Ward, J. R. Pipal, Anhydrous Nickel(II) Halides and their Tetrakis(ethanol) and 1,2-Dimethoxyethane Complexes, *Inorg. Synth.* **1972**, *13*, 154-164.
- <sup>152</sup> D. Fraccarollo, R. Bertani, M. Mozzon, Synthesis and spectroscopic investigation of *cis* and *trans* isomers of bis(nitrile)dichloroplatinum(II) complexes, *Inorg. Chim. Acta* **1992**, *201*, 15-22.
- <sup>153</sup> D. G. Patel, T. B. Mitchell, S. D. Myers, D. A. Carter, F. A. Novak, Approach to Quinone-Based Diarylethene Photochromes, *J. Org. Chem.* **2020**, *85*, 2646-2653.
- <sup>154</sup> R. M. Raj, K. K. Balasubramanian, D. Easwaramoorthy, Diels-Alder trapping of *in situ* generated dienes from 3,4-dihydro-2*H*-pyran with *p*-quinone catalyzed by *p*-toluenesulfonic acid, *Org. Biomol. Chem.* **2017**, *15*, 1115-1121.
- <sup>155</sup> H. Miyamura, F. Tobita, A. Suzuki, S. Kobayashi, Direct Synthesis of Hydroquinones from Quinones through Sequential and Continuous-Flow Hydrogenation-Derivatization Using Heterogeneous Au-Pt Nanoparticles as Catalysts, *Angew. Chem. Int. Ed.* **2019**, *58*, 9220-9224.
- <sup>156</sup> B. H. Lipshutz, S. Ghorai, W. W. Yi Leong, B. R. Taft, D. V. Krogstad, Manipulating Micellar Environments for Enhancing Transition Metal-Catalyzed Cross-Couplings in Water at Room Temperature, *J. Org. Chem.* **2011**, *76*, 5061-5073.
- <sup>157</sup> T. Sperger, C. K. Stirner, F. Schoenebeck, Bench-Stable and Recoverable Palladium(I) Dimer as an Efficient Catalyst for Heck Cross-Coupling, *Synthesis* **2017**, *49*, 115-120.
- <sup>158</sup> M. Liu, S. Onchaiya, L. Y. Fong Tan, M. A. Haghghatbin, T. Luu, T. C. Owyong, R. Hushiarian, C. F. Hogan, T. A. Smith, Y. Hong, 9-Vinylanthracene Based Fluorogens: Synthesis, Structure-Property Relationships and Applications, *Molecules* **2017**, *22*, 2148.
- <sup>159</sup> M. G. Lauer, M. K. Thompson, K. H. Shaughnessy, Controlling Olefin Isomerization in the Heck Reaction with Neopentyl Phosphine Ligands, *J. Org. Chem.* **2014**, *79*, 10837-10848.
- <sup>160</sup> Y. Li, F. Mao, T. Chen, Z. Zhou, Y. Wang, J. Huang, *In Situ* Trapped and Immobilized Palladium Nanoparticles as Active and Clean Catalysts for Suzuki-Miyaura Reaction, *Adv. Synth. Catal.* **2015**, *357*, 2827-2832.
- <sup>161</sup> H. Brunner, G. Olschewski, B. Nuber, Enantioselective Catalyses; 126: Axially Chiral *N,N*-Ligands with Binaphthyl/Bipyridyl Structure, *Synthesis* **1999**, 429-434.

<sup>162</sup> Y. Zhang, V. César, G. Storch, N. Lugan, G. Lavigne, Skeleton Decoration of NHCs by Amino Groups and its Sequential Booster Effect on the Palladium-Catalyzed Buchwald-Hartwig Amination, *Angew. Chem. Int. Ed.* **2014**, *53*, 6482-6486.